

Recovery of valuable products from polytetrafluoroethylene (PTFE) waste

I. J. van der Walt

**Thesis submitted for the degree Doctor of Philosophy at the Potchefstroom
Campus of the North West University**

Promoter: Prof. O. S. L. Bruinsma

Co-promoter: Dr. J. T. Nel

November 2007

**Dedicated to my Father
who inspired me by his example**

ACKNOWLEDGEMENTS

I would like to express my sincere gratitude and appreciation to:

1. God whom gave me the talent to perform this research;
2. My wife Marisa for being very supportive, patient and understanding;
3. My external supervisor: Dr J. T. Nel (Johann), Senior Scientist, Manager, Engineering and Technology Department, Necsa, for his mentorship and guidance;
4. My internal supervisor: Prof. O. S. L. Bruinsma, Research Director: Separation Science and Technology Group, North West University, for his wisdom and guidance;
5. The Necsa, Pelindaba for financial support;
6. The North West University, Potchefstroom campus, for the chance to do this study;
7. Mr. Alfred Grunenberg, Senior Technologist, Engineering and Technology Department, Necsa, for his assistance in the design and build of some of the laboratory equipment;
8. Mr. W. L. Retief, Private contractor, for the linguistic editing of the thesis;
9. Mr. John le Roux, Senior Scientist, Engineering and Technology department, Necsa, for his assistance with Chapters 6 and 8;
10. Mr. Rajen Naidoo, Senior Chemical Engineer, Business development department, Necsa, for his assistance with Chapter 12;
11. Dr. Cornie van Sittert, School of Chemistry, NWU, for her assistance with Chapter 7;
12. Prof. Hein Neomagus, School of Chemical and Minerals Engineering, NWU, for his assistance with Chapter 8;
13. The technicians, Mr. C. C. Fakazi, Mr. G. G. Maluleke and K Moodley for their assistance and operating the laboratory systems.

ABSTRACT

The disposal of PTFE waste presents a global problem from both an ecological and economical perspective. This study was performed to address this problem as well as to understand the mechanism according to which PTFE is depolymerised to form the different products, namely C_2F_4 , C_2F_6 , C_3F_6 , C_3F_8 and $c-C_4F_8$.

Different conceptual reactors were designed and built for different tests on filled and unfilled PTFE. These included a laboratory scale Rotating-kiln Reactor for testing the depolymerisation properties in a horizontal reactor, a Drop-tube Reactor for the continuous depolymerisation of unfilled PTFE, a Paddle Reactor for the continuous depolymerisation of filled as well as unfilled PTFE and a Vibrating Reactor for the evaluation of other fluoropolymers like THV, HTE, ETFE and PFA. Analytical techniques such as GC, GC/MS, TGA and SEM were used to evaluate the different types of PTFE and analyse the gaseous products from the depolymerisation process.

A mechanism by which depolymerisation and product formation takes place was proposed on the basis of experimental data obtained during experimentation on various PTFE depolymerisation systems, utilising different analytical techniques, including a thermodynamic study, a kinetic study and molecular modelling.

For the product formation mechanism a two-route approach was proposed. Route 1 dominated at temperatures < 700 °C, producing mainly C_2F_4 , C_3F_6 and $c-C_4F_8$. Route 2 dominated at temperatures between 700 and 900 °C, producing mainly C_2F_4 , C_2F_6 , C_3F_6 , C_3F_8 , PFIB and $c-C_4F_8$.

A thermodynamic study and molecular modelling was used to evaluate possible product formation reactions in order to propose scientifically sound mechanisms for Routes 1 and 2.

A kinetic study revealed that the order of the depolymerisation reaction is 0.54, and that the reaction proceeds at a rate of $4.03 \times 10^{-3} \text{ s}^{-1}$ at 600 °C. The activation energy for the depolymerisation process was calculated to be $260 \text{ kJ}\cdot\text{mol}^{-1}$.

A Rotating-kiln Plant was designed for the production of HFP from PTFE on a commercial scale. An economic analysis indicated that a $500 \text{ kg}\cdot\text{h}^{-1}$ filled PTFE depolymerisation plant, selling HFP as a product at R55 per kg, is highly profitable.

OPSOMMING

Die wegdoening van PTFE skroot skep tans 'n wêreldwye probleem vanuit beide 'n ekologiese en koste-oogpunt. Hierdie ondersoek is uitgevoer om die probleem aan te spreek sowel as om die meganisme te verstaan waarvolgens PTFE gedepolimeriseer word om die volgende produkte te vorm: C_2F_4 , C_2F_6 , C_3F_6 , C_3F_8 and $c-C_4F_8$.

Verskillende konseptuele reaktore is ontwerp en gebou vir die uitvoer van verskillende toetse op gevulde en ongefulde PTFE. Hierdie reaktore het die volgende ingesluit: 'n laboratoriumskaal Roterende-oond Reaktor om die depolimeriseringseienskappe van PTFE in 'n horisontale reaktor te toets, 'n Vertikale Reaktor (eng. Drop-tube Reactor) vir die depolimerisering van ongefulde PTFE op 'n kontinue grondslag, 'n Pedaalreaktor (eng. Paddle Reactor) vir die depolimerisering van gevulde sowel as ongefulde PTFE op 'n kontinue grondslag en 'n Vibrerende Reaktor vir die evaluering van ander fluoropolimere soos THV, HTE, ETFE en PFA. Analitiese tegnieke soos GC, GC/MS, TGA en SEM is gebruik om verskillende PTFE monsters te evalueer en om die gasprodukte vanaf die depolimeriseringsproses te analiseer.

'n Mekanisme waarvolgens die depolimerisasie van PTFE en opvolgende produkvorming plaasvind is voorgestel op grond van eksperimentele data ingewin vanaf 'n PTFE depolimeriseringstelsel deur gebruik te maak van verskillende analitiese tegnieke, wat 'n termodinamiese studie, 'n kinetiese studie en molekulêre modellering insluit.

Vir die produkvorming is 'n twee-roete meganisme voorgestel. Roete 1 domineer by temperature $< 700\text{ }^\circ\text{C}$, en hoofsaaklik C_2F_4 , C_3F_6 en $c-C_4F_8$ word geproduseer. Roete 2 domineer by temperature tussen 700 en $900\text{ }^\circ\text{C}$ en hoofsaaklik C_2F_4 , C_2F_6 , C_3F_6 , C_3F_8 , PFIB en $c-C_4F_8$ word geproduseer.

Die termodinamiese studie en molekulêre modellering is gebruik om moontlike produkformingsvergelykings te evalueer en sodoende 'n goeie wetenskaplike voorstel te maak vir die Roete 1 en 2 meganismes.

Na 'n kinetiese studie is gevind dat die orde van die depolimeriseringsreaksie 0.54 is, en dat die reaksie teen 'n tempo van $4.03 \times 10^{-3} \text{ s}^{-1}$ by $600 \text{ }^\circ\text{C}$ plaasvind. Die aktiveringsenergie is as $260 \text{ kJ}\cdot\text{mol}^{-1}$ bereken.

'n Roterende-oond aanleg vir die depolimerisering van PTFE op 'n kommersiële skaal met die doel om C_3F_6 te vervaardig, is ontwerp. 'n Ekonomiese analise het getoon dat 'n depolimeriseringsaanleg wat $500 \text{ kg}\cdot\text{h}^{-1}$ gevulde PTFE kan hanteer en HFP teen R55 per kg verkoop, hoogs winsgewend is.

LIST OF PUBLICATIONS

The following is a list of patents and publications by the author:

Publications

1. I. J. Van Der Walt, O. S. L. Bruinsma, *Depolymerization of clean unfilled PTFE waste in a continuous process*, Journal of Applied Polymer Science, Vol. 102, 3, 2752 – 2759 (2006).
2. Van der Walt, I. J., Investigation into depolymerisation of PTFE waste into TFE as a main product, University of Witwatersrand, M.Sc., 2002.
3. Van der Walt I. J., *Die Depolimerisasie van PTFE om TFE en HFP as hoofprodukte te vorm*, S.A. Tydskrif vir Natuurwetenskap en Tegnologie, Vol 4, 2004.

Patents

1. Van der Walt I. J., Nel J. T., Grunenberg A. T., *Depolymerization of Fluoropolymers*, PCT application PCT/IB2006/054414, 2006.
2. Van der Walt I. J., Conversion of solid fluorine and carbon containing materials to useful products – No2, Patent No PCT/IB01/00158, 2002.

Conferences

1. Van der Walt I. J., *The Depolymerisation of Polytetrafluoroethylene (PTFE) Waste With a Continuous Process*, SACEC 2006, Durban, September 2006.
2. Van der Walt I. J., *Die depolimerisasie van PTFE*, Chemie Simposium vir die Suid Afrikaanse Akademie vir Wetenskaplike en Kuns, University of Stellenbosch, Nov. 2004.

Publications submitted or in progress

1. Izak J. van der Walt, Cornelia G. C. E. van Sittert, *A Mechanistic Study of the Depolymerisation of Polytetrafluoroethylene using Molecule Modelling.* (Publication in writing, to be submitted to Journal of Fluorine Chemistry)
2. I. J. Van der Walt, A. T. Grunenburg, J. T. Nel, and O. S. L. Bruinsma, G. G. Maluleke, *The Continuous Depolymerisation of Filled Polytetrafluoroethylene (PTFE).* (Accepted for publication by the Journal of Applied Polymer Science, August 2007)

CONTENTS

	Page
Dedication	ii
Acknowledgements	iii
Abstract	iv
Opsomming	vi
List of Publications	viii
Contents	x
List of Abbreviations	xvii
List of Symbols and Units	xix
List of Chemical Formulas	xx
List of Figures	xxii
List of Tables	xxvi
Chapter 1	
Introduction and Literature Study Regarding the Depolymerisation of Fluoropolymers	
1.1. Introduction and problem statement	2
1.2. Literature review on fluoropolymers	5
1.2.1. The fluorine radical	5
1.2.2. The C-F bond	5
1.2.3. The monomer tetrafluoroethylene (TFE)	5
1.2.4. The polymer polytetrafluoroethylene (PTFE)	8
1.2.4.1. The properties of PTFE	6
1.2.4.2. The manufacturing of PTFE and other fluoropolymers	10
1.2.4.3. Filled PTFE	11
1.3. Market information	12
1.4. The depolymerisation of PTFE waste	13
1.4.1. Considerations for the depolymerisation of PTFE waste	14
1.4.2. Depolymerisation methods	15
1.4.3. Chemical reaction mechanisms proposed in the literature for the depolymerisation of PTFE	17
1.5. Main conclusions from the literature study and the market review	20
1.6. The opportunity	20

INDEX (CONTINUE)

Chapter 2	Purpose and Scope of this Study	
2.1.	Introduction	23
2.2.	The purpose and scope of this study	23
2.3.	The structure of this thesis	25
2.4.	Main objectives of this study	28
Chapter 3	General Description of the Equipment and Analytical Methods Used in this Study	
3.1.	The depolymerisation reactors	30
3.1.1.	Introduction	30
3.1.2.	The Drop-tube Reactor	31
3.1.3.	The Laboratory Rotating-kiln Reactor	33
3.1.4.	The Paddle Reactor	34
3.1.5.	The Vibrating Reactor	37
3.2.	Analytical Methods	38
3.2.1.	Introduction	38
3.2.2.	Gas Chromatography	38
3.2.3.	Gas Chromatography/Mass Spectrometry (GC/MS)	41
3.2.4.	Thermogravimetric analysis (TGA)	43
3.2.5.	Scanning electron microscopy (SEM)	45
3.3.	Conclusions	48
Chapter 4	The Depolymerisation of Unfilled PTFE in a Drop-Tube Reactor	
4.1.	Introduction	50
4.2.	Description of the depolymerisation equipment	50
4.2.1.	Experimental setup	50
4.2.2.	The process	51
4.2.3.	The continuous feeding system	51
4.2.4.	The Drop-tube Reactor	53

INDEX (CONTINUE)

4.2.5. The quench probe	53
4.2.6. The vacuum system	54
4.3. Experimental method	54
4.4. Results and discussion	55
4.4.1. The formation of TFE	58
4.4.2. The formation of HFP	60
4.4.3. The formation of OFCB	61
4.4.4. The formation of HFE	62
4.4.5. The formation of other products	63
4.4.6. Local maxima for the main products TFE, HFE, HFP and OFCB	63
4.5. Conclusions	65
Chapter 5	A Chemical Mechanism for Depolymerisation Product Formation
5.1. Introduction	67
5.2. The proposed reaction mechanism	68
5.2.1. Route 1 (T = 600 to 700 °C)	69
5.2.2. Route 2 (T > 700 °C)	70
5.3. Conclusions	73
Chapter 6	Equilibrium Composition of PTFE Depolymerisation Product Mixture: A Thermodynamic Approach
6.1. General introduction	75
6.2. General background of chemical thermodynamics	75
6.3. Methodology and species selection	79
6.4. Equilibrium composition of depolymerisation species	80
6.5. Evaluation of the proposed Routes 1 and 2 reaction equations	
using experimental data and ΔG° values	83
6.5.1. Background	83
6.5.2. Proposed reactions and calculated ΔG values at 600 and 900°C	83
6.5.3. Discussion	85

INDEX (CONTINUE)

6.6. Conclusions	87
Chapter 7	Molecular Modelling of PTFE Depolymerisation
7.1. Introduction	90
7.2. Molecular modelling	90
7.2.1. Molecular modelling background	90
7.2.2. Methodology	92
7.3. Modelling of the intermediates and products in PTFE depolymerisation	94
7.3.1. The intermediate species	95
7.3.2. The transition state molecules	100
7.3.3. The products	106
7.4. Discussion of the reactions in the two routes of the depolymerisation process	108
7.4.1. Route 1 of the proposed mechanism	109
7.4.2. Route 2 of the proposed mechanism	113
7.5. Conclusions	124
Chapter 8	A Thermogravimetric Investigation of the Kinetics of PTFE Depolymerisation
8.1. Introduction	126
8.2. Theory	126
8.3. Experimental method	128
8.4. Results and discussion	129
8.5. Conclusions	135
Chapter 9	The Characterisation of PTFE Feed Material Before and During Depolymerisation
9.1. Introduction	137

INDEX (CONTINUE)

9.2. Polymer characterisation	138
9.2.1. Feed material	139
9.2.2. Thermogravimetric analysis of different fluoropolymers	139
9.2.3. Thermogravimetric analysis of filled PTFE	142
9.2.4. SEM/EDX analysis of the filler material	143
9.3. <i>In situ</i> ESEM observation of filled PTFE during depolymerisation	145
9.4. Visual observation of the effect of hot PTFE on reactor walls	148
9.5. The residence time of unfilled and filled PTFE in the Paddle Reactor	149
9.5.1. Introduction	149
9.5.2. Experimental procedure	150
9.5.3. Results and discussion	150
9.6. Conclusions	155

Chapter 10 The Depolymerisation of Unfilled and Filled PTFE in a Paddle Reactor

10.1. Introduction	158
10.2. Experimental method	158
10.3. Results and discussion	160
10.3.1. Depolymerisation efficiency of the Paddle Reactor	160
10.3.2. Analyses of the depolymerisation products	161
10.4. Conclusions	169

Chapter 11 Continuous Conversion of Other Fluoropolymer Waste in a Vibrating Reactor

11.1. Introduction	172
11.2. Experimental method	173
11.3. Results and discussion	174
11.3.1. The production of fluorochemicals by the depolymerisation of unfilled and filled PTFE	174

INDEX (CONTINUE)

11.3.2.	The production of fluorochemicals by the depolymerisation of PFA	176
11.3.3.	The production of fluorochemicals by the depolymerisation of FEP	177
11.3.4.	The production of fluorochemicals by the depolymerisation of THV	181
11.3.5.	The production of fluorochemicals by the depolymerisation of ETFE and HTE	182
11.4.	Conclusions	183

Chapter 12 Design of a Depolymerisation Plant for Filled PTFE to Produce HFP

12.1.	Introduction	186
12.2.	Process description	187
12.2.1.	The feed preparation section	187
12.2.2.	The kiln reactor section	187
12.2.3.	The separation section	189
12.2.4.	The gas waste destruction section	190
12.3.	Conceptual design of the HFP plant	190
12.3.1.	The feed material	191
12.3.2.	The products	191
12.3.3.	Determination of the production capacity	192
12.3.4.	Mass balance	192
12.3.5.	Reactor design	194
12.4.	The techno-economy of the process	196
12.5.	Conclusions	200

Chapter 13	Conclusions	201
-------------------	--------------------	-----

References	207
-------------------	-----

Appendix 1	General Calculations	213
-------------------	-----------------------------	-----

Appendix 2	Computer Program Methodology	220
Appendix 3	Evaluation of the Depolymerisation Product Formation Reactions	239
Appendix 4	Residence Time Graphs	247
Appendix 5	Estimated Piloting Costs	255

LIST OF ABBREVIATIONS

Abbreviation	Explanation
CD	Compact Disk
CF	Fluorocarbon
C _x F _y	Fluorocarbon
DFT	Density Functional Theory
ESEM	Environmental Scanning Electron Microscope
EDX	Energy Dispersive X-ray Spectrometer
ETFE	Ethylene-Tetrafluoroethylene copolymer
F/C	Fluorine/Carbon ratio
FEP	Fluorinated-Ethylene-Propylene
FID	Flame Ionisation Detector
GC	Gas chromatograph
GC/MS	Gas Chromatograph/Mass Spectrometer
HFE	Hexafluoroethane
HOMO	Highest Occupied Molecular Orbital
HFP	Hexafluoropropylene
HP	Hewlett Packard
HTE	Hexafluoropropylene-Tetrafluoroethylene-Ethylene copolymer
IRR	Internal Rate of Return
MNDO	Modified Neglect of Differential Overlap
MS	Mass spectrometer
NA	Not Available
ND	Not Detected
NPV	Nett Present Value
OFCB	Octafluorocyclobutane
OFB	Octafluorobutene
OFFP	Octafluoropropane
pa	Per annum
PE	Polyethylene

PFA	Perfluoroalcoxy
PFIB	Perfluoroisobutylene
PM3	Parameterising of MNDO version 3
PTFE	Polytetrafluoroethylene
R22	Freon 22
RF	Radio frequency
RHF	Restricted Hartree-Fock model
SEM	Scanning Electron Microscope
THV	Tetrafluoroethylene-Hexafluoropropylene- Vinilidinefluoride
tpa	tons per annum
TG	Thermogravimetry
TGA	Thermogravimetric analysis
TCD	Thermal conductivity detector
TG/MS	Thermogravimetric/Mass spectrometer
TFE	Tetrafluoroethylene
TFM	Tetrafluoromethane
UHF	Unrestricted Hartree-Fock
USD	United States Dollar
U.S	United States
USA	United States of America

LIST OF SYMBOLS AND UNITS

Symbol	Description	Unit
a	Activity	f/f^0
B	Kinetic constant	-
D	Diameter	m
E_{act}	Activation energy	$\text{kJ}\cdot\text{mol}^{-1}$
f	Fugacity	bar
G	Gibbs free energy	$\text{kJ}\cdot\text{mol}^{-1}$
G°	Standard Gibbs free energy	$\text{kJ}\cdot\text{mol}^{-1}$
H_f	Formation enthalpy	$\text{kJ}\cdot\text{mol}^{-1}$
H_f^\ddagger	Transition state formation energy	$\text{kJ}\cdot\text{mol}^{-1}$
H	Enthalpy	$\text{kJ}\cdot\text{mol}^{-1}$
k	Reaction constants	s^{-1}
K	Temperature	Kelvin
k_0	Reaction rate at 0 Kelvin	s^{-1}
n	Reaction order	-
P	Pressure	kPa
R	Universal gas constant	$\text{J}\cdot\text{K}^{-1}\cdot\text{mol}^{-1}$
t	Time	Second
T	Temperature	$^\circ\text{C}$
T_{ref}	Reference temperature	$^\circ\text{C}$
V	Volume	m^3
λ	Thermal conductivity	$\text{W}\cdot\text{m}^{-1}\cdot\text{K}^{-1}$
α	Alpha	Orbitals
β	Beta	Orbitals
ρ_{gas}	Gas density	$\text{kg}\cdot\text{m}^{-3}$
τ	Solid residence time	sec
τ_{gas}	Gas residence time	sec

LIST OF CHEMICAL FORMULAS

Chemical formula	Abbreviation	Chemical name
$\text{CF}_2^{\bullet\bullet}$	Radical	Difluorocarbene
$\sim\text{CF}_2^{\bullet}$	Radical	PTFE radical
CF_3^{\bullet}	Radical	Trifluorocarbene
CF_4	TFM	Tetrafluoromethane
$\text{C}_2\text{F}_2^{\bullet\bullet}$	Radical	Difluoroethene
C_2F_2		Difluoroethyne
C_2F_4	TFE	Tetrafluoroethylene
$\text{C}_2\text{F}_4^{\bullet\bullet}$, $\text{CF}_2\text{-CF}_2^{\bullet\bullet}$	Radical	Tetrafluoroethane
C_2F_6	HFE	Hexafluoroethane
C_3F_6	HFP	Hexafluoropropylene
C_3F_8	OFFP	Octafluoropropane
$\text{c-C}_4\text{F}_8$	OFCB	Octafluorocyclobutane
C_4F_8	OFB	Octafluorobutene
$\text{C}_8\text{F}_{17}^{\bullet}$	Radical	C8 fluoropolymer fragment
$\text{C}_{10}\text{F}_{21}^{\bullet\bullet}$	Radical	C10 fluoropolymer fragment
$\text{C}_{10}\text{F}_{22}$		C10 fluoropolymer
$\text{C}_{20}\text{F}_{42}$		C20 fluoropolymer
$\text{C}_{40}\text{F}_{82}$		C40 fluoropolymer
$\text{C}_{80}\text{F}_{162}$		C80 fluoropolymer
C_6H_6		Benzene
CO		Carbon monoxide
CO ₂		Carbon dioxide
ETFE		Ethylene-Tetrafluoroethylene copolymer
F	Atom	Fluorine atom
FEP		Fluorinated-Ethylene-Propylene
HF		Hydrofluoric acid
HTE		Hexafluoropropylene-Tetrafluoroethylene-Ethylene copolymer
KOH		Potassium hydroxide

NOx		Nitrogen oxides
PTFE		Polytetrafluoroethylene
PFA		Perfluoroalcoxy
THV		Tetrafluoroethylene-Hexafluoropropylene- Vinilidene fluoride

LIST OF FIGURES

	PAGE
Figure 2.1: Schematic presentation of the structure of the thesis	26
Figure 3.1: The Drop-tube depolymerisation Reactor	31
Figure 3.2: Schematic presentation of a set-up used to visually observe the depolymerisation of PTFE in a rotating reactor	33
Figure 3.3a: Paddle Reactor operated by a technician	35
Figure 3.3b: The Paddle Reactor system that was used for the continuous depolymerisation of filled PTFE	36
Figure 3.4: Vibrating Reactor	37
Figure 3.5: A chromatogram of the specially prepared standard that was used in this study to calibrate the GC	39
Figure 3.6: The main components of a mass spectrometer	42
Figure 3.7: The mass spectrum of OFCB	43
Figure 3.8: A thermogram of the filler content determination and depolymerisation temperature of graphite-filled PTFE	45
Figure 3.9: EDX analysis of glass fibre-filler	47
Figure 3.10: A SEM image of glass fibre-filler after depolymerisation	47
Figure 4.1: Schematic presentation of the Drop-tube system	50
Figure 4.2: Granulated PTFE particles (Units in cm)	52
Figure 4.3: Schematic presentation of the PTFE feed system	52
Figure 4.4: Schematic diagram of the quench probe	54
Figure 4.5: Concentration of TFE formed as a function of temperature and pressure	59
Figure 4.6: Concentration of HFP formed as a function of temperature and pressure	60
Figure 4.7: Concentration of OFCB formed as a function of temperature and pressure	61
Figure 4.8: Concentration of HFE formed as a function of temperature and pressure	62

LIST OF FIGURES (CONTINUE)	PAGE
Figure 6.1: Equilibrium concentration at 700 °C (All fluorocarbon species included)	81
Figure 6.2: Equilibrium concentration at 100 kPa (All fluorocarbon species included)	82
Figure 7.1: A geometrically optimised HFP molecule	91
Figure 7.2: Different stereo isomeric structures of C ₆ H ₆	93
Figure 7.3a: C ₂ F ₄ Molecule	97
Figure 7.3b: C ₂ F ₄ •• Radical	97
Figure 7.4a: CF ₂ •• Singlet	98
Figure 7.4b: CF ₂ •• Triplet	98
Figure 7.5: CF ₃ • Radical	99
Figure 7.6a: C ₂ F ₂ Singlet molecule	100
Figure 7.6b: C ₂ F ₂ •• <i>Cis</i> triplet radical	100
Figure 7.6c: C ₂ F ₂ •• <i>Trans</i> triplet radical	100
Figure 7.7: Visual presentation of the transition state for HFP formation	101
Figure 7.8a: An exothermic energy diagram of HFP formation with a transition state	102
Figure 7.8b: A typical endothermic energy diagram with a transition state	102
Figure 7.8c: A typical exothermic energy diagram without a transition state	102
Figure 7.8d: A typical endothermic energy diagram without a transition state	102
Figure 7.9: Electron movement with HFP formation	103
Figure 7.10: PTFE and CF ₂ transition state species	103
Figure 7.11: TFE Molecule	106
Figure 7.12: HFE Molecule	106
Figure 7.13: HFP Molecule	106
Figure 7.14: OFP Molecule	106
Figure 7.15: OFCB Molecule	106
Figure 7.16: C ₁₀ F ₂₂	106
Figure 7.17: Lengths of C-C bonds of a PTFE radical in Å	108

LIST OF FIGURES (CONTINUE)	PAGE
Figure 7.18: Mechanistic presentation of Route 1	109
Figure 7.19: The enthalpy level diagram of Route 1	111
Figure 7.20: Simplified final reaction scheme	113
Figure 7.21: Mechanistic presentation of Route 2	114
Figure 7.22: Enthalpy profile for the high-temperature sub-mechanism	117
Figure 7.23: Summary of Route 2 of the depolymerisation mechanism	122
Figure 8.1: Isothermal mass loss of PTFE	129
Figure 8.2: A plot of $-\ln(dx/dt)$ vs $\ln(x)$ at different temperatures	130
Figure 8.3: Arrhenius plot of $\ln(k)$ vs $1/T$	133
Figure 8.4: Experimental data vs simulated data (bold curve) at 550 °C, $k=7.82 \times 10^{-4} \text{ s}^{-1}$, $n=0.54$	134
Figure 9.1: Granulated unfilled and graphite-, bronze-, and glass fibre-filled PTFE	139
Figure 9.2: Thermograms of THV, ETFE, PFA and graphite-filled PTFE (heating rate = 5 °C·min ⁻¹)	140
Figure 9.3: Thermogravimetric curves of different filled PTFE samples	142
Figure 9.4a: SEM image of glass fibre filler	144
Figure 9.4b: SEM image of bronze filler	144
Figure 9.4c: SEM image of graphite filler	145
Figure 9.5: Cold PTFE	146
Figure 9.6: PTFE starts to swell	146
Figure 9.7: Surface depolymerisation	146
Figure 9.8: Core of particle melts	146
Figure 9.9: Bottom PTFE boils	147
Figure 9.10: More particles boil	147
Figure 9.11: Particles melts together	147
Figure 9.12: Molten mass boils	147
Figure 9.13: Process continues	147
Figure 9.14: Volume decreased	147

LIST OF FIGURES (CONTINUE)	PAGE
Figure 9.15: Photo of depolymerising PTFE inside the laboratory size, manually turned, Rotating-kiln Reactor (through 45 °) at 400 °C	148
Figure 9.16: Residence time and residence time distribution of unfilled PTFE in the Paddle Reactor	151
Figure 9.17: Residence time of different filled PTFE samples at different reactor angles as a function of paddle rotation speed	153
Figure 9.18: Residence time of unfilled PTFE as a function of paddle rotation speed and reactor angle	154
Figure 10.1: A schematic presentation of the depolymerisation Paddle Reactor and the feed and discharge system	159
Figure 10.2: TFM concentration as produced by the Paddle Reactor	162
Figure 10.3: HFE concentration as produced by Paddle Reactor	163
Figure 10.4: TFE concentration as produced by the Paddle Reactor	164
Figure 10.5: OFP concentration as produced by the Paddle Reactor	165
Figure 10.6: HFP concentration as produced by the Paddle Reactor	166
Figure 10.7: OFCB concentration as produced by the Paddle Reactor	167
Figure 10.8: PFIB concentration as produced by the Paddle Reactor	168
Figure 11.1: A Vibrating Reactor that was used to depolymerise different fluoropolymers	173
Figure 11.2: The TFE yield from FEP depolymerisation	179
Figure 11.3: The HFP yield from FEP depolymerisation	180
Figure 11.4: The OFCB yield from FEP depolymerisation	181
Figure 12.1: Schematic presentation of the PTFE depolymerisation system for filled PTFE	188
Figure 12.2: Depolymerisation product separation facility to purify HFP	190
Figure 12.3: The flow-sheet with recycled streams of a HFP plant	193
Figure 12.4: Sensitivity analysis for the IRR	199
Figure 12.5: Sensitivity analysis for the NPV over a 5 year period	199

LIST OF TABLES

	PAGE
Table 1.1: Fluorochemical species and their structures	7
Table 1.2: A comparison of the physical properties of PTFE and PE	9
Table 1.3: Some properties of filled PTFE	11
Table 1.4: Market value of fluorochemicals (2004)	13
Table 3.1: Repeatability and precision of depolymerisation data at 600 °C and 5 kPa	32
Table 3.2: Calibration results of the GC for the specially prepared standard	41
Table 4.1: Typical experimental parameters for the depolymerisation of unfilled PTFE in the Drop-Tube Reactor	55
Table 4.2: Product gas composition at ca. 600 °C and increasing pressure as determined by GC (Vol %)	56
Table 4.3: Product gas composition at ca. 700 °C and increasing pressure as determined by GC (Vol %)	56
Table 4.4: Product gas composition at ca. 800 °C and increasing pressure as determined by GC (Vol %)	57
Table 4.5: Product gas composition at ca. 900 °C and increasing pressure as determined by GC (Vol %)	57
Table 4.6: Local yield maxima	63
Table 6.1: CF compounds in the HSC5.1 database.	79
Table 6.2: The ΔG° values calculated by HSC5.1 for different reactions at 600 to 900°C	84
Table 6.3: Route 1 reactions at 600 and 700 °C	85
Table 6.4: Route 2 reactions at 800 and 900 °C	86
Table 6.5: Route 1 reactions at 600 to 700 °C	88
Table 6.6: Route 2 reactions at 700 to 900 °C	88
Table 7.1: Comparison of modelled ΔH_f with published values	95

LIST OF TABLES (CONTINUE)	PAGE
Table 7.2: The intermediate species and their formation energies as calculated by molecular modelling	96
Table 7.3: Reaction enthalpies of reactions without activation energies or transition state molecules	104
Table 7.4: Activation energies of reactions with transition state molecules	105
Table 7.5: Formation enthalpies of stable molecules	107
Table 7.6: Enthalpy profile data of Route 1	111
Table 7.7: Formation enthalpy evaluation of fluorine transfer to CF ₂ ^{••}	116
Table 7.8: Enthalpy profile data of Route 2	118
Table 8.1: The n (order of reaction) values for the different temperatures	131
Table 8.2: The k values as calculated over a temperature range of 500 to 620 °C	132
Table 9.1: Chemical structure of the different fluoropolymers	141
Table 9.2: Amount of filler material in filled PTFE samples	143
Table 9.3: Residence time of filled and unfilled PTFE samples in the Paddle Reactor under varying conditions	152
Table 10.1: Solid residue originating from filled and unfilled PTFE, collected after depolymerisation	160
Table 10.2: The GC analyses of the product gas after depolymerisation of graphite-filled PTFE in the Paddle Reactor (Vol %)	161
Table 11.1: Product composition after depolymerisation of unfilled and filled PTFE in the Vibrating Reactor	175
Table 11.2: Results obtained during the depolymerisation of PFA	176
Table 11.3: Products from the depolymerisation of FEP	177
Table 11.4: Results obtained during the depolymerisation of THV	182

Chapter 1

Introduction and literature study regarding the depolymerisation of fluoropolymers

- 1.1. Introduction and problem statement
- 1.2. Literature review on fluoropolymers
 - 1.2.1. The fluorine radical
 - 1.2.2. The C-F bond
 - 1.2.3. The monomer tetrafluoroethylene (TFE)
 - 1.2.4. The polymer polytetrafluoroethylene (PTFE)
 - 1.2.4.1. The properties of PTFE
 - 1.2.4.2. The manufacturing of PTFE and other fluoropolymers
 - 1.2.4.3. Filled PTFE
- 1.3. Market information
- 1.4. The Depolymerisation of PTFE waste
 - 1.4.1. Considerations for the depolymerisation of PTFE waste
 - 1.4.2. Depolymerisation methods
 - 1.4.3. Chemical reaction mechanisms proposed in the literature for the depolymerisation of PTFE
- 1.5. Main conclusions from the literature study and the market review
- 1.6. The opportunity



1.1 INTRODUCTION AND PROBLEM STATEMENT

Life in the previous and twenty first century was and is dominated by technological innovation. Regarding the great inventions and technological progress of the twentieth century, for example: nuclear science across its whole impressive spectrum, space travel, medical advances such as organ transplant breakthroughs, the unravelling of the human genetic code, etc.; these inventions have also invaded our homes, even in the kitchen. A very good example in this regard that springs to mind is non-stick cookware like pots and pans.

Many polymers have been developed, but the real stars in the polymer constellation are the fluorinated variety like polytetrafluoroethylene (PTFE). The success of non-stick cookware is directly attributable to the development to fluoropolymers, especially PTFE. This polymer has one building block, the monomer tetrafluoroethylene (TFE). By linking together TFE building blocks into enormous chains, a very high-molecular-mass polymer is formed, a process that was accidentally discovered by a scientist named Plunkett in 1948 when he did some experiments with TFE.⁽¹⁾ Since then, the synthesis of PTFE, its physical and chemical characteristics, its very diverse application spectrum, etc., have been exhaustively studied in the past.⁽¹⁻⁷⁾ It was especially found that three or four properties of PTFE make it a very valuable and sought-after material. Some of these properties are the following^(6, 7):

- PTFE is chemically inert;
- It exhibits relatively good thermal stability;
- The lubricity of PTFE is exceptional;
- Another very good characteristic of PTFE is its water repellence.

However the main desirable property of PTFE, namely its chemical inertness, also poses an enormous problem with regards to the safe and economic disposal of PTFE.⁽⁷⁻¹⁰⁾ Up to the present, incineration was virtually the only viable disposal method other than expensive and space-consuming landfilling. During the incineration of PTFE very toxic by-products like perfluoroisobutylene (PFIB) might

form under undesirable conditions,⁽¹¹⁻¹⁶⁾ with the result that this waste disposal method is ecologically seriously frowned upon.

During the mechanical manufacturing of PTFE components, more than normal quantities of waste are generated because of its non-melt-processibility. In contrast to other polymers this waste can not be recycled. Manufacturers therefore either have to landfill or store the waste PTFE. It goes without saying that the PTFE industry would seriously welcome the development of a viable waste disposal or treatment method. The disposal problem is exacerbated when the PTFE is filled with various substances like carbon, glass fibre, bronze or molybdenum disulfide particles to preferentially enhance properties like improved creep resistance, increased hardness, better abrasion properties, etc.

A further factor which must not be ignored is that one of the building blocks of PTFE is fluorine, which is quite expensive. The recovery of the fluorine-values, in whatever useable form, is therefore also an important consideration.

Necsa embarked on the manufacturing of high value, highly sought after fluoro-chemical compounds for several years now.⁽¹⁷⁾ These include inorganic (WF_6 , SF_6 , NF_3 , ClF_3 , etc.) as well as organic fluorochemical compounds like (CF_4 , TFE, HFP and OFCB, etc.). HFP for example, is used as an intermediate product to manufacture even more lucrative downstream products like HFPO. This product finds application in speciality low-temperature polymers⁽¹⁸⁾ and OFCB as an etching gas in the silicon industry.⁽¹⁹⁾ Apart from the fact that TFE is, as already mentioned, the basic building block for the manufacturing of PTFE, it can also be converted to HFP, or used directly as a feedstock for the production of other speciality fluorochemicals. TFE however has one main disadvantage, namely that it is a highly unstable and explosive gas which makes the transportation and storage thereof nearly impossible from a safety point of view.⁽²⁰⁾ This forces the manufactures of fluoropolymers and organic fluorochemicals that use TFE in their production processes, to synthesise it in-house and on-site, or use other more stable fluorochemical compounds as intermediate product. One such compound is HFP and is generally being referred to in the fluorochemical industry as "transportable TFE".⁽²¹⁾

An example of the value-added chain, using PTFE as starting material through intermediate products like TFE and HFP, is given below:

PTFE → TFE → HFP → HFPO → Final product

In previous studies⁽²²⁻²⁴⁾ it was found that the depolymerisation of PTFE led to products like TFE, HFP, and OFCB, in various quantities:

PTFE → TFE + HFP + OFCB

This process was exploited by Necsca on commercial scale, but under sub-optimal conditions, whereby clean and unfilled PTFE was depolymerised to give a product mixture of TFE, HFP and OFCB. Subsequently this product mixture has to be separated and purified by a laborious cryogenic distillation processes, putting strain on the economic viability of the whole process.

Necsca mainly used clean and unfilled PTFE in a semi-continuous process. Clean and unfilled PTFE left no residue after polymerisation as all the PTFE is converted into gaseous products. This process was conducted in a drop tube reactor where the to-be-decomposed PTFE was fed vertically through a tube into a crucible which was held at the desired temperature where the depolymerisation took place. Hence the name "Drop-tube Reactor". However, waste PTFE that can be used as feedstock, is also available with filler material which is incorporated in the PTFE to enhance certain physical properties of PTFE e.g. mechanical strength and creep resistance.^(6,7) The use of filled PTFE as a feedstock in the Necsca process was unfortunately not possible as the un-decomposed filler material will be left as a residue at the bottom of the reactor, the reactor will eventually be filled up with these residues and will block the whole system.

Therefore, to conclude, the handling of PTFE waste and especially filled PTFE, poses a huge problem which has to be addressed by the manufactures and processors of PTFE.

1.2 LITERATURE REVIEW ON FLUOROPOLYMERS

As mentioned in Section 1.1, PTFE occupies a unique position in the polymer and related industries due to its exceptional properties. This polymer is manufactured via the polymerisation of the TFE monomer.⁽¹⁻⁷⁾ Thus, although the manufacturing and application of both TFE and PTFE have been exhaustively addressed in literature and industry, there is a shortage of information and experience regarding the destruction of both unfilled and filled PTFE. One of the purposes of this study is to bridge this knowledge gap.

1.2.1 The fluorine radical

Fluorine occurs widely in nature as CaF_2 and is more abundant than chlorine. The great reactivity of F_2 can be contributed to the low dissociation energy of the F-F bond. This is probably because of the strong repulsion of the nonbonding electrons.⁽²⁵⁻²⁷⁾ The fluorine electronic structure is $1s^2 2p^5$ with one unpaired electron in the outer shell, which also explains the high reactivity. This is typical of radicals.⁽²⁸⁾ The existence and contribution of the fluorine atom in the fluorocarbon formation is addressed by Moore.⁽²⁹⁾

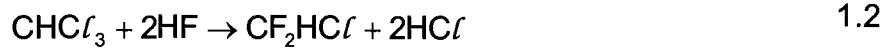
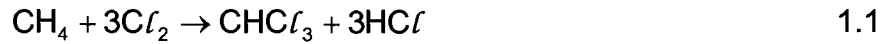
1.2.2 The C-F bond

Although the C-H bond is well known and forms the basis of organic chemistry, much less, as can be expected is known about the C-F bond. The C-H bond energy is $413 \text{ kJ}\cdot\text{mol}^{-1}$, which is smaller than the $484 \text{ kJ}\cdot\text{mol}^{-1}$ bond energy of the C-F bond. The high electron affinity of fluorine is the reason why it reacts with an exothermic reaction with carbon.⁽²⁷⁾

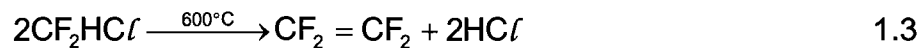
1.2.3 The monomer tetrafluoroethylene (TFE)

At present the TFE monomer is manufactured commercially via thermal decomposition of the freon, chlorodifluoromethane (CF_2HCl) at high temperatures.⁽²⁾ The compound CF_2HCl is also commercially known as R22. This process firstly

involves the manufacturing of R22 by hydrogen substitution of methane with chlorine and then partial fluorination of trichloromethane with hydrofluoric acid, as presented in the reactions below:



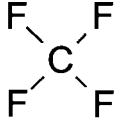
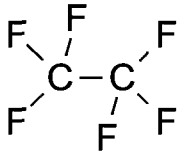
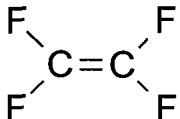
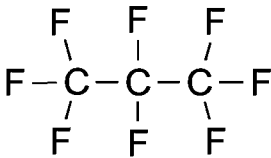
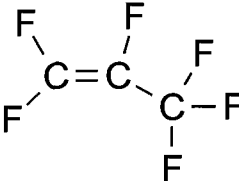
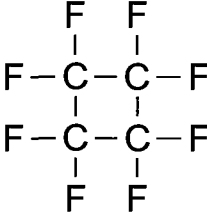
R22 is then continuously fed into a high-temperature reactor at 600 °C to form TFE as main product:



The partial pressure of R22 can be decreased by the addition of steam. Lower partial pressures increase the TFE yield in the above-mentioned reaction scheme. R22 that is not converted to TFE has to be separated from the steam and TFE and recycled back into the reactor. The waste stream contains a low concentration of HCl after pyrolysis inside the reactor. This must be collected and neutralised and generates a waste problem. The R22 route is not a very efficient method. However, this method has been performed safely for many years. The gaseous product that is formed consists of a mixture of TFE, hexafluoropropylene (HFP) and octafluorocyclobutane (OFCB), with TFE as the main product. Separation is needed in order to increase the concentration of TFE. When HFP is needed as the main product, the process parameters are changed and subsequently the TFE yield decreases. The disadvantages of this method are: the production of HCl as a by-product and the low conversion (~20 %) of R22 into products, requiring a large recycle stream.

The monomers are also used for the manufacturing of an increasing number of chemical products such as low-temperature compounds, highly inert oils and some are used as etching agents in the silicon industry. Some of the fluorochemicals and their structures are presented in Table 1.1.

Table 1.1: Fluorochemical species and their structures

Name	Abbreviation	Empirical formula	Structure
Tetrafluoromethane	TFM	CF ₄	
Hexafluoroethane	HFE	C ₂ F ₆	
Tetrafluoroethylene	TFE	C ₂ F ₄	
Octafluoropropane	OFP	C ₃ F ₈	
Hexafluoropropylene	HFP	C ₃ F ₆	
Octafluorocyclobutane	OFCB	c-C ₄ F ₈	

Of these products only OFCB is available on the open market. The required purity specification for the electronic industry is between 99.9 and 99.999 %. The HFP product is not available on the open market in industrial quantities, because every manufacturer produces it in-house to satisfy its own demand from which other downstream fluoropolymers can be manufactured. The purity needed is, however, only 99.5 %. The TFE product is also not available on the open market. The dangers accompanying the manufacturing of this product (auto-ignition point at 220 kPa abs. and low tolerance for oxygen), prevent it from being transported safely over long

distances. Thus it is manufactured under controlled conditions and used for polymerisation on the same site. The other products TFM, HFE and OFP are of low value, although used in large quantities in the electronic industry as flushing gases.

Some properties of TFE⁽³⁰⁾ are: it is a colourless, odourless gas with a molecular mass of $100 \text{ g}\cdot\text{mol}^{-1}$, a boiling point of $-76.3 \text{ }^\circ\text{C}$, a freezing point of $-142.5 \text{ }^\circ\text{C}$. TFE is however a very dangerous and explosive gas as mentioned previously. The flammability limits in air at 1 atm are 14 – 43 % by volume.⁽³⁰⁾ TFE is incapable of explosion at atmospheric pressures, but explodes violently as the loading density of a vessel increases. A safe operating pressure for such a vessel is 2.2 bar abs.^(31, 32)

1.2.4 The polymer polytetrafluoroethylene (PTFE)

In 1938 a Du Pont scientist, Roy Plunkett⁽²⁾, discovered the polymer polytetrafluoroethylene (PTFE) when tetrafluoroethylene (TFE) was accidentally polymerised in a cylinder. This polymer was introduced commercially into the world by the company Du Pont as Teflon[®] in 1946. Pictures of PTFE products are presented on the cover page of this chapter.

It was proposed that the polymerisation process proceeds via a free-radical initiation mechanism.⁽³⁻⁷⁾ Free radical initiators like peroxydisulfides and organic peroxides are used.

Two distinctly different polymerisation methods are used for the homopolymerisation of PTFE. In the one process little or no dispersing agent is used. Vigorous agitation produces a granular resin. In the other process, called aqueous-dispersion polymerisation, precipitation of the resin particles is avoided. The granular product can be moulded while the aqueous dispersion can be converted into a powder for paste extrusion.⁽⁵⁾

1.2.4.1 The properties of PTFE

This very versatile solid polymer has an extremely high average molar mass,

(10^6 to 10^7 g·mol⁻¹) and a viscosity of about 10^9 to 10^{11} Pa·s in its molten state at 380 °C. It is a highly crystalline polymer and has a crystalline melting point of 330 °C. Its high thermal stability is due to the strong carbon-fluorine bonds and characterises PTFE as a very useful high-temperature polymer.^(1, 3, 4) A summary of some of the physical properties of PTFE is given in Table 1.2 and is compared to those of polyethylene (PE).

Table 1.2: A comparison of the physical properties of PTFE and PE

Property	PTFE	PE
Density (g·cm ⁻³)	2.2 to 2.3	0.9 to 1.0
Melting point (°C)	342 first and 327 second*	105 to 140
Dielectric constant (at 1 kHz)	2.0	2.3
Dynamic coefficient of friction	4×10^{-2}	3.3×10^{-1}
Surface energy (dyne·cm ⁻¹)	18.0	33.0
Chemical resistance	Excellent. No known solvent	Susceptible to attack by hot hydrocarbons
Thermal degradation temp. (°C)	505	404
E_{act} (kJ·mol ⁻¹)	339	264
Melt viscosity (Pa·s)	10^9 to 10^{11}	-
Refractive index	1.3	1.5
Chain-branching propensity	No	Yes

* The melting point of PTFE changes after being heated for the first time. This is because of the sintering of the polymer at high temperature.

PTFE, with its good chemical, electrical and surface properties was accepted with open arms by the industry. Since then other fluoropolymers were discovered possessing unique properties that only fluoropolymers can provide. Amongst these, several variants of PTFE, as well as a variety of co-polymers with ethylene, vinylidene fluoride, hexafluoropropylene (HFP) as co-monomers, were produced and their uses range from PTFE coatings on cookware to thermally stable components exhibiting excellent operating properties in industrial machinery.

1.2.4.2 The manufacturing of PTFE and other fluoropolymers

Commercially PTFE is manufactured by two different polymerisation techniques that result in two different physical forms of a chemically identical polymer.⁽²⁾ Suspension polymerisation produces a granular resin, whilst emulsion polymerisation produces a coagulated dispersion which is often referred to as a fine powder.

The suspension-polymerised PTFE is usually produced by addition of a coagulant to the TFE after initiation, while emulsion-polymerised PTFE is made via the addition of an emulsification agent. Emulsion-polymerised PTFE behaves entirely differently to suspension-polymerised PTFE because of the difference in physical structure. Coagulated dispersions are processed by a cold extrusion process. Emulsion polymerised PTFE is usually processed according to latex processing techniques.

In 2006, the main manufacturers of PTFE included Daikin Kogyo (Polyflon), Du Pont (Teflon[®]), Hoechst (Hostaflon), ICI (Fluon), Ausimont (Algoflon and Halon), and the CIS (Fluoroplast). The People's Republic of China also manufactures some PTFE products.

The discovery of PTFE was a big step forward for materials science. The fact that PTFE was not melt-processible, as a result of its high viscosity, was one of the only drawbacks. The pursuit for more easily processible polymers with the same properties as PTFE led to the discovery of Fluorinated Ethylene Propylene (FEP) co-polymer, which could be melted in an extruder. When compared to PTFE, the only major disadvantage was that of reduced thermal stability. The Ethylene

Tetrafluoroethylene co-polymer (ETFE) addresses the need for a mechanically stronger polymer. Many of the unique properties of PTFE are lost when co-polymers with different properties are manufactured, but the advantage is that the waste can be recycled by means of melt-processing.^(6, 7)

1.2.4.3 Filled PTFE

In the case of co-polymers, TFE can be mixed with a second or third monomer and polymerised into a polymer with specific properties. Another way to address some of the weaknesses of PTFE is to incorporate a solid filler^(3, 7), producing a polymer that has all the previously mentioned good properties, as well as improved creep resistance, abrasion resistance or other properties. Filled granular PTFE compounds belong to the most significant PTFE commodities because of the large volumes of consumption. Unfilled and filled PTFE can be used for the manufacturing of an increasingly wide variety of products. Table 1.3 summarises some of the advantages and properties of PTFE filled with different fillers.⁽³⁻⁷⁾

Table 1.3: Some properties of filled PTFE

Filler	Additional advantages	Thermal conductivity (Wm·K ⁻¹)
Unfilled PTFE		0.24
Carbon-filled (15%*)	Better abrasion properties, reduces creep, increases hardness and thermal conductivity	0.63
Glass fibre-filled (15 to 40%)	Better creep performance	0.41
Bronze-filled (60%)	Reduces deformation under load and raises the thermal and electrical conductivity.	0.57
Molybdenum disulfide-filled (5%)	Increases hardness while decreasing friction.	NA**

* The (%) designates the typical amount of filler in the PTFE.

** NA = Not Available

1.3 MARKET INFORMATION

The U.S. demand for fluoropolymers in 2002 was estimated at 60 000 tpa, with PTFE accounting for over 40 % of this demand.⁽³³⁾ This would result in an approximate 12 000 tpa PTFE landfill burden in the U.S. alone. World consumption in 2001 was 112 000 tpa.

The *Freedonia*⁽³³⁾ market research report estimates that the global market for fluorochemicals would be worth USD 12.9 billion by 2007. Global trade in the fluorine performance chemicals and polymers excluding the low-molecular-weight polymers is probably 1.5 to 2 times the US merchant market size of approximately USD 4.1 billion. The global trade in low-molecular-mass polymers is probably only 1.2 to 1.5 the size of the U.S. merchant market because U.S. companies such as DuPont and 3M dominate this sector of the market.

The global market for low-molecular mass polymers is approximately USD 600 million. The average growth-rate over the previous five years (1997 to 2002) has been 5 % per year. This is a performance-chemical market and is therefore characterized by a high degree of technical support for customers and also a large research and development support for new compounds and new applications for existing compounds. Du Pont and 3M dominate about 50 % of the global market. A number of relatively large US, European and Japanese companies own a smaller share of the market. Some of them are Dyneon, Imperial Chemical Industries, Daikin and Ausimont.

Whilst growth will continue to be sluggish due to meagre gains in the large fluorocarbon sector, it represents a considerable improvement over the losses registered during the past decade (when the major impact of the chlorofluorocarbon phase-out was felt). In addition, strong growth opportunities are expected in fluoropolymers, especially with respect to newer melt-processible varieties, specialty fluorine gases, such as nitrogen-trifluoride and specialty organic chemicals. Continued downward price-pressure is expected in key markets such as polymers.

The three fluorochemicals which are most abundantly used are TFE, HFP and OFCB. Table 1.4 presents the production cost in 2004 and market values for these products.

Table 1.4: Market value of fluorochemicals (2004)⁽³³⁾

Product	Production cost (USD per kg)	Selling price (USD per kg)
HFP	7.5 to 8	10 to 15
c-C ₄ F ₈	NA	70 to 85
TFE	5.0 to 5.4	NA

* NA = Not Available

Governments world-wide are introducing legislation to force manufacturers to be responsible for waste generated. This causes large companies to accumulate tremendous amounts of waste that need to be treated by a suitable technique in order to reduce the volume of waste to be land filled.

1.4 THE DEPOLYMERISATION OF PTFE WASTE

As previously mentioned, the inert properties of PTFE can unfortunately be a disadvantage from a waste point of view. PTFE waste can be in the form of shavings, turnings, off-cuts and chunks and can sometimes amount to as much as 50 % of the final product.^(21, 35) It is not possible to re-use PTFE waste by melt processing as is the case with other polymers, for example polyethylene.⁽⁶⁾ Unfilled PTFE waste can be ground into a fine powder form and can be re-used as a filler material in, for example, paint and cement. Grinding is not an option for filled PTFE and currently all filled PTFE waste is regarded as unwanted. This forces PTFE processors and manufacturers to dispose of these types of PTFE waste in landfill sites. This is an expensive option (the international cost in 2006 was typically \$2 to \$3 per kg PTFE), due to the cost associated with land filling, the loss of the highly valuable fluorine values that are contained in the waste, and the long-term negative environmental effects due to the non-biodegradable property of the waste PTFE. However, it is

currently the only option available because incinerating the polymer poses a big health threat to the community, as toxic gases are emitted in alarming quantities.⁽¹¹⁻¹⁵⁾ In some cases ultra-fine particles are formed that can be extremely toxic, and causes illness which is generally defined as polymer fever.⁽³²⁾

1.4.1 Considerations for the depolymerisation of PTFE waste

Extensive research has been done in the laboratory⁽¹⁴⁻¹⁹⁾ with regard to the depolymerisation process of PTFE and the chemistry thereof. The most basic method of depolymerisation involves the heating of PTFE by means of a furnace to above the thermal degradation temperature (ca. 505 °C). During this process several factors need to be considered:

1. What is the purpose of the depolymerisation? If destruction is the purpose, the off-gas has to be destroyed by an appropriate method.⁽³⁴⁾ If the end-product is to be re-used, then careful consideration should be given to the depolymerisation process parameters, because this can influence the product yields;⁽²²⁻²⁴⁾
2. What are the safety concerns? Safety is of paramount importance because very toxic perfluoroisobutylene (PFIB) and ultra-fine particles can be produced during the depolymerisation process. The toxicity (LD 50) of PFIB was reported to be 0.045 mg/l;^(11-16, 32)
3. What product is needed? The depolymerisation process parameters can be tailored to favour preferred species;^(22-24, 35)
4. What depolymerisation process is favoured? There are generally three options:
 - a. If operation at sub-atmospheric pressures is possible and the desired product is TFE, then vacuum depolymerisation can be performed.^(22-24, 35) The disadvantage of this process is the high system integrity that is necessary to be able to operate at low pressures and prevent air leaks. Air leaks can form toxic and explosive mixtures if in contact with the depolymerisation product. The advantage is the fact that no carrier gas is present and less separation steps are necessary;

- b. If HFP, OFCB or other long-chain compounds are the desired products, the depolymerisation process can be performed at higher pressures because longer-chain-length products are generally formed at these conditions;^(22-24, 35-37)
 - c. When TFE is the desired product, and the process needs to proceed at ambient pressures, steam depolymerisation can be performed. The disadvantage is the large amount of waste generated in terms of HF.^(8, 38, 39)
5. The following are possible depolymerisation systems:
- a. A reduced pressure (1 to 100 kPa abs) depolymerisation system;⁽²²⁻²⁴⁾
 - b. A steam depolymerisation system;^(8, 38, 39)
 - c. A fluidised bed and steam depolymerisation system.⁽³⁸⁾

1.4.2 Depolymerisation methods

The process of depolymerising PTFE via vacuum pyrolysis is extensively described in the literature.^(22-24, 40-42) Various means of heating were used, including resistance heating (the depolymerisation reactor is heated electrically by means of external heaters) and steam heating (the depolymerisation reactor is heated by means of resistance heating and the addition of steam to reduce the partial pressure of the product, with a resulting increase in the TFE yield at ambient pressure^(38, 39)). These methods employ kiln reactors and fluidised bed reactors for the depolymerisation process and have the advantage that the depolymerisation reaction takes place at ambient pressures. However, it is anticipated that large volumes of low concentration HF waste are formed during the depolymerisation process and this causes the reactor and down stream systems to be manufactured from diluted-HF resistant materials.

Steam heating has the advantage that the system operates at atmospheric pressure with a smaller chance of air leaking inwards and causing a possible explosion. One of the disadvantages is the large amount of waste produced by condensation of the steam (10 to 20 parts steam for 1 part TFE). The steam is contaminated with a low percentage of hydrofluoric acid and must be treated accordingly. When reduced pressure depolymerisation is used, the amount of waste is reduced to an almost

negligible amount. It also decreases the capital cost of the reactor system, because normal stainless steel can be used instead of exotic materials that are HF-resistant, e.g. Inconel.

The literature revealed that most of the depolymerisation experiments were performed in a laboratory for research purposes only, and were not scaled up for production purposes. These laboratory-scale experiments have been successfully performed for many years.^(7-10, 22-24, 34-39)

Recently research was done on the optimisation of a production process for TFE, HFP and OFB isomers.⁽³⁵⁾ This research was done with a reactor using a flow rate of 250 to 1000 g·h⁻¹ PTFE and with nitrogen as a carrier gas, or as a partial pressure reducer. The product was frozen in sample holders and analysed by means of gas chromatography. This work was done on a laboratory scale reactor and the TFE, HFP and OFCB concentrations were determined as a function of temperature, pressure and gas residence time. During these experiments a carrier gas was used.

Van der Walt developed a 2 kg·h⁻¹ semi-continuous PTFE depolymerisation laboratory system.⁽²²⁻²⁴⁾ The composition of the product that was produced by this system was dependant on the pressure and the temperature at which the reaction took place. The maximum TFE yield was obtained at 600 °C and 5 kPa. Different ratios of the main products (TFE, HFP and OFCB) as a function of temperature and pressure were obtained. From this experimental data it was possible to predict maximum yields of HFE (C₂F₆), TFE, HFP and OFCB at reduced pressures and within a temperature range of 600 to 900 °C. For a system operating continuously this may be valuable information. For optimisation of a specific product, the operating parameters can be varied during operation. Depending on the product, a selectivity i.t.o. TFE of up to 95 % can be obtained. This is described in more detail in Chapter 4 of this study.

To the best of my knowledge, there is currently no commercial plant world-wide that depolymerises PTFE on a continuous basis.^(6, 8-10)

The global waste production rate of PTFE is estimated to be 12 000 tpa in the USA alone. The landfill cost associated with this is estimated to be USD 24 million pa. The intrinsic value of the F-compounds produced from the waste is estimated to be USD 120 million pa (based only on the HFP price of USD 10 kg⁻¹). The global annual value of PTFE waste therefore is estimated at USD 144 million pa.

1.4.3 Chemical reaction mechanisms proposed in the literature for the depolymerisation of PTFE

The mechanism of any depolymerisation process is difficult to predict although the mechanism for the depolymerisation of PTFE is relatively uncomplicated when compared to those of other polymers, because the structure consists of homogeneous and linear polymer chains. Using GC/MS, TG/MS and FTIR for product analysis, a good prediction of the mechanism could be made.

Lewis and Naylor proposed a mechanism for the depolymerisation process where PTFE was unzipped to form exclusively TFE double radicals ($\cdot\text{CF}_2\text{-F}_2\text{C}\cdot$).⁽⁴³⁾ One of these radicals may then form a double bond exothermally to afford TFE, or at higher pressures two radicals can combine to form HFP and OFCB in secondary reactions. No mention was made of the formation of HFE or OFP in the product mixture. Experimentation was performed in a batch reactor since the aim of this experimentation was not to depolymerise PTFE on a continuous basis.

Morisaki performed TG/MS experiments with PTFE in order to determine the activation energy of TFE and HFP that were produced via the combination of different intermediate fractions formed inside a mass spectrometer.⁽⁴⁴⁾ He also proposed a mechanism where TFE was formed by depolymerisation of PTFE into difluorocarbene radicals ($\text{CF}_2\cdot$). HFP and OFCB were also part of a secondary reaction of one TFE molecule with either another TFE molecule to form a C₄-compound or a difluorocarbene radical to form HFP. Meissner *et al* proposed a similar reaction mechanism, but, according to them, TFE is the primary product and only OFCB forms from TFE in a secondary reaction. HFP actually forms in a tertiary reaction from OFCB decomposition according to them.⁽³⁵⁾ They performed their experiments in a semi-continuous reactor. PTFE was fed into the reactor and at

different fixed residence times, the product gas was quenched by freezing with a liquid nitrogen quench. The PTFE feed rates for these experiments were very small compared to experimentation by vd Walt⁽²²⁻²⁴⁾.

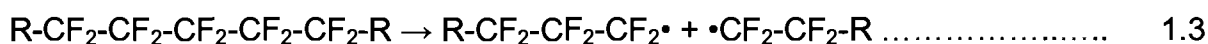
The process of depolymerisation can take place via one of two routes, which are temperature-driven: random depolymerisation, where the polymer chain randomly breaks into fragments (high temperatures, typically 700 to 900°C), and chain depolymerisation or unzipping (low temperatures, typically 450 to 700°C).⁽⁴³⁾ Random depolymerisation takes place in three steps:

1. Initiation where a PTFE chain randomly splits into pieces of variable length.
2. Depropagation where stepwise ejection of monomer molecules from the radical-ends takes place. The monomer rapidly diffuses away from the reaction site.
3. Termination is possible via different routes, namely direct evaporation, disproportionation and radical combination.^(45, 46) If the depolymerisation is complete, termination might only mean that the depolymerisation products stabilise when cooled.

Cox *et al* determined the activation energy of the depolymerisation process as 318.2 kJ·mol⁻¹ with a first order calculation.⁽⁴⁷⁾ Siegle *et al* experimentally determined the activation energy to be 347.5 kJ·mol⁻¹ in a single-step process.⁽⁴⁶⁾ Carroll and Manche proposed that the depolymerisation of PTFE takes place in two steps, indicating two activation energies, 353.55 kJ·mol⁻¹ and 191.21 kJ·mol⁻¹.⁽⁴⁸⁾ The order of the depolymerisation process was chosen to be zero. Kinetic calculations on the first mechanism were done by analysing TGA data from the depolymerisation process.^(9, 49)

The depolymerisation process was generally divided into three stages: initiation, propagation to TFE and propagation to other products (HFP and OFCB). The following mechanism has been proposed:^(8, 35, 44)

Initiation:



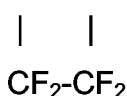
Propagation to TFE:



Propagation to HFP:



Propagation to OFCB:



The HFP and OFCB products form in the gas phase from TFE. The different reactions for production of TFE, HFP and OFCB have different orders and different activation energies for the forward and reverse reactions. Equilibrium constants were calculated for the reactions.^(50, 51) This falls outside of the scope for this thesis and will not be discussed here but will be pursued in future work.

1.5 MAIN CONCLUSIONS FROM THE LITERATURE STUDY AND THE MARKET REVIEW

After reviewing the literature and market information, the following main conclusions can be made:

1. Better disposal of PTFE is a matter that needs attention;
2. The current manufacturing of the monomer TFE is via a R22 route;
3. Currently depolymerisation of PTFE is not carried out commercially. Proposals have been made to depolymerise PTFE by means of steam. This however creates a lot of downstream products and demands higher integrity of the plant necessary for depolymerisation;
4. Different reaction mechanisms for the manufacturing of TFE, HFP and OFCB were proposed by various researchers where TFE is the main depolymerisation product and HFP and OFCB form as products of secondary reactions in the gas phase;
5. It was proposed that the depolymerisation process takes place via two mechanistic routes. These routes are temperature-dependant;⁽³³⁾
6. The depolymerisation of filled PTFE was not mentioned in the literature;
7. Molecular modelling of fluorocarbon molecules, radical species and transition state species to evaluate the depolymerisation and product formation mechanism, have not yet been done.

1.6 THE OPPORTUNITY

As discussed in the above-mentioned paragraphs, huge problems exist in the handling of PTFE waste, but at the same time it creates several opportunities for new, innovative and creative solutions to the problem.

These opportunities can be summarised as follows:

- A method is required to destroy waste PTFE in a safe, and ecological responsible manner;

- Current depolymerisation processes are sub-optimal and more research is required to determine the optimal window of parameters by which PTFE can be depolymerised;
- The output in terms of the production of valuable downstream fluoro-chemical products and the consequent recovery of expensive fluorine values, has to be maximised;
- A process is needed whereby filled PTFE can also be treated but with a continuous process;
- A basic, theoretical and fundamental knowledge of the depolymerisation process in terms of thermodynamic calculations, molecular modelling and reaction mechanisms is needed in order to have a better fundamental understanding of the depolymerisation process;
- A commercial scale depolymerisation plant, that is based on sound scientific results and designed according to chemical engineering principles is needed to address the waste PTFE problem with the ultimate goal to produce high value intermediate and final fluorochemical products (such as HFP), using PTFE waste.
- A techno-economical feasibility study is needed for the above mentioned plant.

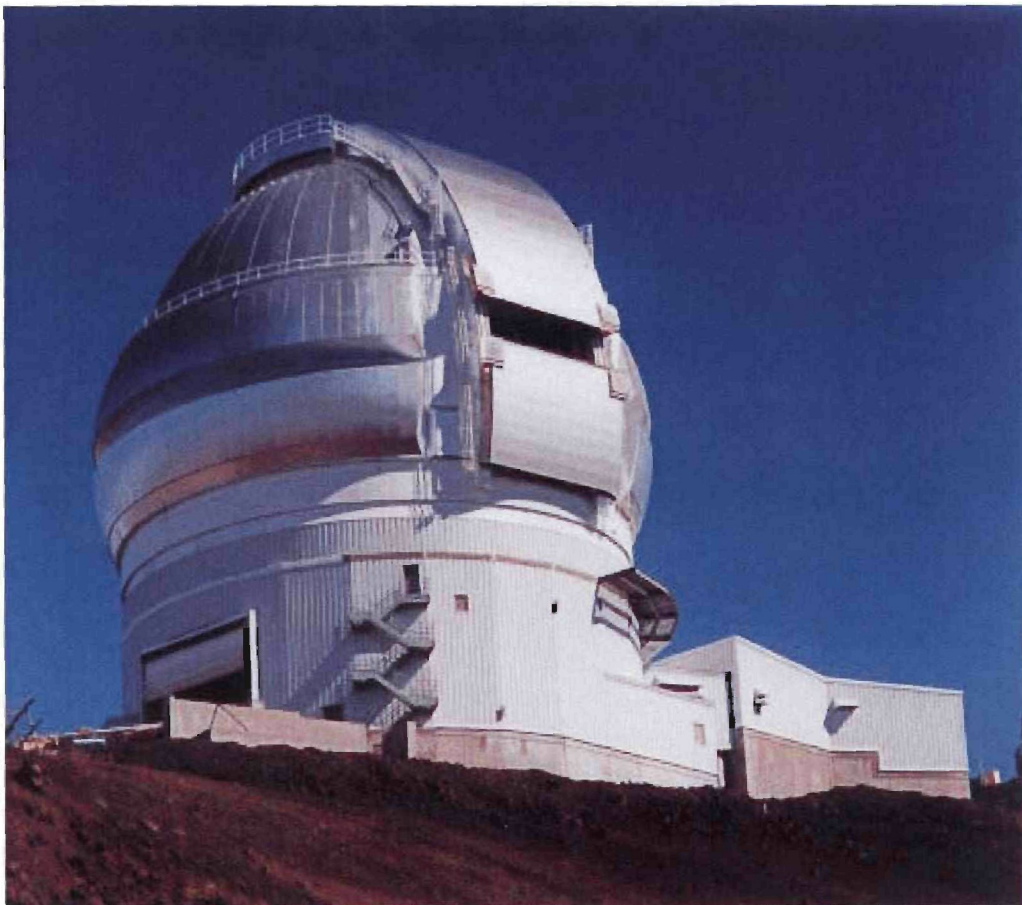
This study is therefore to present and develop some solutions to the problem of the handling of PTFE waste and to contribute to the abovementioned opportunities. These challenges became the driving force behind this study. The purpose and main objectives of this study will be discussed in more detail in Chapter 2 of this thesis.

Chapter 2

Purpose and Scope of this Study

- 2.1 Introduction
- 2.2 The purpose and scope of this study
- 2.3 The structure of this thesis
- 2.4 Main objectives of this study

BIG SCOPE



2.1 INTRODUCTION

As indicated in Chapter 1 of this thesis, there exists some clear and definitive opportunities which justify more research and development. There is firstly a lack of understanding of the basic knowledge and theoretical background of the depolymerisation process of PTFE in terms of thermodynamics, kinetics, mechanism of depolymerisation product formation and molecular modelling. On a more technical ground, there is secondly the need to develop reliable reactor systems in which fluoropolymers and more specifically PTFE (filled and unfilled) systems can be depolymerised on a continuous basis without blockages. According to the literature, no such systems exist on a commercial basis. The literature reports quite a lot of laboratory results that were generated on small scale and in batch experiments. Lastly, the need for a commercial plant to address the problem of PTFE waste, but at the same time manufactured much needed valuable downstream products, offers a huge opportunity to be explored.

In this chapter the purpose and scope of the thesis will be outlined. All the aspects which will be discussed in the following chapters will briefly be mentioned. The thesis can roughly be structured according to the following three topics: Background, Science and Technology.

2.2 THE PURPOSE AND SCOPE OF THIS STUDY

The purpose of this study is to address some of the abovementioned aspects, as well as some of the opportunities outlined in Chapter 1. The approach in this study was therefore twofold: Firstly to propose additional and complementary mechanisms for the depolymerisation and product formation of PTFE, and secondly to develop a reactor able to depolymerise unfilled as well as filled PTFE on a continuous basis as an industrial solution for a worldwide problem. The main products (TFE, HFP and OFCB) formed during this process are useable, with HFP the most sought after. It is therefore the aim to manufacture HFP at the highest yield and with the lowest concentration of unwanted or toxic by-products (HFE, OFP and PFIB) and to optimise the window of parameters by which this goal can be achieved.

It is anticipated to propose a mechanism that is based on what is currently available in the literature, as well on the results generated in previous work⁽²²⁻²⁴⁾. This mechanism, in addition to other reported proposed mechanisms^(8, 35, 44) will include the formation of the products carbon, HFE and octafluoropropane (OFP) as they were experimentally observed in previous work.

In order to qualify the proposed mechanism a variety of analytical techniques was used, which will be discussed in detail in Chapter 3. Further, thermodynamic calculations of the equilibrium concentrations of the depolymerisation species and the Gibbs free energy for the different proposed reaction equations at the experimental temperature and pressure ranges will be studied. The proposed mechanism will further be evaluated by molecular modelling of the formation energies of the different products and the intermediate species. Energy diagrams will be constructed and a detailed study will be done to determine the preferred reaction series describing the mechanistic routes towards the observed products. The role of the F atom in HFE and OFP formation will be evaluated.

An isothermal thermogravimetric study on PTFE depolymerisation will be done. An attempt will be made to determine the order and calculate activation energy of the depolymerisation process.

In order to find a scaleable reactor and depolymerisation system that is able to depolymerise unfilled as well as filled PTFE on a continuous basis, the PTFE as well as the filler material will be characterised according to particle size, general particle morphology, type of filler material and the flow properties of hot and cold PTFE in a rotating kiln. With this information a laboratory reactor system will be designed and tested. The depolymerisation of different fluoropolymers will also be evaluated with PTFE as a reference.

In addition to the development of such a reactor system, a concept chemical engineering design and costing will be done on a system that will be able to depolymerise 500 kg·h⁻¹ filled PTFE on a continuous basis with the aim to produce HFP as a main product. A detail chemical engineering design, with process flow

diagrams, mass and energy balances, process and instrumentation diagrams, design and specification of main equipment, falls however outside the scope of this thesis. The author is however hopeful that this thesis will stimulate further study in this regard.

From the available literature, and as discussed in Chapter 1, the depolymerisation of PTFE always produces a mixture of products and in various ratios.⁽²²⁻²⁴⁾ It is obvious that these product mixtures have to be separated in terms of main products and have to be purified of unwanted contamination. Several possible methods can be investigated in this regard, for example cryogenic distillation, separation by gas membranes and absorption/desorption techniques. These aspects fall however also outside the scope of this thesis and can also form a study on its own right.

The kinetics of the depolymerisation reaction of PTFE is also another important aspect that is recognised by the author. Again it is felt that this very important aspect can form a study on its own and will only be briefly addressed in this study.

2.3 THE STRUCTURE OF THIS THESIS

The structure of the thesis is divided into three sections namely a background section a scientific section where research results are reported and a technology section where different reactors were developed for the depolymerisation of PTFE.

The structure of this thesis is schematically presented in Figure 2.1.

The Depolymerisation of Fluorocarbons



Figure 2.1: Schematic presentation of the structure of the thesis

The schematic outlay of the thesis can be explained in more detail as follows:

1. **The Background Section:** In this section the problems associated with PTFE waste are identified and discussed. This is followed by a literature study on the depolymerisation of PTFE and different depolymerisation processes that have been mentioned in the available literature. From the literature and market research, certain opportunities were identified that could be worthwhile for further research. Subsequently, the purpose and the scope of the study are defined and the structure evolved to address the anticipated research. The equipment and analytical methods used in the study and their suitability to satisfy the analytical requirements for the study was discussed. This background discussion spans Chapters 1, 2 and 3.
2. **The Science Section:** In this section the different analytical methods will be employed to analyse the proposed depolymerisation and product formation mechanism. These methods include a thermodynamic study, molecular modelling and a thermogravimetric study (Chapters 4, 5, 6, 7 and 8);
3. **The Technology Section:** The technology section where the different experimental reactors will be discussed. A fairly simple reactor, the Drop-tube Reactor, which was able to generate quick results with unfilled PTFE, was developed and discussed. In order to address the problem with filled PTFE the filler material, from filled PTFE, will firstly be characterised after which the Paddle Reactor will be discussed. A Vibrating Reactor for depolymerising other fluoropolymers will be presented and then a commercial design solution for the waste PTFE problem will be presented and discussed. (Chapters 4, 9, 10, 11 and 12).

2.4 MAIN OBJECTIVES OF THIS STUDY

The main objective of this study is to propose a method to treat and beneficiate filled and unfilled PTFE waste by producing a high value, sought-after product namely HFP. In order to optimise the HFP concentration and to understand the chemistry, a mechanism for the formation of depolymerisation products, based on PTFE depolymerisation experiments, will be proposed. This mechanism will be scrutinised and refined by means of scientific reasoning using thermodynamic, molecular modelling and kinetically based arguments.

Finally an industrial scale system will be proposed and designed based on a cost analysis and a preliminary techno economic study.

It is realised that in order to develop a complete holistic approach to the very wide field of the depolymerisation of PTFE, several other important aspects must also be investigated. This will make this thesis however too comprehensive and falls therefore outside the scope of this particular study. Each of these can follow a study in its own right. They are for example:

- Kinetics of the depolymerisation product formation;
- Detail chemical engineering design;
- Separation methods of the fluorocarbon products.

Chapter 3

General Description of the Equipment and Analytical Methods Used in this Study

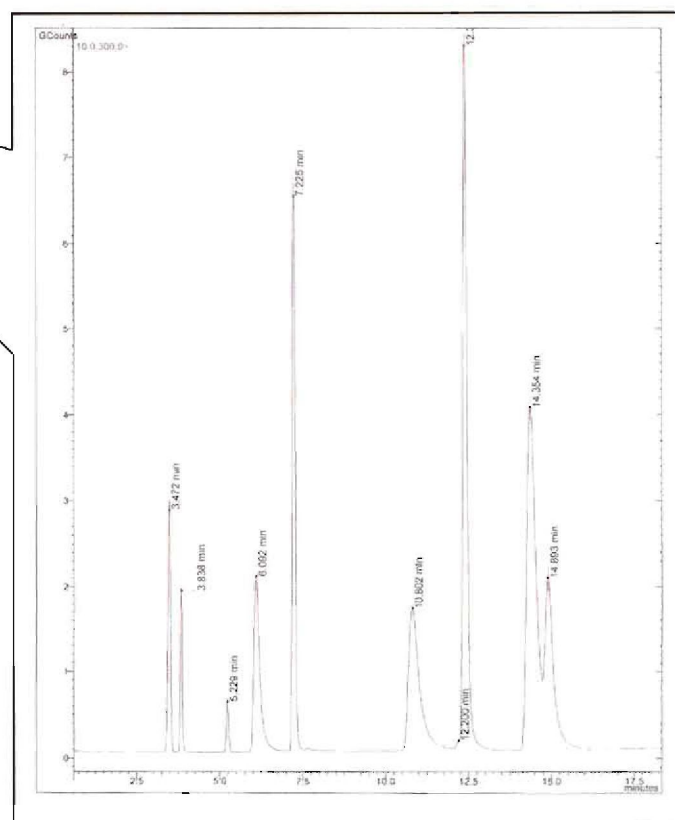
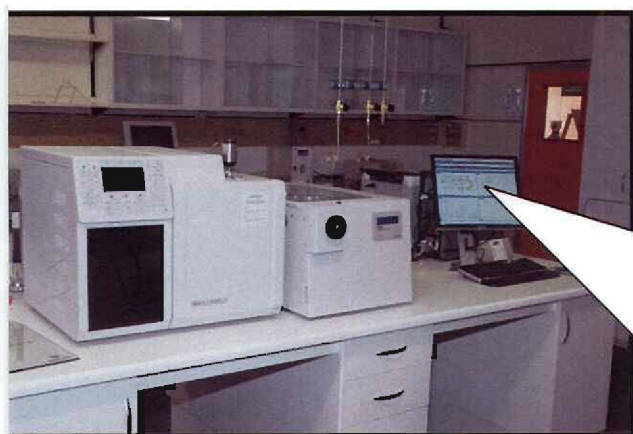
3.1. The Depolymerisation Reactors

- 3.1.1. Introduction
- 3.1.2. The Drop-tube Reactor
- 3.1.3. The Laboratory Rotating-kiln Reactor
- 3.1.4. The Paddle Reactor
- 3.1.5. The Vibrating Reactor

3.2. Analytical Methods

- 3.2.1. Introduction
- 3.2.2. Gas Chromatography
- 3.2.3. Gas Chromatography/Mass Spectrometry (GC/MS)
- 3.2.4. Thermogravimetric Analysis (TGA)
- 3.2.5. Scanning Electron Microscopy (SEM)

3.3. Conclusions



As indicated in Chapters 1 and 2, the opportunity exists to develop a process for the continuous depolymerisation of filled and unfilled PTFE and to manufacture valuable downstream products from the product gas stream. In order to develop such a process, various types of reactors were envisaged. The purpose of this chapter is to describe these reactor systems and the various aspects of the depolymerisation process that they will help understand. The analytical methods used for characterisation and during experimentation will also be discussed. Therefore, this chapter is divided into two main parts, namely the description of the depolymerisation reactors and a discussion of the analytical techniques that were used.

3.1 THE DEPOLYMERISATION REACTORS

3.1.1 Introduction

In order to understand the depolymerisation process of PTFE, different methods were used to test different aspects of the process. Tests were performed to evaluate different fluoropolymer feedstock (filled and unfilled PTFE), to evaluate the residence time of PTFE inside the reactor, to observe the depolymerisation process inside the reactor and to test different reactor concepts.

The different types of reactors that were developed are the following:

- A Drop-tube Reactor to study the depolymerisation products of unfilled PTFE on a continuous basis;
- A laboratory scale Rotating-kiln Reactor to observe the mechanical interaction of hot PTFE with the reactor walls during the depolymerisation process;
- A Paddle Reactor for the development of continuous process for the depolymerisation of filled and unfilled PTFE;
- A simple Vibrating Reactor to test the depolymerisation of PTFE and compare it to other fluoropolymers.

These systems, the reactors and the equipment used to conduct this research will be described in detail below.

3.1.2 The Drop-tube Reactor

For the depolymerisation process to be tested and to qualify the system and the depolymerisation product composition against values reported in the literature^(8-10, 22-24), a Drop-tube Reactor was developed. This reactor system that was able to depolymerise unfilled PTFE on a continuous basis, producing useable high-value monomers, was designed and developed during this study. A picture of this reactor is shown in Figure 3.1 and schematically presented in Chapter 4, Figure 4.1.

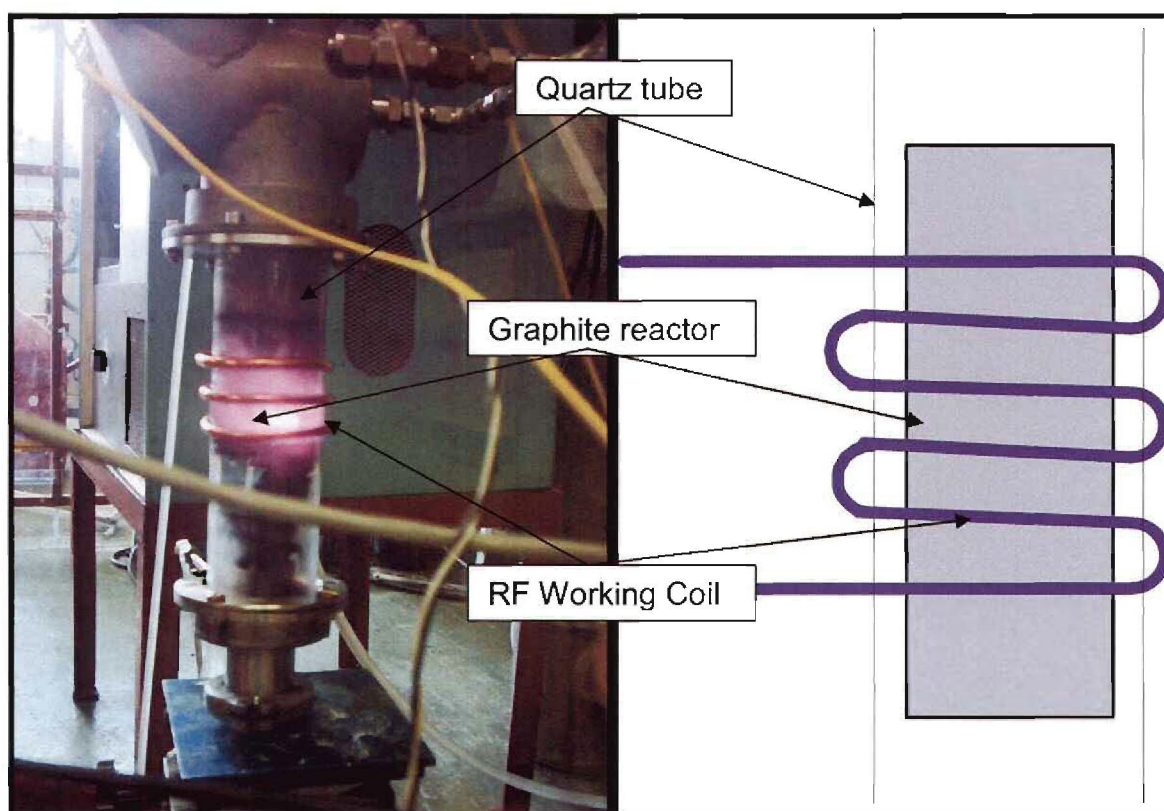


Figure 3.1: The Drop-tube depolymerisation Reactor

The process can be described as follows: The PTFE that is to be depolymerised, is fed via a feed hopper from the top into the graphite reactor that is situated inside a quartz tube within the working coil of a radio frequency (RF) generator. The RF generator heats the graphite reactor and the PTFE is depolymerised at certain temperatures that could be changed by adjusting the power of the RF generator. The

product gases that evolved were quenched downstream by means of a rotating continuous self cleaning quench probe, before it was analysed by a gas chromatograph. This quench probe was made up of double annular water cooled concentric tubes. This type of quenching method was chosen because it doesn't contaminate the product mixture as would be the case with a gas/gas or a gas/liquid quench method. The annular quench was designed to quench the depolymerisation product at a high quench rate of up to $1 \times 10^6 \text{ }^\circ\text{C} \cdot \text{s}^{-1}$.⁽⁵²⁾

In order to be able to develop reaction mechanisms the Drop-tube Reactor was used. Because of its short residence time, only primary products TFE, HFP and OFCB were formed. The reactor has a great flexibility with respect to temperature and pressure; however it can not be used for depolymerisation of filled PTFE. A 100 tpa PTFE depolymerisation system has been tested. The results of all the experiments conducted on this system are presented in Chapter 4.

Repeatability and precision

In order to evaluate the repeatability and the precision of the experimental data, the average of 3 analyses of the product gas, for the experiments performed between 600 to 900 °C and at different pressures (ca. 10, 20, 50 and 80 kPa), were used. Table 3.1 shows the average, repeatability and precision of three analyses performed at similar experimental conditions.

Table 3.1: Repeatability and precision of depolymerisation data at 600 °C and 5 kPa

	T (°C)	P (kPa)	C ₂ F ₆ (%)	C ₂ F ₄ (%)	C ₃ F ₆ (%)	C ₃ F ₈ (%)	c-C ₄ F ₈ (%)	PFIB (%)	Total gas yield (%)
	600	5	ND	94.0	5.3	ND	0.6	ND	99.9
	615	5	ND	93.9	5.2	ND	0.8	ND	99.9
	606	5	ND	93.8	5.4	ND	0.6	ND	99.8
Average	607	5	ND	93.9	5.3	ND	0.7	ND	99.9
Standard deviation	7.5	0		0.1	0.1		0.1		0.05

The standard deviation of the analytical data points for TFE, HFP and OFCB is 0.1 for all the analyses, and for the temperature it was 7.5. This indicates a good repeatability of the system, the analytical sampling and GC analysis. The standard deviation for OFCB was also 0.1 %. This is an indication that a fault of 14 % can be made as appose to a 0.1 % fault for TFE. As OFCB is a minor product for these experimental conditions, even a 14 % fault will not influence the final average product mixture significantly. The temperature control of the reactor is good as only a ~1 % temperature difference was measured. The remainder of data points presented in Chapter 4 were calculated in similar fashion. All the data reported in this thesis, was the average of at least three analytical results.

3.1.3 The Laboratory Rotating-kiln Reactor

The flow properties of filled PTFE under high-temperature conditions were investigated by visually observing the depolymerisation process in a laboratory scale Rotating-kiln Reactor. At the beginning of this study, the hypothesis was made that when PTFE is depolymerised, it might undergo different physical phases. Upon heating it is proposed that the phase changes from a solid phase polymer, through a viscous semi-liquid phase to eventually be vaporised. Should the PTFE stick to the walls during depolymerisation, it would be difficult to use a tubular reactor, because the bad heat transfer properties of PTFE may cause incomplete depolymerisation and eventually lead to blocking of the reactor. For this experiment a 100 mm long, 50 mm diameter, open-ended stainless steel kiln reactor was used to observe the flow of PTFE at the depolymerisation temperature (See Figure 3.2).

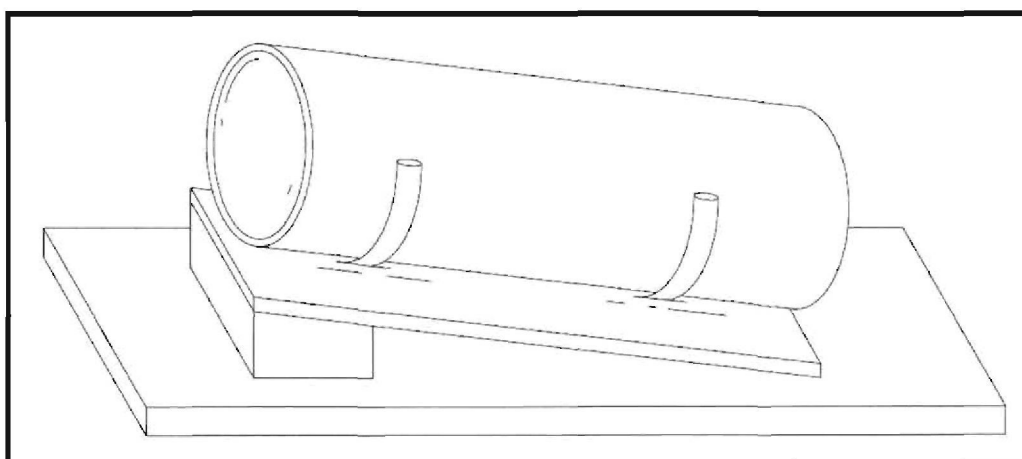


Figure 3.2: Schematic presentation of a set-up used to visually observe the depolymerisation of PTFE in a rotating reactor

The kiln was positioned inside a muffle oven where the reactor was heated to the desired temperature. A thermocouple was inserted into the reactor and positioned against the inner wall in an attempt to measure the wall temperature directly.

This system was operated inside a well-ventilated fume cupboard because of the toxicity of some of the envisaged gaseous depolymerisation products.

The kiln temperature was increased from ambient temperature to a temperature of 600 °C over a two-hour period. When a temperature of 400 °C was reached, a 5 g glass fibre-filled PTFE sample was introduced into the front end and the depolymerisation process observed as the temperature increased. While rotating the kiln the glass fibre-filled PTFE was completely depolymerised and the residue (filler) was discharged at the lower end. The experiment continued until no PTFE was left inside the reactor. These results are discussed in Chapter 9 of this thesis.

3.1.4 The Paddle Reactor

Tests with filled PTFE in the Drop-tube Reactor could only be conducted in a batch mode because the reactor gradually filled up with filler material that cannot be depolymerised. Therefore, during this study a reactor was designed for the continuous depolymerisation of unfilled as well as filled PTFE. This required a system where the depolymerisation of PTFE would be able to take place inside a kiln-type reactor and that the filler material could be successfully and continuously be separated from the depolymerisation gas. It was also unsure if the filler material (the un-depolymerised residue) would stick to the sides of the reactor with subsequent bad heat transfer properties and eventually failure due to blockages.

The reactor that was designed to address these possible foreseeable problems is shown in Figure 3.3a. It consisted of a kiln (tube) and paddles on the inside thereof to conduct a continuous scraping action against the inside of the reactor wall. The reactor and paddle screw were made of Inconel 600 to be chemically resistant at elevated temperatures, and had an inside diameter of 150 mm and a length of 1

meter. The tube had an inlet at the top of the feed-side and two outlets at the top and bottom of the discharge-side, as schematically presented in Figure 3.3b. A screw feeder supplied PTFE continuously from a hopper to the inlet of the reactor. A quench probe was mounted onto the top outlet of the reactor. The Paddle Reactor can be operated at temperatures of up to 800 °C and pressures in the range of 10 to 100 kPa. In order to be able to perform the research under reduced pressure conditions the following measures were taken:

- The whole reactor system was designed to be air tight;
- A vacuum pump was installed at the outlet of the system after the filter;
- The filler residue was accumulated *in situ* through the bottom outlet of the reactor. The filler collection bin was designed to collect filler material on a continuous basis for a period of 8 hours (1 working day) before it needed to be emptied.

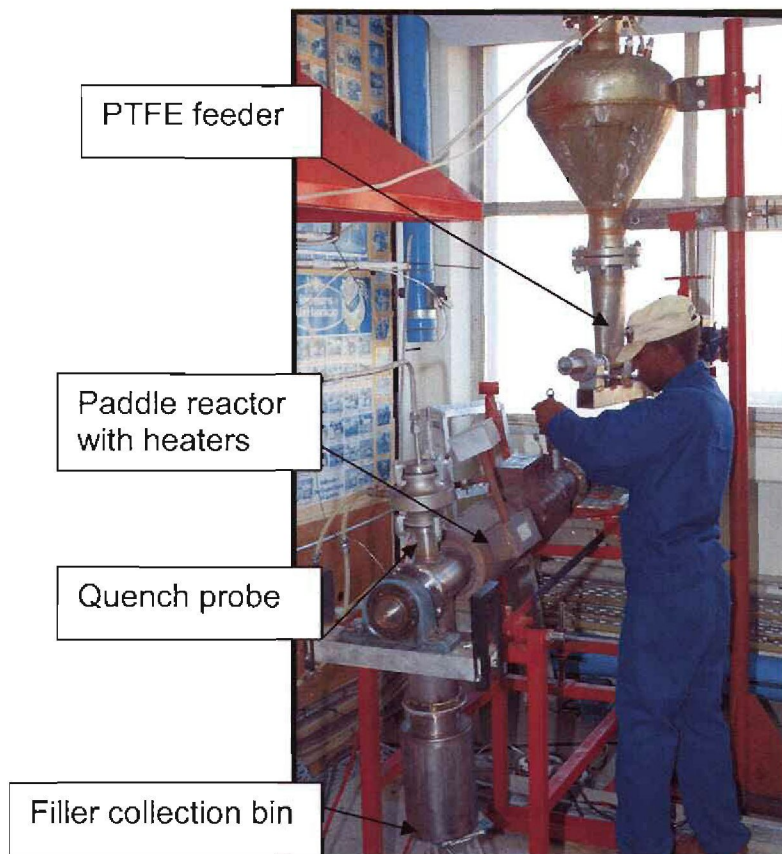


Figure 3.3a: Paddle Reactor operated by a technician

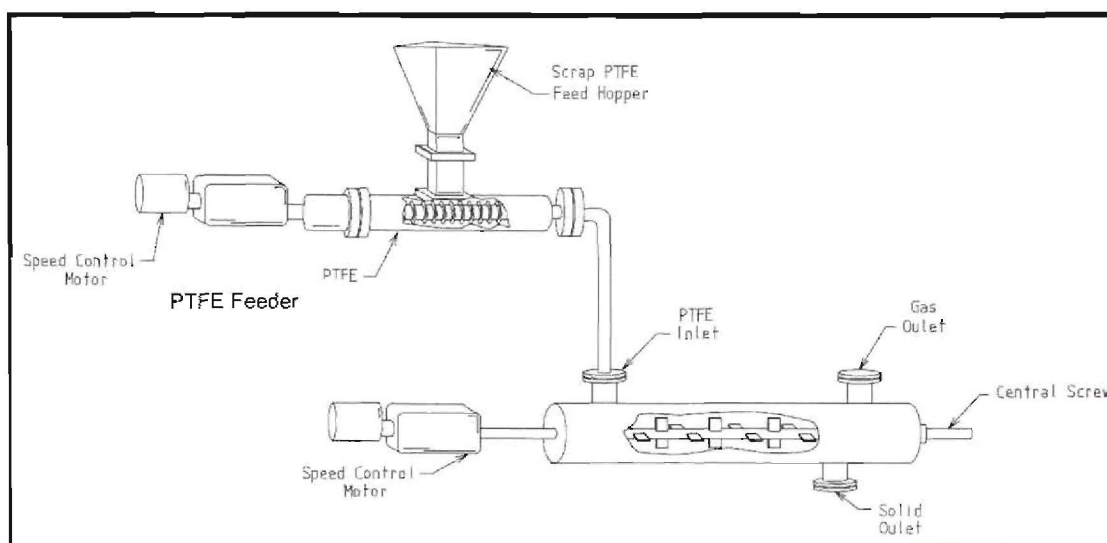


Figure 3.3b: The Paddle Reactor system that was used for the continuous depolymerisation of filled PTFE

Two externally mounted heaters (not shown in Figure 3.3b), were clamped around the reactor, and supplied a maximum of 6 kW of energy to the system. Temperature controllers controlled the energy input in order to sustain the pre-set temperature. The temperature of the reactor outer wall was measured by means of a type K thermocouple.

The centrally mounted paddle screw consisted of two parts, namely a short screw below the feeder inlet (not shown), while equally spaced paddles at right angles to one another, occupied the rest of the axis. The paddles cleared the reactor wall by a small margin to transport the PTFE and filler material through the reactor and to increase the area of contact between the PTFE and the hot reactor wall. The scraping action of the paddles against the wall prevented the filler residue from sticking to the wall and blocking the reactor, and also increased the heat transfer between the PTFE and the hot wall. The reactor was mounted onto a stand, the angle of which could easily be adjusted.

Thus two experimental series were performed in order to qualify the reactor for the depolymerisation process. The first was the determination of the residence times of PTFE at different reactor conditions in order to optimise the depolymerisation efficiency, and the second was to convert such a reactor into a depolymerisation

system to depolymerise unfilled as well as filled PTFE for extended periods of time. The results of all the experiments conducted on this system are presented in Chapter 10.

3.1.5 The Vibrating Reactor

The depolymerisation of other fluoropolymers was evaluated in a Vibrating Reactor using clean, unfilled PTFE as a reference. This reactor is shown in Figure 3.4 and was used because of its simplicity and simple maintenance. The property difference between PTFE and the other fluoropolymers could cause experimental difficulties.

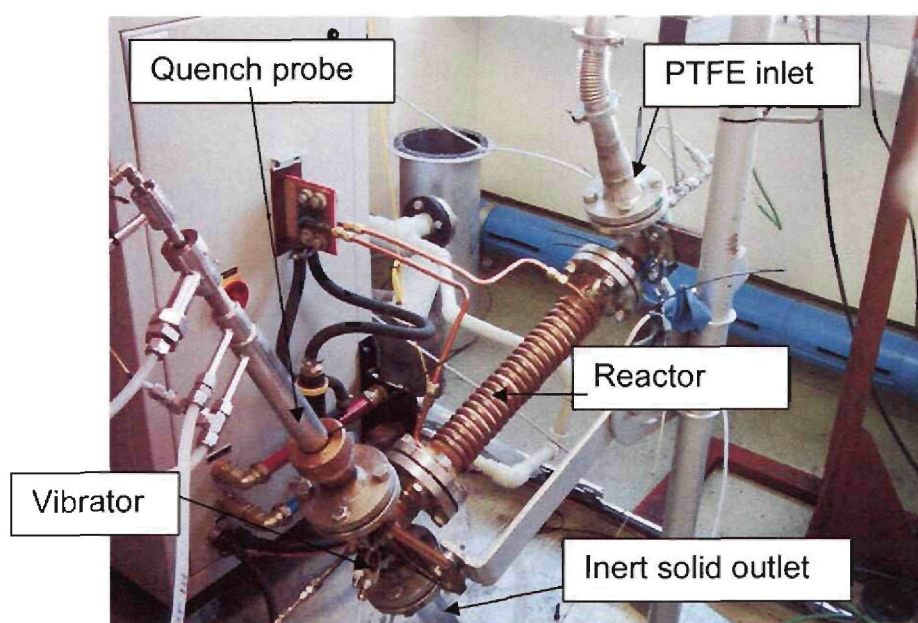


Figure 3.4: Vibrating Reactor

Filled and unfilled PTFE were depolymerised in this reactor for fluoropolymers such as Perfluoroalcoxy (PFA), Fluorinated-Ethylene-Propylene (FEP), Ethylene-Tetrafluoroethylene copolymer (ETFE), Hexafluoropropylene-Tetrafluoroethylene-Ethylene copolymer (HTE) and Tetrafluoroethylene-Hexafluoropropylene-Vinilidene fluoride (THV). The reactor consisted of a 50 mm diameter, 500 mm long stainless steel pipe and was heated by means of a 20 kW radiofrequency induction generator. The polymer was fed into the reactor by means of a screw feeder. A vibrator that was fixed to the outlet side of the reactor propagated the PTFE through the reactor for the depolymerisation process. Inert solid residue was accumulated

and the product gas quenched before analysis as with the Paddle Reactor. These results are presented in Chapter 11.

3.2 ANALYTICAL METHODS

3.2.1 Introduction

In order to characterise the PTFE feed samples, the filler materials and the depolymerisation products, a variety of analytical instrumentation was used.

With regard to the feed material, it was important to determine the size, quantity, morphology and type of filler material that is encapsulated inside the PTFE. This can have a major effect on the depolymerisation system if the filler material cannot withstand the depolymerisation conditions.

The different analytical methods used, and their applicability to this study, will be discussed below.

3.2.2 Gas Chromatography

General background of gas chromatography

Chromatography is one of the most widely-used methods for separating closely-related chemical species. In addition it can be employed for qualitative as well as quantitative determination of the separated species.

A gas chromatograph consists of an injection port where a gas sample is injected into a separation column. This column is situated inside a temperature-controlled oven and separates the sample into its constituents. The separated species are identified by means of a detector at the outlet of the column. Different types of columns (e.g. packed and capillary columns) and detectors (e.g. FID, TCD, etc.) can be used depending on the application and the species to be separated and detected.^(53, 54)

A gas sample is injected into an inert gas stream (usually helium) which is called the mobile phase that constantly flows through the stationary phase of the column. The stationary phase of a packed column can consist of any one of a wide variety of

separating media, for example, zeolites, graphite, alumina and inert solids with an active chemical deposited onto the surface. When the mobile phase with the sample flows over the stationary phase, certain species are retained longer inside the column than others. This gives rise to the separation of the different species in the sample mixture. Separation can take place according to two different mechanisms and the separation columns can generally be divided into two main groups, namely active and inactive columns. Active columns separate the sample according to the charges on the molecule. Molecules with different charges will be retained differently inside the column.

Inactive columns separate the sample according to the physical size of the different species inside the sample mixture. For example in an inactive column a gas like CF_4 will elute before C_4F_8 , because C_4F_8 is a larger molecule. The time it takes for a species to pass through a column is called the retention time. The retention time is dependant on many variables like the mobile phase flow rate, column temperature, type of stationary phase, length of the column and matrix of the sample.

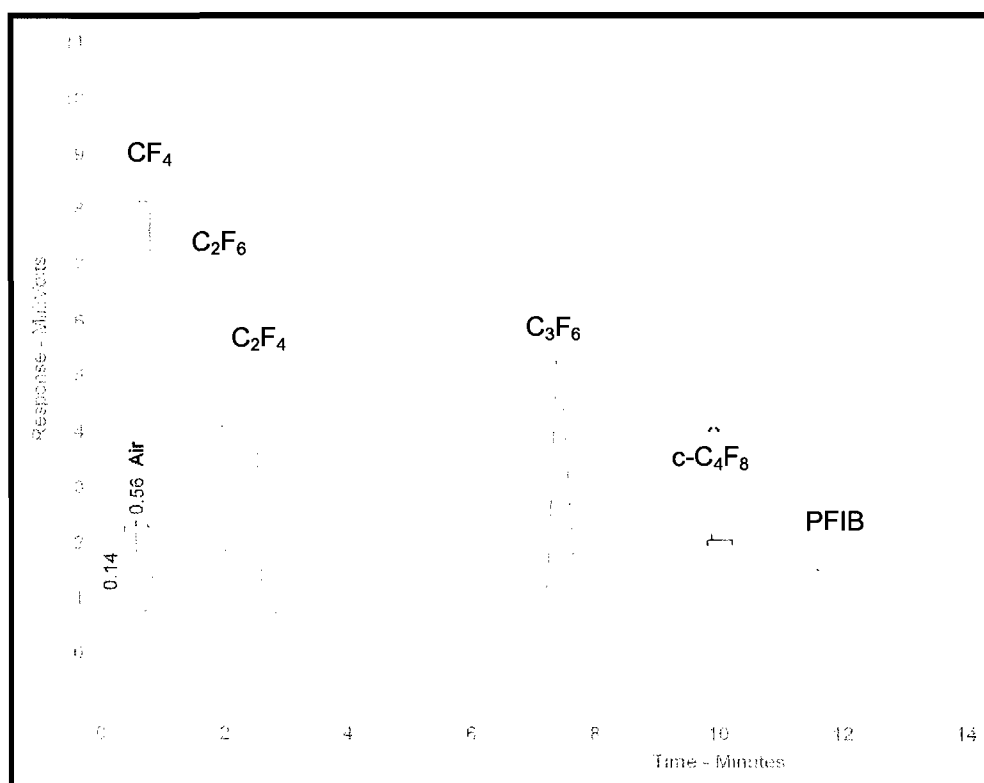


Figure 3.5: A chromatogram of the specially prepared standard that was used in this study to calibrate the GC

Instrumentation

During this study a Varian 3600 gas chromatograph was used which was equipped with a Haysep N, 2 meter packed column from Scientific Supply Services cc. The GC was equipped with a thermal conductivity detector (TCD) and He was used as the mobile phase. The signal from the detector was analysed by means of Chrompack commercial software (from Scientific Supply Services cc) and a chromatogram was produced for each analysis. The integrated peak area for each peak was used for quantification purposes.

The suitability of gas chromatography for this study

The products to be analysed for in this study were gaseous fluorocarbon compounds including CF_4 , C_2F_6 , C_2F_4 , C_3F_6 , $\text{c-C}_4\text{F}_8$ and PFIB. A typical gas chromatogram of a gas mixture containing this variety of perfluorinated compounds that were analysed during this study is shown in Figure 3.5. The retention times and calibrated identities for each of the compounds are indicated on top of each peak. In this study the response factors of the detector were not calculated and the area under the peak was used as the measurement of concentration.

Method

The sample was continuously flushed through a six-port valve, which was connected inline to the process, and a sample was pneumatically injected into the injection port of the GC. The temperature of the injection port was controlled at 120 °C. The GC was programmed with a temperature program where the temperature was increased from 80 to 140 °C within the first two minutes and then the temperature was regulated at 140 °C for 8 more minutes. All of the depolymerisation products eluted within 12 minutes.

The GC was calibrated by a standard, especially prepared by Pelindaba Analytical Labs, which is an accredited analytical laboratory. The calibration results are presented in Table 3.2. Peak identification was conducted and confirmed with a mass spectrometer (See Section 3.2.3 for more detail).

Table 3.2: Calibration results of the GC for the specially prepared standard

Peak No.	Component	Retention time (min)	Prepared concentration (Vol %)	Integrated peak area (Vol %)
1	Air	0.56	2	2.01
2	CF ₄ (TFM)	0.77	10	10.45
3	C ₂ F ₆ (HFE)	1.90	15	16.13
4	C ₂ F ₄ (TFE)	2.46	15	16.76
5	C ₃ F ₆ (HFP)	7.38	40	37.41
6	c-C ₄ F ₈ (OFCB)	9.88	15	13.53
7	C ₄ F ₈ (PFIB)	11.65	3	2.82

These values are not corrected, but the analyses during experimentation were corrected for air because it does not participate in the depolymerisation reactions.

3.2.3 Gas Chromatography/Mass Spectrometry (GC/MS)

General background of GC/MS⁽⁵⁵⁾

Mass spectrometry (MS) is an analytical technique whereby components of a sample are bombarded with an electron beam, converted into rapidly moving gaseous ions and separated by means of their mass-to-charge ratio. This enables a sample to be analysed in terms of, for example:

1. Qualitative and quantitative information on organic as well as inorganic complex mixtures;
2. Information on the structure of a wide variety of complex organic species;
3. The isotopic ratios of atoms in samples;
4. The structure and composition of solid surfaces.

The block diagram in Figure 3.6 shows the main components of a mass spectrometer.

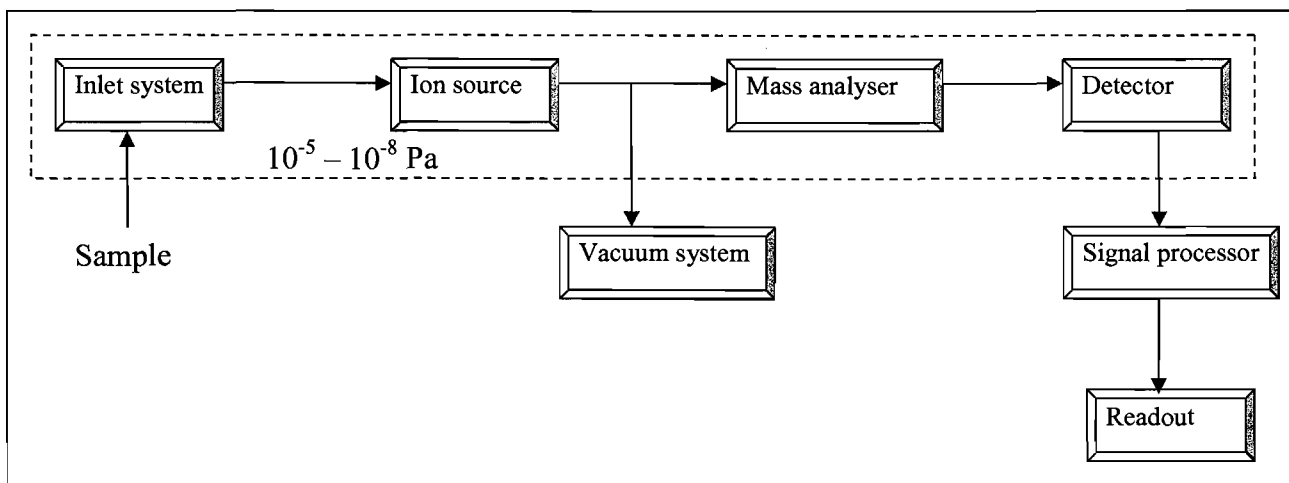


Figure 3.6: The main components of a mass spectrometer

In the case of the GC/MS, a GC is used to separate the product mixture before each compound (identified by the particular peak) is injected into the mass spectrometer. A 30 m CP-PoraPlot-Q 0.32 mm capillary column (by SMM cc) was used inside the GC. In the GC/MS configuration, it can be said that the mass spectrometer acts as a sophisticated detector for the GC.

The inlet system and the ion source are usually combined into one component. One micromole or less of the sample is introduced into the inlet system. In the inlet system solids and liquids are evaporated and fragmented into gaseous ions by bombarding the evaporated product with electrons, ions, photons or molecules. The ionised gas enters the mass analyser and gets separated by means of the mass analyser, according to their mass-to-charge ratio. The data from the mass analyser is then converted into an electrical signal by the detector and the readout gives a mass spectrum. Figure 3.7 is a presentation of the mass spectrum for OFCB. Each of the lines represents the mass number of a fraction of the sample molecule. The height of the lines represents the abundance of these fractions. Every molecule has, for this reason, a unique fingerprint spectrum.

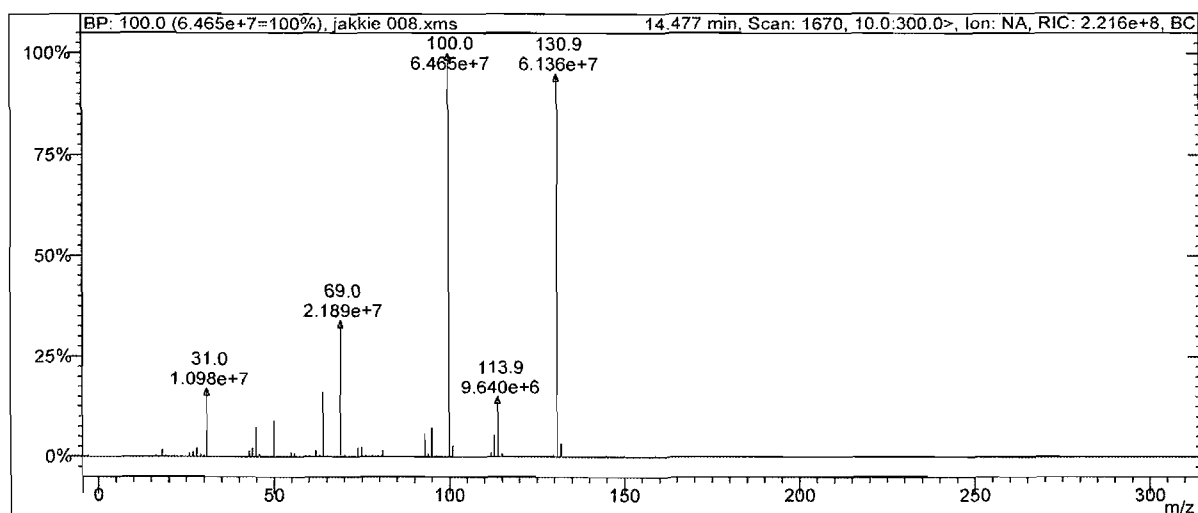


Figure 3.7: The mass spectrum of OFCB

The use of GC/MS in this study

The mass spectrometer was used in this study to identify the different species that formed during the depolymerisation process of PTFE and also for calibration purposes. Once the different peaks have been identified, the in-line GC that was used on the systems was calibrated accordingly. The GC/MS used during this study was a Hewlett Packard (HP 5970 quadrupole mass spectrometer and a HP 5890 GC). The GC was fitted with the same capillary column and it was programmed with a temperature program to optimise the peak separation efficiency of the column. The temperature program used started at 25 °C and was linearly increased to 140 °C within 20 minutes.

3.2.4 Thermogravimetric Analysis (TGA)

General description of Thermogravimetric Analysis

Thermogravimetric Analysis (TGA) is widely used in determining mass loss from solid samples when heated to a specific temperature.⁽⁵⁵⁾ The percentage mass loss as a function of temperature or time is generally the output that is obtained. The degradation rate, under a specific atmosphere and at a specific temperature, can also be measured by this method. A brief description of the operation of the instrument follows.

Instrumentation

A Perkin Elmer PGS2 TGA instrument was used during this study. The instrument used was a counter-balance instrument with the sample holder and furnace contained within a quartz tube. The sample is positioned in a platinum pan supported by a platinum stirrup, which hangs inside the furnace. The furnace is designed for high heating and cooling rates and good thermal coupling to the sample. After a sample is loaded, it is counter-balanced and zeroed in order for the mass loss to be measured. The furnace was continuously purged with nitrogen gas when samples were being heated to prevent oxidation and to flush gaseous residue, resulting from heating, before they can disturb or contaminate the balance mechanism.

Technique

In order to accurately determine decomposition temperatures of the PTFE samples, the increment by which the instrument increases the temperature must be very small, typically 1 to 5 °C·min⁻¹. In this study ~5 mg samples were used.

In this study TGA was used as a method to accurately determine the amount of filler in a filled PTFE sample and to determine the depolymerisation kinetics (Chapter 8). This is a very important aspect of this study because the filler (residue that will be left over after depolymerisation) will be a waste product that needs to be disposed of. In commercially available PTFE, the filler content is generally less than 30 %. The following samples were used and were obtained from an industrial supplier: Bronze-filled, graphite-filled and glass fibre-filled PTFE.

Figure 3.8 is a typical thermo-analytical curve with a first derivative of the weight loss for a PTFE sample that was filled with a residue. In this specific example, the TGA results showed that the amount of filler in the sample was 26.72 %. The depolymerisation started at 540 °C, showed a maximum rate at 590 °C and was completed at 600 °C. The filler contained inside the PTFE does not take part in the depolymerisation reaction and remains un-reacted in the instrument.

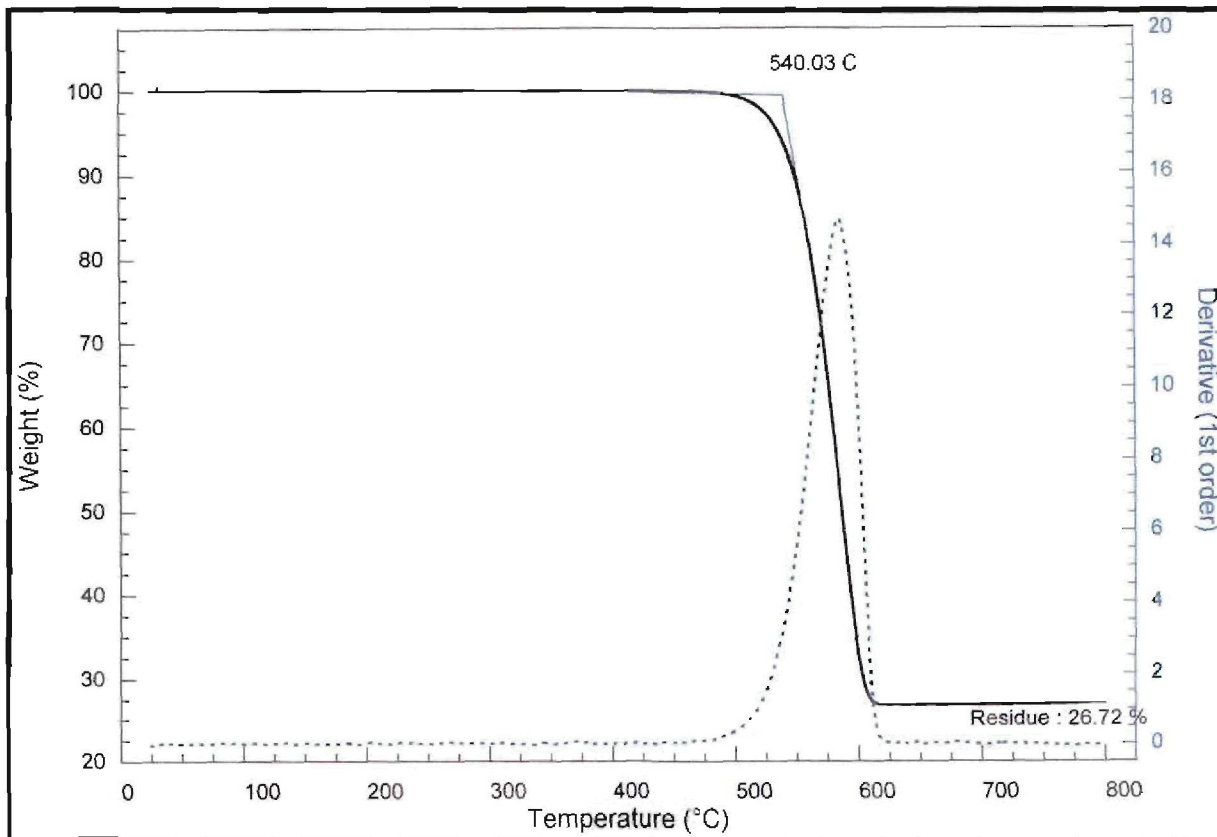


Figure 3.8: A thermogram of the filler content determination and depolymerisation temperature of graphite-filled PTFE

TG analyses results of the unfilled and filled PTFE as well as the difference in depolymerisation temperature between THV, ETFE, PFA and filled PTFE will be discussed in Chapter 9.

The PTFE depolymerisation rate at different isothermal temperatures was analysed. This data will be discussed and analysed in Chapter 8.

3.2.5 Scanning Electron Microscopy (SEM)

Background information on scanning electron microscopy

In an electron microscope a sample is bombarded with electrons from an electron gun. This bombardment of the sample surface produces secondary electrons that are detected by a photomultiplier tube, amplified and projected onto a screen. The bombarding electrons also cause X-rays to be emitted by the sample. These X-rays

can be used in determining the atomic composition of the sample. This technique is called electron diffraction X-ray spectroscopy (EDX).

Instrumentation and methodology

In this study a SEM with an electron diffraction X-ray detector coupled to it was used to determine the type and morphology of the filler in filled PTFE. A Phillips XL20 SEM that was equipped with a heating stage was used in this study. The EDX was used to determine the elemental composition of the filler material. This information can be used to determine if the filler material can withstand the depolymerisation process conditions.

For visual observation of the depolymerisation of PTFE on the micro scale, the SEM was used in the low vacuum mode with the heating stage for microscopy in the so-called ESEM mode. With the ESEM mode, a small quantity of glass fibre-filled PTFE was depolymerised with the heating stage, starting at a temperature of 450 °C. As the polymer was slowly heated the depolymerisation process was observed and recorded *in situ* on the computer.⁽⁵⁶⁾ A copy of this is included at the back cover of this thesis. To access the video the file "Depolymerisation" must be opened with Windows Media Player. As the depolymerisation process is slow in the beginning, the viewer is recommended to fast forward it to near the end. These observations are explained in Chapter 9.

A typical electron diffraction X-ray (EDX) analysis of glass fibre-filled PTFE is presented in Figure 3.9. From these results it could be deduced that the filler could possibly be CaSiO_3 with some impurities. Some fluorine was detected on the filler surface. This might be the result of incomplete depolymerisation. This observation is further discussed in Chapter 9.

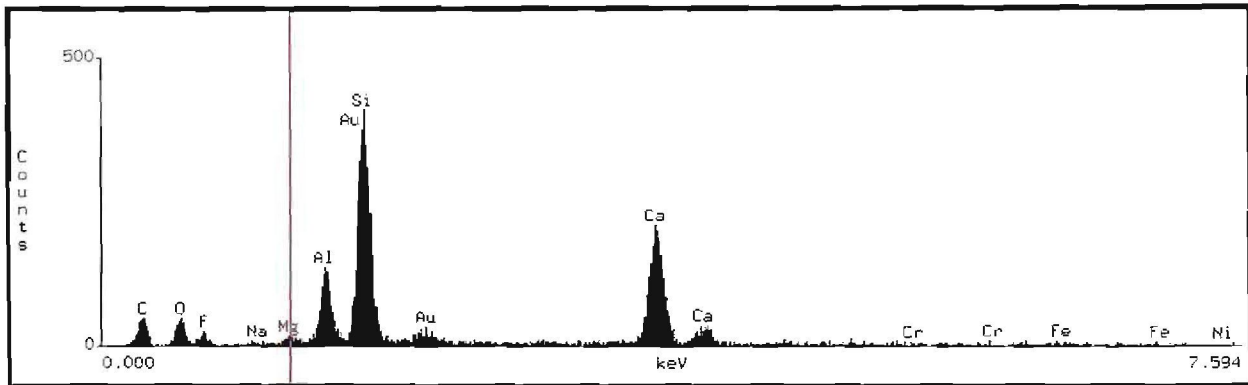


Figure 3.9: EDX analysis of glass fibre-filler

Figure 3.10 is a SEM image of glass fibre-filler, after depolymerisation, taken at 1000 x magnification. This filler is in the form of small needle-like particles of 10 μm in diameter and some more than 100 μm in length.

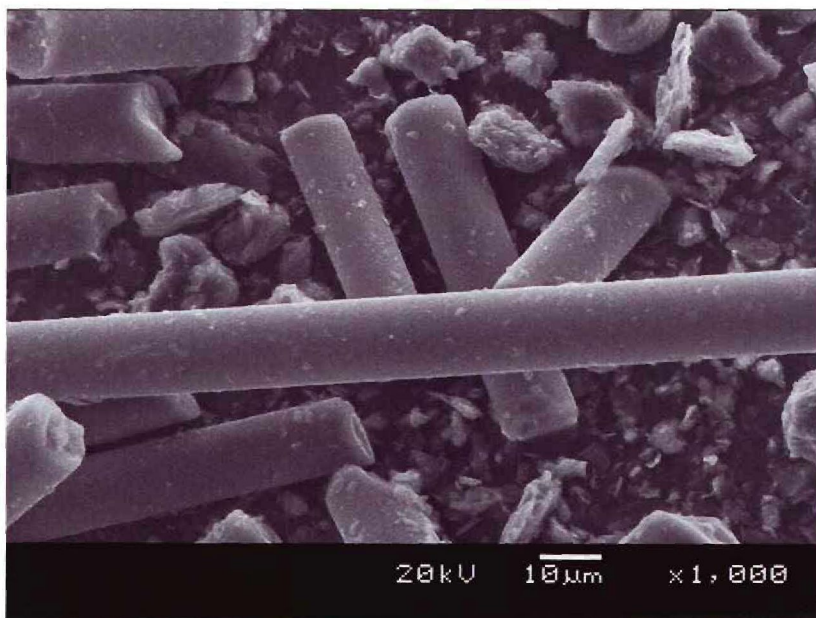


Figure 3.10: A SEM image of glass fibre-filler after depolymerisation

When the image is analysed it is observed that fine particular matter is still present on the fibre surface, which means that all of the polymer did not depolymerise completely. This observation was confirmed with experiments where the depolymerisation efficiency was determined. This is un-depolymerised PTFE. It is also observed that the filler does not only contain needle-like fibres, but also contains fine particular matter of $\sim 20 \mu\text{m}$ and smaller. More images will be discussed in Chapter 9.

3.3 CONCLUSIONS

- Four different reactor systems are used to study and prove different aspects of the depolymerisation of PTFE and other fluoropolymers. These are:
 - Depolymerisation of unfilled PTFE in a Drop-tube Reactor (Chapter 4);
 - Visual observation of the depolymerisation process using a laboratory scale Rotating-kiln Reactor (Chapter 9);
 - Depolymerisation of unfilled and filled PTFE using a Paddle Reactor on a continuous basis (Chapter 10);
 - Depolymerisation experiments evaluating other fluoropolymers using a simple Vibrating Reactor (Chapter 11).
- A variety of analytical methods are used to analyse the different samples (depolymerisation gas and solid particles) most effectively. These are:
 - GC to analyse the gaseous product on an in-line basis;
 - GC/MS to verify the GC analysis of the gaseous products on an *ad-hoc* basis;
 - TGA to measure the depolymerisation temperature of different fluoropolymers as well as the different filled PTFE samples. TGA was also used to determine the quantity of filler material in the filled PTFE samples. This method was further used for isothermal depolymerisation in order to determine the rate of the depolymerisation process at different temperatures and the activation energy;
 - SEM to visually observe the morphology of the filled PTFE samples as well as the filler material before and after it was used in PTFE. In the low vacuum mode (ESEM) with a heating stage the depolymerisation process of glass fibre-filled PTFE was recorded *in situ*.

The results obtained by means of these analytical techniques are presented in detail in the following chapters, where the specific research and the development on the different reactors and the parameters that were investigated, are presented.

Chapter 4

The Depolymerisation of Unfilled PTFE in a Drop-Tube Reactor

4.1. Introduction

4.2. Description of the depolymerisation equipment

4.2.1. Experimental setup

4.2.2. The process

4.2.3. The continuous feeding system

4.2.4. The Drop-tube Reactor

4.2.5. The quench probe

4.2.6. The vacuum system

4.3. Experimental method

4.4. Results and discussion

4.4.1. The formation of TFE

4.4.2. The formation of HFP

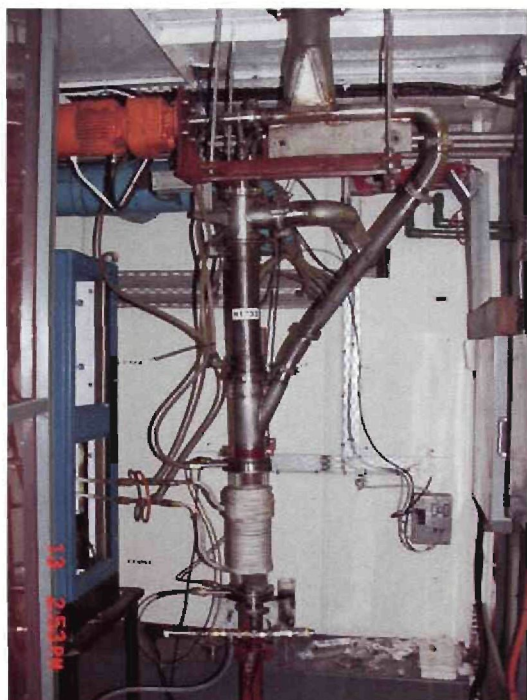
4.4.3. The formation of OFCB

4.4.4. The formation of HFE

4.4.5. The formation of other products

4.4.6. Local maxima for the main products TFE, HFE, HFP and OFCB

4.5. Conclusions



*I. J. Van Der Walt, O. S. L. Bruinsma,
Depolymerization of clean unfilled PTFE waste in
a continuous process, Journal of Applied
Polymer Science, 102, 3, 2752 – 2759 (2006).*

4.1 INTRODUCTION

As indicated in Chapter 1 and 2, the depolymerisation of unfilled PTFE waste by means of a continuous process was described by Van der Walt and Bruinsma⁽²²⁻²⁴⁾ and applied by Necca. However, much more investigation was needed to optimise this process and these investigations will form the basis of this chapter. This process was patented in 2002.⁽²⁴⁾ In this chapter the depolymerisation system, the Drop-tube Reactor, will be described and the experimental results, generated within an experimental window, between ~5 to ~80 kPa (abs) and between ~600 to ~900 °C will be presented.

4.2 DESCRIPTION OF THE DEPOLYMERISATION EQUIPMENT

4.2.1 Experimental setup

A schematic diagram of the Drop-tube Reactor is presented in Figure 4.1. It is also described in Chapter 3, Paragraph 3.1.2. No carrier gas was used in the process, resulting in higher purity products and therefore simplifying the separation process.

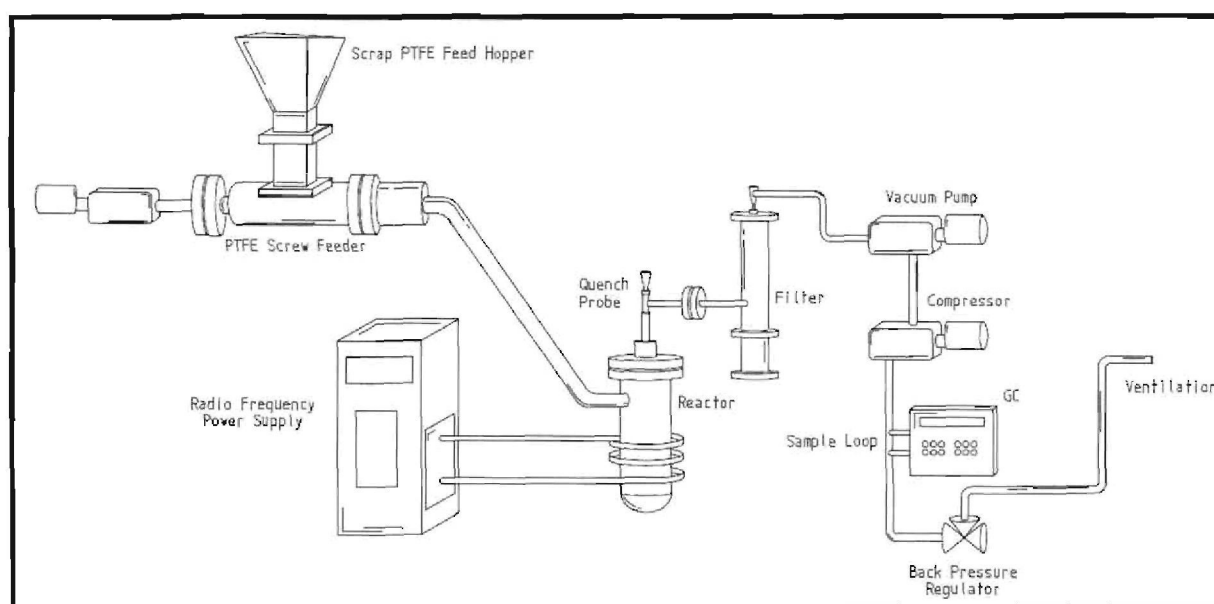


Figure 4.1: Schematic presentation of the Drop-tube system

A radio frequency (RF) power supply (induction generator) was used as a heating source. The energy efficiency of the induction generator was > 80 %. The RF

generator was operated at a frequency of 800 kHz and a maximum of 10 kW power could be applied. The main reason for using RF induction as a heating source was the advantage of quick start-up and shut-down times, and the quick response time for *in situ* temperature changes.

The Drop-tube Reactor consisted of a graphite crucible situated inside a quartz tube as described in Chapter 3 (Figure 3.1). This reactor was positioned inside the working coil of the induction generator which heated the reactor homogeneously in a relatively short time period (5 to 10 min) to the required operating temperature.

4.2.2 The process

The PTFE granules were continuously fed via a screw feeder into the reactor, where it was depolymerised. The product gas was evacuated through an automated self-cleaning quench probe, attached to the top of the reactor. A Gortex PTFE bag filter was used to remove any fine particulates that might still be present in the product gas stream after quenching. The product gases were analysed on-line with a gas chromatograph (GC).

The following equipment needed for the continuous Drop-tube Reactor system will be discussed: the continuous feeding system, the depolymerisation reactor and the quench probe.

4.2.3 The continuous feeding system

Consistent transport of the PTFE into the reactor is an important operating criterion. The feed rate of the PTFE must be carefully controlled to correlate with the capacity of the system and the amount of energy being supplied by the RF generator. An excessive feed rate can result in the reactor being blocked.

PTFE waste (shavings, off-cuts, used parts, etc.⁽⁵⁷⁾) comes in a wide variety of different shapes and sizes. These physical differences make it difficult to feed PTFE waste at a consistent continuous rate by means of a screw feeder. This problem was overcome by compressing the scrap PTFE at an elevated temperature (~450 °C) into billets and then granulating it into roughly equal-sized particles of 1 to 2 mm (Figure

4.2). These granulated particles were free-flowing and could easily be fed by the screw feeder without any blockages occurring.



Figure 4.2: Granulated PTFE particles (Units in cm)

In this system, PTFE was continuously fed to the screw feeder from a hopper that was connected to the top of the screw feeder body with a vacuum seal. This is schematically presented in Figure 4.3.

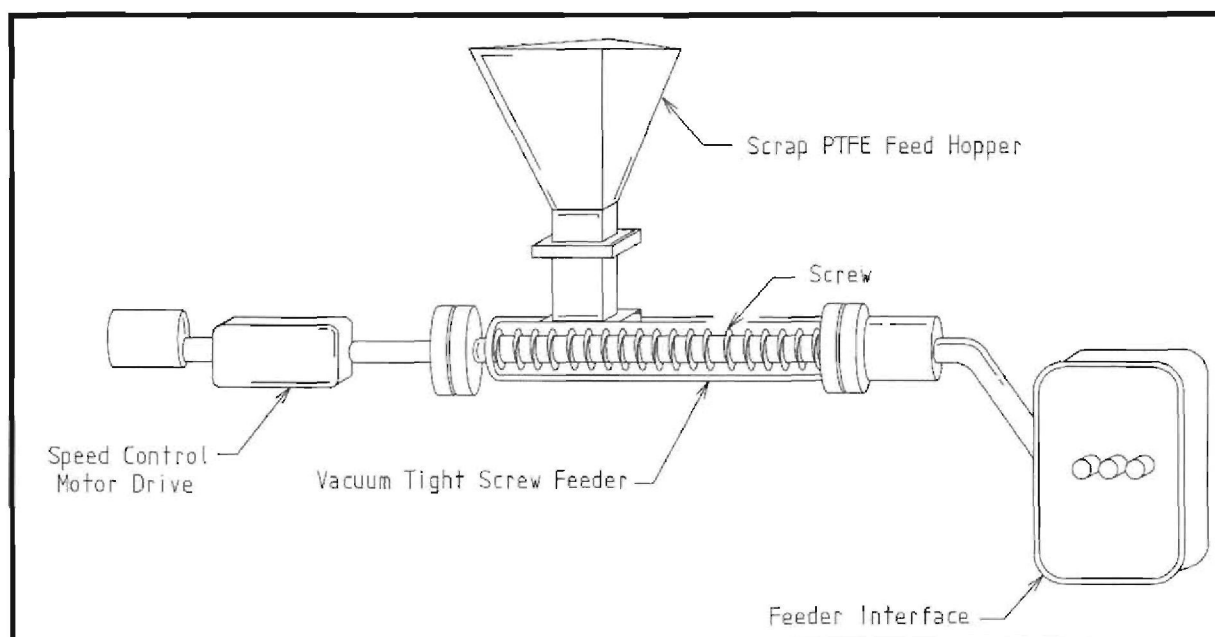


Figure 4.3: Schematic presentation of the PTFE feed system

A variable speed motor was used to regulate the rotating speed of the feeding screw. The reactor was situated below the feeder interface and the quench probe above, while the feeder inlet protruded from the side (see Figure 4.3). The feeder was calibrated according to the speed of the motor and was able to feed between 0.5 and 5 kg·h⁻¹. Because of the size and the design, the reactor was able to depolymerise a maximum of 2 kg·h⁻¹ PTFE on a continuous basis, which falls within the range of the feeder. Experiments at higher feed rates were performed, but blockages occurred because of droplet formation as a result of a high depolymerisation gas flow rate inside the reactor.

4.2.4 The Drop-tube Reactor

The Drop-tube Reactor consisted of a cylindrical graphite crucible (200 mm in length, 63 mm outer diameter and with a 5 mm wall thickness), situated inside a quartz tube (300 mm in length and 70 mm outer diameter with a 3 mm wall thickness). This reactor was situated inside the working coil of the RF generator as presented in Figure 3.1. The quartz tube enabled visual observation of the depolymerisation process inside the reactor as well as optical temperature measurements. The temperature of the reactor was measured by means of a Minolta Land Cyclops infrared optical pyrometer, suitable to measure temperatures between 600 and 3000 °C. According to the suppliers of this instrument, the temperature measurement was accurate within 0.5 %. The pyrometer was situated at a right angle to the reactor wall for temperature measurement in the middle of the wall.

4.2.5 The quench probe

Rapid quenching (up to 10⁶ °C·s⁻¹ as discussed in Section 3.1.2) is a very important process step to ensure high yield (> 93 %) of TFE, one of the primary products. This was achieved by means of an annular water-cooled, double-tube, self-cleaning quench probe (Figure 4.4). The quench probe consisted of an inner and outer annulus with scrapers. During operation the inner annulus was continuously rotated tangentially backwards and forwards with respect to the outer annulus. Any solid particles that deposited or re-polymerised on the walls of the quench probe were scraped off and fell back into the reactor, or were removed from the gas stream by

the filter. The vacuum system ensured transfer of the product gas through the annulus of the probe.

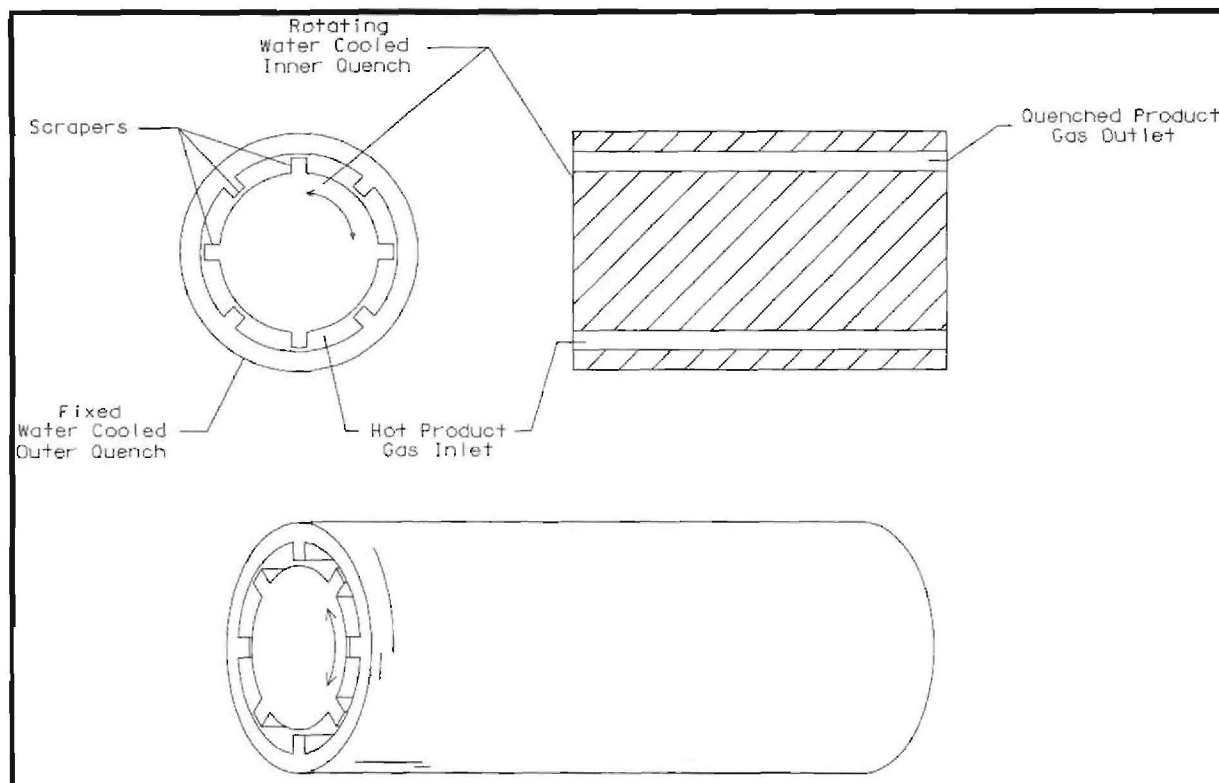


Figure 4.4: Schematic diagram of the quench probe

4.2.6 The vacuum system

A dry vacuum pump (Varian Star, $25 \text{ m}^3 \cdot \text{h}^{-1}$) was used to achieve the reduced pressures inside the reactor, as indicated in Figure 4.1. A dry pump was used to prevent the product from being contaminated with vacuum oil.

4.3 EXPERIMENTAL METHOD

A summary of typical experimental conditions for the continuous depolymerisation laboratory system is presented in Table 4.1. The system was operated continuously for 24 hours with in-line analyses performed at 30 minute intervals. Due to the complexity of the system, only one experiment per day could be performed. This caused the amount of experiments that were done to be stretched over a long period of time (1 year).

Table 4.1: Typical experimental parameters for the depolymerisation of unfilled PTFE in the Drop-tube Reactor

Parameter	Value
Power (kW)	1.82 to 5.04
Pressure (kPa (abs))	5 to 80
Temperature (°C)	600 to 900
PTFE feed rate (kg·h ⁻¹)	2.0
Energy input (MJ·kg ⁻¹ PTFE)	3.3 to 9.1

Depending on the required temperature, the electrical power supplied to the system varied between 1.82 and 5.04 kW. The feed rate of the PTFE was fixed at 2 kg·h⁻¹. An operational window, with respect to the temperature and pressure was chosen to perform the experiments in. The temperature window ranged from ~600 to ~900 °C and the pressure window between ~5 and ~80 kPa (abs.). The specific energy input for this system was calculated to be between 3.3 and 9.1 MJ·kg⁻¹.

4.4 RESULTS AND DISCUSSION

The depolymerisation product mixture invariably contained TFE, HFE, HFP and OFCB as the main products. When the depolymerisation parameters were kept constant, the concentration of the products, as determined by the on-line GC, varied by less than 5 %. During this 24 hour cycle no blockages occurred at a feed rate of 2 kg·h⁻¹. As calculated for the Drop-tube Reactor, with a PTFE feed rate of 2 kg·h⁻¹, the gas residence time was ~2 s. This calculation is explained in Appendix 1.

A summary of the experimental results is presented in Tables 4.2 to 4.5 and in Figures 4.5 to 4.8. The standard deviation for these results is 0.1 % for the species concentration and 7.5 % for the temperature.

Table 4.2: Product gas composition at ca. 600 °C and increasing pressure as determined by GC (Vol %)

T (°C)	P (kPa)	Feed rate (kg·h ⁻¹)	Power (kW)	C ₂ F ₆ (%)	C ₂ F ₄ (%)	C ₃ F ₆ (%)	C ₃ F ₈ (%)	c-C ₄ F ₈ (%)	PFIB (%)	Total gas yield (%)
607	5	2.0	1.82	ND	93.9	5.3	ND	0.7	ND	99.9
611	8	2.0	1.82	ND	93.5	5.6	ND	0.7	ND	99.8
609	16	2.0	1.82	ND	90.4	8.0	ND	1.5	ND	99.9
612	17	2.0	1.82	ND	88.1	9.3	ND	2.5	ND	99.9
603	22	2.0	1.82	ND	79.0	12.6	ND	8.3	ND	99.9
612	21	2.0	1.82	ND	81.4	12.4	ND	6.0	ND	99.8
603	52	2.0	1.82	ND	69.8	16.7	ND	13.4	ND	99.9
604	51	2.0	1.82	ND	70.3	16.5	ND	13.2	ND	100.0
623	82	2.0	1.82	ND	58.7	20.7	ND	20.4	ND	99.8
631	84	2.0	1.82	ND	55.0	22.4	ND	22.4	0.05	99.8

ND = Not Detected

Table 4.3: Product gas composition at ca. 700 °C and increasing pressure as determined by GC (Vol %)

T (°C)	P (kPa)	Feed rate (kg·h ⁻¹)	Power (kW)	C ₂ F ₆ (%)	C ₂ F ₄ (%)	C ₃ F ₆ (%)	C ₃ F ₈ (%)	c-C ₄ F ₈ (%)	PFIB (%)	Total gas yield (%)
701	5	2.0	2.4	ND	92.6	4.1	ND	3.1	0.2	100.0
704	9	2.0	2.4	ND	87.2	6.3	ND	6.4	0.1	100.0
706	14	2.0	2.4	ND	81.1	9.1	ND	9.6	0.1	99.9
713	14	2.0	2.4	ND	81.4	9.2	ND	8.9	0.3	99.8
708	20	2.0	2.6	ND	64.5	19.8	1.7	13.8	ND	99.8
706	21	2.0	2.6	ND	75.9	13.5	ND	10.4	ND	99.8
717	53	2.0	2.6	ND	45.1	31.9	1.1	21.3	0.4	99.8
715	53	2.0	2.6	0.7	39.6	38.5	1.3	19.0	0.5	99.6
720	82	2.0	2.6	1.8	18.1	48.0	3.2	27.5	1.1	99.7
720	82	2.0	2.6	2.4	23.5	45.3	1.7	25.1	1.7	99.7

ND = Not Detected

Table 4.4: Product gas composition at ca. 800 °C and increasing pressure as determined by GC (Vol %)

T (°C)	P (kPa)	Feed rate (kg·h ⁻¹)	Power (kW)	C ₂ F ₆ (%)	C ₂ F ₄ (%)	C ₃ F ₆ (%)	C ₃ F ₈ (%)	c-C ₄ F ₈ (%)	PFIB (%)	Total gas yield (%)
805	5	2.0	3.66	0.6	89.3	5.7	ND	4.2	0.1	99.9
809	9	2.0	3.66	0.7	81.1	12.0	0.2	6.1	0.5	99.9
806	11	2.0	3.66	0.8	76.5	15.9	0.3	6.2	0.1	99.8
815	14	2.0	3.66	0.9	63.7	28.1	0.6	6.3	0.2	99.8
813	14	2.0	3.66	0.5	63.3	32.6	0.8	2.4	0.2	99.8
827	21	2.0	3.7	3.3	30.0	59.9	2.6	3.5	0.4	99.7
825	21	2.0	3.7	2.3	32.9	57.0	2.0	5.1	0.5	99.8
812	56	2.0	3.99	16.9	13.9	58.2	6.3	3.4	0.9	99.6
817	52	2.0	3.99	15.8	14.8	60.6	5.0	2.7	0.8	99.7
801	82	2.0	3.56	11.8	17.0	58.7	4.3	7.1	1.0	99.9
805	82	2.0	3.56	9.0	12.8	61.0	4.5	10.7	1.7	99.7

ND = Not Detected

Table 4.5: Product gas composition at ca. 900 °C and increasing pressure as determined by GC (Vol %)

T (°C)	P (kPa)	Feed rate (kg·h ⁻¹)	Power (kW)	CF ₄ (%)	C ₂ F ₆ (%)	C ₂ F ₄ (%)	C ₃ F ₆ (%)	C ₃ F ₈ (%)	c-C ₄ F ₈ (%)	PFIB (%)	Total gas yield (%)
901	5	3.0	5.84	ND	0.5	80.2	16.1	ND	3	0.1	99.9
923	10	3.0	5.84	ND	0.4	78.5	17.9	0.1	2.4	0.5	99.8
927	9	3.0	5.84	ND	0.3	77.9	19.2	0.2	2	0.2	99.8
904	15	3.0	5.84	ND	0.6	72.1	22.3	0.3	3.9	0.7	99.9
902	17	3.0	5.84	ND	0.5	70.5	24.5	0.5	3.7	ND	99.7
907	20	3.0	5.84	ND	0.8	63.5	31.0	0.4	3.9	0.1	99.7
901	52	3.0	5.84	6.3	73.2	4.4	11.2	0.9	3.1	0.9	100.0
923	55	3.0	5.84	7.8	77.1	3.3	10.1	0.8	0.5	0.1	99.7
927	55	3.0	5.84	5.0	71.9	4.2	17.3	1.1	ND	0.2	99.7
904	83	3.5	5.84	ND	4.2	68.1	18.7	0.9	7.8	ND	99.7
902	83	3.5	5.84	ND	3.9	67.9	18.7	1.0	8.3	ND	99.8
903	82	3.5	5.84	ND	3.8	68.3	19.2	0.9	7.6	ND	99.8

ND = Not Detected

From these tables it is clear that TFE, HFP and OFCB are the main products of the depolymerisation of PTFE. The product HFE, although a major product at 900°C and 50 kPa, is a by-product as it does not have a significant commercial value. The products OFP and PFIB are low yield by-products at the depolymerisation conditions of the Drop-tube Reactor.

These products will be discussed in more detail by focussing on the maximum production rate conditions for the products that were analysed. A computer program called Axum 5.0B for Windows by Mathsoft, Inc. is used for the graphical presentation of the analytical data as a function of temperature and pressure. Axum uses the Marquardt-Levenberg nonlinear least squares algorithm to fit the curves.

4.4.1 The formation of TFE

When Figure 4.5 is analysed it is observed that in order to obtain a high TFE yield (volume %), two different experimental conditions can be applied: For yields of > 90 % TFE, a temperature of ~ 600 °C and a pressure of < 10 kPa, is needed. This high yield at low pressure gradually decreases with increasing temperature. Another high yield area at a temperature of 920 °C and a pressure of > 80 kPa is observed. At a temperature of 920 °C and ~ 50 kPa the TFE yield decreased to below 3.4 %. This might indicate the formation of other products, for example HFE and OFB.

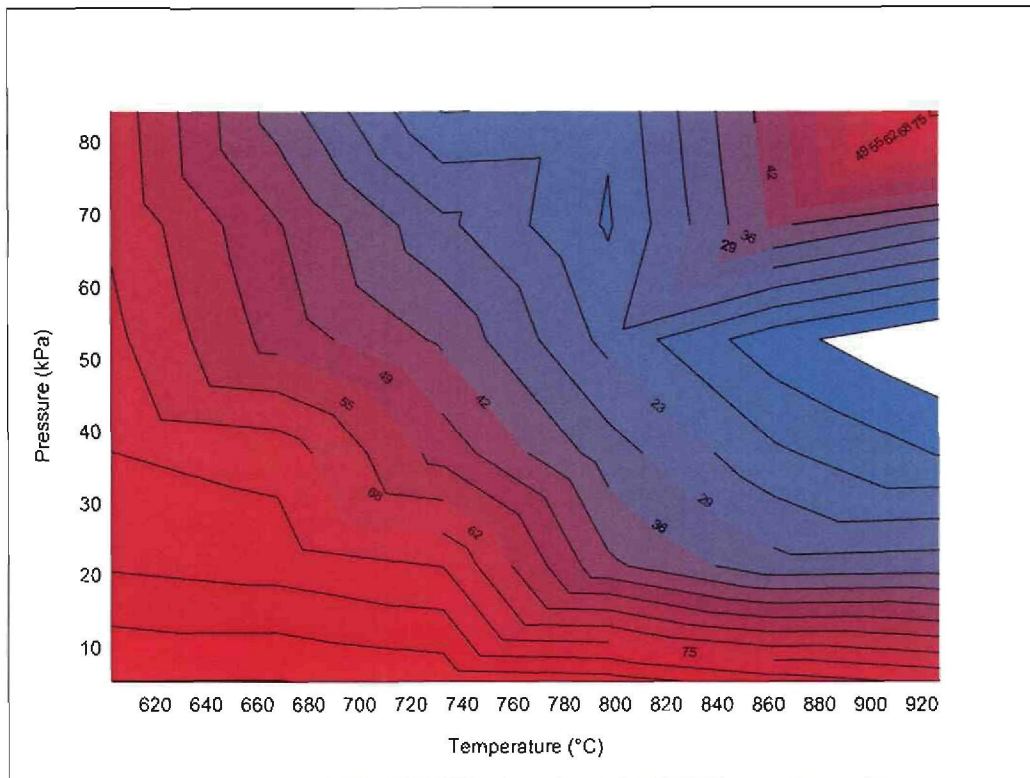


Figure 4.5: Concentration of TFE formed as a function of temperature and pressure

The high TFE yield found at low pressure and at 600 °C is in line with literature⁽¹⁻⁷⁾. This can be contributed to the depolymerisation process of PTFE. While it generally seems as if the TFE yield from the depolymerisation process is inversely proportional to the reaction temperature, another maximum for TFE production can be observed at ~900 °C and ~80 kPa which might indicate another mechanism at the high temperature conditions.

Obviously it is important to know what other compounds are formed at conditions where the TFE yield is low and also what impurities are present in the high TFE-yield regions.

4.4.2 The formation of HFP

Figure 4.6 is a presentation of the HFP yield over the temperature and pressure window. For maximization of the HFP yield, two experimental conditions could be identified. A sharp maximum of 64 % HFP was observed at a temperature of > 800 °C and a pressure of ca. 20 kPa. A much broader maximum of 57 % HFP was observed at a temperature of 800 °C and a pressure of 70 to 80 kPa. There is a definite trend to suggest that an increase in temperature and pressure will increase the HFP yield. HFP is a high-value, sought-after product and will be discussed in Chapter 12.

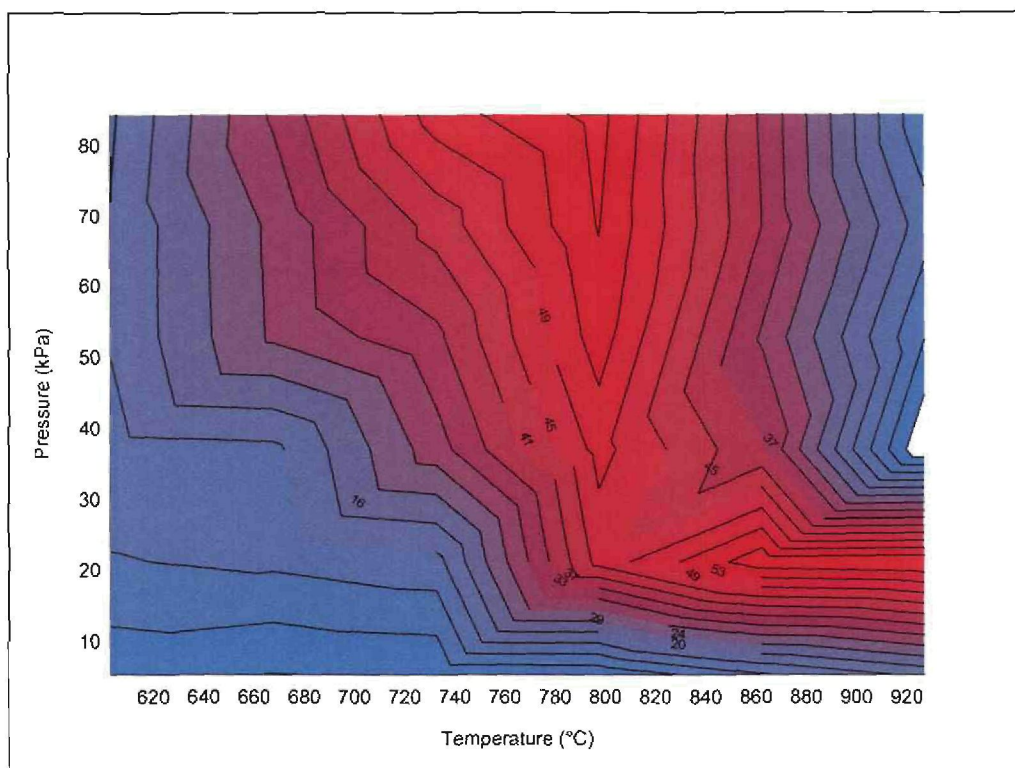


Figure 4.6: Concentration of HFP formed as a function of temperature and pressure

The HFP yields observed in this graph are in line with the literature⁽¹⁻⁷⁾. Even higher yields were observed in some cases⁽³⁵⁾. The HFP yield can generally be related to the temperature and pressure indicating that a high TFE molecule density (high pressure) and a high temperature is advantageous to HFP formation. The HFP graph seems to be the inverse of the TFE graph. This might indicate that at certain

experimental conditions TFE reacts to form HFP. At 80 kPa it seems that the HFP reaches a well defined Gaussian maximum, while at lower pressures, 20 to 40 kPa the maximum is distorted, probably by the formation of another product. A lower yield maximum is observed at 850 to 900 °C and 20 kPa. In this case another mechanism may be involved, but the two maxima are not significantly separated to be certain. HFP can also, under the right conditions, be converted back into TFE or OFCB.

4.4.3 The formation of OFCB

Figure 4.7 presents the OFCB yield within the operational window. A maximum OFCB yield of 25 % could be obtained at a temperature of 700 °C and a pressure of 80 kPa. There is a definite trend towards higher yields at higher-pressure conditions and at 700 °C. OFCB is a low-volume, high-value product (in terms of market demand) which is safe to manufacture and transport.

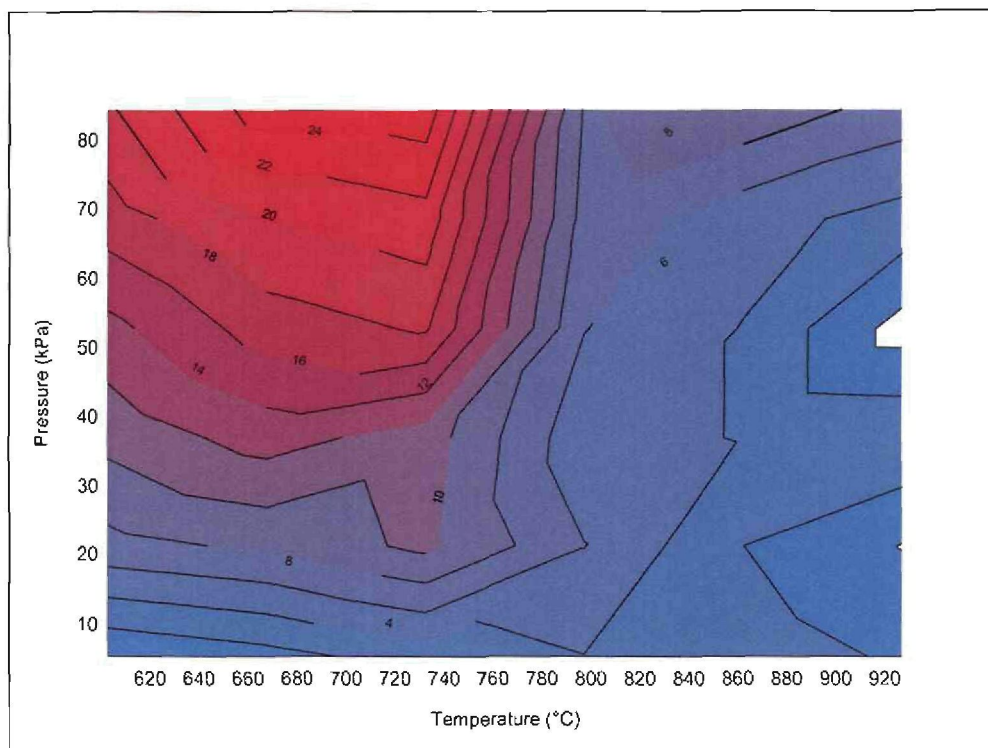


Figure 4.7: Concentration of OFCB formed as a function of temperature and pressure

The OFCB yield is in line with values found in the literature^(1-7, 35). The one prominent maximum peak indicates that only one mechanism is involved in the OFCB formation.

4.4.4 The formation of HFE

Figure 4.8 is a presentation of the HFE concentration within the experimental parameters. No HFE was detected at low-temperature and -pressure conditions, but at 700 to 900 °C, however, HFE was detected in significant amounts. The highest yield of 77.1 % HFE was recorded at 900 °C and 50 kPa.

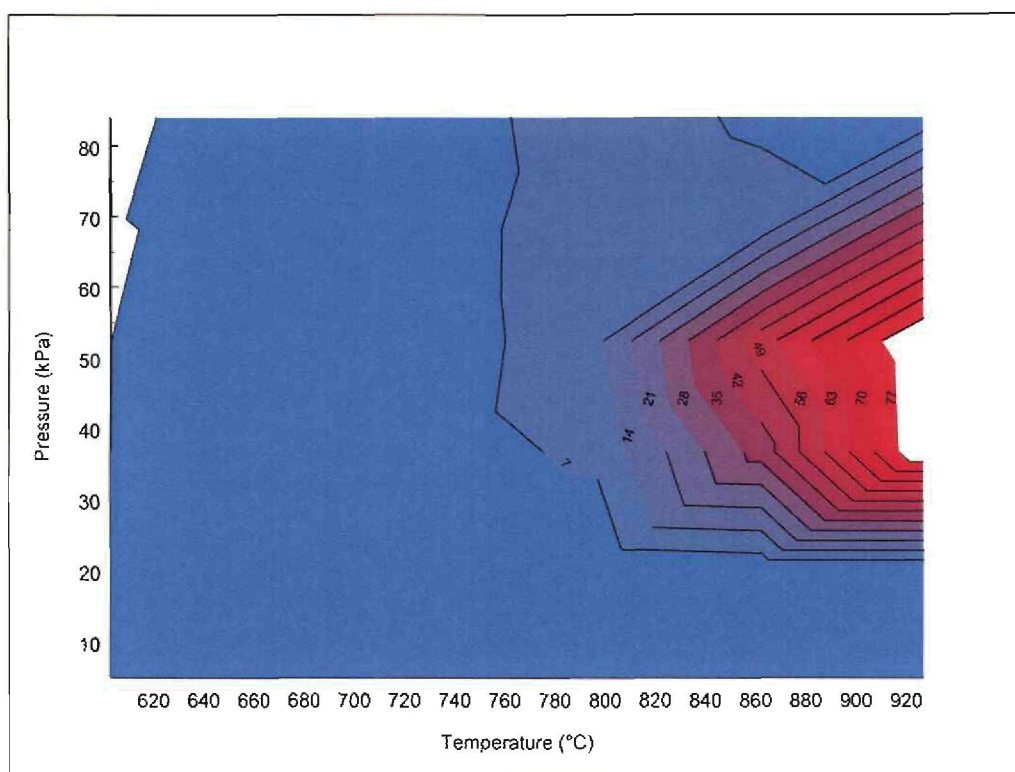


Figure 4.8: Concentration of HFE formed as a function of temperature and pressure

The formation of HFE was not quantitatively reported in the literature, but is unmistakable. The well defined maximum gives one a good indication of the process parameters where HFE could be formed and is also an indication that one mechanism is involved. TFM, HFE and OFP has an F/C ratio of > 3 while PTFE has a F/C ratio equal to 2. This is the reason why the formation of these products (mainly

HFE) is accompanied by the formation of a fine solid carbon deposition, either inside the depolymerisation reactor or in the filter. During prolonged experimentation this may cause operational problems. This is one reason to avoid depolymerisation at intermediate pressures (30 to 60 kPa) and temperatures above 800 °C.

HFE as well as other perfluorinated products are low-value products with limited use in the industry. For this reason it is regarded as a waste product in the fluorocarbon manufacturing process. Therefore, conditions should be chosen to minimise this product.

4.4.5 The formation of other products

Other perfluorinated products were also formed during depolymerisation: TFM, OFP, 1- and 2- octafluorobutylene and PFIB. The product TFM was only observed in significant, but low, yields at 900 °C indicating possible formation temperatures of > 900 °C. The minor product PFIB seems to form in slightly higher concentrations with increasing temperature. There also seems to be a direct relation to the pressure. These products will not be discussed in this chapter, but some of them are included in discussions in further chapters.

4.4.6 Local maxima for the main products TFE, HFE, HFP and OFCB

From Figure 4.5 to 4.8 local maxima of the different products could be identified and are presented in Table 4.6.

Table 4.6: Local yield maxima

	Concentration (Vol %)	Temperature (°C)	Pressure (kPa)
TFE	80 to 94	600 to 900	5
	68	900	82
HFP	61	800	82
	48	720	82
OFCB	27	700	84
HFE	77	920	55

The TFE yield reached a maximum of 94 % at low pressure and temperature. The yield gradually decreased as the temperature increased. The same trend was followed when the pressure was increased, but the yield was more sensitive to a change in pressure than in temperature. Another main product is HFP. The HFP yield had the opposite trend than TFE. Local maxima (48 % and 61 %) for HFP were observed at 720 and 800 °C and 82 kPa. The highest yield for OFCB was 27 % at 700 °C and 84 kPa. The trend showed that the yield might increase if the pressure could be increased. One of the unwanted products, HFE, showed a sharp increase in yield towards 900 °C and 55 kPa. As this is not a high-value product and HFE formation is accompanied by C formation, these reactor conditions must be avoided. TFM was only observed at 900 °C and PFIB in low concentrations over the whole temperature range. For production purposes the formation of these products must be minimised because of separation and toxicological constraints.

4.5 CONCLUSIONS

A $2 \text{ kg}\cdot\text{h}^{-1}$ continuous PTFE depolymerisation laboratory system, featuring a Drop-tube Reactor, was successfully developed, built, commissioned and tested. The system could be operated for 24 hours continuously without any problems.

It was found that the product composition is dependant on the pressure and the temperature at which the reaction takes place. Different ratios of the main products (TFE, HFP and OFCB), as a function of temperature and pressure, were obtained. The HFP yield reached maxima of 48 % and 61 % at 720 and 800 °C respectively at 82 kPa. The optimum TFE yield was obtained at 600 °C and 5 kPa and the optimum OFCB yield at 700 °C and 84 kPa. From this experimental data it is possible to predict maximum yields and product gas compositions (different ratios of HFE, TFE, HFP and OFCB) at reduced pressures and within a temperature range of 600 to 900 °C.

If a certain product is required, the operating parameters, to optimise the yield of this product, can be varied during operation. The formation of certain products should however be avoided. PFIB, for example, is toxic and TFM, OFP and HFE forms carbon deposits when produced, causing blockages. These products are also not high value products. The best conditions where the main wanted products (TFE, HFP and OFCB) are formed are 700 to 800 °C at 84 kPa.

Note that this is a research setup that is used to screen pressure and temperature conditions at short residence times in order to optimise the main products and to develop a chemical mechanism (Chapters 5 to 7).

A second mechanism seems to be responsible for additional formation of some of the main products such as TFE and HFP at higher temperatures. The formation of TFM, HFE and OFP is accompanied by subsequent carbon deposition.

This research can also be scaled up or modified for use of filled PTFE depolymerisation (Chapters 9 to 12)

Chapter 5

A Chemical Mechanism for Depolymerisation Product Formation

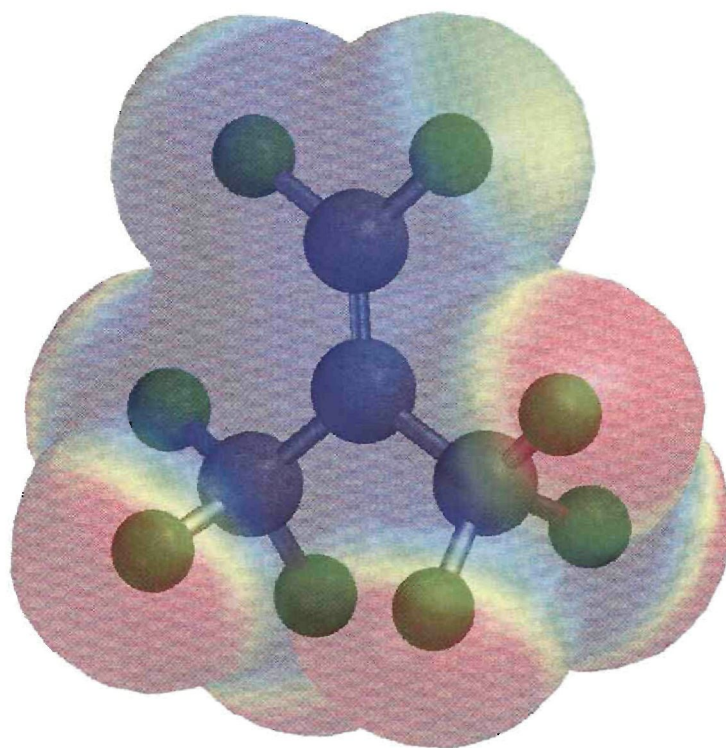
5.1. Introduction

5.2. The proposed reaction mechanism

5.2.1. Route 1 ($T = 600$ to 700 °C)

5.2.2. Route 2 ($T > 700$ °C)

5.3. Conclusions



5.1 INTRODUCTION

The depolymerisation process of PTFE is complex and involves many species and their reactions with each other. In this chapter a mechanism will be proposed to identify the possible dominant reactions involving the formation of the major species, tetrafluoroethylene (TFE), hexafluoroethane (HFE), hexafluoropropylene (HFP), octafluoropropane (OFP) and octafluorocyclobutane (OFCB). This proposed mechanism is based on the experimental data presented in Chapter 4 and the hypothesis is made that the mechanism proceeds according to a split mechanism. The first part of the mechanism dominates at low temperatures (600 to 700 °C) and the second part dominates at higher temperatures (700 to 900 °C). This is in contrast to some literature as discussed in Chapter 1.^(8, 35, 44) These authors proposed a single mechanism where TFE forms from PTFE and HFP and OFCB forms in a secondary reaction from TFE. The products TFM, HFE and OFP were not part of these mechanisms. They, however, have a higher F/C ratio than PTFE which will invariably lead to carbon deposition with negative operational and economic consequences.

For the purpose of this study it is accepted that the depolymerisation process proceeds according to the following series of events (as per reactor system in Chapter 4):

- The PTFE is fed into a hot reactor;
- Depolymerisation and thermal fragmentation of the polymer takes place inside the reactor;
- Intermediate gaseous fluorocarbon species form;
- Collisions occur between the intermediate species and the polymer fragments and thereby sometimes transferring a F atom to the intermediate species;
- Product formation starts to take place, which is a function of the reactor temperature, reactor pressure and residence time inside the reactor;
- At the quench probe the intermediate species are stabilised via rapid quenching;
- At the outlet of the quench probe a stable product mixture is found.

The products found after final quenching, therefore represent the stable final products after the above sequence of events have occurred, and do not necessarily reveal the reaction paths followed during their production.

5.2 THE PROPOSED REACTION MECHANISM

Following the results presented in Chapter 4, and taking into account the series of events as described above, the following mechanism is proposed:

PTFE consists of helical, un-branched chains of polymerized TFE monomers. When a polymer is exposed to thermal excitation ($> 400\text{ }^{\circ}\text{C}$) it undergoes cross-linking or chain scission. In PTFE random chain scission predominates with thermal excitation (initiation). When the depolymerisation results (Chapter 4) were analysed, it was found that a wider product variety was produced at high temperatures (700 to 900 $^{\circ}\text{C}$) than at low temperatures (600 to 700 $^{\circ}\text{C}$). At low temperatures only three major products were found namely TFE, HFP and OFCB. At high temperatures though, two more major products were formed, namely the perfluorinated products HFE and OFP and to a lesser extent TFM and PFIB. For this reason the following hypothesis is presented:

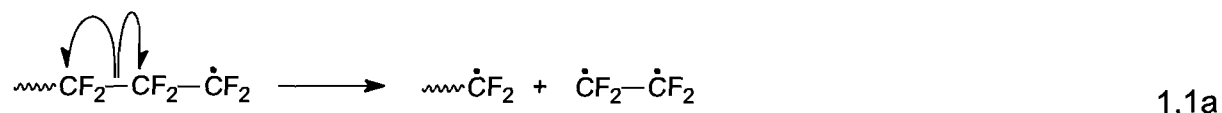
A two-part mechanism is proposed where depolymerisation or unzipping of the PTFE chain dominates the first route (hereafter called Route 1) at 600 to 700 $^{\circ}\text{C}$. Route 1 is dominated by the presence of the $\text{C}_2\text{F}_4^{\bullet\bullet}$ radical as intermediate species. During reactions conforming to the second mechanistic route (hereafter called Route 2), PTFE is pyrolysed into smaller fractions ($\text{CF}_2^{\bullet\bullet}$), at a temperature above 700 $^{\circ}\text{C}$. A hypothesis is made that F transfer reactions from PTFE and subsequent carbon formation are permitted at temperatures above 700 $^{\circ}\text{C}$.

The initiation reaction for the two routes is the same. Initiation takes place via random chain scission at depolymerisation temperatures. It is therefore accepted that for the purpose of this discussion, the depolymerisation process will start with a broken PTFE chain or a PTFE radical ($\text{---CF}_2\text{---CF}_2\text{---CF}_2^{\bullet}$)

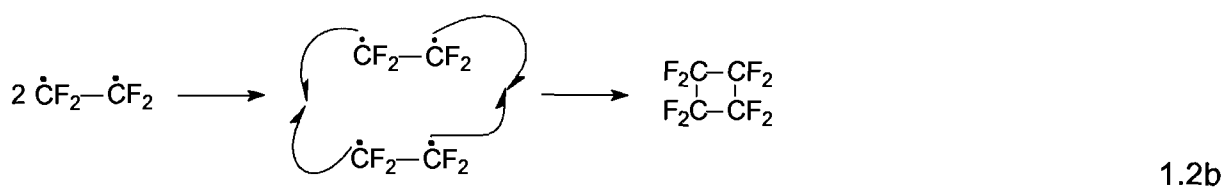
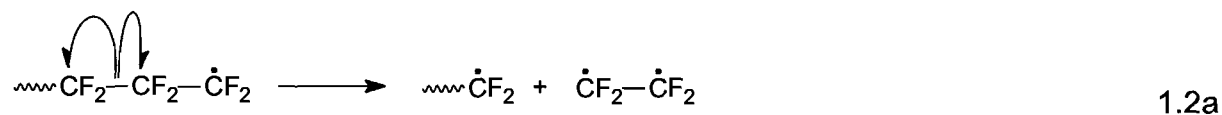
The proposed mechanism is represented by the following reaction equations in Routes 1 and 2, based on the results presented in Chapter 4:

5.2.1 Route 1 (T = 600 to 700 °C):

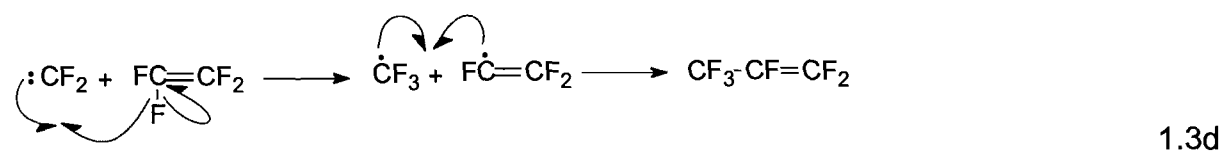
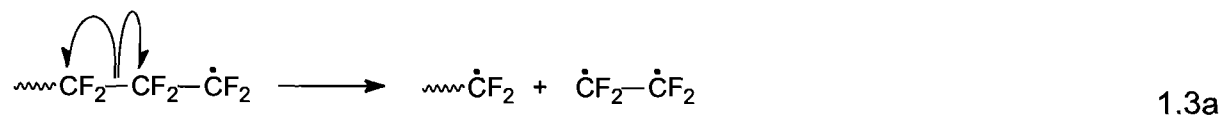
(1.1) TFE formation via unzipping:



(1.2) OFCB formation:



(1.3) HFP formation:



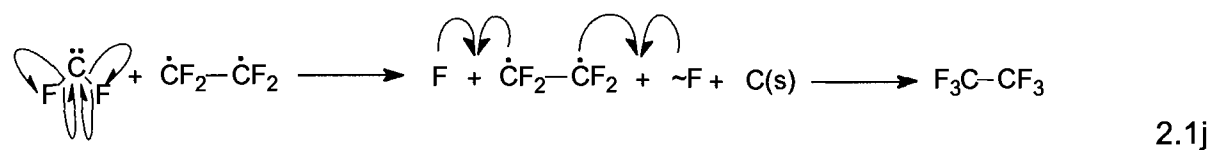
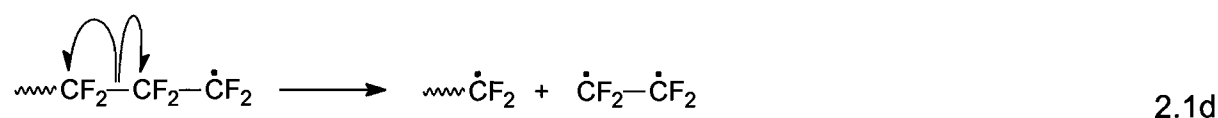
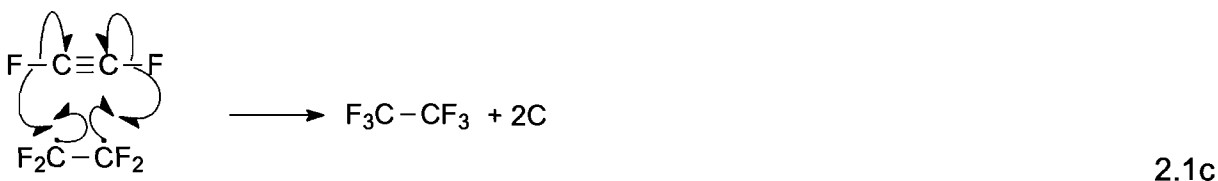
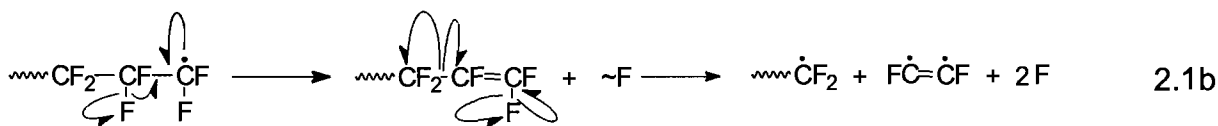
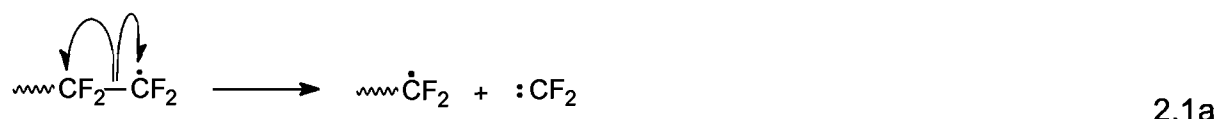
In Route 1, PTFE converts directly to a PTFE radical by the process of chain scission (1.1a). This PTFE radical can selectively form TFE, by the process of unzipping, forming a stable double bond (1.1b). This process, called unzipping, will be discussed in Chapter 7. The formation of HFP and OFCB is minimised by the low pressure because of a low radical concentration. At higher pressures though, the radical concentration becomes sufficient to promote the formation of HFP and OFCB. The product OFCB forms simply by a combination of two $\text{CF}_2\text{-CF}_2^{\bullet\bullet}$ radicals (1.2a and 1.2b). This is a very stable product and high yields can be obtained at the optimum pressure conditions. With the formation of HFP (1.3a to 1.3e), two $\text{CF}_2\text{-CF}_2^{\bullet\bullet}$ radicals combine, transfer a $\text{CF}_2^{\bullet\bullet}$ radical and form HFP and $\text{CF}_2^{\bullet\bullet}$. Combination of two of these $\text{CF}_2^{\bullet\bullet}$ radicals may also form a TFE molecule. A more plausible possibility is the combination of the $\text{CF}_2^{\bullet\bullet}$ radical with another $\text{CF}_2\text{-CF}_2^{\bullet\bullet}$ radical to also form HFP. These $\text{CF}_2^{\bullet\bullet}$ radicals are not stable at the low temperature conditions and will rapidly react. Experimental results in Chapter 4 confirmed Route 1 because of the high selectivity of TFE formation when PTFE was depolymerised at 10 kPa. At higher pressures HFP and OFCB were formed, but the TFE formation reaction still dominated.

5.2.2 Route 2 ($T > 700\text{ }^\circ\text{C}$):

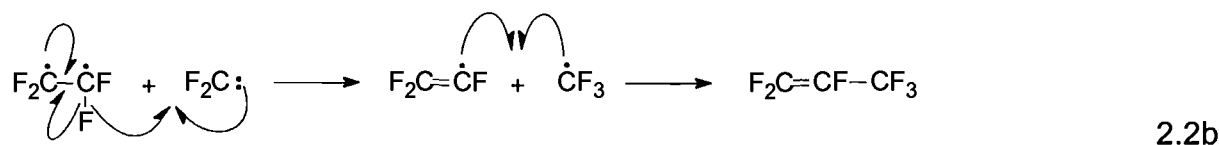
In Route 2, the formation of highly reactive intermediates like $\text{C}_2\text{F}_4^{\bullet\bullet}$, $\text{C}_2\text{F}_2^{\bullet\bullet}$ and $\text{CF}_2^{\bullet\bullet}$ as well as F transfer from PTFE is proposed. This route is not covered by literature. Under these conditions not enough thermal energy was applied for a free fluorine radical formation (Chapter 6, Figure 6.1), but transfer reactions from PTFE to radicals are permitted. This reaction is accompanied by a solid carbon deposition. The reaction mechanism is presented as follows for the formation of the main products: TFE, HFE, HFP, OFP and OFCB (Route 1 form the basis of Route 2):

2.1 HFE formation via F-transfer from PTFE:

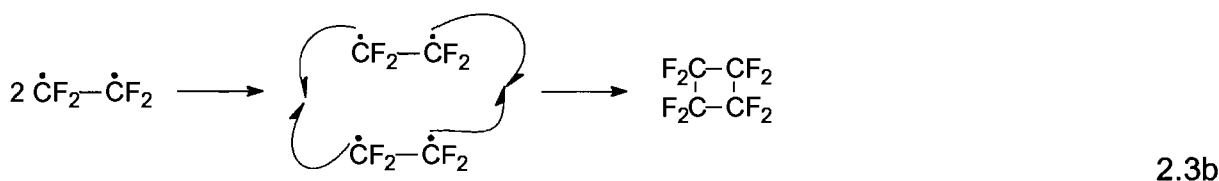
Only for illustration purposes will the fluorine, which is being transferred from PTFE, be indicated as $\sim\text{F}$. Thermodynamically, free fluorine does not exist in significant concentrations. Therefore a transfer reaction is proposed. This will be further discussed in Chapter 6 and 7.



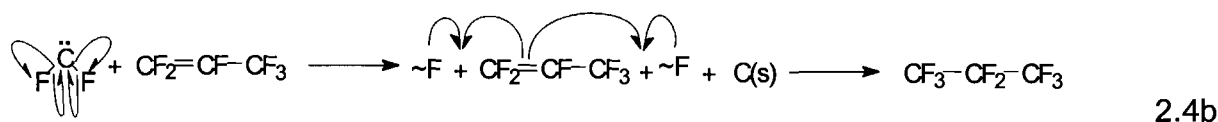
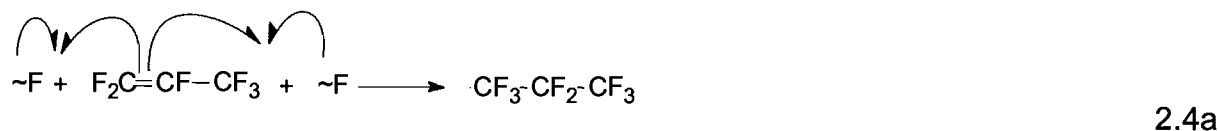
2.2 HFP formation via ••CF₂ radicals:



2.3 OFCB formation via ••CF₂ radicals:



2.4 OFP formation from HFP and F transfer from PTFE:



TFE, HFP and OFCB are formed via the same reactions proposed in Route 1. The formation of these products is also pressure-dependant. During the formation of HFE and OFP the formation of carbon would be expected. As indicated in Equations 2.1c, 2.1j and 2.4b, the presence of carbon was observed. This was also experimentally observed. For HFE and OFP to form the F/C ratio must increase implicating solid carbon formation.

Other octafluorobutylene (OFB) isomers including PFIB formed in insignificant amounts. For the purpose of this discussion, only the formation of OFCB is presented because it is the most abundant of the isomers.

5.3 CONCLUSIONS

In this chapter, a mechanism for the depolymerisation of PTFE is proposed. This mechanism is based on the experimental data generated in previous work as presented in Chapter 4. From this work it is concluded that the depolymerisation process follows two mechanistic routes: a low-temperature and a high-temperature route.

In the low-temperature route TFE, HFP and OFCB are formed as the main products while in the high-temperature route, HFE and OFP are also found as main products. Along with the main gaseous product formation a carbon deposit was formed because the F/C ratio increased with the formation of HFE and OFP

In further support of this mechanism, the next chapter will deal with the stability at equilibrium conditions of the intermediate species and products to distinguish whether the product distribution is close to equilibrium or whether reaction kinetics play a major role. In Chapter 7 a molecular modelling study will be made of the intermediate species, the transition state species as well as the product molecules and their formation energies in order to evaluate the mechanism proposed in this chapter.

In Chapter 8, TGA will be used in determining the activation energy of the depolymerisation process along with the rate constant and reaction order.

Chapter 6

Equilibrium Composition of PTFE Depolymerisation

Product Mixture:

A Thermodynamic Approach

- 6.1. General introduction
- 6.2. General background of chemical thermodynamics
- 6.3. Methodology and species selection
- 6.4. Equilibrium composition of depolymerisation species
- 6.5. Evaluation of the proposed Routes 1 and 2 reaction equations using experimental data and ΔG° values
 - 6.5.1. Background
 - 6.5.2. Proposed reactions and calculated ΔG values at 600 and 900 °C
 - 6.5.3. Discussion
- 6.6. Conclusions

$$\Delta G = \Delta H - T\Delta S$$

$$G = H - TS$$

$$H_i(T) = \Delta H_{f,i}(T_{ref}) + \int_{T_{ref}}^T C_{p,i} dT + \sum \Delta H_{tr}$$

$$\Delta G = \int_{p_1}^{p_2} \frac{nRT \cdot dp}{p} = nRT \cdot \ln \frac{p_2}{p_1}$$

$$G - G^\circ = RT \cdot \ln \frac{f \cdot \prod (a_i)^{\nu_i}}{f^\circ \cdot \prod (a_i)^{\nu_i}} = K$$

$$\Delta G = \Delta H - T\Delta S = \int_{p_1}^{p_2} \Delta V \cdot dp$$

6.1 GENERAL INTRODUCTION

In Chapter 4 the spectrum of gaseous PTFE depolymerisation products at different temperatures and pressures was presented. In Chapter 5, a hypothetical mechanism was proposed in order to explain the formation of the products observed. This mechanism supports the possibility of two routes, namely a route at the lower temperature region where the formation of TFE, HFP and OFCB is explained and a route at the higher temperature region where it is explained that HFE and OFP is additionally formed via F transfer reactions (F atoms are transferred from PTFE only at higher temperatures).

In this chapter, the equilibrium composition of the depolymerisation products and radicals will be calculated based on chemical thermodynamics. After a short overview of the background of chemical thermodynamics and the numerical methods to calculate multi-component product mixtures, the equilibrium product distribution will be generated in order to assess whether the products formed in the Drop-tube Reactor are at, or close to equilibrium.

A commercially available thermodynamic computer package, HSC Chemistry Version 5.1, HSC5.1⁽⁵⁸⁾, was used to perform all thermodynamic calculations. The conditions that were given as input parameters in the program are similar to the experimental conditions used in Chapter 4, namely temperatures between 600 and 900 °C, and pressures between 1 and 100 kPa.

Finally, the reactions in the proposed mechanism will be analysed. This will be done in order to qualify or disqualify the reactions in the proposed mechanism.

6.2 GENERAL BACKGROUND OF CHEMICAL THERMODYNAMICS

For a reversible process taking place at constant temperature and pressure, and involving a volume change V_1 to V_2 , the work done is $P(V_2 - V_1)$ or $P\Delta V$. The relationship between the net amount of energy available, or the Gibbs free energy (G) and the enthalpy of the system (H), is given by the following equations:^(59, 60)

$$G = H - TS \quad 6.1$$

S denotes the entropy of the system in $\text{kJ}\cdot\text{mol}^{-1}$. The basis for chemical thermodynamics is this Gibbs equation. The change in Gibbs free energy between two states of a system at constant temperature will be:

$$dG = VdP - SdT \quad 6.2$$

If G is integrated for a change in pressure at a constant temperature when the volume and pressure are known, then:

$$\Delta G = G_2 - G_1 = \int_{P_1}^{P_2} VdP \quad 6.3$$

If V is substituted by $V = nRT/P$, assuming that at moderate pressures the ideal gas law holds, we obtain:

$$\Delta G = \int_{P_1}^{P_2} \frac{nRT \cdot dP}{P} = nRT \cdot \ln \frac{P_2}{P_1} \quad 6.4$$

When the volume is not known, the fugacity (*f in bar*) is used. The fugacity is a thermodynamic function used in the place of partial pressure in reactions involving real gases and mixtures. The fugacity of a liquid or a solid is the fugacity of the vapour with which it is in equilibrium. The Gibbs free energy equation can then be described by the following at equilibrium conditions:

$$G = RT \cdot \ln f + B \quad 6.5$$

where B is a constant only dependant on the temperature and the nature of the substance. In order to determine the free energy a reference Gibbs free energy, G° , is introduced by:

$$G^\circ = RT \cdot \ln f^\circ + B \quad 6.6$$

and that

$$G - G^\circ = RT \cdot \ln \frac{f}{f^\circ} \quad 6.7$$

Now $f/f^\circ = a$ (activity). If a is substituted then:

$$G = G^\circ + RT \ln a \quad 6.8$$

For evaluation of the change in free energy:

$$\Delta G = \Delta G^\circ + RT \ln \frac{a_2}{a_1} \quad 6.9$$

where ΔG° is the standard Gibbs free energy in $\text{kJ}\cdot\text{mol}^{-1}$ and a_2/a_1 is the reaction activity ratio.

For the reaction $\nu_a A \leftrightarrow \nu_b B$ the equilibrium constant $K = (a_B)^{\nu_b} / (a_A)^{\nu_a}$.^(59, 60) At equilibrium conditions $\Delta G = 0$ and the equilibrium constant $K = a_2/a_1$. Therefore, at equilibrium conditions:

$$\Delta G^\circ = -RT \ln K \quad 6.10$$

where K , for a generalised reaction is defined as:

$$K = \frac{\prod_i (a_i^{\nu_i})}{\prod_j (a_j^{\nu_j})} \quad 6.11$$

where the indices i and j refer to the product and reagent species, respectively and ν_i and ν_j are the stoichiometric numbers in the reaction equation. A negative value for

ΔG thus gives an equilibrium constant, K , larger than 1, thus favouring the formation of the products from the reagents.

The enthalpies of the different compounds in the reaction occurring at temperature T are calculated as;

$$H_i(T) = \Delta H_{f,i}(T_{ref}) + \int_{T_{ref}}^T C_{p,i} dT' + \sum \Delta H_{tr} \quad 6.12$$

where T_{ref} is the reference temperature in K, (in this case 298.15 K), and ΔH_f is the enthalpy of formation, in $\text{kJ}\cdot\text{mol}^{-1}$, at the reference temperature. The heat of formation for a fluorocarbon compound is based on the reaction;



where the formation enthalpies of C and F are the reference enthalpies, equal to zero. The last term in the enthalpy equation accounts for the enthalpy changes in the form of phase transitions between T_{ref} and T .

The entropies of the different compounds are calculated as:

$$S_i(T) = S_i(T_{ref}) + \int_{T_{ref}}^T (C_{p,i} / T) dT' \quad 6.14$$

where the heat capacity is calculated with the Kelley equation:

$$C_p = A + B \cdot 10^{-3} \cdot T + C \cdot 10^{-5} \cdot T^{-2} + D \cdot 10^{-6} \cdot T^2 \quad 6.15$$

The four parameters A, B, C and D are available in the HSC5.1 database or can be obtained from other literature sources.^(61, 62)

The equilibrium composition is calculated using the Gibbs free energy minimization method where the most stable phase combination is found and the composition is

calculated where the Gibbs free energy for the complete system reaches its minimum, subject to mass balance and fixed temperature and pressure conditions as discussed by White W. B.⁽⁶³⁾ In the HSC5.1 package this numerical algorithm, called GIBBS, is used.

6.3 METHODOLOGY AND SPECIES SELECTION

A detailed procedural discussion of the HSC5.1 computer program is given in Appendix 2.

Fluorocarbon products in the HSC5.1 database

The CF-products contained in the HSC5.1 database are given in Table 6.1 and have been grouped in three categories: carbons, CF molecules and CF radicals.

Table 6.1: CF compounds in the HSC5.1 database.

Carbons		Molecules		Radicals	
Symbol	Compound	Symbol	Compound	Symbol	Compound
C(g)	Graphite	CF ₄ (g)	Tetrafluoromethane	CF ^{•••} (g)	Carbon monofluoride
C(D)	Diamond	C ₂ F ₂ (g)	Difluoroethyne	CF ₂ ^{••} (g)	Difluorocarbene
C(A)	Amorphous C	C ₂ F ₆ (g)	Hexafluoroethane	CF ₃ [•] (g)	Carbon trifluoride
C ₁₋₅ (g)	Gaseous C ₁ -C ₅	C ₂ F ₄ (g)	Tetrafluoroethene	C ₂ F [•] (g)	Fluoroethyne
C ₆₀ (g)	Fullerene gas	C ₄ F ₈ (g)	Octafluoro-2-butene	C ₂ F ₃ [•] (g)	Fluoroethene
C ₆₀ (s)	Fullerene solid	C ₄ F ₈ (g)	Octofluorocyclobutene	C ₂ F ₅ [•] (g)	Pentafluoroethyl
		C ₄ F ₁₀ (g)	Decafluorobutane	C ₂ CF ^{••} (g)	Monofluorocyclopropene ?
		C ₆ F ₆ (g)	Hexafluorobenzene	C ₃ F ₇ [•] (g)	Heptafluoropropyl
		C ₁₂ F ₁₀ (g)	Decafluorobiphenyl	C ₇ F ₈ [•] (g)	Perfluorotoluene
		F ₂ (g)	Difluorine	F [•] (g)	Fluorine

The main products that are not included in the HSC5.1 database are HFP and PTFE.

All of the products in the database were used when the equilibrium concentrations were calculated. Omission of some of these products might lead to inaccurate calculations.

6.4 EQUILIBRIUM COMPOSITION OF DEPOLYMERISATION SPECIES

To study the equilibrium composition with regard to thermodynamic considerations, all the fluorocarbon species in the HSC5.1 database were selected. Included in this species list was fluorine and carbon since they also play a part in the final depolymerisation product formation. For the calculation to be performed, 1 kmol of TFE was selected to act as carbon and fluorine source (starting material). The species TFE was chosen for the simulation, because of the F/C ratio of 2, which is the same as the F/C ratio of PTFE. As this is an equilibrium calculation it is not relevant which species is chosen for the starting material as long as the F/C ratio is 2.

All compounds in the HSC5.1 database

Figure 6.1 is a presentation of the equilibrium concentration for the species at a constant temperature of 700 °C over a pressure range of 1 to 100 kPa. The dominant reaction is the formation of carbon and CF₄, according to:



The other products only feature in very low concentrations, but can be observed when using the log scale. Although analytical detection of these species becomes problematic at concentrations lower than 10⁻³ mol, it is interesting to see that their formation is possible, but not in significant yields.

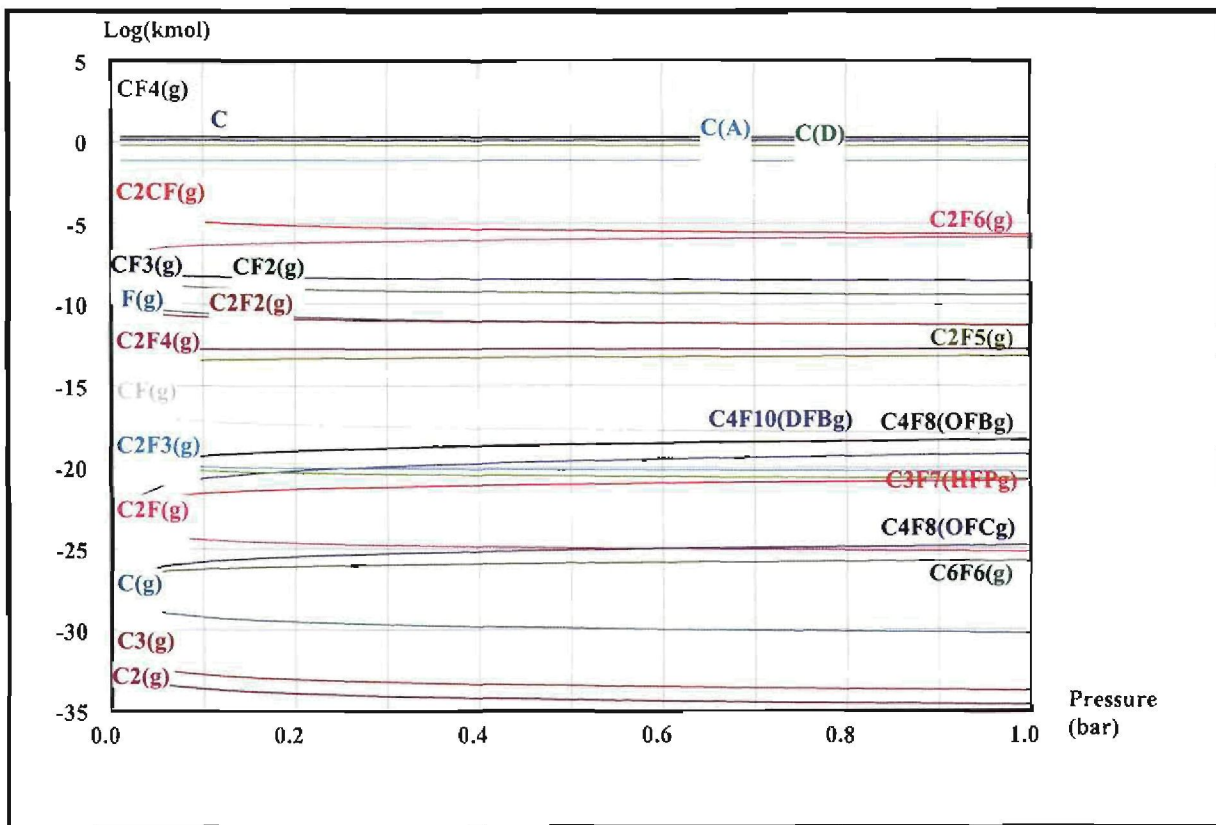


Figure 6.1: Equilibrium quantities at 700 °C from 1 kmol of C₂F₄. All fluorocarbon species included

To compare the species dependency on temperature, a similar equilibrium analysis was done where the pressure was kept constant at 100 kPa, and the temperature was varied between 25 and 1000 °C. This data is presented in Figure 6.2.

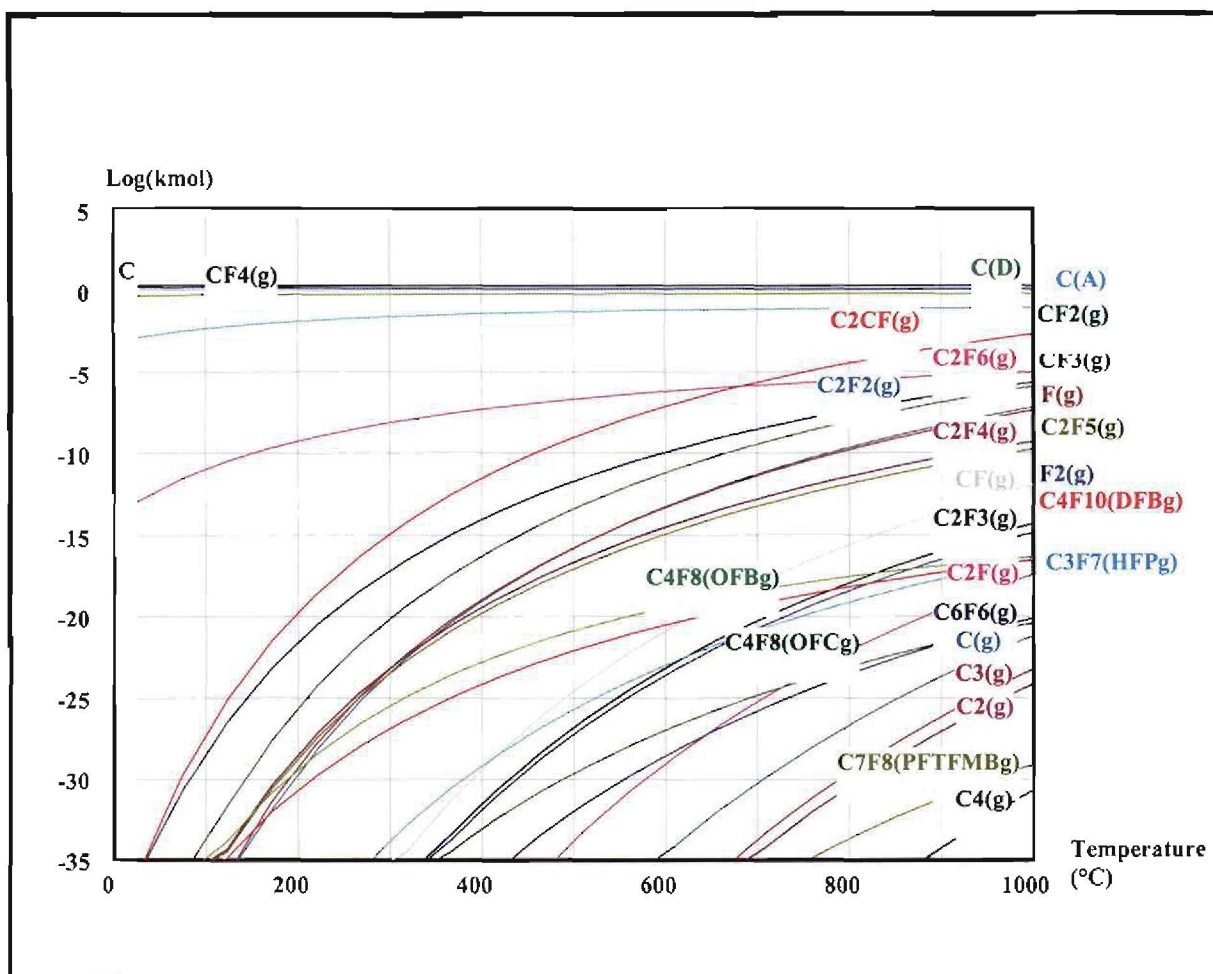


Figure 6.2: Equilibrium quantities at 100 kPa from 1 kmol C_2F_4 . All fluorocarbon species included

From Figures 6.1 and 6.2 it can be observed that the equilibrium distribution of the fluorocarbon species is more dependent on temperature than on pressure. Although the temperature dependence of the concentration is obvious, the species CF_4 and carbon are still thermodynamically favoured over the whole temperature range, but the radical species CF_2 , CF_3 , C_2CF and C_2F_2 are present in more substantial quantities at higher temperatures. The radical C_2CF does not form part of the proposed model and will be disregarded. The product C_2CF is an equilibrium species and was not observed during analysis, therefore stressing the kinetic dependence of the depolymerisation reactions.

The species presented in Figures 6.1 and 6.2 are the fluorocarbon species at equilibrium conditions with TFE as carbon and fluorine source. When these species are compared to the products obtained in Chapter 4, no correlation can be found,

because experimentally, CF_4 and carbon were only found in small concentrations at high temperatures (900 °C). The explanation seems obvious: kinetics rather than thermodynamics dictates product formation under the experimental conditions and short residence time that were used in the Drop-tube Reactor. An Ellingham plot of the fluorocarbon species, available in the HSC database, which might be involved in the depolymerisation product formation, is included in Appendix 3.

6.5 EVALUATION OF THE PROPOSED ROUTES 1 AND 2 REACTION EQUATIONS USING EXPERIMENTAL DATA AND ΔG° VALUES

6.5.1 Background

Under the conditions of Route 1 (low-temperature region), as discussed in Chapter 5, the unzipping reaction dominated the reactions, leading to the formation of mainly TFE as confirmed experimentally in Chapter 4. According to the proposed mechanism, the F transfer and formation of the $\text{CF}_2^{\bullet\bullet}$ radicals only start to feature significantly under the conditions of Route 2 high-temperature region. The reactions governing these mechanistic routes will be studied in this chapter using HSC5.1, and an attempt will be made to use thermodynamic considerations to qualify or disqualify the proposed reactions.

6.5.2 Proposed reactions and calculated ΔG values at 600 and 900 °C

The reactions for the formation of the four prominent products (C_2F_6 , C_2F_4 , C_3F_6 and *c*- C_4F_8) will be evaluated. The reactions and associated ΔG° values as calculated by HSC5.1 are presented in Table 6.2. No reactions with more than two reactant molecules were included in the mechanism as such reactions are highly unlikely to occur.

A thermodynamic evaluation of each proposed reaction was done by HSC5.1 and the change in the standard Gibbs free energy (ΔG°) for the reaction as a function of temperature is presented in Appendix 3. When ΔG° has a negative value the reaction

proceeds predominantly in a forward direction. When, on the other hand, ΔG° has a positive value the reaction takes place predominantly in the reverse direction.

Note that OFP is not part of the proposed products. The reason for this is that OFP does not form part of the HSC database and reaction calculations could therefore not be done. OFP is however regarded as a product and is subsequently included in the discussions in Chapter 7.

Table 6.2: The ΔG° values calculated by HSC5.1 for different reactions at 600 to 900°C

Reaction number	Chemical reaction	ΔG°_{600} (kJ·mol ⁻¹)	ΔG°_{900} (kJ·mol ⁻¹)
<i>TFE formation:</i>			
6.1	$C_2F_2(g) + 2F(g) \rightarrow C_2F_4(g)$	-603.76	-521.49
6.2	$CF_2^{**}(g) + CF_2^{**}(g) \rightarrow C_2F_4(g)$	-138.50	-87.12
<i>HFE formation:</i>			
6.3	$C_2F_4(g) + 2F(g) \rightarrow C_2F_6(g)$	-535.84	-486.11
6.4	$C_2F_4(g) + CF_2^{**}(g) \rightarrow C_2F_6(g) + C(s)$	-61.56	-53.78
6.5	$C_2F_4(g) + C_2F_2(g) \rightarrow 2C + C_2F_6(g)$	-85.58	-70.81
6.6	$C_2F_2(g) + 4F(g) \rightarrow C_2F_6(g)$	-1193.40	-1023.65
<i>HFP formation:</i>			
6.7	$C_2F_4(g) + CF_2^{**}(g) \rightarrow C_3F_6(g)$	-193.67	-184.01
6.8	$3CF_2^{**}(g) \rightarrow C_3F_6(g)$	-332.17	-271.12
<i>OFCB formation:</i>			
6.9	$C_2F_4(g) + C_2F_4(g) \rightarrow c-C_4F_8(g)$	-38.11	18.85
6.10	$C_3F_6(g) + CF_2^{**}(g) \rightarrow c-C_4F_8(g)$	17.06	115.74
6.11	$4CF_2^{**}(g) \rightarrow c-C_4F_8(g)$	-288.22	-155.38

Note that ΔG° is negative for all but two reactions (for the formation of OFCB, Equations 6.9 (except for the 600 °C ΔG° value) and 6.10). Reaction 6.10 and the high temperature Reaction 6.9 will therefore not be considered in further discussions. This is in contrast with the experimental data in Chapter 4, indicating that kinetic effects do play a significant role in the depolymerisation product formation process. It must also be noted that ΔG° generally becomes less negative at the higher temperatures. This shows that the equilibrium for these reactions shift to the left with an increase in temperature. Another important observation is that these reactions, in

a multi-component system, take part in the same reactant mixture and compete with one another for the formation of the same intermediate species at a given set of conditions. For this reason the different reactions cannot be compared to one another according to the ΔG° values only. The relative concentration of the intermediate species must be known for such a comparison to be made, but this falls outside the scope of this discussion.

6.5.3 Discussion

In this section an attempt has been made to reason why some reactions will take place more predominantly via Route 1 and others more predominantly via Route 2, with the experimental data of Chapter 4 as reference. All of the proposed reactions, for the two routes, are thermodynamically possible. During this reasoning it must be kept in mind that free fluorine is not available for reaction at the depolymerisation temperatures. It is therefore proposed that fluorine is transferred from the PTFE chain to a radical at higher temperatures due to a concerted F transfer reaction.

Route 1

Table 6.3 presents the possible reactions that will take place when Route 1 is dominating. These reactions were chosen because only TFE, HFP and OFCB formed as products at these conditions.

Table 6.3: Route 1 reactions at 600 and 700 °C

Reaction number	Chemical reaction
6.2	$2CF_2^{\bullet\bullet} \rightarrow C_2F_4$
6.7	$C_2F_4 + CF_2^{\bullet\bullet} \rightarrow C_3F_6$
6.9	$C_2F_4(g) + C_2F_4(g) \rightarrow c-C_4F_8(g)$

The temperature where Route 1 takes place is too low for significant amounts of fluorine transfer reactions to take place. For this reason all the reactions that make use of F transfer will not be considered for the low-temperature route. These include equations 6.1, 6.3, 6.4, 6.5 and 6.6. The reactions 6.1, 6.8, 6.11 are ternary or higher reactions and will also not be considered further.

Route 2

The products HFE and OFP (experimentally observed) can only form if there is a reaction between radicals and fluorine in order to increase the F/C ratio to a value greater than 2. Table 6.4 summarises the reactions that are proposed for the temperature range of 800 to 900 °C.

Table 6.4: Route 2 reactions at 800 and 900 °C

Reaction number	Chemical reaction
6.2	$2CF_2^{\bullet\bullet} \rightarrow C_2F_4$
6.4	$C_2F_4(g) + CF_2^{\bullet\bullet}(g) \rightarrow C_2F_6(g) + C(s)$
6.5	$C_2F_4 + C_2F_2 \rightarrow 2C + C_2F_6$
6.7	$C_2F_4 + CF_2^{\bullet\bullet} \rightarrow C_3F_6$
6.9	$C_2F_4(g) + C_2F_4(g) \rightarrow c-C_4F_8(g)$

The formation of HFE is accomplished by the reaction of an intermediate radical species ($C_2F_4^{\bullet\bullet}$ or $2CF_2^{\bullet\bullet}$) with C_2F_2 or PTFE via a fluorine transfer reaction. These reactions are accompanied by the deposition of solid carbon. According to experimental data, the formation of HFE was only observed at temperatures between 800 and 900 °C along with the formation of carbon. As fluorine transfer is necessary for HFE formation it can therefore be accepted that fluorine is not available for reaction at temperatures < 800 °C because these products are not found according to data presented in Chapter 4. Reactions 6.4, and 6.5, are therefore possible. More than one reaction is presented for the formation of some products because all the species reside in the same product mixture and one cannot distinguish between certain reactions taking place in preference to others.

This can only be done by measuring the rates of the individual reactions, and will not be done as part of this thesis.

6.6 CONCLUSIONS

The equilibrium concentration distribution does not correspond to the distribution of products found with the Drop-tube Reactor (Chapter 4). The dominant equilibrium reaction in the operating window is:



These products were not observed experimentally and therefore Reaction 6.17 is not the major reaction during the depolymerisation process in the Drop-tube Reactor.

No evidence could be found to support thermodynamics playing a role in the depolymerisation reactions, as investigated experimentally in Chapter 4. The conclusion is therefore made that the depolymerisation product formation, as presented in Chapter 4, is dominated by kinetics. It is anticipated that the product distribution will be different for longer residence times and that proper reactor design will play an important role in product yield optimisation. Another reactor with a longer gas phase residence time than the Drop-tube Reactor will be discussed in Chapters 10 to 12.

A number of reactions were evaluated according to their ΔG° values within a temperature range of 600 to 900 °C. Only combination reactions were considered, as it is proposed that the decomposition of gaseous products does not take place during the depolymerisation process. It was found (using the HSC5.1 thermodynamic computer program) that free fluorine is not available in significant amounts at temperatures below 1000 °C. In order for HFE and OFP to be formed it was proposed that fluorine transfer reactions takes place between the polymer and the radicals. These reactions only takes place during Route 2 reactions. The reactions that are presented in Tables 6.5 (Route 1) and 6.6 (Route 2) are all thermodynamically possible but thermodynamic considerations can not narrow the mechanism down further. For this purpose kinetic considerations needs to be employed.

Table 6.5: Route 1 reactions at 600 to 700 °C

Chemical reaction
$C_2F_4(g) + C_2F_4(g) \rightarrow c-C_4F_8(g)$
$C_2F_4 + CF_2^{**} \rightarrow C_3F_6$
$2CF_2^{**} \rightarrow C_2F_4$

Table 6.6: Route 2 reactions at 700 to 900 °C

Chemical reaction
$2CF_2^{**} \rightarrow C_2F_4$
$C_2F_4(g) + CF_2^{**}(g) \rightarrow C_2F_6(g) + C(s)$
$C_2F_4 + C_2F_2 = 2C + C_2F_6$
$C_2F_4 + CF_2^{**} \rightarrow C_3F_6$
$C_2F_4(g) + C_2F_4(g) \rightarrow c-C_4F_8(g)$

The final product composition presented by thermodynamics, does in most cases correspond to the composition determined experimentally, but the reactions proposed the ones with the least negative ΔG° values. For this reason these reactions are not the most likely reactions to take place, but the only acceptable ones from the proposed model. The reason for this phenomenon is most probably that kinetic effects overshadow those of thermodynamics.

Chapter 7

Molecular Modelling of PTFE Depolymerisation

7.1. Introduction

7.2. Molecular modelling

7.2.1. Molecular modelling background

7.2.2. Methodology

7.3. Modelling of the intermediates and products in PTFE depolymerisation

7.3.1. The intermediate species

7.3.2. The transition state molecules

7.3.3. The products

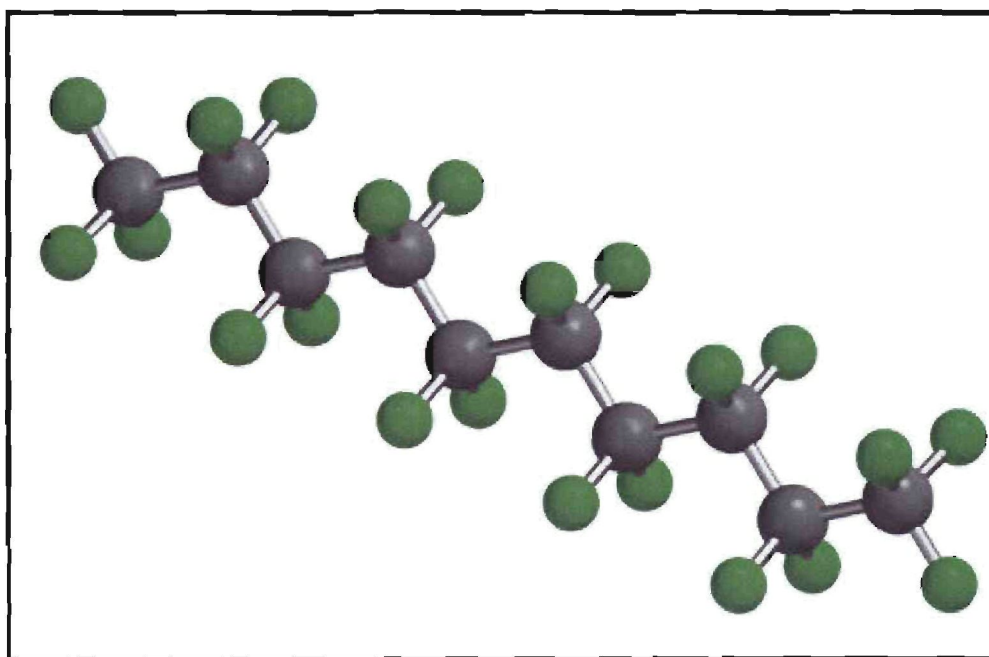
7.4. Discussion of the reactions in the two routes of the depolymerisation process

7.4.1. Route 1 of the proposed mechanism

7.4.2. Route 2 of the proposed mechanism

7.5. Conclusions

Parts of this chapter will be submitted for publication in the Journal of Fluorine Chemistry.



7.1 INTRODUCTION

The depolymerisation mechanism proposed in Chapter 5 was thermodynamically studied in Chapter 6. In this chapter, molecular modelling is used to study the depolymerisation products, their intermediate species and the reaction routes. The objective of this chapter is to propose a series of reactions for the depolymerisation and subsequent recombination reactions to form stable products, as determined by molecular modelling. Another objective is to support the thermodynamic observations (Chapter 6) from a molecular modelling point of view, by calculating the ΔH_f values of the geometrically optimised molecules and radicals involved in the proposed model (Chapter 5).

In this chapter a background of molecular modelling will briefly be given, after which a summary of the formation enthalpies ΔH_f of the different species involved in depolymerisation will be discussed. A different representation of the two mechanistic routes will be given and discussed based on the molecular modelling results. Finally, the calculated ΔH_f values will be used for drawing energy diagrams of the individual reactions within each mechanistic route. This will determine if a reaction will be endothermic or exothermic and identify the most probable reactions in order to propose the final depolymerisation mechanism.

7.2 MOLECULAR MODELLING

7.2.1 Molecular modelling background

The aim of molecular modelling is not to completely describe the molecule, but just the necessary parameters for a given situation. A good model is therefore a good representation of the molecule for a specific situation. Outside of the given situation the model may be a totally wrong representation.

A good example is the representation of sodium chloride. The formula for sodium chloride is NaCl and as such offers good representation of the stoichiometric composition of table salt, just as it having a cubic structure is a good representation

of the crystal structure thereof. The formula NaCl does however not give any information about the crystal structure of salt.

In the recent past the mathematical calculations involved in modelling were too complex for even the largest super computer. Computers are nowadays fast enough and have large enough storage capacity to be able to calculate various characteristics of a chemical reaction in a relatively short time. Even a personal computer is able to execute molecular modelling within a relatively short time, depending on the size of the system being investigated.

When chemical species are modelled, they can be simplified in order to make the calculation less complex. It is not advisable to try to model a chemical species and calculate the positional change for all the atoms in 1 mol of solution (6×10^{23} atoms for each mol)

Strictly speaking a molecule should be described by solving the Schrödinger equation for the specific molecule. This is a very complex method. An easier method is to use a mechanical model where wave mechanics are not used. Such a mechanical model is mathematically simple and gives fairly accurate results. For example, Figure 7.1 is a visual presentation of a geometrically optimised HFP molecule. In such a model the directions, bond lengths, bond angles and energies needed to twist these angles and lengths are described with mathematical equations. Bonds are described as stretching and bendable springs and Hook's law can be applied to this action.

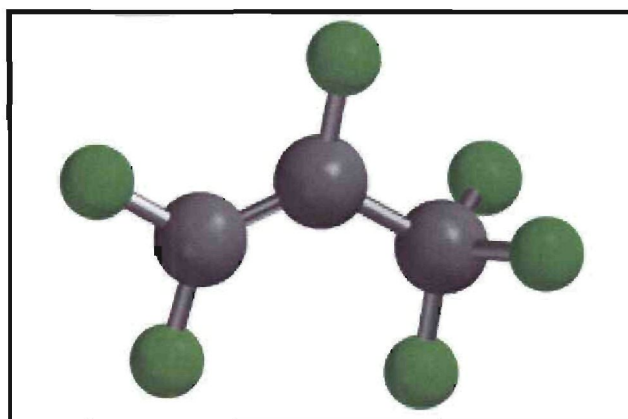


Figure 7.1: A geometrically optimised HFP molecule

7.2.2 Methodology

In this study a commercially available computer program from Wavefunction, called Spartan '04 v 1.0.3 was used.⁽⁶⁴⁾ The program was operated on a HP Intel Pentium IV 3.2 GHz computer and was used to model the depolymerisation products of PTFE, intermediate species and their transition states.

The steps required to perform this are:

1. *Choose the best modelling program.* The first step when an attempt is made to model a molecule is to choose a modelling program that supports the correct force fields and that is parameterised for the elements to be used. For this purpose a mathematical algorithm is used to obtain the minimum energy accurately in a short time;
2. *Perform a convergence action.* The bond lengths and angles are varied to find the minimum energy for the whole molecule;
3. *Find the local and/or global minima.* Some molecules such as C_6H_{12} can have more than one minimum of which one is that of the most stable isomeric structure (Figure 7.2). These stable minima are called the local minima and the most stable isomeric structure is called the global minimum. The modelling program will search for the most stable structure that is closest to the original drawing. This may only be a local minimum;

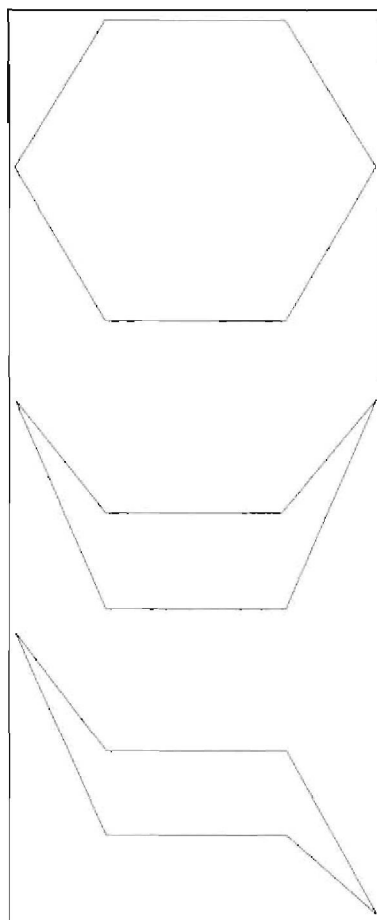


Figure 7.2: Different stereo isomeric structures of C₆H₁₂

4. *Perform thermodynamic calculations using quantum mechanical models.* The basis of the quantum mechanical molecule model is the Schrödinger equation. Simplifications must be adopted in order to apply this equation practically. Different quantum mechanical models used in the molecular modelling differ in degree of simplification;
 - a. *Ab initio methods:* Methods where the Schrödinger equation is adapted in order to model larger molecules are called *ab initio* methods. Hartree-Fock calculation methods are only used for molecules with a few atoms for which every electron can be accounted for. The Density Functional Theory (DFT) calculation method is another *ab initio* method used mainly when transition metal complexes are modelled. The Hartree-Fock method, in this case, is less successful and one of the reasons is that the atomic base sets are not combined to describe the very long distance interactions that are found at bond-breaking;

- b. *Open and closed peel (outer electron shell) systems*: A distinction is made between orbitals with one (open) or two (closed) spin electrons. The two orbitals are called α and β . This system is exceptionally adequate to describe radicals and paramagnetic molecules, for example the $\text{CF}_3\cdot$ radical where one orbital is empty and the other filled with one electron. This system is described by the Unrestricted Hartree-Fock (UHF). The Restricted Hartree-Fock model (RHF) is used for closed systems where both positive and negative spin are found in the same orbital for example a TFE molecule;
- c. *Semi-empirical methods*: Using only the valence electrons and only the most important overlaps in the atomic orbitals of the molecule a simplified calculation can be performed. The inner electrons will have very little overlap with the orbitals of other atoms and are seen as constant and are therefore parameterised. This method is called the semi-empirical method and much larger atoms than with *ab initio* methods can be modelled in a shorter time-span. To reduce the calculation time, the overlapping integral of orbitals that develop between different atoms must be eliminated and the error that is hereby created must be reduced. A variety of algorithms and sets of parameters were developed in order to decrease the calculation time for modelling of numerous molecules. Modified Neglect of Differential Overlap (MNDO) was one of the first models where s- and p-orbitals were successfully eliminated. The parameterising of MNDO version 3 (PM3) was an improvement on the MNDO method. These models are mainly used for modelling of organic molecules.

7.3 MODELLING OF THE INTERMEDIATES AND PRODUCTS IN PTFE DEPOLYMERISATION

In this study different modelling methods were evaluated and the results compared against values reported in the literature. For the modelling of depolymerisation products that would only contain fluorocarbons, it was found that the *ab initio* and DFT calculations did not give satisfactory energy values because the force-fields

were not parameterised for fluorocarbons. The depolymerisation molecules, radicals and transition state molecules were subsequently modelled with the PM3 semi-empirical method and the equilibrium geometry and formation energy results obtained coincided with published results as indicated in Table 7.1.^(61, 62)

Table 7.1: Comparison of modelled ΔH_f with published values

Molecule	Modelled ΔH_f	ΔH_f from Daubert & Danner ⁽⁶²⁾
TFM	-941.8	-933.2
HFE	-1329.6	-1343.9
TFE	-703.8	-658.6
OFFP	-1733.7	-1703.2
HFP	-1156.4	-1080.0
OFCB	-1573.2	-1528.0

From the results presented in Table 7.1, a good comparison was found from the modelled ΔH_f values and those published by Daubert and Danner. Therefore it was decided to use the PM3 semi-empirical method in all further calculations. The procedure to use the program is explained in Appendix 2.

Molecular modelling in this study was also done in order to investigate the proposed depolymerisation mechanism as described in Chapter 5. During the depolymerisation process the intermediate species form from the unzipping process. Before the depolymerisation molecules form, the intermediate species go through a transition state. These three steps are modelled and the results presented here.

7.3.1 The intermediate species

During the depolymerisation process, numerous intermediate species or radicals are produced. Modelling of these radicals is done by means of changing the multiplicity of the radical before the calculation is done. The multiplicity of a molecule reflects the number of the unpaired electrons therein. A neutral molecule with no unpaired electrons has a multiplicity of one. It is then said that this molecule is in the singlet state. If a molecule is a radical and has one unpaired electron, then the multiplicity is two. It is then said that such a radical is in the doublet state, and so on.

Some of the species like $\text{CF}_2^{\bullet\bullet}$, C_2F_2 may be in the singlet, doublet or triplet state. In some cases the same molecule may have local energy minima in the singlet as well as the triplet state, one of which is usually more stable than the other. This may be two electronic configurations, or different physical structures like a *cis* and a *trans* configuration of the same molecule. This may be important for the model because in certain cases the one configuration may be more susceptible to chemical attack than the other.

In this study, molecular modelling was done for a variety of depolymerisation intermediate species using PM3. The species investigated and their formation enthalpies ΔH_f ($\text{kJ}\cdot\text{mol}^{-1}$) are presented in Table 7.2.

Table 7.2: The intermediate species and their formation energies as calculated by molecular modelling

Radical formula	Formation enthalpy ΔH_f ($\text{kJ}\cdot\text{mol}^{-1}$)	Figure no./ Description
F atom Doublet	79.04	
$\text{C}_2\text{F}_4^{\bullet\bullet}$ Triplet	-571.10	Figure 7.3a
CF_3^{\bullet} Doublet	-558.70	Figure 7.5
$\text{CF}_2^{\bullet\bullet}$ Singlet	-205.39	Figure 7.4a
$\text{CF}_2^{\bullet\bullet}$ Triplet	-108.14	Figure 7.4b
$\text{C}_2\text{F}_2^{\bullet\bullet}$ <i>Cis</i> Triplet	124.81	Figure 7.6b
$\text{C}_2\text{F}_2^{\bullet\bullet}$ <i>Trans</i> Triplet	152.46	Figure 7.6c
$\text{C}_{10}\text{F}_{21}^{\bullet}$	-4188.62	$\text{C}_{10}\text{F}_{22}$ minus a F
$\text{C}_{10}\text{F}_{20}^{\bullet\bullet}$	-3875.30	
$\text{C}_{10}\text{F}_{19}^{\bullet}$	-3548.88	
$\text{C}_{10}\text{F}_{18}$	-3221.11	
$\text{C}_9\text{F}_{17}^{\bullet}$	-3137.31	
C_8F_{17}	-3399.44	
$\text{C}_9\text{F}_{18}^{\bullet\bullet}$	-3469.72	
$\text{C}_7\text{F}_{15}^{\bullet}$	-2983.39	
$\text{C}_6\text{F}_{13}^{\bullet}$	-2581.60	

The formation energy for an F atom and *Cis* and *Trans* $C_2F_2^{\bullet\bullet}$ are positive implicating the instability of these radicals at the depolymerisation conditions as set out in Chapter 4. The more negative the formation energy the higher the bonding energy per mol, so it is obvious that ΔH_f decreases with larger molecules, which in itself does not mean that a specific bond in a molecule is stronger or weaker.

The results obtained for some of the species at their most stable state, as calculated by the modelling program, are visually presented in Figures 7.3 to 7.6. Here the electron density (electron cloud) around a molecule is visually presented by animating the highest occupied molecular orbital (HOMO) electron cloud on the geometrically optimised species. A blue area represents an area with low electron density while the red area represents an area of high electron density.

The C_2F_4 and $C_2F_4^{\bullet\bullet}$ species

The two geometries for TFE, for example, could be optimised with the singlet multiplicity, in Figure 7.3a, and the triplet multiplicity, in Figure 7.3b. This occurs during the unzipping reaction of the PTFE chain, when the chain is split up into the monomer radicals and, under the correct conditions, forms TFE. The singlet TFE molecule in Figure 7.3a with an electron density of 23.4 e/au between the C-atoms and $\Delta H_f = -703.8 \text{ kJ}\cdot\text{mol}^{-1}$ is more stable than the triplet $C_2F_4^{\bullet\bullet}$ radical in Figure 7.3b with an electron density of 19.6 e/au between the C-atoms and $\Delta H_f = -571.1 \text{ kJ}\cdot\text{mol}^{-1}$. This higher electron density in the singlet molecule is an indication of a stronger bond and therefore a more stable molecule. This can be visualised when the highest occupied molecular orbital (HOMO) electron cloud is animated on top of the $C_2F_4^{\bullet\bullet}$ radical. Of the two, the TFE singlet molecule is more stable, as can be expected.

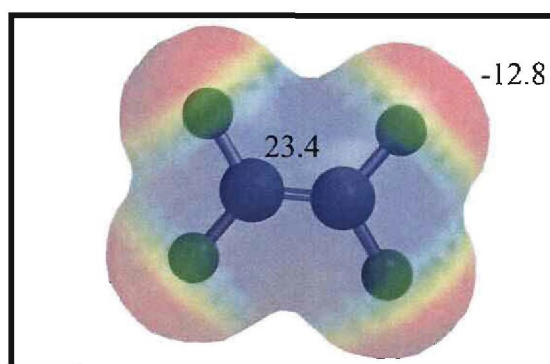


Figure 7.3a: C_2F_4 Molecule

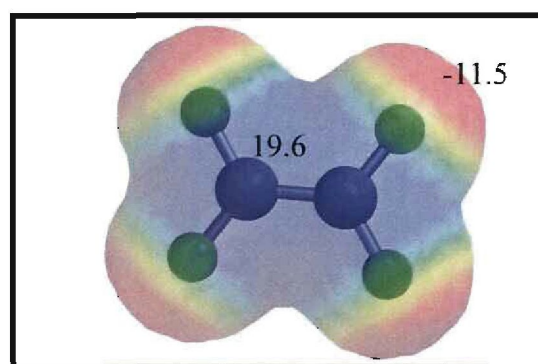


Figure 7.3b: $C_2F_4^{\bullet\bullet}$ Radical

The big atoms represent carbon and the small atoms represent fluorine.

The unit for electron density is given as electrons per atomic unit (e/au). The charges on the red and blue regions change slightly if the radical is compared to the molecule. The charge on the fluorine molecule only slightly differs from one another, while the charge on the two carbon atoms differs significantly. This is because the two unpaired electrons render the charge on the carbons more negative in the radical.

The CF₂•• singlet and CF₂•• triplet species

Another example is the CF₂•• radical (Figure 7.4), which can also have a singlet and triplet multiplicity. The singlet CF₂•• (Figure 7.4a $\Delta H_f = -205.39 \text{ kJ}\cdot\text{mol}^{-1}$) is more stable than the triplet CF₂•• (Figure 7.4b $\Delta H_f = -108.14 \text{ kJ}\cdot\text{mol}^{-1}$). This can be visualised when the highest occupied molecular orbital (HOMO) electron cloud is animated on top of the CF₂•• simulation. In the singlet molecule, the electron pair that was supposed to be situated on the carbon atom is hybridised into the electron cloud of the fluorine atoms. The electron cloud around the triplet CF₂•• radical, shows that the free electron pair is still positioned on the carbon atom, and the radical is not as polarised as the singlet radical.

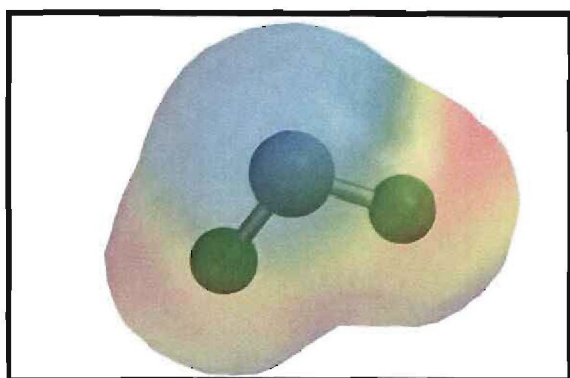


Figure 7.4a: CF₂•• Singlet

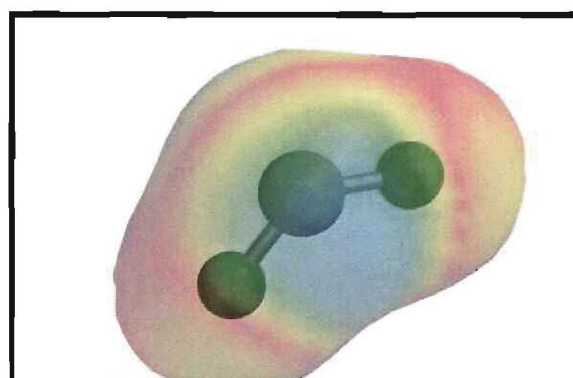


Figure 7.4b: CF₂•• Triplet

The CF₃• radical

The CF₃• radical (Figure 7.5) is more stable ($\Delta H_f = -558.70 \text{ kJ}\cdot\text{mol}^{-1}$) than the CF₂•• ($\Delta H_f = -205.39 \text{ kJ}\cdot\text{mol}^{-1}$) radical in Figure 7.4a. This is because the electrons are spread out more symmetrically over the radical. The carbon atom is situated slightly

out of the plane from the fluorine atoms. The one free electron is situated on the carbon atom and not delocalised with the other electrons. This is visualised by animating the highest occupied molecular orbital (HOMO) electron cloud onto the $\text{CF}_3\cdot$ radical.

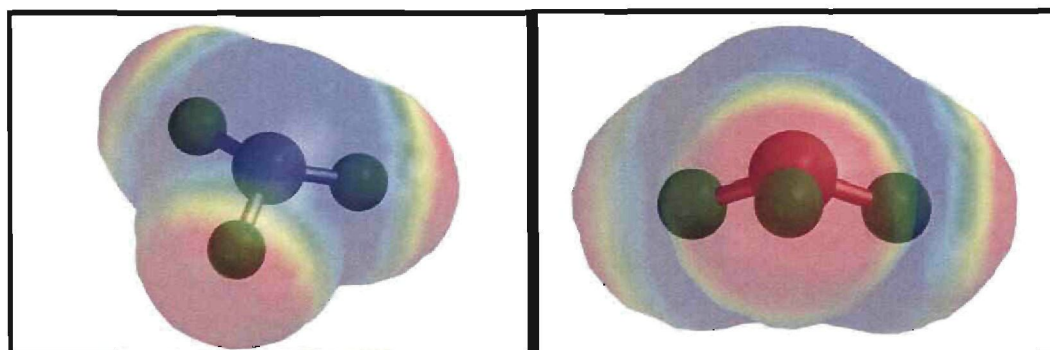


Figure 7.5: $\text{CF}_3\cdot$ Radical

The singlet C_2F_2 molecule and the cis and trans triplet $\text{C}_2\text{F}_2\cdot\cdot$ radicals

The singlet linear C_2F_2 molecule (Figure 7.6a) is more stable ($\Delta H_f = -48.43 \text{ kJ}\cdot\text{mol}^{-1}$) than the *cis* and *trans* triplet $\text{C}_2\text{F}_2\cdot\cdot$ radicals (Figure 7.6b and c) ($\Delta H_f = 124.81 \text{ kJ}\cdot\text{mol}^{-1}$ and $\Delta H_f = 152.46 \text{ kJ}\cdot\text{mol}^{-1}$ respectively) and therefore the singlet can be expected to feature in higher concentrations than the triplet radicals. When the electron densities are analysed, it is found that the *cis* radical is slightly polar. The *trans* radical and the linear molecule are non-polar. In the linear molecule the free electrons combine to form a more stable triple bond. This compound is not stable at ambient conditions, unlike its hydrocarbon counterpart acetylene, which is fairly stable. The highest occupied molecular orbital (HOMO) electron cloud is visualised by modelling this cloud onto the different C_2F_2 species.

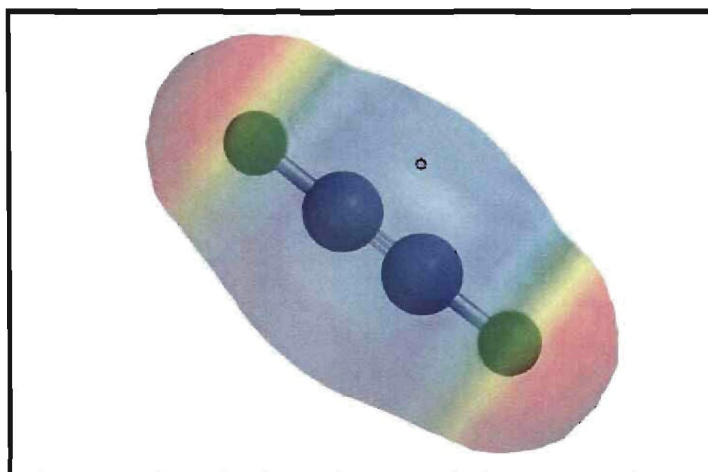


Figure 7.6a: C_2F_2 Singlet molecule

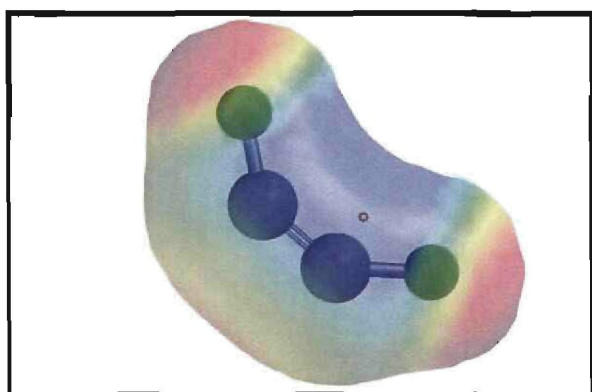


Figure 7.6b: $C_2F_2^{\bullet\bullet}$ *Cis* triplet radical

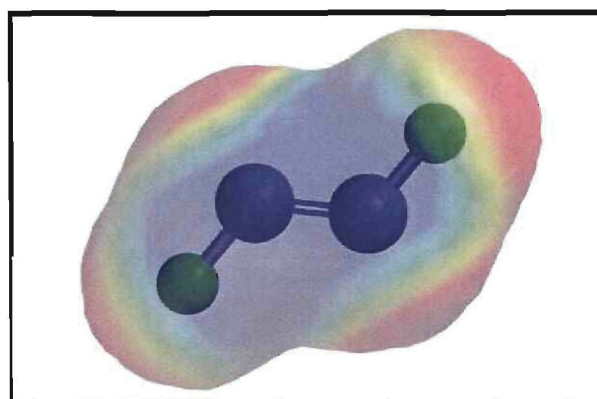


Figure 7.6c: $C_2F_2^{\bullet\bullet}$ *Trans* triplet radical

7.3.2 The transition state molecules

During the product formation- or termination process, intermediate species combine and form transition state products. These short-lived products will continue to react to form final products, because the final products are more stable than the intermediate species. In order for a transition state product to form, a certain amount of activation energy needs to be applied to the reactants. For the reaction to proceed exothermically, the formation energy (ΔH_f) of the reaction products must be lower than that of the reagents. Two specific transition states will be discussed, as they are of importance for the depolymerisation process.

The formation of an HFP molecule

When Spartan calculates a transition state molecule, the frequency calculation module must be activated. This function within the program enables one to obtain a fingerprint frequency table, which can be compared to an infrared spectrum of the

particular species. In addition an imaginary frequency might be calculated amongst the real frequencies. If this is the case, then a transition state molecule was simulated.

Figure 7.7 gives a visual presentation of the transition state that forms when two $C_2F_4^{\bullet\bullet}$ radicals combine to form HFP. This is only one step in a series of steps and therefore the double bond is already formed. This is part of the proposed mechanism for HFP formation as will be discussed shortly. Here it can visually be observed that the bond between the two carbon atoms, 1 and 2, of one of the $C_2F_4^{\bullet\bullet}$ molecules is breaking, while a bond is formed between carbon atoms 2 and 3. This already gives the propane chain of HFP. Together with this, the fluorine atom number 9 is shifted from carbon 3 to the newly added carbon number 2. The final step is the formation of the double bond between carbon atoms 3 and 4. In this process a HFP molecule and a $CF_2^{\bullet\bullet}$ radical are formed.

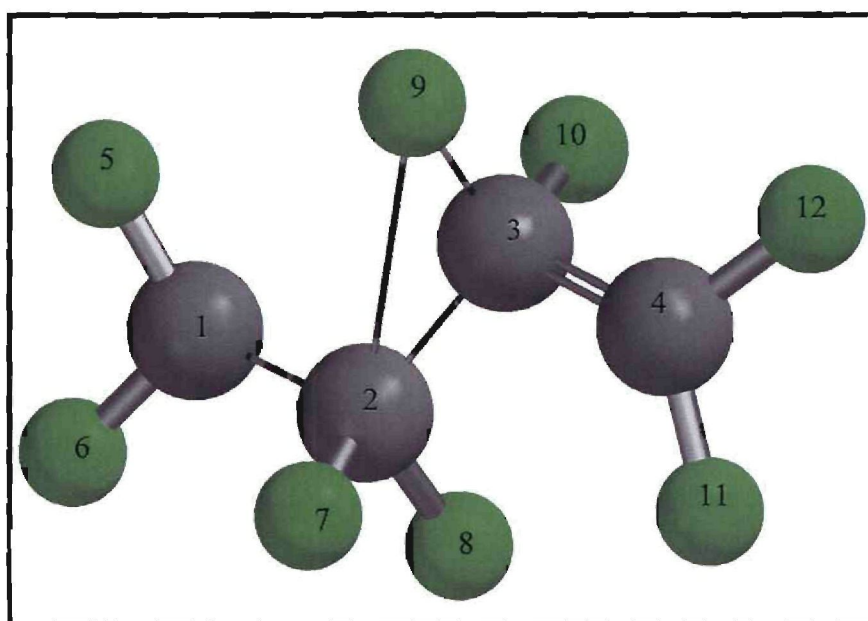


Figure 7.7: Visual presentation of the transition state for HFP formation

The energy diagram of this reaction is presented in Figure 7.8a. The determination of the energy diagrams of the different reactions will be discussed in Section 7.4 of this chapter.⁽⁶⁵⁾ From a kinetic perspective there can be four types of reactions as visualized in Figures 7.8 a to d.

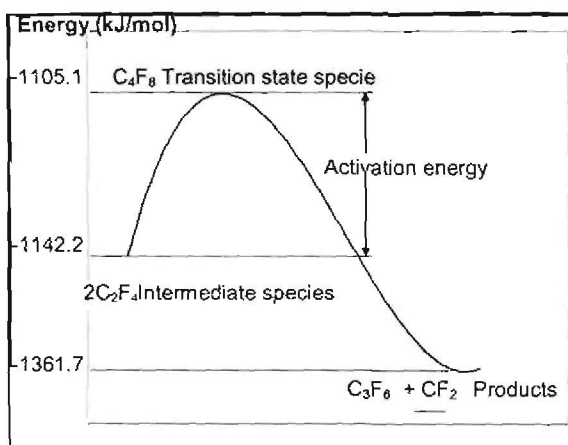


Figure 7.8a: An exothermic energy diagram of HFP formation with a transition state

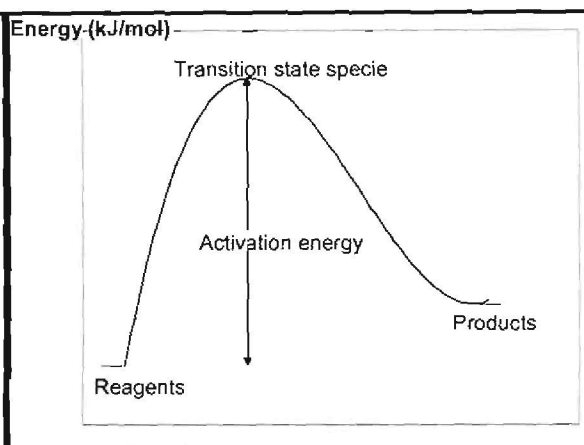


Figure 7.8b: A typical endothermic energy diagram with a transition state

Figure 7.8a is an example of a binary exothermic reaction with a transition state producing a stable end product as well as a radical that can participate in another propagation or a termination reaction.

In Figure 7.8b the activation energy, which is larger than the enthalpy difference between the reagents and the products, determines how the reaction rate depends on the temperature.

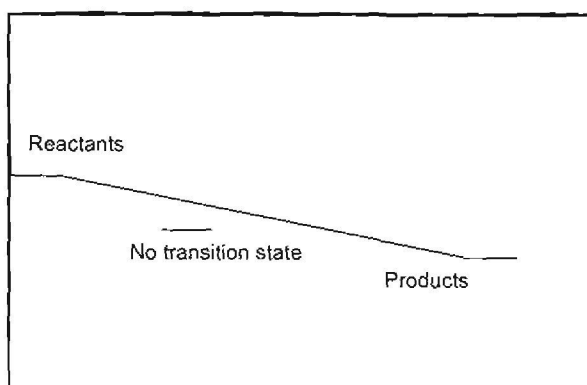


Figure 7.8c: A typical exothermic energy diagram without a transition state

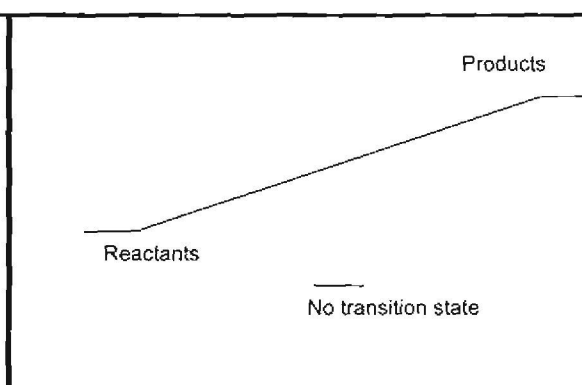


Figure 7.8d: A typical endothermic energy diagram without a transition state

In Figure 7.8c the enthalpy difference between the reagents and products is negative indicating that there is no activation energy. This is an exothermic reaction with no transition state molecule involved.⁽⁶⁵⁾

In Figure 7.8d the enthalpy difference between the reagents and products is in fact the activation energy. This is an endothermic reaction and there is no transition state molecule involved in this reaction.⁽⁶⁵⁾

In order to minimise energy and to use all the radicals with the HFP formation, three $C_2F_4^{\bullet\bullet}$ molecules react in a $CF_2^{\bullet\bullet}$ exchange reaction as indicated in Figure 7.9. When this reaction takes place, two HFP molecules will form.

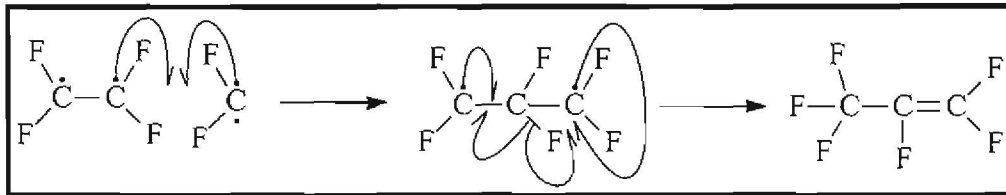


Figure 7.9: Electron movement with HFP formation

The formation of a CF_3^{\bullet} radical

For further illustration purposes Figure 7.10 is a visual presentation of a transition state PTFE molecule transferring a fluorine to a $CF_2^{\bullet\bullet}$ radical in order to yield a CF_3^{\bullet} radical. This reaction will be discussed in Section 7.4.2.

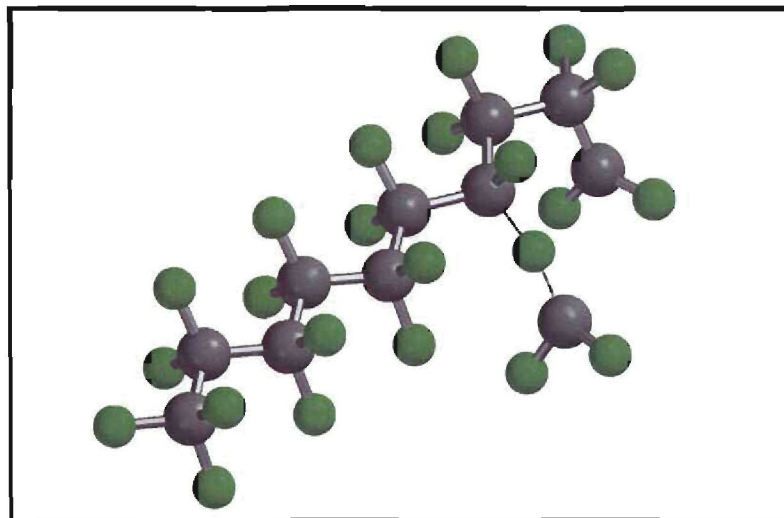


Figure 7.10: PTFE and CF_2 transition state species

Table 7.3 summarises the reaction enthalpies of the reactions, where the transition state molecules does not affect the reaction enthalpy of the particular reaction in the PTFE depolymerisation process. All the F atoms represent a C₁₀F₂₂ PTFE chain loosing an F atom in a transfer reaction.

Table 7.3: Reaction enthalpies of reactions without activation energies or transition state molecules

Formula of transition state molecule	Formation enthalpy ΔH_f^\ddagger (kJ·mol ⁻¹)	Reaction enthalpies (kJ·mol ⁻¹)	Descriptive reactions
2CF ₂ ••	-412.82	-293.04	2CF ₂ •• → TFE
C ₂ F ₄ ••	-596.00	-132.72	C ₂ F ₄ •• → TFE
C ₂ F ₄ •• + 2F	-1321.67	-40.87	C ₂ F ₄ •• + 2F → HFE
c-C ₄ F ₈	-1187.39	-431.04	2C ₂ F ₄ •• → OFCB

For these reactions the ΔH_f^\ddagger value is smaller than the ΔH_f for the starting molecule/s (Figures 7.8c and d). Therefore it is plausible to accept that these exothermic reactions will proceed without a transition state and thus without an activation energy (ΔH_f products - ΔH_f reagents).

Table 7.4 summarises the activation energies needed for the reactions to proceed towards the endpoint. These reactions are all exothermic reactions, meaning that ΔH_f products < ΔH_f reagents. Transition state molecules play a significant role in these reactions.

Table 7.4: Activation energies of reactions with transition state molecules

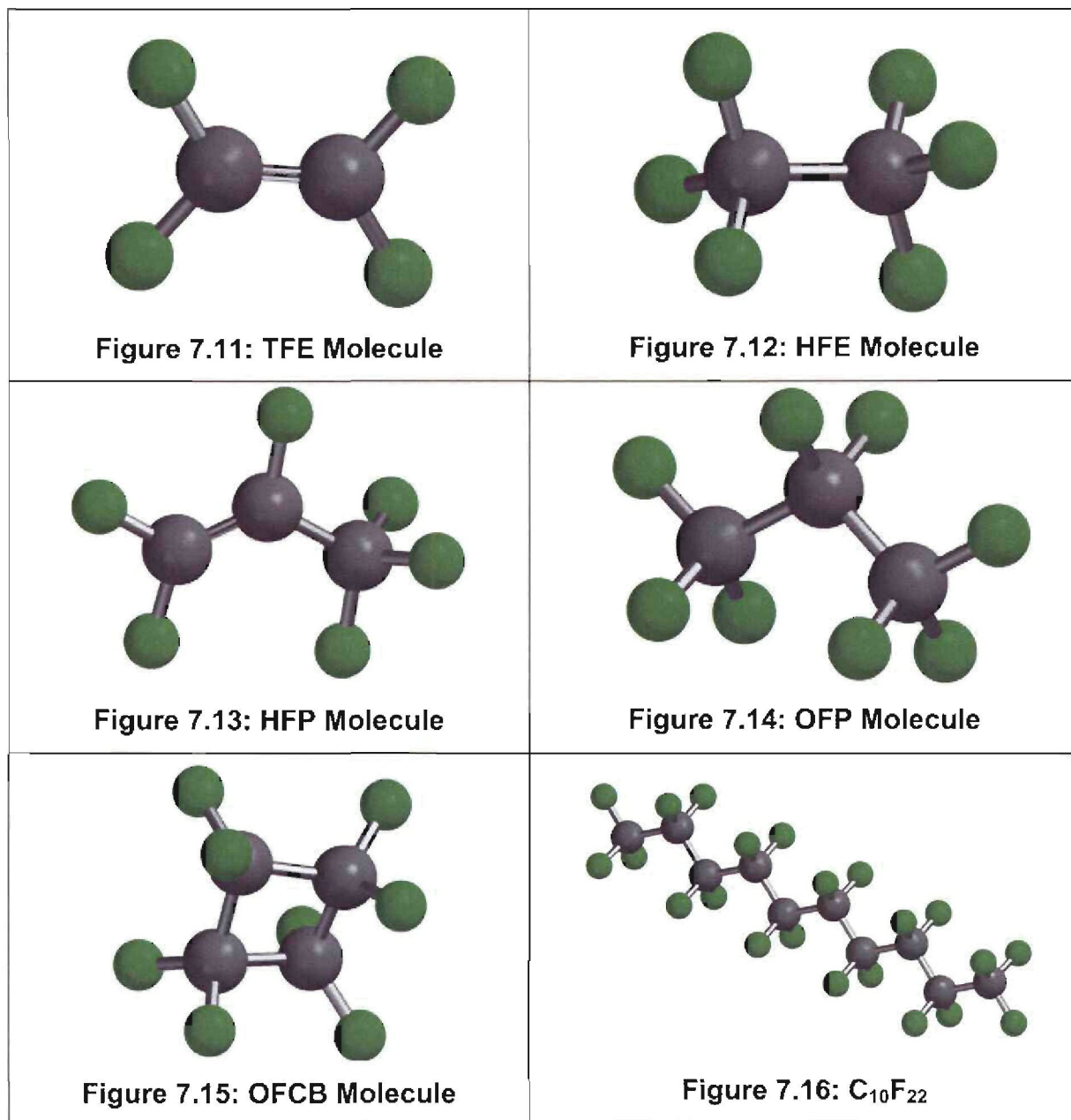
Transition state molecules			
Formula of transition state molecule	Formation enthalpy ΔH_f^\ddagger (kJ·mol ⁻¹)	Activation energies (kJ·mol ⁻¹)	Descriptive reactions
CF ₃ •	-123.21	441.02	CF ₂ •• + F → CF ₃ •
C ₂ F ₂ + 2F	-592.62	173.49	C ₂ F ₂ + 2F → TFE
C ₃ F ₈	-1726.08	147.97	HFP + 2F → OFP
C ₂ F ₄ •• + CF ₂ ••	-398.11	378.38	C ₂ F ₄ •• + CF ₂ •• → HFP
2CF ₃ •	-315.90	801.5	2CF ₃ • → HFE
			Figure 7.8a
C ₃ F ₆	-1105.10	37.1	2C ₂ F ₄ •• → HFP + CF ₂ ••
C ₁₀ F ₂₁ •	-3997.73	190.89	C ₁₀ F ₂₁ • → C ₉ F ₁₉ • + CF ₂ ••
C ₁₀ F ₂₁ • losing C ₂ F ₄ ••	-4128.14	60.48	C ₁₀ F ₂₁ • → C ₈ F ₁₇ • + C ₂ F ₄ ••
C ₁₀ F ₂₁ • losing F	-4197.97	392.26	C ₁₀ F ₂₁ • → C ₁₀ F ₂₀ •• + F
C ₁₀ F ₁₉ • losing C ₂ F ₂	-3421.94	766.68	C ₁₀ F ₁₉ • → C ₈ F ₁₇ • + C ₂ F ₂
C ₁₀ F ₂₂ losing F	-4549.80	437.88	C ₁₀ F ₂₂ → C ₁₀ F ₂₁ • + F

These formation enthalpy values can be used for the calculation of the activation energy needed for a specific reaction to take place. If the ΔH_f^\ddagger of the transition state is more than the sum of the ΔH_f of the reagents (i.e. $\Sigma\Delta H_f$ reagents - ΔH_f^\ddagger = a positive value) then the amount of activation energy that would be needed for the reaction to take place is equal to the difference between the $\Sigma\Delta H_f$ reagents and the ΔH_f^\ddagger (Figures 7.8 a and b).

The information obtained here is obtained for the energy supplied to the reactions at room temperature. A whole number of molecules and transition state molecules are modelled for all of the possible reactions. This does not necessarily comply with the proposed mechanism presented in Chapter 5, but may be wider in order to try to evaluate all the different permeations for the formation of the different end products.

7.3.3 The products

Figures 7.11 to 7.16 visually represent the geometrically optimised molecules of the depolymerisation of PTFE namely TFE, HFE, HFP, OFP, OFCB and $C_{10}F_{22}$.



Grey atoms are carbon, green atoms are fluorine.

The product molecules were selected based on the results in Chapter 4 and the formation energies (ΔH_f) of the depolymerisation molecules were calculated and presented in Table 7.5. Interestingly enough OFCB was found to be a stable compound because of the strong electron affinity of the fluorine atom. This is in contrast to $c-C_4H_8$ which is not stable at ambient conditions.

Table 7.5: Formation enthalpies of stable molecules

Depolymerisation molecules		
Formula	Formation enthalpies ΔH_f (kJ·mol ⁻¹)	Figure no.
C ₁₀ F ₂₂	-4547.46	Figure 7.16
C ₂ F ₂	-48.43	Figure 7.6a
C ₂ F ₄	-703.82	Figure 7.11
C ₂ F ₆	-1329.65	Figure 7.12
C ₃ F ₈	-1733.70	Figure 7.14
C ₃ F ₆	-1156.37	Figure 7.13
c-C ₄ F ₈	-1573.24	Figure 7.15

The C-C bond lengths in PTFE and PTFE radicals

To simplify the modelling process different chain length fluorocarbons were modelled, namely C₁₀F₂₂, C₂₀F₄₂, C₄₀F₈₂ and C₈₀F₁₆₂. The reason for this was to see if the bond lengths change significantly with chain length. It was found that there is no significant difference in C-C bond lengths for different chain lengths and therefore for the depolymerisation calculations, the C₁₀F₂₂ molecule was used to model PTFE in order to cut down on computational time. For a C₈₀F₁₆₂ chain this required almost 4 hours computational time, but for a C₁₀F₂₂ chain, a much more reasonable 5 minutes is sufficient.

Modelling of the C₁₀F₂₁ PTFE chain indicated that the C-C bond length of the radical side of the PTFE chain (C1 and C2) is shorter (1.535 Å) than the C-C bond lengths of the rest of the polymer chain (1.602 Å) as schematically presented in Figure 7.17.

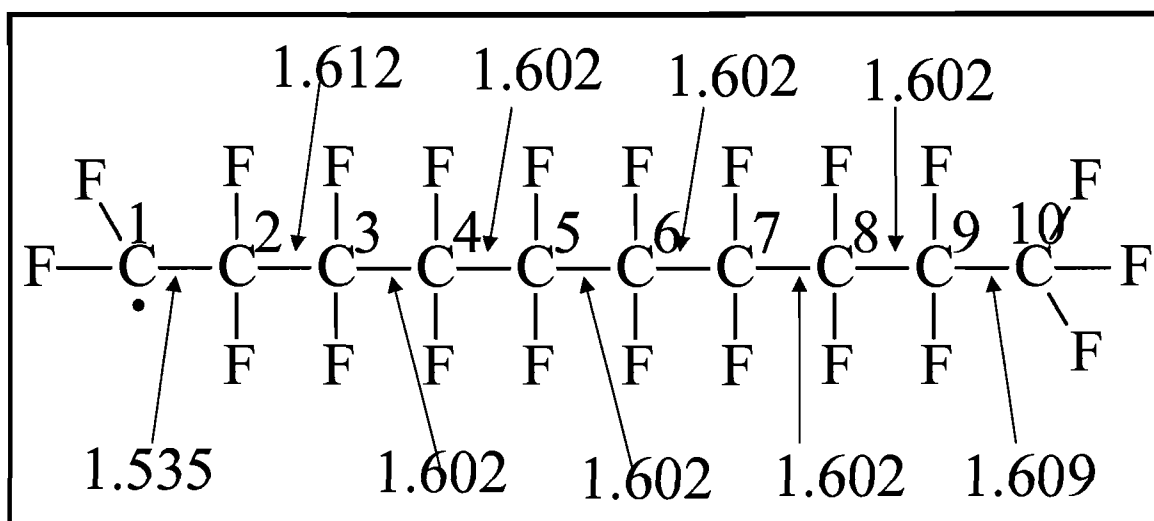


Figure 7.17: Lengths of C-C bonds of a PTFE radical in Å

This is an indication of a stronger bond between C1 and C2, than in the rest of the C-C bonds. The bond length of the C-C bond next to it (C2 and C3) however is longer (1.612 Å) than the rest (this indicates a weaker bond). This is an indication that the $C_2F_4^{\bullet\bullet}$ radical at the end of a PTFE chain will detach before other bonds in the chain will break. This supports the proposed “unzipping” mechanism and therefore explains the formation of TFE as a main product during experimentation. The C-C bond length on the other end of the chain is also slightly longer (1.609 Å) than the rest. This might be the cause of steric hindrance from the three fluorine molecules.

7.4 DISCUSSION OF THE REACTIONS IN THE TWO ROUTES OF THE DEPOLYMERISATION PROCESS

The following discussion about the energies involved in the product formation will be done in conjunction with the proposed mechanism as discussed in Chapter 5. Molecular modelling is a well-recognised method and complements thermodynamic calculations in supporting the proposed mechanism. It also incorporates some kinetic considerations through the calculation of the transition states of the reactions and the subsequent calculation of the activation energies of the reactions.

Initiation for the two mechanistic routes is the same. A PTFE chain breaks into shorter chains because of molecular vibrations at high temperature. It is therefore

accepted that for the purpose of this discussion, the depolymerisation process will continue from a $C_{10}F_{21}\cdot$ PTFE radical chain.

The two hypothetical mechanistic routes for the depolymerisation are represented in Figures 7.18 and 7.19. These two routes include the reactions that are reasonably possible in the proposed mechanism. In the following sections the probability of the reactions taking place will be evaluated. The most probable reactions will form part of the final proposed depolymerisation mechanism.

7.4.1 Route 1 of the proposed mechanism

Route 1 (Figure 7.18) follows an unzipping reaction and not a chemical decomposition, where shorter chain molecules, like $CF_2\cdot\cdot$, can be produced from the PTFE chain. In this route, just enough energy is supplied for the unzipping reaction to start taking place.

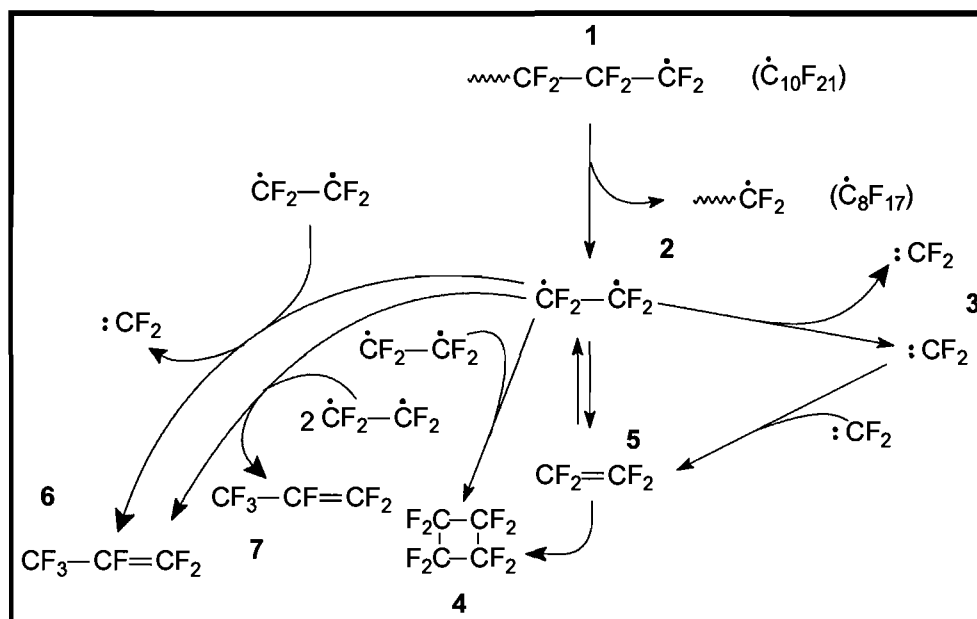


Figure 7.18: Mechanistic presentation of Route 1

The main products that are formed at the low temperature (600 to 700 °C) are TFE, HFP and OFCB. In the unzipping reaction a $C_2F_4\cdot\cdot$ radical (point 2) is formed. The major reaction at low pressure is the stabilisation of the triplet C_2F_4 to form the singlet C_2F_4 (TFE) species (point 5). Furthermore, two $C_2F_4\cdot\cdot$ radicals can combine to form OFCB as shown in point 4. The combination of three triplet C_2F_4 molecules to form

two molecules HFP (point 7) is another possible low-temperature reaction, but this a third order reaction which is not very probable. Lastly the triplet $C_2F_4^{**}$ may dissociate into two difluorocarbene molecules (point 3). These possible low-temperature reactions will be evaluated in order to predict the most probable mechanism.

Evaluation of Route 1 in terms of an energy level diagram

The enthalpy profile, as shown in Figure 7.19 was compiled for Route 1. The numbers at the different enthalpy levels correspond to the numbered reactions as indicated in Figure 7.18. The stoichiometry of a reaction must be kept intact when compiling an enthalpy profile. An example of the calculation of the enthalpy levels in Figure 7.19 is given below (Equation 7.1), using the $C_{10}F_{21}^{\bullet}$ radical as the reference:



The other enthalpies levels are calculated accordingly. The enthalpy diagram of Route 1 is presented in Figure 7.19.

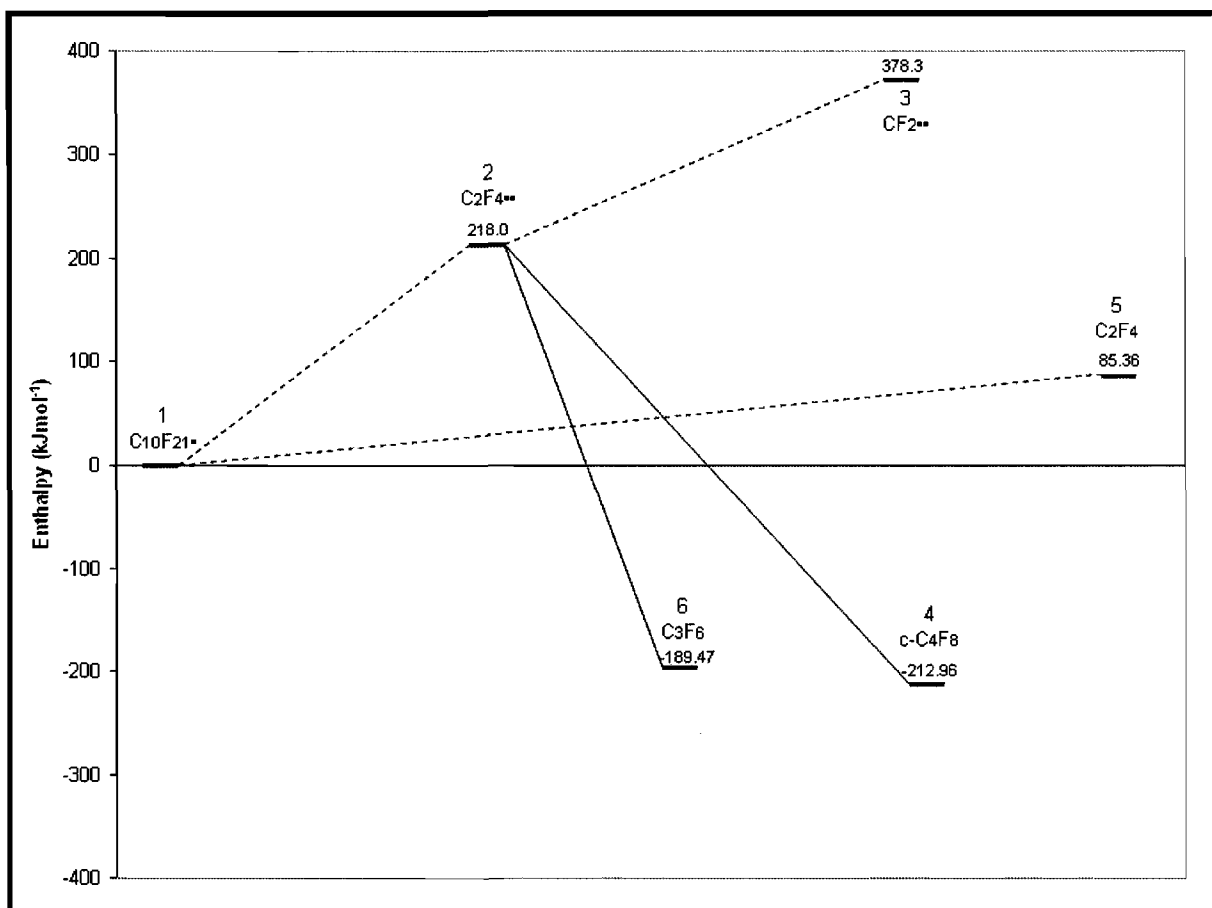


Figure 7.19: The enthalpy level diagram of Route 1

The reaction equations and corresponding energies for the individual reactions are summarised in Table 7.6. The energies discussed here will be the relative reaction energies as calculated above.

Table 7.6: Enthalpy profile data of Route 1

Reaction equation	Reaction enthalpy relative to $C_{10}F_{21}^{\bullet}$ (H_r^0)	Reaction equations
No.	($kJ \cdot mol^{-1}$)	
2	218.08	$C_{10}F_{21}^{\bullet} \rightarrow C_8F_{17}^{\bullet} + C_2F_4^{\bullet\bullet}$
6	-189.47	$C_{10}F_{21}^{\bullet} + C_2F_4^{\bullet\bullet} \rightarrow C_9F_{19}^{\bullet} + C_3F_6$
4	-212.96	$C_{10}F_{21}^{\bullet} + C_2F_4^{\bullet\bullet} \rightarrow C_8F_{17}^{\bullet} + c-C_4F_8$
3	378.39	$C_{10}F_{21}^{\bullet} \rightarrow C_8F_{17}^{\bullet} + 2CF_2^{\bullet\bullet}$
5	85.36	$C_{10}F_{21}^{\bullet} \rightarrow C_8F_{17}^{\bullet} + C_2F_4$

It was observed that reactions 4 and 6 are exothermic reactions and reactions 2, 3 and 5 endothermic.

Unzipping

At point 2 the polymer chain separates into a C_8F_{17} fragment and a $C_2F_4^{\bullet\bullet}$ radical. The relative reaction enthalpy of this reaction is $218.08 \text{ kJ}\cdot\text{mol}^{-1}$ and the activation energy for this reaction is $60.48 \text{ kJ}\cdot\text{mol}^{-1}$.

OFCB formation

At point 4, two $C_2F_4^{\bullet\bullet}$ radicals, one from the matrix and the other from the PTFE chain, combine to form OFCB along with a $C_8F_{17}^{\bullet}$ fragment, with a relative reaction enthalpy of $-212.95 \text{ kJ}\cdot\text{mol}^{-1}$. This value is different than reported in Table 7.3 ($-431.04 \text{ kJ}\cdot\text{mol}^{-1}$) and the reason is, that in this case, 2 TFE radicals from the matrix are involved in the OFCB formation and no PTFE chain. The reaction of point 4 is a complex reaction and no single transition state could be calculated.

TFE formation

The enthalpy for the TFE molecule, point 5, is higher than that of the initial reagents, but lower than the intermediate radical. This reaction is endothermic and according to modelling calculations, there is no transition state for this reaction. The fact that TFE forms the major product of the depolymerisation process and the yield is pressure-dependant might be an indication that the reaction entropy plays an important role in the product formation.

HFP formation

The HFP molecule, point 6, is at a lower enthalpy ($-189.47 \text{ kJ}\cdot\text{mol}^{-1}$) than the reactants and therefore the reaction is exothermic. This reaction does proceed via a transition state molecule as is indicated in Figure 7.8a.

$CF_2^{\bullet\bullet}$ radical formation

The formation of two $CF_2^{\bullet\bullet}$ radicals when the $C_2F_4^{\bullet\bullet}$ radical dissociates (point 3) needs more energy ($378.39 \text{ kJ}\cdot\text{mol}^{-1}$) to form than the intermediate product (TFE radical) at point 2. Another reaction where $CF_2^{\bullet\bullet}$ can be formed is via the dissociation of the polymer chain. This is an endothermic reaction. According to the

thermodynamic calculations in Chapter 6, as well as previously mentioned modelling, this radical will only form at higher temperatures. The formation of a $\text{CF}_2^{\bullet\bullet}$ radical directly from the PTFE chain is not probable because of the shortening of the terminal C-C bond on the PTFE chain, during the unzipping process, as discussed previously. For this reason the $\text{CF}_2^{\bullet\bullet}$ radical is not formed in significant amounts from the PTFE chain and is not included in the route 1 mechanism

Final simplified mechanism for Route 1

A summary of the reactions taking place in Route 1 of the depolymerisation mechanism is presented in Figure 7.20.

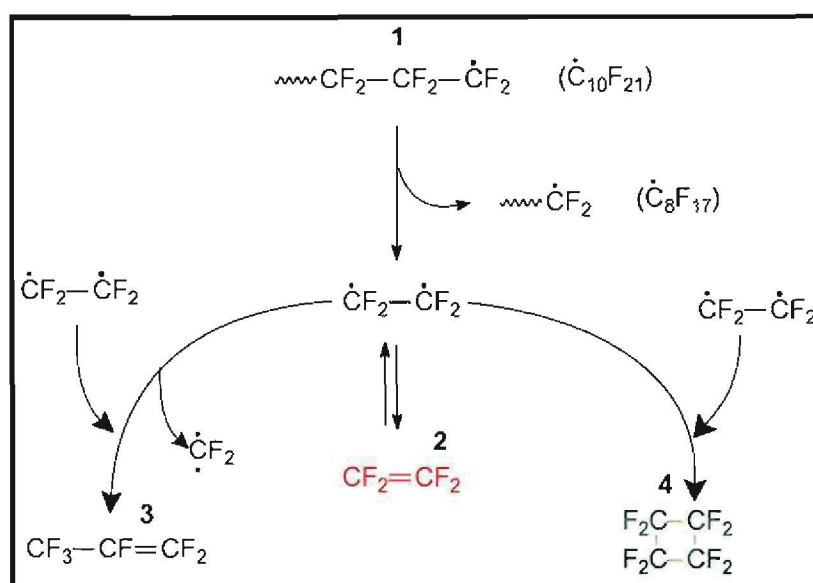


Figure 7.20: Simplified final reaction scheme

The reactions forming TFE, HFP and OFCB are the only reactions proposed to take place in Route 1. According to this final proposal, all the reactions take place via the TFE radical, which originates from the unzipping process of PTFE.

7.4.2 Route 2 of the proposed mechanism

When depolymerisation takes place at the higher temperatures (700 to 900°C), other molecules become more prominent. It was experimentally found that the main products that form during the depolymerisation of PTFE at the higher temperature range are TFE, HFP, OFCB, HFE and OFP and PFIB. A possible mechanistic route by which these products are formed is presented in Figure 7.21. Other minor

products like C_4F_{10} and C_4F_8 isomers also form, but are not included in this mechanism. One of the C_4F_8 isomers, perfluoroisobutylene (PFIB), may under certain conditions form as a major product (up to 25 % as indicated in Chapter 10). This product is very toxic (as discussed in Section 1.1 and 1.4) and one of the main drives during experimentation is to minimise the formation of PFIB.

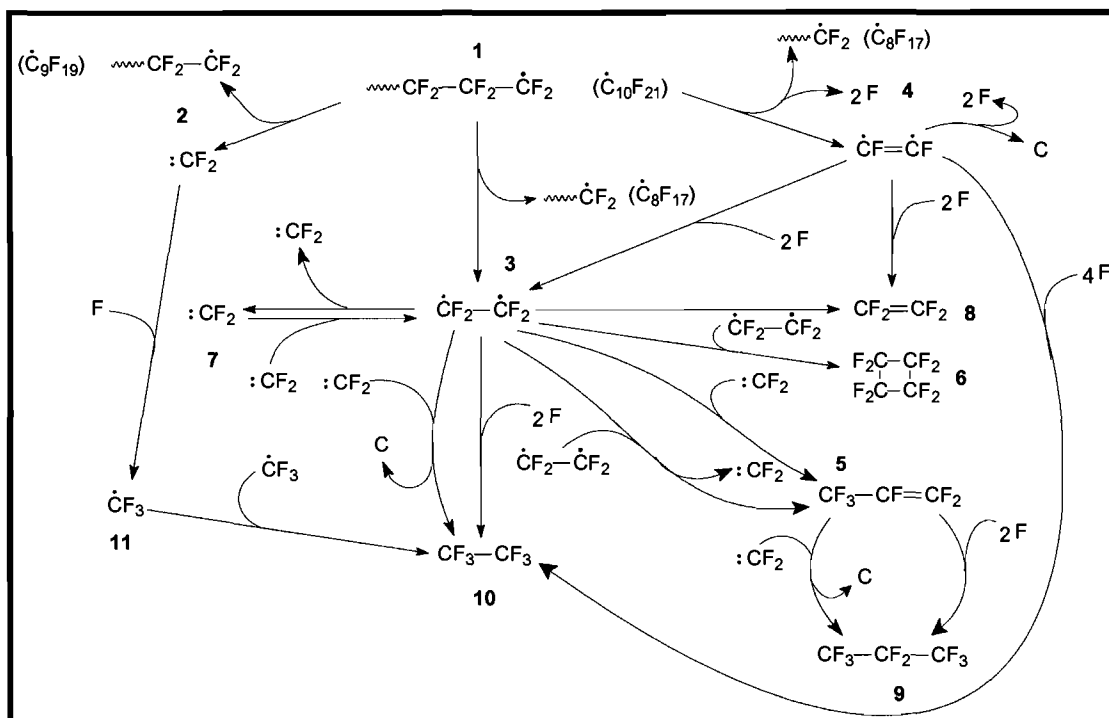


Figure 7.21: Mechanistic presentation of Route 2

After the initiation reaction, the $C_2F_4^{\bullet\bullet}$ radical (point 3) is only one of the products that form. Other products are difluorocarbene ($CF_2^{\bullet\bullet}$) (point 2) and difluoroethyne (C_2F_2).

F participation

F is only available in insignificant concentrations because of the positive formation enthalpy. It is however proposed that F (point 4) participates in product formation by concerted transfer reactions from the polymer or C_2F_2 to the intermediate products, $CF_2^{\bullet\bullet}$, C_2F_2 , HFP, etc.

TFE and OFCB formation

The formation of TFE (point 8) and OFCB (point 9) from the depolymerisation process follows the same route as for the Route 1 (points 3, 6 and 8 in Figure 7.16).

HFP formation

HFP however, may form via various reactions (point 5). The first reaction is similar to that proposed for Route 1, where two $C_2F_4^{\bullet\bullet}$ radicals combine to form HFP and a $CF_2^{\bullet\bullet}$ radical. Secondly, the $C_2F_4^{\bullet\bullet}$ radical may react with difluorocarbene ($CF_2^{\bullet\bullet}$), and also form HFP.

OFP formation

The product OFP may form via a fluorine transfer reaction to HFP from either the polymer chain or the $CF_2^{\bullet\bullet}$ radical (point 9). These reactions are accompanied by solid carbon deposition.

CF_3^{\bullet} radical formation

One possible reaction to produce HFE is for two CF_3^{\bullet} radicals to react. The CF_3^{\bullet} radicals (point 11) can only form if one of the $CF_2^{\bullet\bullet}$ radicals undergoes a fluorine transfer reaction from the polymer chain. The reaction where a fluorine atom is transferred to a $CF_2^{\bullet\bullet}$ radical is an energetically sound reaction, and the overall energy is less than that before the transfer. This is indicated in Table 7.7, where the CF_3^{\bullet} radical is more stable than the $CF_2^{\bullet\bullet}$ radical by an amount of $353.3 \text{ kJ}\cdot\text{mol}^{-1}$.

Table 7.7: Formation enthalpy evaluation of fluorine transfer to CF₂••

Molecule/radical	ΔH_f	Average C-F bond length
	(kJ·mol ⁻¹)	(Å)
CF ₂ ••	-205.39	1.29
CF ₃ •	-558.70	1.31
C ₁₀ F ₂₂	-4547.46	1.35
Energy difference between CF ₂ •• and CF ₃ •	353.30	
Average energy needed to break a C-F bond of a polymer chain.	326.93	

The average amount of energy needed to break a C-F bond from a polymer chain is 326.93 kJ·mol⁻¹ (this was calculated by averaging a number of the ΔH_f of a polymer chain losing fluorine atoms). This means that the transfer energy whereby a PTFE chain transfers a fluorine atom to a CF₂•• radical, will lower the total reaction energy by 26.37 kJ·mol⁻¹. This is accentuated by the fact that the C-F bond length of a polymer chain is 1.35 Å, as opposed to a 1.29 Å C-F bond length of a CF₂•• radical. Less energy would be needed to break a C-F bond on a polymer than a C-F bond on a CF₂•• radical.

There is a slight reduction in energy throughout the energy profile of the fluorine transfer reaction. The energy reduction, however, is not enough to cause spontaneous, exothermic CF₃• formation, but reactions as a result of collisions between a CF₂•• radical and the polymer chain will most probably result in CF₃• formation. The collision-dependence of the CF₃• formation signifies the pressure-dependence of the reaction.

HFE formation

The last major product that is formed during the depolymerisation reaction is HFE (point 10). The formation of this product is also dependant on a fluorine transfer reaction. There are several possible reactions that may lead to the formation of HFE.

The first and most probable is the combination of two $\text{CF}_3\cdot$ radicals (point 11). Other reactions by which HFE may form from $\text{C}_2\text{F}_4^{\bullet\bullet}$, is by de-fluorination of a PTFE chain radical and deposition of solid carbon, as well as with F transfer by collision of a $\text{C}_2\text{F}_2^{\bullet\bullet}$ radical with a polymer chain.

The Route 2 enthalpy level diagram

The second route as depicted in Figure 7.21 was also analysed according to an enthalpy profile diagram. This route is much more complex because of the formation of HFE and OFP, and the occurrence of the $\text{CF}_2^{\bullet\bullet}$ radical. Different reactions will be discussed for the different products. Generally it is accepted that the route resulting in the lowest enthalpy will be dominant. This is however not always the case, as will be shown for the OFP formation. The enthalpy profile for Route 2 is shown in Figure 7.22. The enthalpy shown on the y-axis is given in the unit $\text{kJ}\cdot\text{mol}^{-1}$.

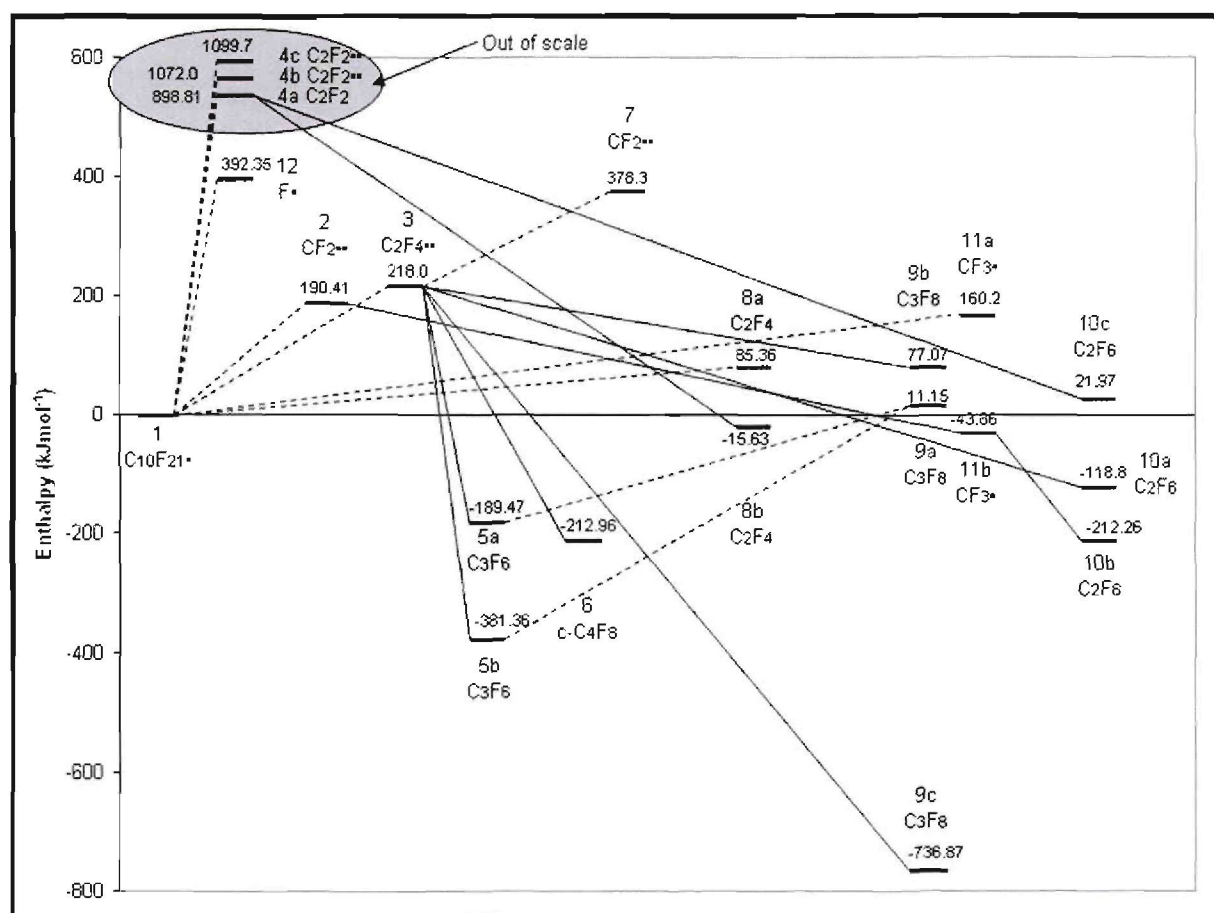


Figure 7.22: Enthalpy profile for the high-temperature sub-mechanism

This mechanistic route also starts with a C₁₀F₂₁ PTFE radical fragment. It is also assumed that CF₂•• and C₂F₄•• radicals are available in the matrix of this depolymerisation product mixture.

The chemical equations that correspond to each product on the enthalpy diagram are presented in Table 7.8.

Table 7.8: Enthalpy profile data of Route 2

Reaction equation	Reaction enthalpy relative to C ₁₀ F ₂₁ • (H _r ⁰)	Reaction equations
No.	(kJ·mol ⁻¹)	
2	190.41	C ₁₀ F ₂₁ • → C ₉ F ₁₉ • + CF ₂ ••
3	218.08	C ₁₀ F ₂₁ • → C ₈ F ₁₇ • + C ₂ F ₄ ••
4a	898.81	C ₁₀ F ₂₁ • → C ₈ F ₁₇ • + 2F + C ₂ F ₂
4b	1072.06	C ₁₀ F ₂₁ • → C ₈ F ₁₇ • + 2F + C ₂ F ₂ ••
4c	1099.71	C ₁₀ F ₂₁ • → C ₈ F ₁₇ • + 2F + C ₂ F ₂
5b	-189.47	C ₁₀ F ₂₁ • + C ₂ F ₄ •• → C ₉ F ₁₉ • + C ₃ F ₆
6	-212.96	C ₁₀ F ₂₁ • + C ₂ F ₄ •• → C ₈ F ₁₇ • + c-C ₄ F ₈
8a	85.36	C ₁₀ F ₂₁ • → C ₈ F ₁₇ • + C ₂ F ₄
8b	-15.53	C ₁₀ F ₂₁ • + C ₂ F ₂ → C ₁₀ F ₁₉ • + C ₂ F ₄
9a	11.15	C ₁₀ F ₂₁ • + C ₃ F ₆ → C ₁₀ F ₁₉ • + C ₃ F ₈
9b	77.07	C ₁₀ F ₂₁ • + C ₂ F ₄ → C ₈ F ₁₅ • + CF ₂ • + C ₃ F ₈
10a	-118.8	C ₁₀ F ₂₁ • + C ₂ F ₄ → C ₁₀ F ₁₉ • + C ₂ F ₆
10b	-212.26	2CF ₃ • → C ₂ F ₆
10c	21.97	C ₁₀ F ₂₁ • + C ₂ F ₂ → C ₁₀ F _{17(radical)} + C ₂ F ₆
11a	160.21	C ₁₀ F ₂₁ • → C ₉ F ₁₈ •• + CF ₃ •
11b	-43.86	C ₁₀ F ₂₁ • + CF ₂ •• → C ₁₀ F ₂₀ • + CF ₃ •

Reaction 5a and 9c are improbable ternary reactions and have therefore been disregarded.

F reactions

At these temperatures the fluorine radical, at point 12, is not formed in significant concentrations as a stable, free radical as indicated in Chapter 6. The formation energy for this radical is rather high ($392.35 \text{ kJ}\cdot\text{mol}^{-1}$) if compared to that of the TFE radical (point 3). Although F appears in an insignificant concentration, F atoms are available in concerted transfer reactions from a PTFE chain to a fluorine recipient like $\text{CF}_2^{\bullet\bullet}$.

$\text{CF}_2^{\bullet\bullet}$ radical formation

The $\text{CF}_2^{\bullet\bullet}$ radical, at points 2 and 7, can be formed by two different reactions. The first reaction, as indicated in Table 7.8, is that of $\text{CF}_2^{\bullet\bullet}$ formation via PTFE chain cracking. The other reaction is via the breaking of a $\text{C}_2\text{F}_4^{\bullet\bullet}$ radical's C-C bond to form two $\text{CF}_2^{\bullet\bullet}$ radicals. The total relative enthalpy for the first reaction is $190.41 \text{ kJ}\cdot\text{mol}^{-1}$ and for the second reaction, $378.39 \text{ kJ}\cdot\text{mol}^{-1}$. The latter is in accordance with findings from Chapter 6 where the cracking of a C_2F_4 is thermodynamically not permitted. Two $\text{CF}_2^{\bullet\bullet}$ radicals are formed by the reaction at point 7 and this is double the amount of energy for the formation of one molecule at point 2 (different routes use the same amount of energy). The reaction for point 7 will therefore be disregarded.

CF_3^{\bullet} radical formation

The CF_3^{\bullet} radical formation and a fluorine transfer both from a PTFE chain (point 11a), increases the total energy of the reaction to $160.21 \text{ kJ}\cdot\text{mol}^{-1}$. However, the CF_3^{\bullet} radical formation via a $\text{CF}_2^{\bullet\bullet}$ radical from the matrix and a fluorine transfer reaction from a PTFE chain reduces the energy of the reaction to $-43.86 \text{ kJ}\cdot\text{mol}^{-1}$ (point 11b). For this reason CF_3^{\bullet} radicals will form at conditions where an F is available via transfer reaction and this opens the opportunity for HFE and OFP formation.

$\text{C}_2\text{F}_4^{\bullet\bullet}$ radical formation

The $\text{C}_2\text{F}_4^{\bullet\bullet}$ radical formation also may occur via two different reactions. The first reaction is formation via an unzipping process of the PTFE chain (point 3), with a relative energy of $218.08 \text{ kJ}\cdot\text{mol}^{-1}$. Another reaction, which is not shown, is the formation of $\text{C}_2\text{F}_4^{\bullet\bullet}$ via addition reaction of two $\text{CF}_2^{\bullet\bullet}$ radicals. This reaction is endothermic and the $\text{C}_2\text{F}_4^{\bullet\bullet}$ radical concentration via this reaction is also not

significant. It is therefore proposed that the main source of $C_2F_4^{\bullet\bullet}$ radicals are via unzipping of the PTFE chain. The fact that the $C_2F_4^{\bullet\bullet}$ radical forms the basis of a large number of the other reactions is a good indication that the applied thermal energy for the depolymerisation reaction is above $218.08 \text{ kJ}\cdot\text{mol}^{-1}$. The large role that kinetics plays is very clear in this case in particular.

C₂F₂ formation

Another product that is thermodynamically stable (Chapter 6) is the difluoroethyne (C_2F_2 , $F-C=C-F^{\bullet\bullet}$) molecule (point 4). This molecule may exist as a *cis* or *trans* radical, or as a difluoroethyne molecule. According to modelling results the existence of this molecule, in all its forms, is only possible at high energy inputs. The relative formation energy of the C_2F_2 molecules, via the proposed reactions, range between $898.81 \text{ kJ}\cdot\text{mol}^{-1}$ for the ethyne, to $1099.71 \text{ kJ}\cdot\text{mol}^{-1}$ for the *cis* C_2F_2 molecule. The existence of these molecules is highly unlikely even at the high-temperature depolymerisation conditions (800 and 900 °C).

HFP formation

The C_3F_6 (HFP) molecule (point 5) is more stable than the previously discussed species. According to the model, HFP can form via two different reactions. The first reaction is where a $C_2F_4^{\bullet\bullet}$ radical from the matrix reacts with a $C_2F_4^{\bullet\bullet}$ radical that originated from a $C_{10}F_{21}$ PTFE chain. The total relative energy for this reaction is $-189.47 \text{ kJ}\cdot\text{mol}^{-1}$. Figure 7.9 presents an electron diagram of this reaction. A second reaction for the formation of HFP follows the splitting of the C-C bond of a $C_2F_4^{\bullet\bullet}$ radical as part of a $CF_2^{\bullet\bullet}$ transfer reaction with two $C_2F_4^{\bullet\bullet}$ molecules, in order to form two HFP molecules. This reaction results in the formation of HFP at a lower energy ($-381.36 \text{ kJ}\cdot\text{mol}^{-1}$) than the first reaction, however the H_r^0 of reaction 5a is exactly double that of 5b. It is also an improbable ternary reaction and for this reason. Reaction 5a will be disregarded. Reaction 5b is therefore the preferred reaction.

OFCB formation

The OFCB molecule shown at point 6 can only form when two $C_2F_4^{\bullet\bullet}$ molecules react with one another to afford the cyclic compound. This reaction reduces the total reaction enthalpy to $-212.96 \text{ kJ}\cdot\text{mol}^{-1}$, making this an exothermic reaction. The OFCB

reaction is one of the most energetically viable reactions. OFCB is also one of the most stable fluorocarbon molecules because of the extraction of de-stabilising electrons from the ring by the fluorine atoms.⁽⁶⁶⁾

TFE formation

The TFE molecule, at point 8, can again form via two reactions. The first reaction is where C_2F_2 reacts with fluorine to form TFE. Even if the fluorine is substituted from a PTFE chain, the energy to form C_2F_2 is too high to overcome, and this reaction will not take place to a significant extent. The second reaction for TFE formation is via double bond formation of the last two carbons of a PTFE chain and the subsequent ejection of TFE from the chain (unzipping). With the relative reaction enthalpy of $85.36 \text{ kJ}\cdot\text{mol}^{-1}$ the formation of TFE directly from PTFE is very probable. The TFE yield at low temperatures is high, which can be explained because the unzipping reaction dominates depolymerisation. At higher temperatures the unzipping reaction competes with other reactions and the TFE yield would decrease. It is therefore proposed that the TFE formation still mainly takes place via the unzipping reaction.

OFP formation

The perfluorinated product OFP, at point 9, can form via three possible reactions. The first (point 9c) and most unlikely reaction is when PTFE transfers fluorine and $CF_2^{\bullet\bullet}$ radicals, along with $C_2F_4^{\bullet\bullet}$ from the matrix, to yield OFP. The fact that this is a four molecule reaction and that fluorine transfer is needed makes this reaction not likely because of the positive formation energy (Table 7.2). The second most stable reaction (point 9a) is where fluorine is transferred from PTFE to HFP. This reaction seems to be the most viable of the three reactions, with a total enthalpy of $11.15 \text{ kJ}\cdot\text{mol}^{-1}$. The third reaction (point 9b) uses one $C_2F_4^{\bullet\bullet}$ radical from the matrix and another from a PTFE chain. In the same reaction fluorine is transferred from the PTFE chain to form OFP. The total enthalpy for this reaction is $77.07 \text{ kJ}\cdot\text{mol}^{-1}$, which does not make it the preferred reaction for the OFP formation.

HFE formation

There are three proposed reactions whereby HFE (point 10) can be formed. The first reaction (point 10c) makes use of the C_2F_2 molecule and that four fluorine atoms are transferred from the PTFE chain. The total energy necessary for this reaction is

higher than the initial available energy and therefore this reaction is not expected to be the source of a high concentration of HFE. The total energy of the reaction at the second (point 10a) and third (point 10b) reactions both decrease. In the second reaction, fluorine is transferred to $C_2F_4^{**}$ from the PTFE chain to form HFE and the total reaction enthalpy reduction is $-118.8 \text{ kJ}\cdot\text{mol}^{-1}$. In the third reaction, two $CF_3\cdot$ radicals react with one another to form HFE. This reaction reduces the total reaction enthalpy by the largest amount of $-212.26 \text{ kJ}\cdot\text{mol}^{-1}$. Reaction point 10a and b are both preferred reactions, which were found to take place at higher pressures (50 to 100 kPa) where the collision probability is higher.

Final simplified mechanism for Route 2

A summary of the reactions taking place in Route 2 of the depolymerisation mechanism is presented in Figure 7.23.

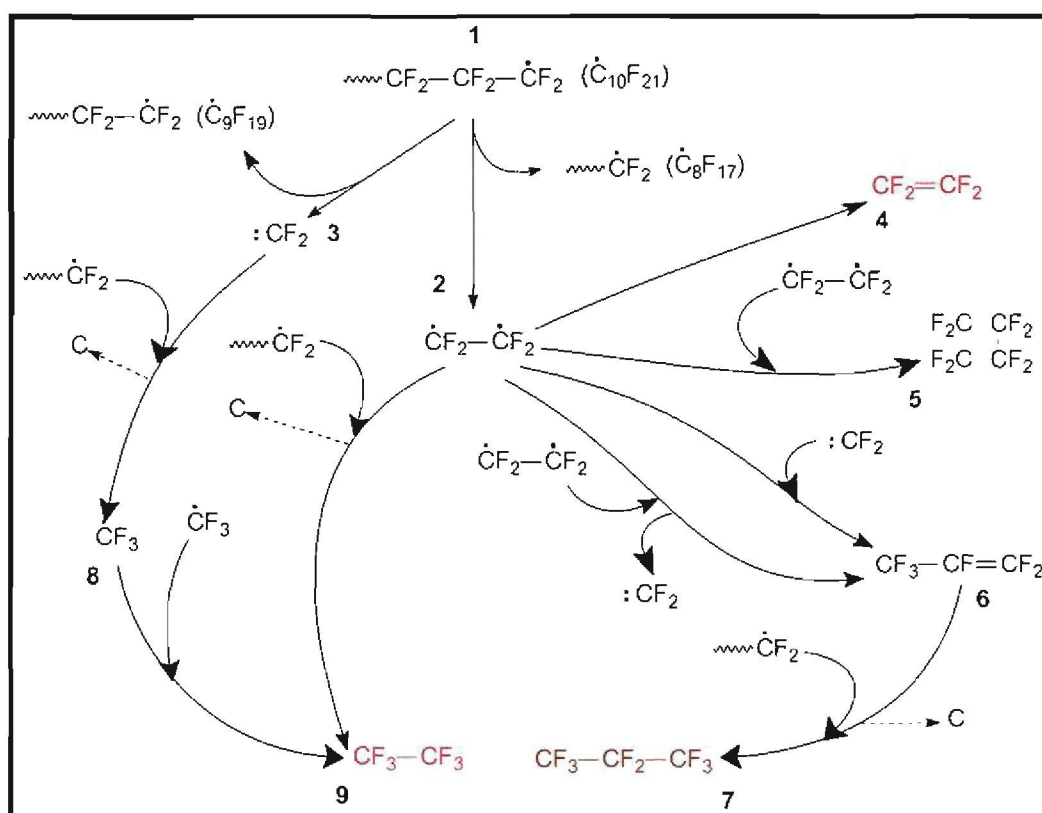


Figure 7.23: Summary of Route 2 of the depolymerisation mechanism

In Route 2, it was proposed that TFE, HFP and OFCB were formed via the same reactions as in Route 1 and HFE as well as OFP (perfluorinated products) will

additionally form via F transfer reactions from PTFE. These reactions only took place significantly at high temperatures ($> 700\text{ }^{\circ}\text{C}$).

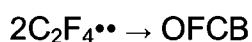
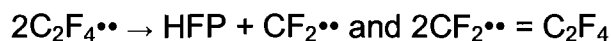
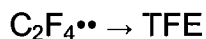
7.5 CONCLUSIONS

According to the results presented in Chapter 4, it was proposed that the product formation after the depolymerisation of PTFE occurs according to two mechanistic routes. In this chapter the process of molecular modelling was applied in supporting the individual reaction equations that are proposed for the mechanism for the depolymerisation of PTFE as presented in Chapter 5.

The formation energies for the individual radicals, molecules and transition species were calculated after their geometries were optimised. From this data the two energy diagrams for the two proposed mechanistic routes were drawn and analysed. Finally, according to thermodynamic and some kinetic considerations, the two final mechanistic routes were proposed.

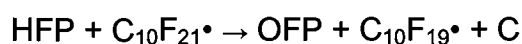
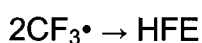
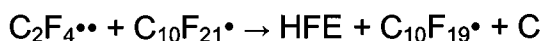
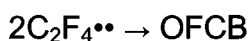
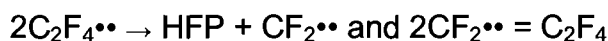
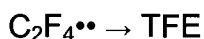
Route 1 at low temperature (600 to 700 °C):

Route 1



and Route 2 at high temperature (700 to 900 °C).

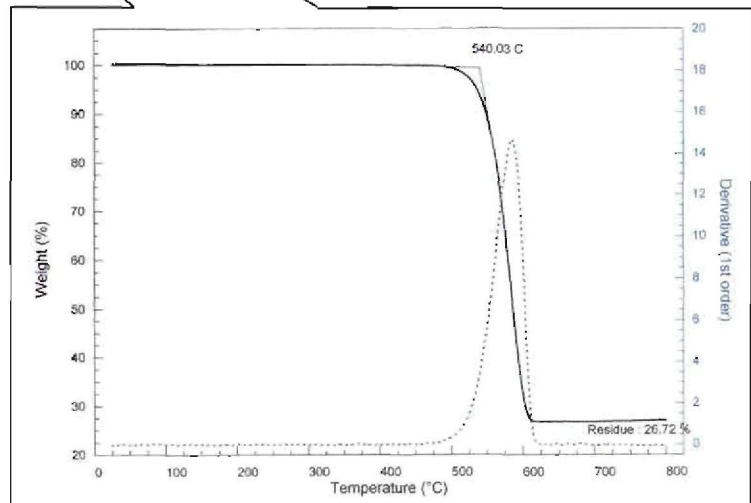
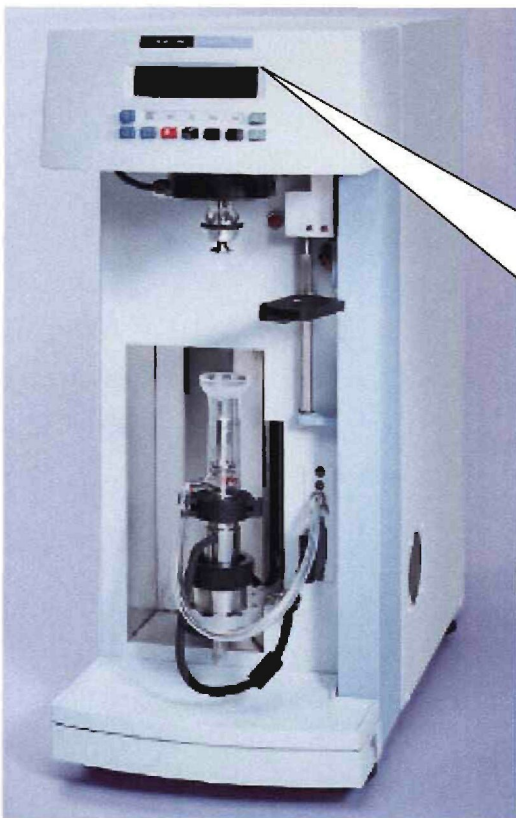
Route 2



Chapter 8

A Thermogravimetric Investigation of the Kinetics of PTFE Depolymerisation

- 8.1 Introduction
- 8.2 Theory
- 8.3 Experimental method
- 8.4 Results and discussion
- 8.5 Conclusions

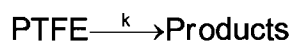


8.1 INTRODUCTION

The purpose of this chapter is to study the depolymerisation kinetics of PTFE by means of isothermal mass loss data. This data obtained during the thermal decomposition of PTFE, can be used to provide kinetic information (order of reaction (n), rate constants (k) and the activation energy (E_{act})) of the PTFE depolymerisation process at different temperatures. The calculated n , k and E_{act} values can be substituted into appropriate equations to obtain the calculated mass losses at each temperature. A graphic comparison (an overlay of experimental and calculated plots) between the experimental and calculated isothermal mass losses will then verify the validity of the calculated n , k and E_{act} values.

8.2 THEORY

The kinetics of the depolymerisation of PTFE is described according to:^(67, 68)



The following general rate equation is used for data analysis:

$$-\frac{dx}{dt} = k \cdot x^n \tag{8.1}$$

where x is the PTFE mass, in mg, at time t , relative to the initial mass; ($x = m/m_0$), k is the depolymerisation rate constant, in s^{-1} , and n is the order of the reaction, usually varying between 0.5 and 1.

The two kinetic constants, k and n , can be obtained from experimental results by taking the logarithm of Equation 8.1:

$$-\ln\left(\frac{dx}{dt}\right) = \ln k + n \ln x \quad 8.2$$

Hence a plot of the left hand side of Equation 8.2 $\ln(dx/dt)$ versus $\ln x$, will yield a plot with the slope equal to n , the reaction order. The y-intercept at $\ln x = 0$ gives k , the rate constant. When Equation 8.2 is integrated the following equation (8.3) is found. The derivation of this equation is shown in Appendix 1:

$$x = {}^{1-n}\sqrt{1 - (1-n)kt} \quad 8.3$$

Equation 8.3 can be used to simulate the TGA diagram, once the reaction order and the rate constant have been determined. The temperature dependence of the rate constant can subsequently be analysed using the Arrhenius equation (Equation 8.4). In this way the activation energy (E_{act} in $\text{kJ}\cdot\text{mol}^{-1}$) can be determined.

$$k = k_0 e^{-E_{act}/RT} \quad 8.4$$

Where k_0 is the pre-exponential rate constant, R is the universal gas constant and T the reaction temperature. An Arrhenius plot gives the activation energy and the pre-exponential rate constant:

$$\ln(k) = -\frac{E_{act}}{R} \times \frac{1}{T} + \ln(k_0) \quad 8.5$$

8.3 EXPERIMENTAL METHOD

Isothermal TG analysis of unfilled PTFE was performed using a Perkin Elmer PGS2 TG analyser working on a counterbalance principle. Approximately 5 mg of an unfilled PTFE sample was introduced into the TG analyser and the instrument zeroed. This sample was heated to a predetermined temperature at a heating rate of $40\text{ }^{\circ}\text{C}\cdot\text{min}^{-1}$ with nitrogen as a carrier gas, at a flow of $30\text{ ml}\cdot\text{min}^{-1}$, and kept constant at the predetermined temperature for 40 minutes. The following temperatures were investigated: 500, 510, 520, 530, 540, 550, 560, 580, 600 and $620\text{ }^{\circ}\text{C}$.

Experimentation at higher temperatures was attempted, but the isothermal method does not work at too high temperatures ($> 620\text{ }^{\circ}\text{C}$), as the PTFE is already depolymerising to a large extent while heating up is still in progress. This experimentation was therefore abandoned.

8.4 RESULTS AND DISCUSSION

The thermogram in Figure 8.1 presents the isothermal mass loss of PTFE at different temperatures ranging from 500 to 620 °C.

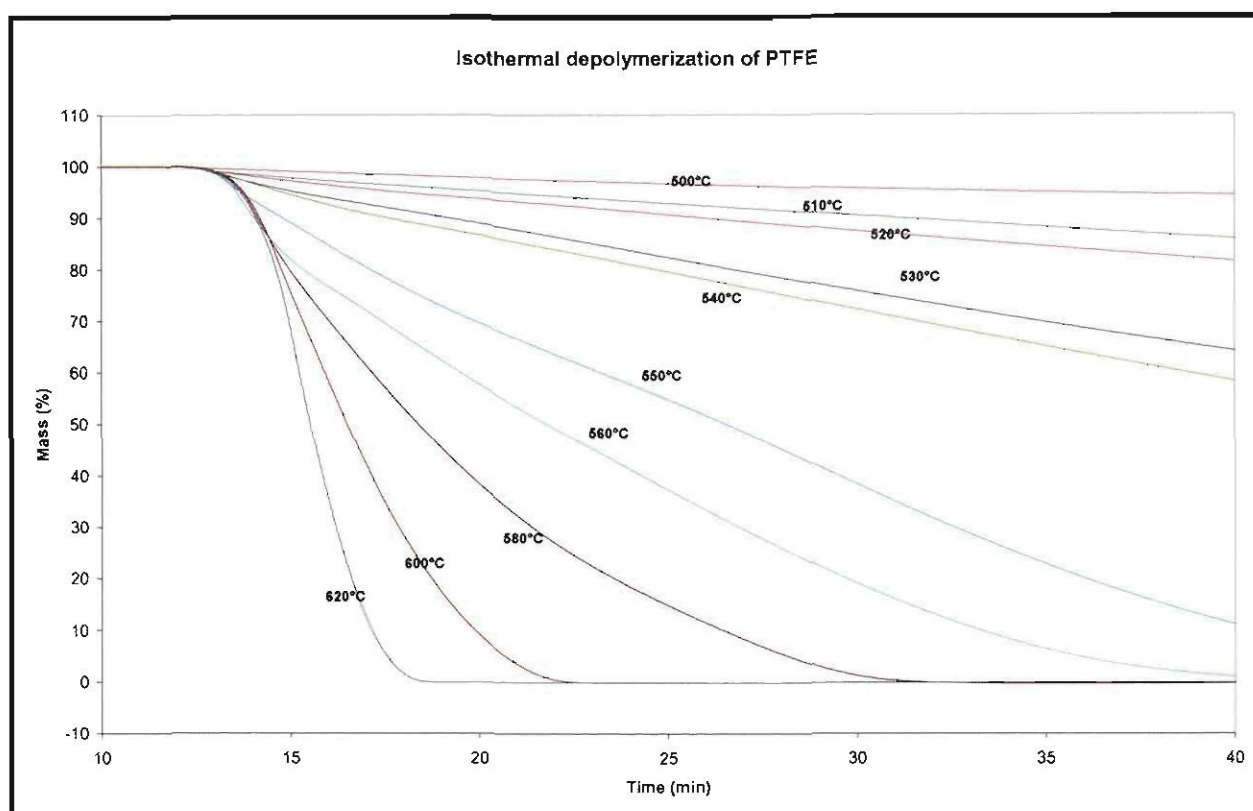


Figure 8.1: Isothermal mass loss of PTFE

With a heating rate of $40\text{ °C}\cdot\text{min}^{-1}$ it takes 12 minutes to reach 500 °C. As can be seen from Figure 8.1, at this temperature the depolymerisation rate is low and the amount of PTFE depolymerised below 500 °C can be ignored. Above 580 °C, however, the initial shape of the three curves clearly indicates that depolymerisation below the isothermal set point can no longer be ignored. For this reason, in the data analysis, only the later section of the curve is used. Thermograms above 620 °C clearly cannot be measured as all PTFE has already been depolymerised before the set point is reached. The two curves at 520 and 540 °C do not follow the regular pattern of the other thermograms. For an unknown reason they seem to closely resemble 510 and 530 °C thermograms.

The data presented in Figure 8.1 was transferred into Figure 8.2, using Equation 8.2.

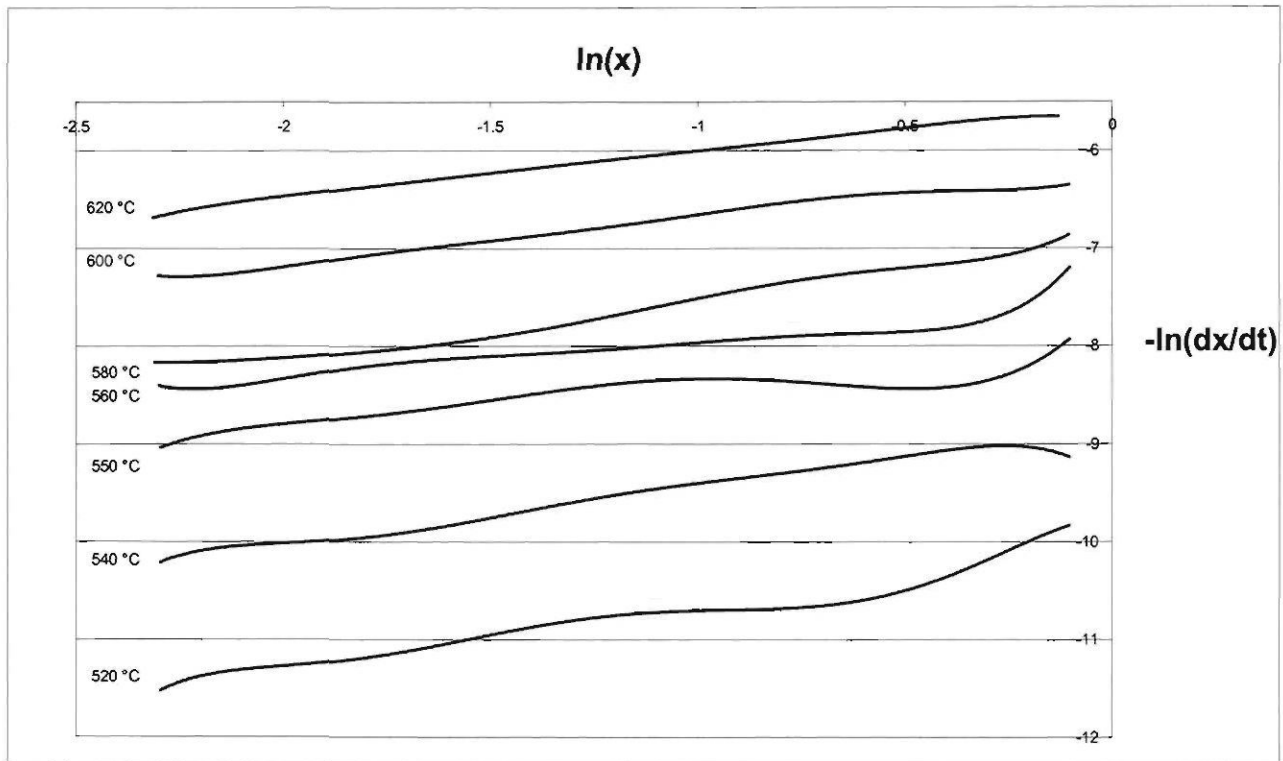


Figure 8.2: A plot of $-\ln(dx/dt)$ vs $\ln(x)$ at different temperatures

Note that $x = (m/m_0)$, and initially $\ln(x) = 0$.

Some of the graphs in Figure 8.2 (520, 550 and 560 °C) presented some irregularities at the beginning of the experiment, which may be contributed to the sample shape.

The order of the reaction (n) and the reaction rate constants (k), as calculated from data in Figure 8.2, where n , the slope and k , the y-intercept, are presented in Tables 8.1 and 8.2 respectively.

Table 8.1: The n (order of reaction) values for the different temperatures

T (°C)	Slope (n)
530	0.48
540	0.57
550	0.66
560	0.57
580	0.48
600	0.47
620	0.50
Average	0.54 ± 0.08

As is evident from the table, the slopes (order of the reaction) do not differ significantly nor systematically and in the further analysis the average n value of 0.54 will be used. It is important to remember that the order is not the order for the product formation reactions, but for the PTFE depolymerisation reaction.

Conesa and Font in 2001 and Doyle in 1961 found the order of the depolymerisation process to be zero.^(9, 49) This is in contrast to the order found in this study, possibly because in this study a wider temperature range was investigated.

The 0.54 reaction order was used to calculate the values for k by best fit of Equation 8.4. This data is presented in Table 8.2

Table 8.2: The k values as determined over a temperature range of 500 to 620 °C

T (°C)	Rate Constant (k (s⁻¹))
500	$3.79 \cdot 10^{-5}$
510	$8.51 \cdot 10^{-5}$
520	$9.09 \cdot 10^{-5}$
530	$2.60 \cdot 10^{-4}$
540	$2.88 \cdot 10^{-4}$
550	$7.82 \cdot 10^{-4}$
560	$1.14 \cdot 10^{-3}$
580	$1.94 \cdot 10^{-3}$
600	$4.03 \cdot 10^{-3}$
620	$9.45 \cdot 10^{-3}$

As presented in Table 8.2 the reaction constants, k, increase from $3.79 \cdot 10^{-5} \text{ s}^{-1}$ to $9.45 \cdot 10^{-3} \text{ s}^{-1}$, which indicates that the reactions at 620 °C take place at a rate approximately two orders of magnitude faster than at 500 °C. This is in accordance with work done by Wall⁽⁶⁹⁾ who found the reaction constant k at 500 °C to be $5.51 \cdot 10^{-5} \text{ s}^{-1}$.

The Arrhenius plot is presented in Figure 8.3 using the data from Table 8.2.

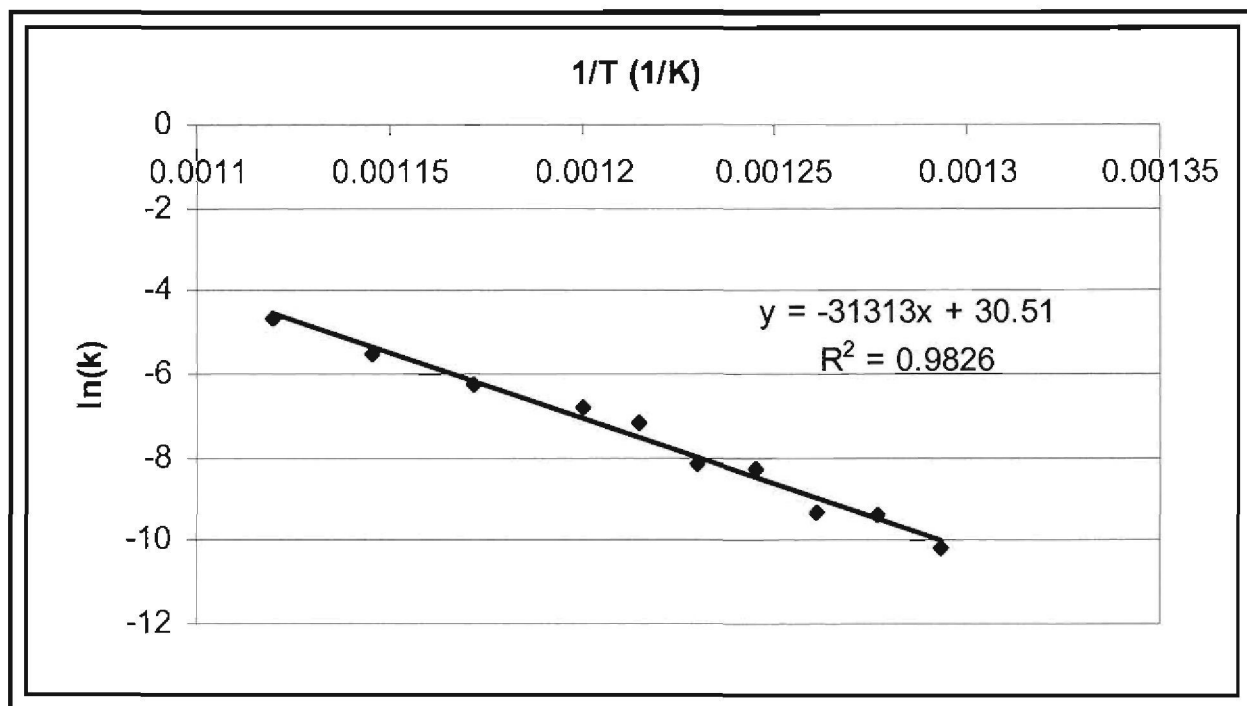


Figure 8.3: Arrhenius plot of $\ln(k)$ vs $1/T$

The data can be described by one activation energy equal to $260 \text{ kJ}\cdot\text{mol}^{-1}$ and a pre-exponential factor $k_0=1.78\times 10^{13} \text{ s}^{-1}$. The straight line is an indication that the calculated order of 0.54 for the depolymerisation process seems correct.

This activation energy for the depolymerisation process is a little less, but still in line with activation energies stated in the literature for example: Cox *et al* determined the activation energy to be $318.2 \text{ kJ}\cdot\text{mol}^{-1}$,⁽⁴⁷⁾ Siegle *et al* determined the activation energy to be $347.5 \text{ kJ}\cdot\text{mol}^{-1}$,⁽⁴⁶⁾ Carroli and Manche who proposed that the depolymerisation of PTFE takes place in two steps, indicating two activation energies, $353.55 \text{ kJ}\cdot\text{mol}^{-1}$ and $191.21 \text{ kJ}\cdot\text{mol}^{-1}$.⁽⁴⁸⁾ Wall calculated an activation energy of $166 \text{ kJ}\cdot\text{mol}^{-1}$, but used radiation depolymerisation which is highly dependent on the sample thickness.⁽⁶⁹⁾

Simulation of the thermograms

In order to validate the reaction rate model given by Equation 8.1 the full thermograms were simulated, an example of which is given in Figure 8.4 at 550 °C.

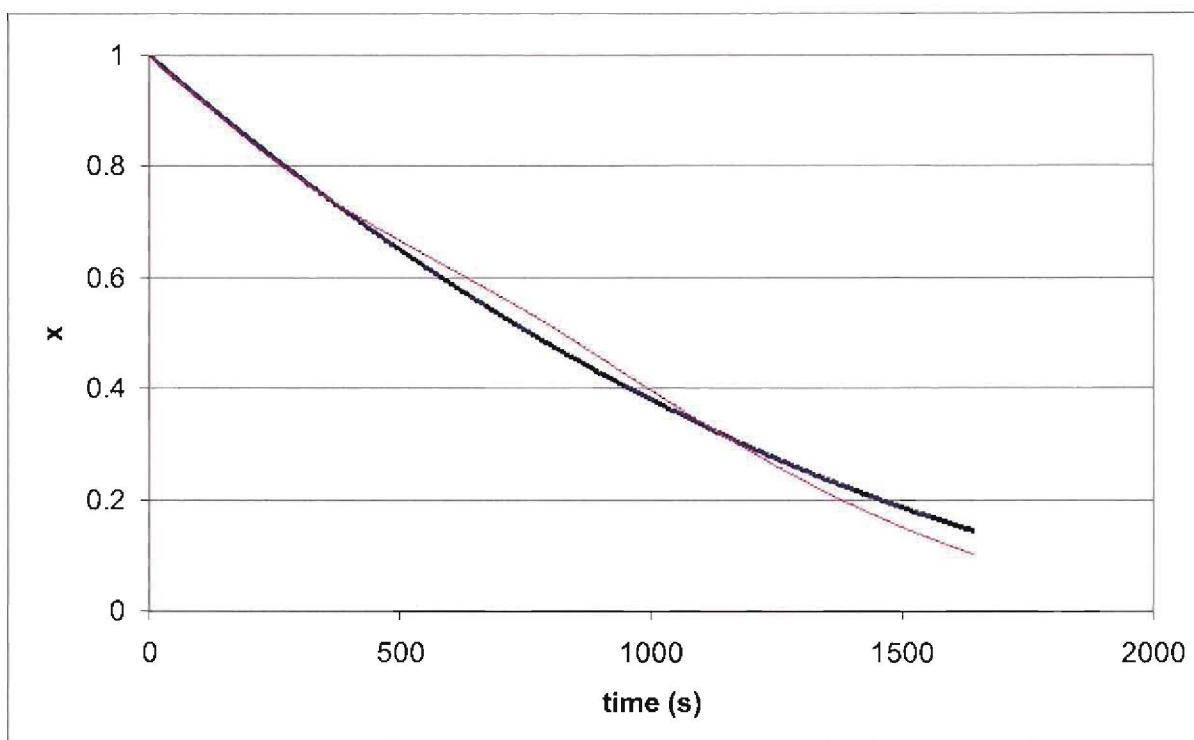


Figure 8.4: Experimental data vs simulated data (bold curve) at 550 °C, $k=7.82 \times 10^{-4} \text{ s}^{-1}$, $n=0.54$

Although the position of the simulated curve corresponds well with the experimental values, the shape is different. The experimental curve is closer to a straight line. This might well be a consequence of the fact that the PTFE sample has a continuous molecular weight distribution and that the isothermal depolymerisation rate continuously decreases with the degree of depolymerisation (i.e. the continuous re-distribution of the molecular weight during depolymerisation). This phenomenon is observed in all thermograms.

8.5 CONCLUSIONS

Isothermal TGA data was used to calculate the order (n), rate constant (k) and activation energy (E_{act}) of the depolymerisation process for unfilled PTFE over a temperature range of 500 to 620 °C. It was determined that the order of the depolymerisation reaction is 0.54 ± 0.08 and the rate constants, at different temperatures, were calculated to increase from $3.79 \cdot 10^{-5} \text{ s}^{-1}$ to $9.45 \cdot 10^{-3} \text{ s}^{-1}$ as the temperature is changed from 500 °C to 620 °C. This order is in contrast to the values found in the literature by Doyle⁽⁴⁹⁾, Conesa and Font⁽⁹⁾, Cox *et al*⁽⁴⁷⁾ and Siegle *et al*⁽⁴⁶⁾.

The activation energy was calculated to be $260 \text{ kJ} \cdot \text{mol}^{-1}$ and the pre-exponential factor $k_0 = 1.78 \cdot 10^{13} \text{ s}^{-1}$. This activation energy differ significantly from the energies reported in the literature by Cox *et al*, Siegle *et al* and Carroll and Manche⁽⁴⁶⁻⁴⁸⁾ (Chapter 1). A possible explanation is the sample preparation of the PTFE before it is introduced into the TGA oven. This experimentally determined value is the activation energy for the depolymerisation process of PTFE into TFE. The activation energy according to Chapter 7 is $218.08 \text{ kJ} \cdot \text{mol}^{-1}$.

The fact that the simulated isothermal diagram closer resembles a straight line as opposed to the model seems to indicate that the depolymerisation rate for a PTFE sample is not constant. It is postulated that this is a direct consequence of the continuous re-distribution of the molecular weight of the polymer during depolymerisation.

Chapter 9

The Characterisation of PTFE Feed Material Before and During Depolymerisation

9.1. Introduction

9.2. Polymer characterisation

9.2.1. Feed material

9.2.2. Thermogravimetric analysis of different fluoropolymers

9.2.3. Thermogravimetric analysis of filled PTFE

9.2.4. SEM/EDX analysis of the filler material

9.3. *In situ* ESEM observation of filled PTFE during depolymerisation

9.4. Visual observation of the effect of hot PTFE on reactor walls

9.5. The residence time of unfilled and filled PTFE in the Paddle Reactor

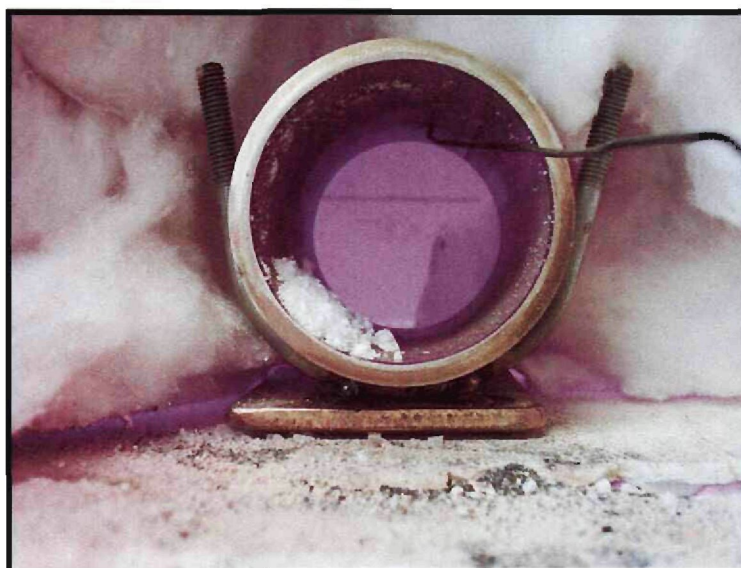
9.5.1. Introduction

9.5.2. Experimental procedure

9.5.3. Results and discussion

9.6. Conclusions

The results presented in this chapter was accepted for publication by the author in Journal of Applied Polymer Science on 2007/09



9.1 INTRODUCTION

As discussed in Chapter 3, PTFE is often filled with filler materials like graphite, bronze, glass fibre, etc., in order to enhance certain physical characteristics of the polymer. Unfilled as well as filled PTFE can be depolymerised to form a variety of high-value products. The purpose of this chapter is to characterise different filled PTFE samples in order to determine their ability to be depolymerised.

For filled PTFE to be successfully depolymerised, the filler material must not take part in the reaction as this may lead to unnecessary product contamination for example low-melting metal contamination, hydrocarbons, and more. For this reason the different filler materials must be evaluated for compliance with the depolymerisation conditions.

One of the main objectives of this study was to develop a system whereby filled PTFE can be depolymerised on a continuous basis. At the beginning of this study the following hypotheses and criteria were made regarding such a system:

1. During the depolymerisation step the PTFE does not stick to the walls of the reactor;
2. Forward movement and positive flow properties of the PTFE are assumed;
3. The PTFE feed material is free-flowing;
4. The flow properties of the solid residue (filler) after the depolymerisation process are such that it can be removed from the reactor on a continuous basis;
5. No blockages occur in the reactor, quench or off-gas systems;
6. The residence time in the reactor is such that the feed material has enough time to be fully depolymerised;
7. The system can be optimised to produce desired products like tetrafluoroethylene (TFE), hexafluoropropylene (HFP) and octafluorocyclobutane (OFCB), and minimise unwanted products like hexafluoroethane (HFE), octafluoropropane (OFP) and perfluoroisobutylene (PFIB).

A hypothesis can further be made that the following properties will have an influence on the depolymerisation process of PTFE, especially when the development of a continuous depolymerisation system is envisaged:

1. Particle size of the feed material;
2. Type of filler;
3. Particle size of the filler;
4. Physical shape of the filler (fibres, rough edges);
5. Melting point of the filler;
6. Chemical stability of the filler material at the envisaged depolymerisation temperature;
7. Flowability of the filled PTFE feed material as well as that of the filler material;
8. The flow property characteristics of the viscous PTFE mass in the depolymerisation process.

Several experiments were performed in order to test the different aspects of continuous depolymerisation inside a horizontal reactor:

1. Polymer and filler characterisation;
2. Mechanical properties of PTFE during the depolymerisation process inside a laboratory scale Rotating-kiln Reactor;
3. Residence time of unfilled as well as filled PTFE samples inside a Paddle Reactor.

9.2 POLYMER CHARACTERISATION

The amount of filler material added to PTFE may vary for different applications. For a depolymerisation system to operate continuously, it must be able to separate the filler residue from the gaseous product while the system is in operation. Sintering or a build-up of the filler residue inside the reactor will ultimately cause blockages. Therefore, the depolymerisation temperature of filled PTFE, where the filler has a relatively low melting point, must be chosen with care. The flow properties of the feed

material and the filler residue must also be taken into account during the depolymerisation system design.

9.2.1 Feed material

In this study, four types of free-flowing granulated PTFE, namely graphite-, glass fibre-, bronze-filled and unfilled PTFE were used (Figure 9.1). Pure filler material was also obtained from the suppliers for evaluation purposes.

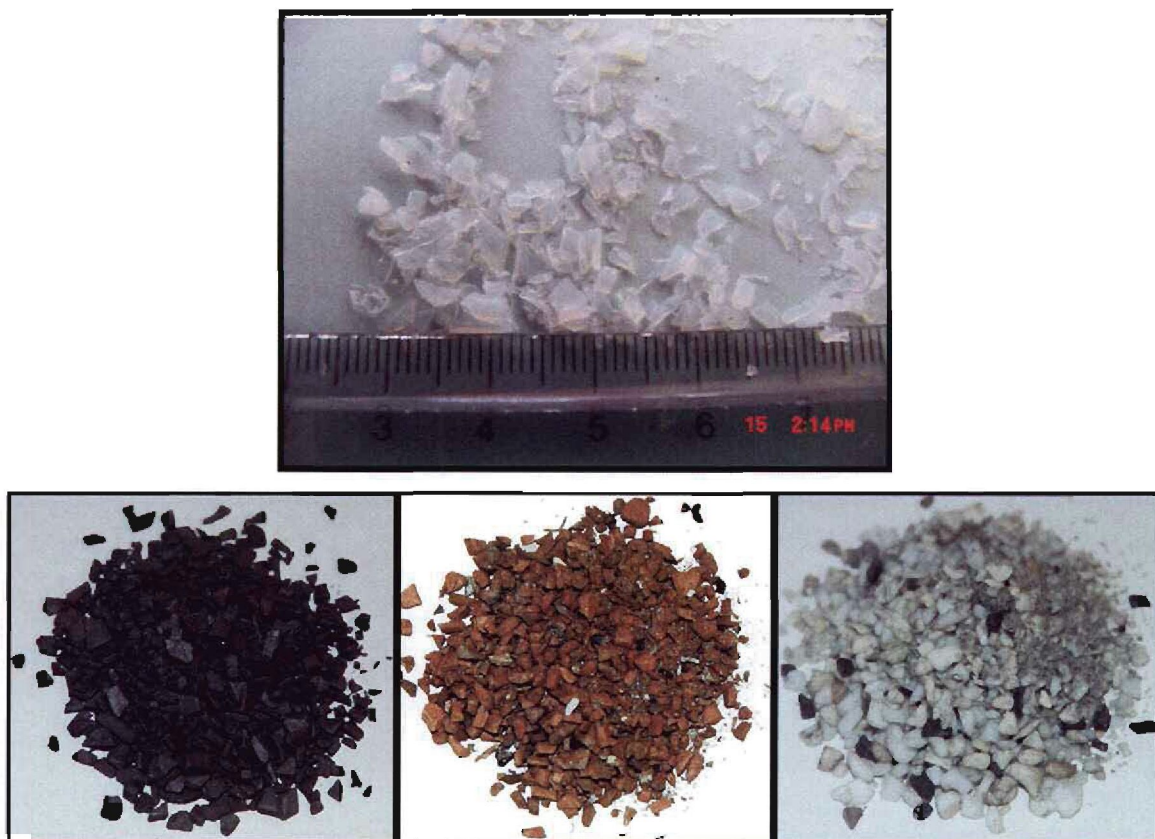


Figure 9.1: Granulated unfilled and graphite-, bronze-, and glass fibre-filled PTFE

9.2.2 Thermogravimetric analysis of different fluoropolymers

Different fluoropolymers were evaluated in order to determine if they could be distinguished from one another by means of thermogravimetric (TG) analysis. Six different samples (tetrafluoroethylene-hexafluoropropylene-vinilidene fluoride copolymer (THV), ethylene-tetrafluoroethylene copolymer (ETFE),

Hexafluoropropylene-Tetrafluoroethylene-Ethylene copolymer (HTE), perfluoroalcoxy (PFA), Fluorinated-Ethylene-Propylene (FEP) and polytetrafluoroethylene (PTFE)) were analysed, and the results are presented in Figure 9.2. In the latter case a 20 % graphite-filled PTFE sample was used, thus the lack of complete weight loss. This however did not influence the depolymerisation temperature significantly because of the slow temperature increase by the TG instrument.

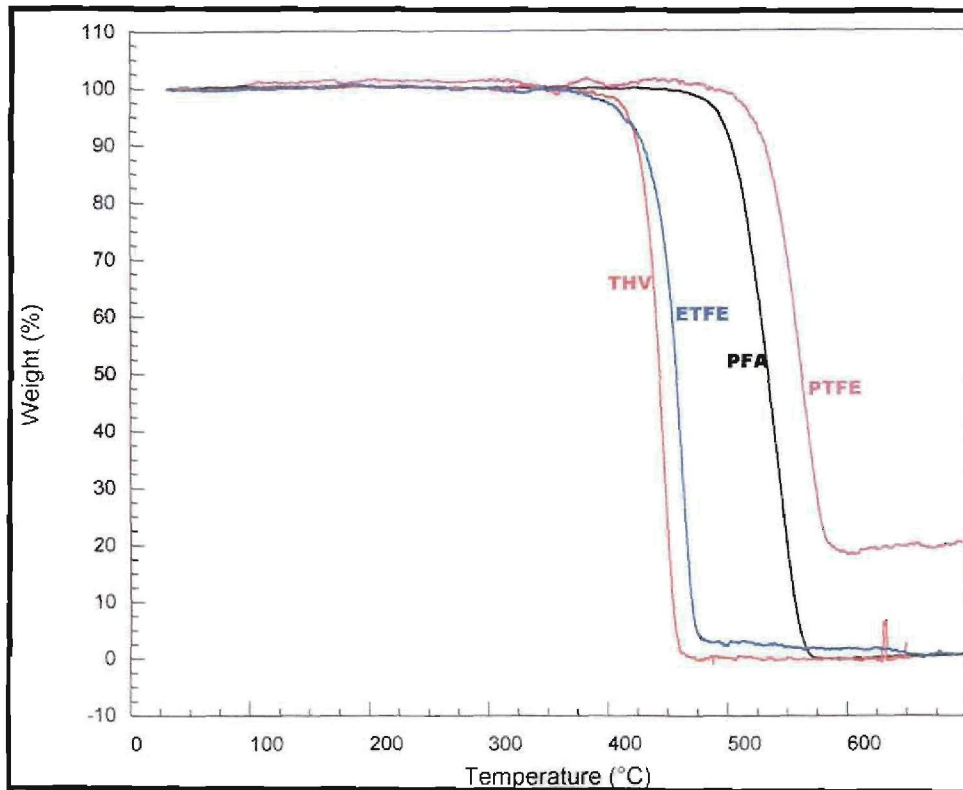


Figure 9.2: Thermograms of THV, ETFE, PFA and graphite-filled PTFE (heating rate = 5 °C·min⁻¹)

The chemical structures of these polymers are presented in Table 9.1.

Table 9.1: Chemical structure of the different fluoropolymers

PTFE	$\begin{array}{cccccc} & \text{F} & \text{F} & \text{F} & \text{F} & \text{F} \\ & & & & & \\ \sim & \text{C} & - & \text{C} & - & \text{C} & - & \text{C} & - & \text{C} & \sim \\ & & & & & \\ & \text{F} & \text{F} & \text{F} & \text{F} & \text{F} \end{array}$	ETFE	$\begin{array}{cccccc} & \text{F} & \text{F} & \text{H} & \text{H} & \text{F} & \text{F} \\ & & & & & & \\ \sim & \text{C} & - & \text{C} & - & \text{C} & - & \text{C} & - & \text{C} & \sim \\ & & & & & & \\ & \text{F} & \text{F} & \text{H} & \text{H} & \text{F} & \text{F} \end{array}$
FEP	$\begin{array}{cccccc} & \text{F} & \text{F} & \text{F} & \text{F} & \text{F} & \text{F} \\ & & & & & & \\ \sim & \text{C} & - & \text{C} & - & \text{C} & - & \text{C} & - & \text{C} & \sim \\ & & & & & & \\ & \text{F} & \text{F} & \text{F} & \text{C} & \text{F} & \text{F} \\ & & & & & & \\ & & & & \text{F} & & \text{F} \end{array}$	HTE	$\begin{array}{cccccc} & \text{F} & \text{F} & \text{F} & \text{F} & \text{H} & \text{H} \\ & & & & & & \\ \sim & \text{C} & - & \text{C} & - & \text{C} & - & \text{C} & - & \text{C} & \sim \\ & & & & & & \\ & \text{F} & \text{F} & \text{F} & \text{C} & \text{H} & \text{H} \\ & & & & & & \\ & & & & \text{F} & & \text{F} \end{array}$
PFA	$\begin{array}{cccccc} & \text{F} & \text{F} & \text{F} & \text{F} & \text{F} & \text{F} \\ & & & & & & \\ \sim & \text{C} & - & \text{C} & - & \text{C} & - & \text{C} & - & \text{C} & \sim \\ & & & & & & \\ & \text{F} & \text{F} & \text{F} & \text{O} & \text{F} & \text{F} \\ & & & & & & \\ & & & & \text{C} & & \\ & & & & & & \\ & & & & \text{F} & & \text{F} \end{array}$	THV	$\begin{array}{cccccc} & \text{F} & \text{F} & \text{F} & \text{F} & \text{H} & \text{F} \\ & & & & & & \\ \sim & \text{C} & - & \text{C} & - & \text{C} & - & \text{C} & - & \text{C} & \sim \\ & & & & & & \\ & \text{F} & \text{F} & \text{F} & \text{C} & \text{H} & \text{F} \\ & & & & & & \\ & & & & \text{F} & & \text{F} \end{array}$

It was observed that the THV and ETFE depolymerisation temperatures are close to one another at ~ 425 °C. The depolymerisation temperature for PFA is ~ 500 °C, and for PTFE ~ 525 °C. From these results it can be concluded that it is possible to distinguish between the different polymers using the dissociation temperature determined by TG analysis, except for ETFE and THV. This is a proven analytical method for qualification and identification of the fluoropolymers. These results also show that the TGA can be used to qualify/identify industrial polymers as well as the identification of waste fluoropolymers that can be used for depolymerisation i.t.o. waste treatment.

As will be discussed further in this study (Chapter 11) the characterisation of waste fluoropolymers before the depolymerisation process, is a very important consideration, because not all types of fluoropolymers are suitable for a specific system and can lead to blockages of the reactor. Other problems can be blockages of the quench system and product gas contamination.

The TGA method determines the depolymerisation temperature for different polymers. The depolymerisation temperatures of THV, ETFE and PFA differ significantly from that of PTFE. PTFE depolymerises at approximately 540 °C, PFA at 510 °C, THV and ETFE both at approximately 440 °C as can be seen in Figure 9.2. These decomposition temperatures are specific to the type of polymer. The

depolymerisation properties of different fluoropolymer samples will be discussed in Chapter 11.

9.2.3 Thermogravimetric analysis of filled PTFE

TG analysis was employed to determine the amount of filler in the feed material, as well as the thermal stability of the filler at the depolymerisation temperatures that were used in this study.

The results obtained from the TG analyses are presented in Figure 9.4. Filled PTFE samples were analysed and found to have different amounts of filler material encapsulated in the PTFE.

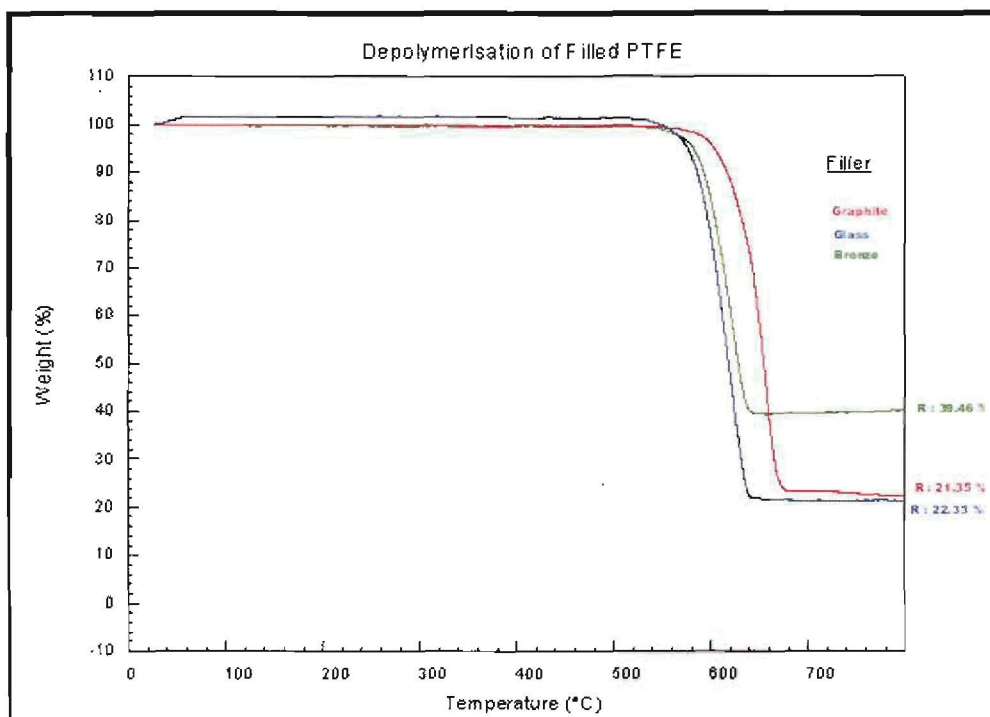


Figure 9.3: Thermogravimetric curves of different filled PTFE samples

The results of the depolymerisation inside the TGA and the amount of filler material contained is presented in Table 9.2.

Table 9.2: Amount of filler material in filled PTFE samples

Filled PTFE sample	Wt % Filler
Graphite-filled PTFE	21.35
Bronze-filled PTFE	39.46
Glass fibre-filled PTFE	22.33

An important result additional to the filler content is the stability of the different filler materials. If there were any significant weight loss in the last section of the thermogravimetric curve (Figure 9.3), then that filler material could not be used in the depolymerisation process. The fillers used in this study proved to be stable at the depolymerisation conditions.

9.2.4 SEM/EDX analysis of the filler material

The unused filler (filler not yet incorporated into PTFE) was examined with a scanning electron microscope (SEM) and the elemental composition thereof confirmed by an Energy Dispersive X-ray Spectrometer (EDX) detector.

SEM/EDX analyses confirmed the elemental composition of the fillers. The graphite filler consisted mainly of carbon with some traces of sulphur. The glass fibre filler consisted mainly of silicon and calcium, with traces of aluminium, and the bronze-filler was confirmed to be a tin-copper alloy.

SEM analysis was done to examine the morphology of the fillers because this might have an influence on the feed properties. According to the SEM analyses, the particle size distribution of all the fillers was between 10 to 100 μm . SEM images of the different filler materials are presented in Figures 9.4a to c. The glass fibres were 50 to 100 μm in length and 10 μm in diameter rods (Figure 9.4a). The bronze and graphite filler particles (Figures 9.4b and 9.4c) were finely-divided and of irregular shape. These images represent the filler (from the supplier) before it was introduced into the PTFE matrix.

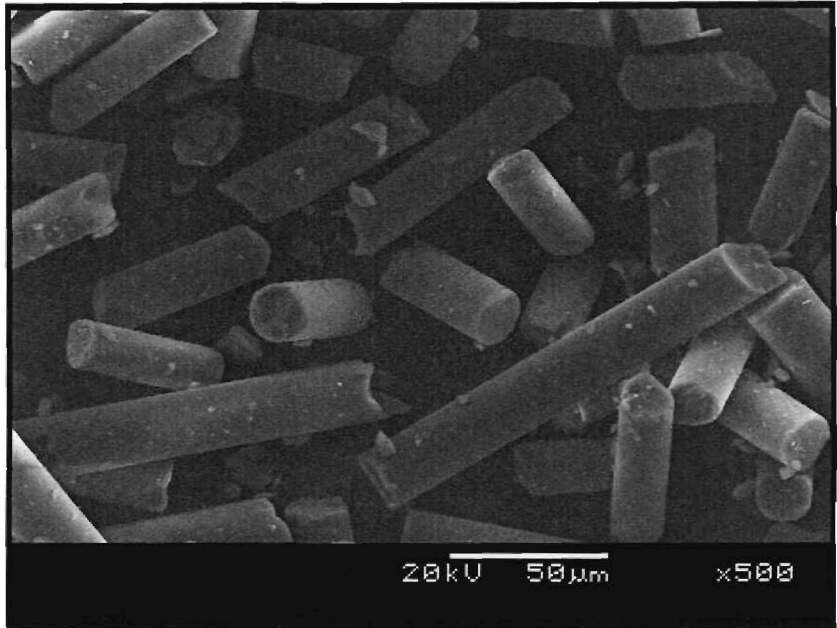


Figure 9.4a: SEM image of glass fibre filler

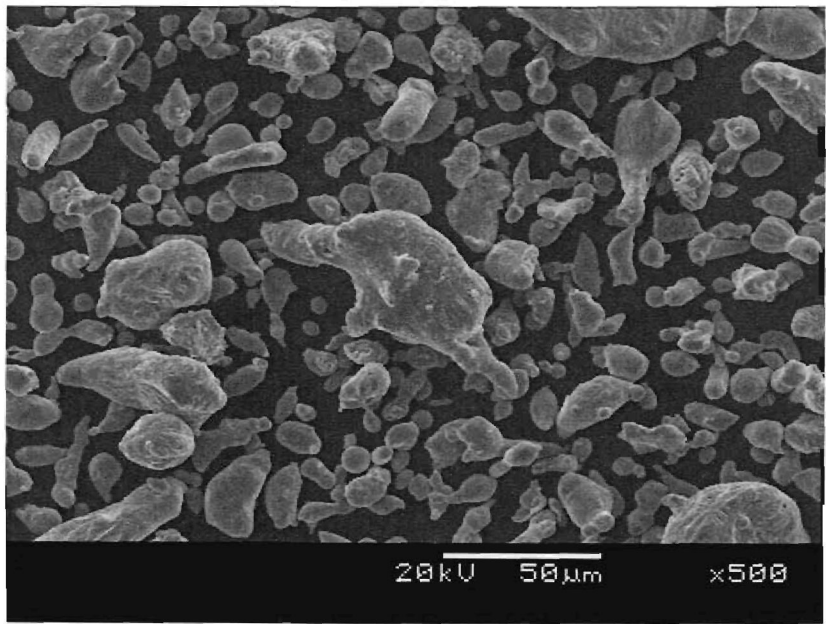


Figure 9.4b: SEM image of bronze filler

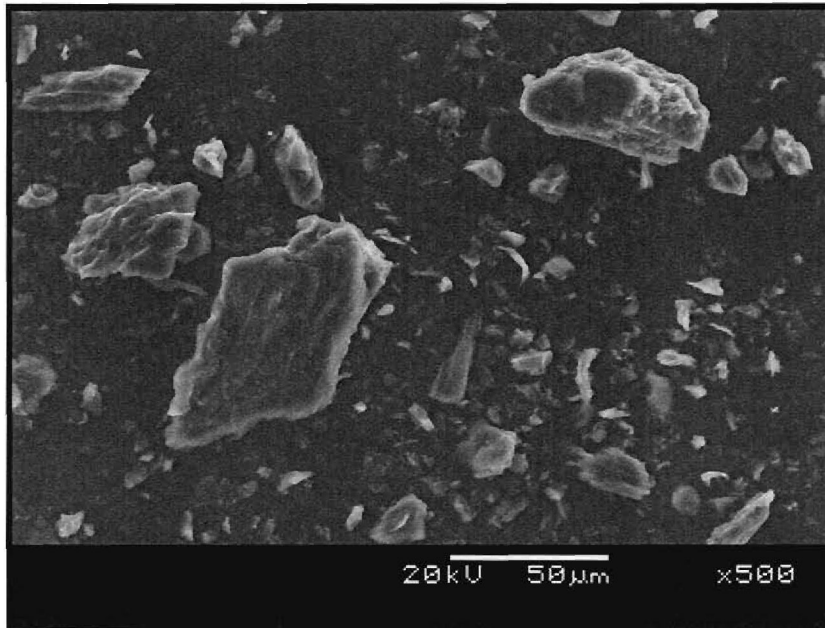


Figure 9.4c: SEM image of graphite filler

It was found that all the filler materials investigated in this study, were free-flowing and a conclusion was made that after depolymerisation of filled PTFE, the residue filler should pose no problem regarding their flowability in a continuous system. In such a system, the filler material has to be removed on a continuous basis, for example in the Paddle Reactor or in a rotating oven. Even seemingly problematic filler shapes like for instance needle-like fillers must be removed from the reactor.

9.3 *IN SITU* ESEM OBSERVATION OF FILLED PTFE DURING DEPOLYMERISATION

Environmental Scanning Electron Microscopy (ESEM) is a technique where an enclosed hotplate is installed inside a SEM while the instrument is operated in an alternative atmosphere under low vacuum. Inside this hotplate compartment a separate ventilation system is operational. This enables one to observe, for instance decompositions under different atmospheres (Chapter 3, Section 3.2.5). In this study the ESEM mode was used to observe the depolymerisation process of glass fibre-filled PTFE at 450 °C. A CD with the video of this process is included inside the back cover of this thesis. (Opening of the file is described in section 3.2.5)

A series of photos are presented in Figures 9.5 to 9.14 of the glass fibre-filled PTFE being depolymerised isothermally at 450 °C in different stages of the depolymerisation process. These pictures were taken as the PTFE increased to 450 °C. Here it can clearly be seen that the PTFE starts to become a highly viscous liquid before the viscosity decreases as the temperature increases. At a later stage the polymer boils as the depolymerisation process takes place. The filler material can always be seen and never takes part in the depolymerisation process.

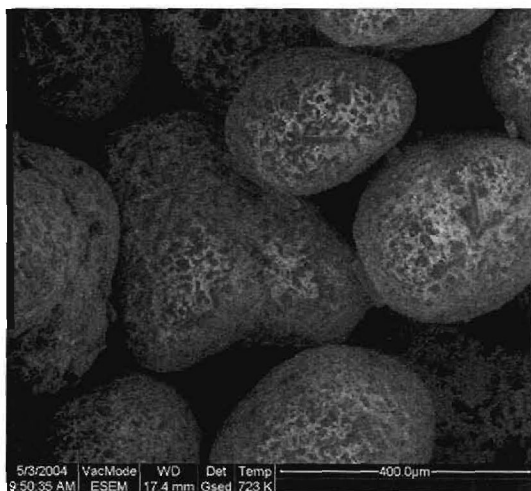


Figure 9.5: Cold PTFE

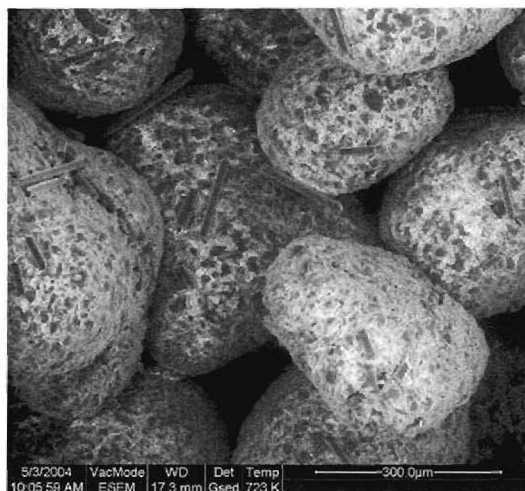


Figure 9.6: PTFE starts to swell

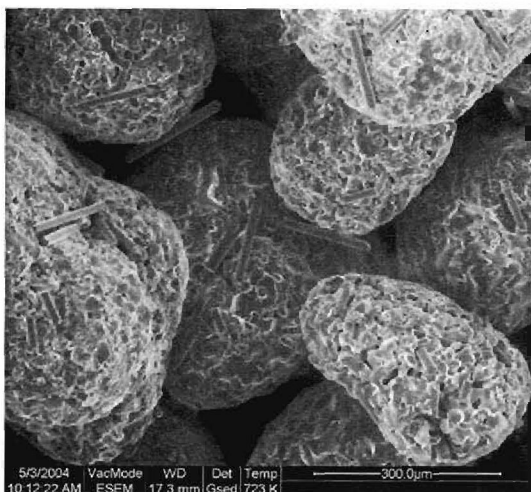


Figure 9.7: Surface depolymerisation

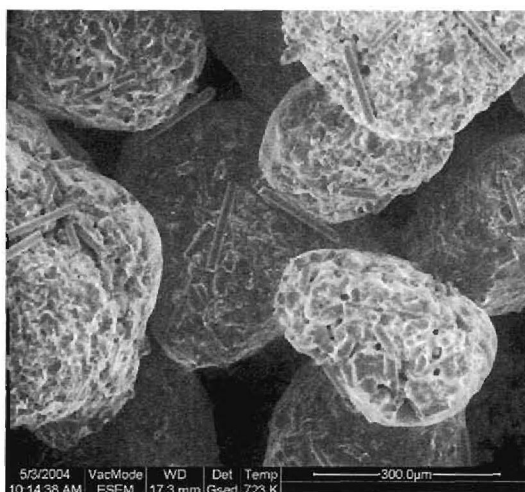


Figure 9.8: Core of particle melts

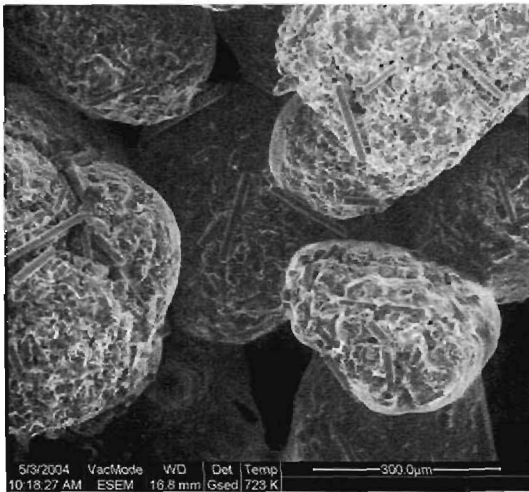


Figure 9.9: Bottom PTFE boills

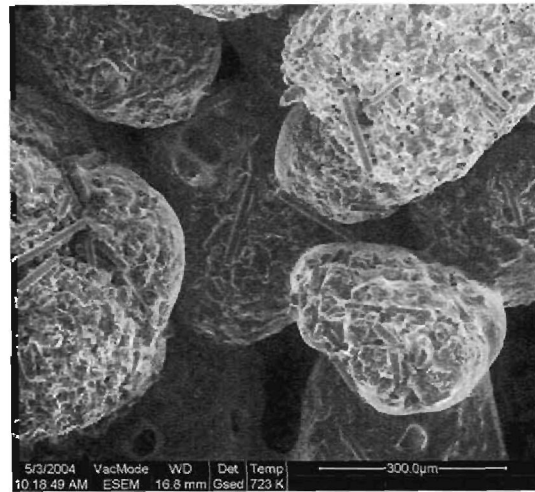


Figure 9.10: More particles boil

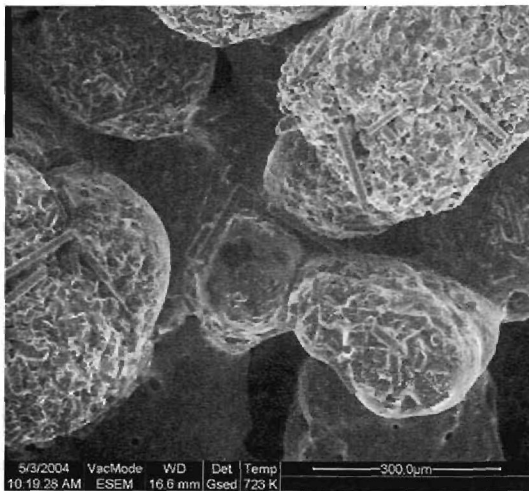


Figure 9.11: Particles melt together

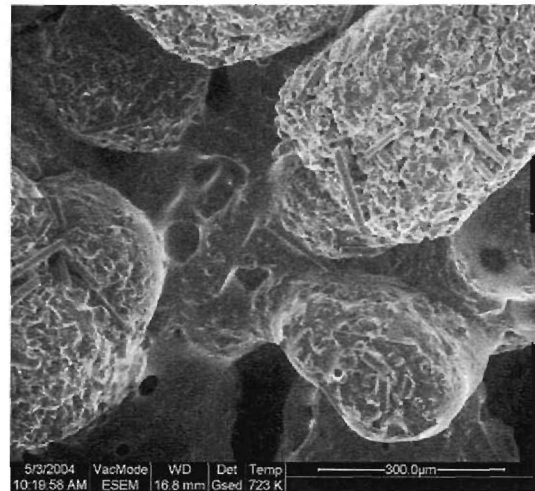


Figure 9.12: Molten mass boils

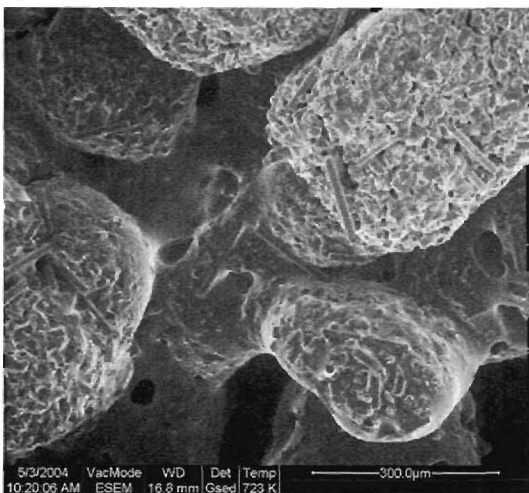


Figure 9.13: Process continues

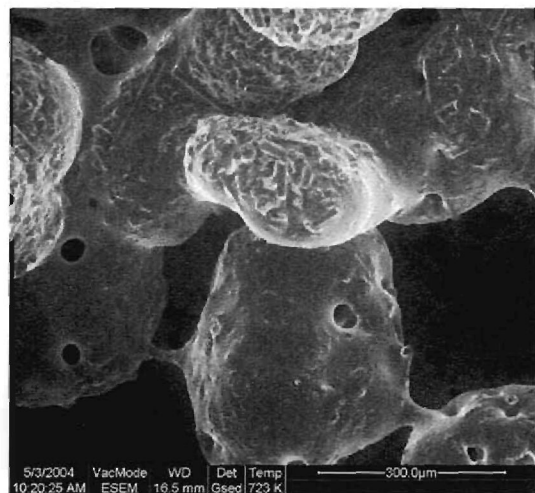


Figure 9.14: Volume decreased

Note that at this temperature of 450 °C the depolymerisation time was relatively long, in the order of 30 min. Heat transfer limitations at the hot stage may, however, also have slowed down the process.

9.4 VISUAL OBSERVATION OF THE EFFECT OF HOT PTFE ON REACTOR WALLS

The purpose of this section was to visually observe the effect of hot PTFE on the hot walls of a laboratory scale Rotating-kiln Reactor. The experimental setup and conditions are described in detail in Chapter 3. It was observed that the PTFE did not stick to the sides of the reactor before or during the depolymerisation process. During repeated rotation of the tube reactor through 45°, the following photo was taken (see Figure 9.15).

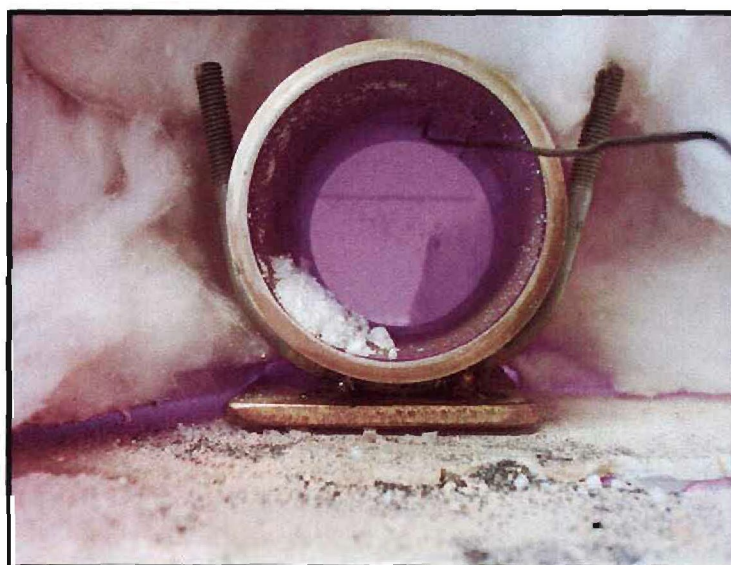


Figure 9.15: Photo of depolymerising PTFE inside the laboratory size, manually turned, Rotating-kiln Reactor (through 45°) at 400 °C

At 400 °C the glass fibre-filled PTFE exhibited a sweaty texture and slid back when the kiln was rotated through 45°. At 450 °C the PTFE had a fluffy texture but it was still solid and slid back when the kiln was rotated through 45°. At 500 °C the PTFE formed a high viscosity cake, but did not stick to the kiln wall. It still slid back when the tube was rotated through 45°. At 520 °C, the PTFE became opaque to transparent in appearance, but still slid back when the kiln was rotated through

45 °. At 550 °C, the volume of the PTFE seemed to increase. In appearance it was now totally transparent and started to form a thick and viscous liquid. At 580 °C the PTFE started to “boil” (sublimate) and white gas fumes appeared. This thick viscous mass rolled back when the tube was rotated through 45 °, without sticking to the walls. The volume reduced rapidly at 590 °C as the material was vaporised. Only the undepolymerised filler residue remained.

This experiment proved that:

1. Filled PTFE can be depolymerised on a continuous basis inside an inclined reactor;
2. The hot PTFE inside the reactor did not stick to the sides, but slid back to the bottom of the kiln during rotation;
3. The PTFE as well as the undepolymerised filler moved easily through the reactor.

It can therefore be concluded that filled PTFE can be depolymerised on a continuous basis in a declined reactor such as a Rotating-kiln Reactor. No problems should be expected regarding the sticking of hot PTFE to the reactor walls and the filler material also free-flows through the back end of the reactor where it can be discharged.

9.5 THE RESIDENCE TIME OF UNFILLED AND FILLED PTFE IN THE PADDLE REACTOR

9.5.1 Introduction

Determination of the mean residence time and the residence time distribution of the feedstock inside the reactor is an important property to know in designing a reactor. If depolymerisation is not efficient, it means that PTFE is not completely depolymerised and, in the case of filled PTFE, the filler material is still covered with polymer. To optimise the depolymerisation efficiency, experimentation at the required depolymerisation temperature must be performed where the residence time can be varied. For safety purposes, these experiments were performed at ambient temperatures and a relation between the actual residence time (the actual time that

the filler material spends inside the reactor during a hot experimental run) and the measured residence time (the residence time measurements of filled PTFE inside the Paddle Reactor without heat applied) was experimentally determined. Room temperature is actually the worst scenario in terms of residence time because the cold PTFE consists of hard, low-friction particles which move effortlessly through the reactor. A description of the system used for the residence time experiments was given in Chapter 3 (the Paddle Reactor). With this reactor the paddle rotation speed and reactor angle was varied in order to vary the residence time.

9.5.2 Experimental procedure

A given amount of polymer granules was introduced into the Paddle Reactor at time zero. The mass of the granules was recorded continuously with time, in order to determine the mean residence time and the residence time distribution inside the oven. The variable operating parameters were the inclination angle of the oven (2° , 4° , 6° and 7°) and the rotation speed of the paddles (2, 4.5, 7, 9.5 and 12 rpm). Four different PTFE samples were tested: unfilled-, bronze-filled-, graphite-filled- and glass fibre-filled PTFE.

9.5.3 Results and discussion

A typical result is presented in Figure 9.16. This particular sample (unfilled PTFE at a reactor angle of 4° and a paddle rotation speed of 7 rpm) took 330 seconds to completely pass through the reactor while it takes ~ 90 seconds for the first granules to leave the oven. The mean residence time for this sample was 161 seconds. The time at the peak of the first derivative was used as a measure of residence time through the reactor. This corresponds to approximately half of the sample that had moved through the reactor.

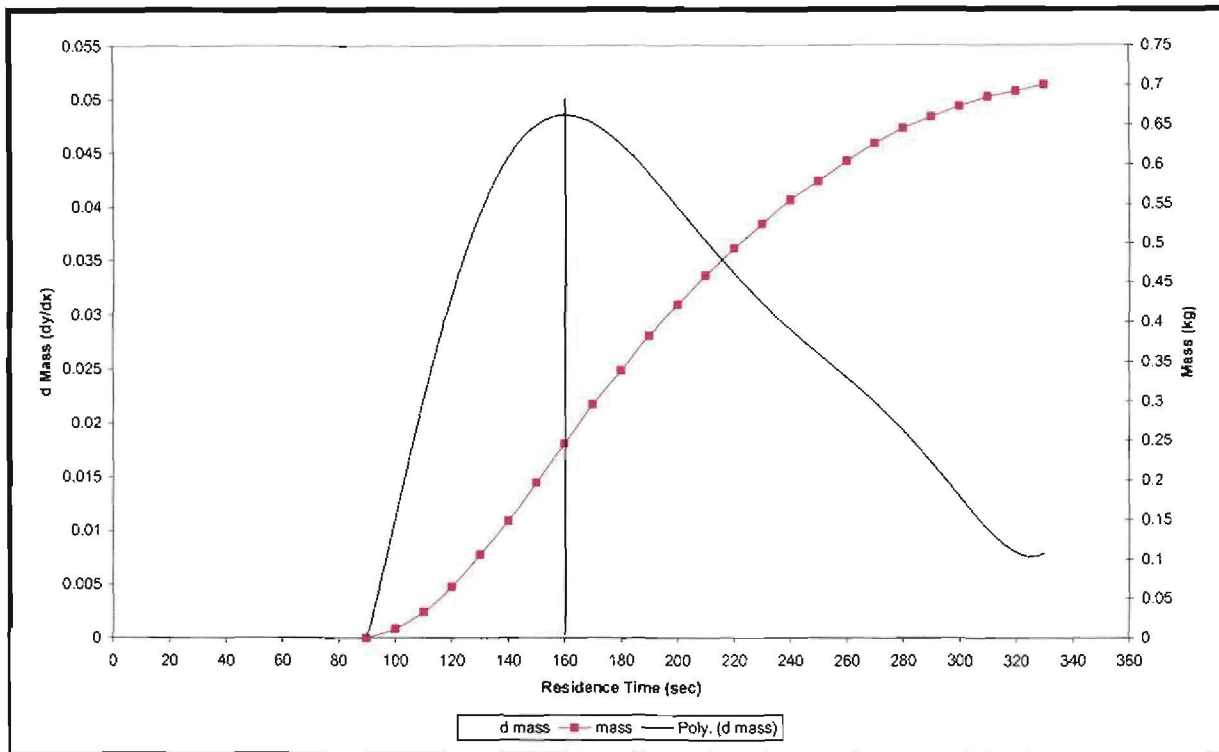


Figure 9.16: Residence time and residence time distribution of unfilled PTFE in the Paddle Reactor

This experiment was repeated for the four filled PTFE samples at different angles (2° , 4° , 6° and 7°) and different rotation speeds (2, 4.5, 7, 9.5 and 12 rpm) of the paddle screw. The results of this series of experiments are presented in Table 9.3.

Table 9.3: Residence time of filled and unfilled PTFE samples in the Paddle Reactor under varying conditions

Reactor Angle (°)	PTFE Sample	Paddle Speed (rpm)				
		2.0	4.5	7.0	9.5	12.0
Mean Residence Time (s)						
2	Unfilled	650	277	164	121	100
4	Unfilled	521	238	161	127	102
6	Unfilled	433	179	112	104	84
7	Unfilled	374	170	148	91	83
2	Bronze	634	278	223	194	114
4	Bronze	575	221	158	149	124
6	Bronze	366	178	122	85	77
7	Bronze	432	197	141	91	74
2	Graphite	636	263	170	126	94
4	Graphite	554	248	172	137	106
6	Graphite	462	197	120	100	84
7	Graphite	440	200	129	100	83
2	Glass	655	308	220	203	122
4	Glass	504	242	165	129	105
6	Glass	455	189	127	98	76
7	Glass	444	227	153	99	83

When the mean residence time is plotted against the paddle rotation speed for the different angles, (2, 4, 6 and 7 degrees declined), it can be observed that the residence time of PTFE inside the reactor increases as the angle decreases and the rotation speed of the paddle screw decreases. The mean residence time of the PTFE varied between 74 seconds for bronze-filled PTFE at a reactor angle of 7 ° and paddle screw speed of 12 rpm, to 655 seconds for glass fibre-filled PTFE at a reactor angle of 2 ° and a paddle screw speed of 2 rpm. Figure 9.17 presents the

dependence of the residence time on the filler material as a function of different reactor angles and different paddle rotation speeds. Individual graphs for 2, 4, 6 and 7 degrees are presented in Appendix 4 for more clarity.

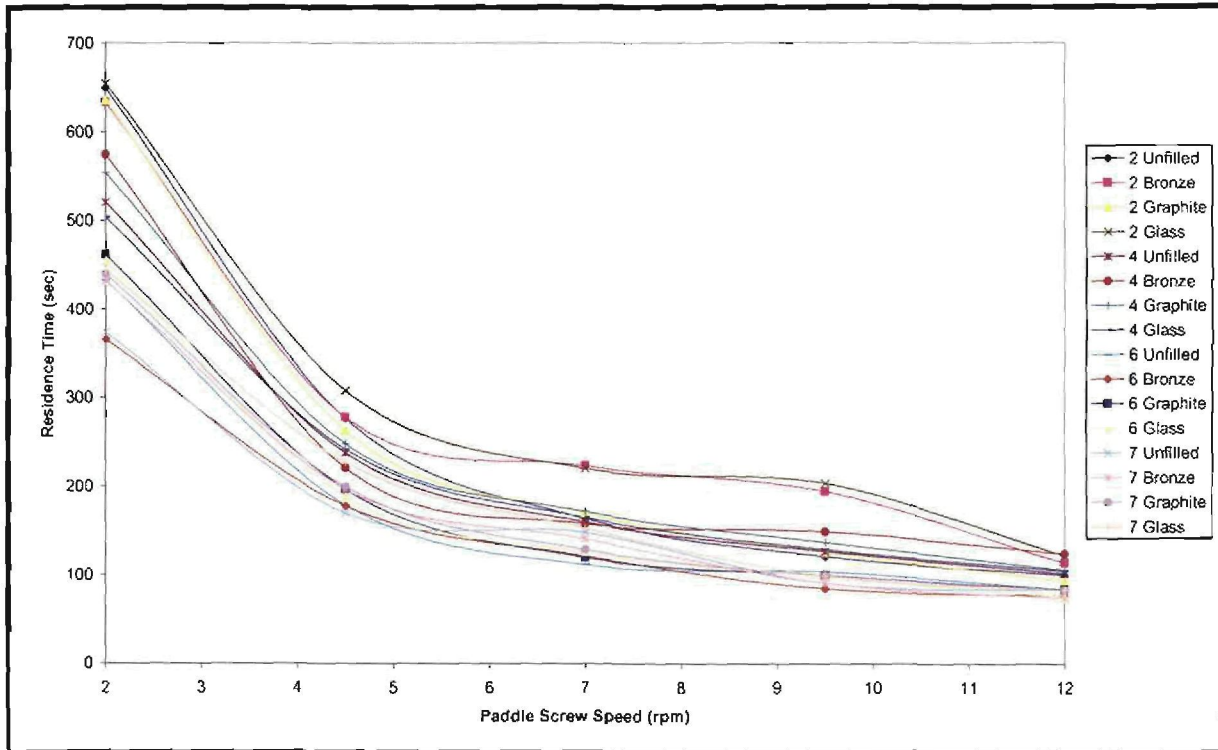


Figure 9.17: Residence time of different filled PTFE samples at different reactor angles as a function of paddle rotation speed

Generally the trends of the different samples at the different parameter settings are the same. From Figure 9.17 it can be seen that the mean residence time is less sensitive at paddle rotation speeds of > 5 rpm. At a low speed (2 rpm) though, the residence time increases significantly, in most cases almost doubling the time the samples spend in the reactor.

Another parameter that was investigated was the reactor angle. The effect of the reactor angle on the residence time is greater at slow paddle rotation speeds than at high rotation speeds. The general trend is also an increase in the residence time with decreasing reactor angle. This is the case for all four the samples.

Figure 9.18 is a three dimensional contour graph of the residence time of unfilled PTFE as a function of paddle rotation speed and reactor angle.

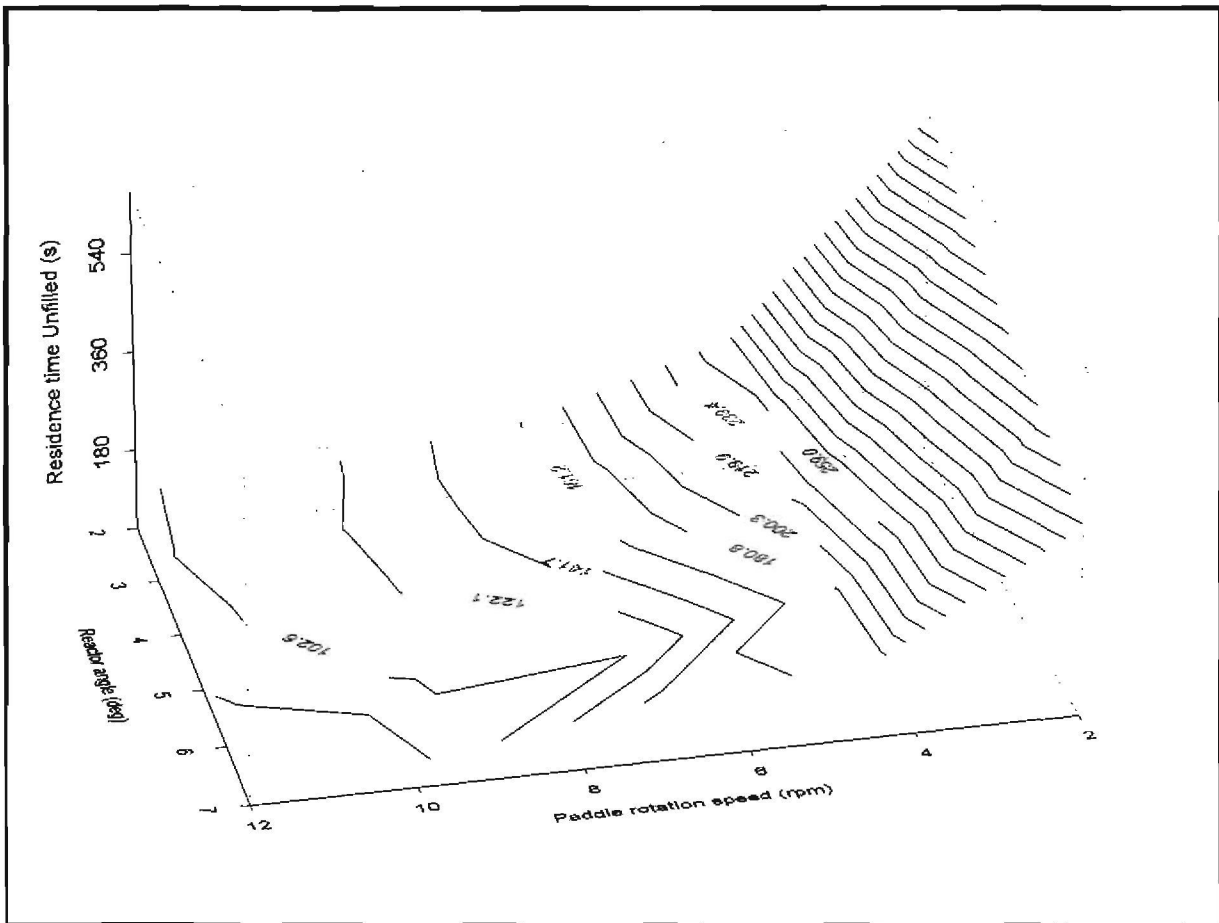


Figure 9.18: Residence time of unfilled PTFE as a function of paddle rotation speed and reactor angle

In this figure the large effect of the paddle rotation speed is clear. A sharp increase in the residence time, for all the reactor angles, when the paddle rotation speed was decreased from 4 to 2 rpm was observed. At the higher rotation speeds the residence times can be up to two orders of magnitude less. Graphs for the filled PTFE samples are included in Appendix 4.

In order to choose a paddle rotation speed and a reactor angle where experiments can be performed, the sensitivity of the system to change must be evaluated. For example at paddle rotation speeds of higher than 6 rpm, there is little change in residence time when the reactor angle is varied. However at a paddle rotation speed of 2 rpm, the residence times varies over-abundantly when the reactor angle is changed. At a paddle rotation speed of ~4 rpm, there is a significant change in residence time when the reactor angle is varied, but the change is manageable.

9.6 CONCLUSIONS

Upon analysis of the TGA polymer characterisation results it was found that the depolymerisation temperature of PTFE was at least 25 °C higher than any of the other polymer test samples. The polymer that closest resembled the PTFE depolymerisation temperature was PFA.

From the TG analyses it was found that the filler content of the PTFE may differ. The test samples typically contained between 20 to 40 % filler. Another result from the filler content test was the observation that the filler material that is to be used in this study is stable at the depolymerisation temperature and therefore will not contaminate the depolymerisation product.

The SEM analyses show that the filler materials differ in physical appearance as well as chemical composition. Glass fibre filler for example exhibits rod-like structures as opposed to the more rounded form of graphite and bronze fillers.

It was visually observed that the PTFE did not stick to the sides of a stainless steel tube reactor (laboratory Rotating-kiln Reactor) during the depolymerisation process upon rotation.

The type of filler material did not influence the residence time needed for complete depolymerisation significantly. The residence time can be accommodated by manipulating the reactor angle and the paddle rotation speed only. For the set-up used in this study, the longest residence time observed was 655 seconds for glass fibre-filled PTFE, at a reactor angle of 2 degrees and a paddle rotation speed of 2 rpm. The shortest residence time was 74 seconds for graphite-filled PTFE at a reactor angle of 7 degrees and a paddle rotation speed of 12 rpm.

At paddle rotation speeds of < 4 rpm the residence time becomes very sensitive for change. It is therefore suggested that experimentation be done at paddle rotation speeds of ~ 4 rpm where the change in residence time is manageable. The change in

reactor angle poses a less severe change in residence time beyond 4° and this is also the suggested reactor angle.

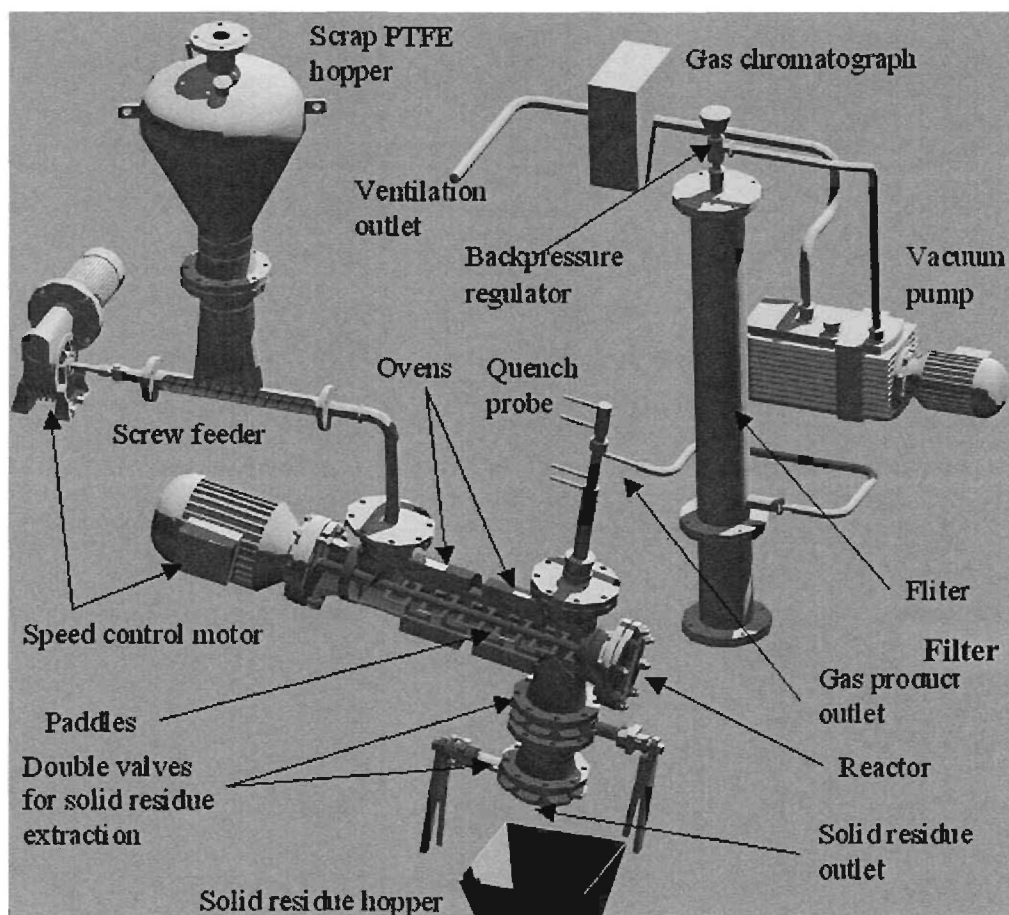
The results obtained in this chapter are very important input parameters for the chemical engineering design of a commercial plant as described in Chapter 12. Some of these parameters are:

- Depolymerisation temperature (energy inputs) required for the different fluoropolymers;
- The residence time will determine the size of the reactor and it must be sufficient to ensure complete depolymerisation ;
- The amount of filler (un-depolymerised fraction) is important in determination of the capacity of feed hoppers, waste hoppers and the amount of material that can be accommodated inside a typical rotating kiln reactor;
- The flowability of the feed material.

Chapter 10

The Depolymerisation of unfilled and filled PTFE in a Paddle Reactor

- 10.1. Introduction
- 10.2. Experimental method
- 10.3. Results and discussion
 - 10.3.1. Depolymerisation efficiency of the Paddle Reactor
 - 10.3.2. Analyses of the depolymerisation products
- 10.4. Conclusions



I. J. Van der Walt, A. T. Grunenbug, J. T. Nel, and O. S. L. Bruinsma, G. G. Maluleke, *The Continuous Depolymerisation of Filled Polytetrafluoroethylene (PTFE)*. (Accepted for publication at the Journal of Applied Polymer Science, August 2007)

10.1 INTRODUCTION

The Depolymerisation of PTFE, as described in Chapter 4, was done at temperatures between 600 to 900 °C and at or below atmospheric pressure (between 10 and 100 kPa). The Drop-tube Reactor described in Chapter 4 was not able to depolymerise filled PTFE on a continuous basis because the filler accumulated inside the reactor, which eventually blocked. The depolymerisation of filled PTFE by a continuous process requires a reactor design where the reactor is able to separate the product gases and the filler material, and dispose of the filler on a continuous basis, while the PTFE is being depolymerised.

In this chapter the development of such a continuous process whereby unfilled as well as filled PTFE waste can be converted into useful products like TFE, HFP and OFCB will be described, while the formation of other less wanted species like TFM, HFE, OFP and PFIB will also be discussed.

10.2 EXPERIMENTAL METHOD

A detail description of the Paddle Reactor system as shown in Figure 10.1 is given in Chapter 3.

During these experimentation, special precautions were taken when working at sub-atmospheric pressures, because TFE and oxygen (that can accidentally leak in), can under certain conditions form an explosive mixture.

At the start of each experiment the reactor was heated to the required temperature. The system was continuously evacuated to the desired pressure. After reaching a stable temperature, the PTFE was fed at a constant rate into the reactor via the screw feeder. When the PTFE entered the reactor, the paddle screw forced it into the hot zone and the depolymerisation process started. As soon as the gaseous products were generated, they were quenched by the quench probe at the reactor outlet. After quenching, the product gas was analysed by an inline GC and confirmed by a GC/MS. The filler material remaining after the depolymerisation process passes through the reactor and accumulates in the solids residue hopper.

The PTFE was fed at a rate of $1 \text{ kg}\cdot\text{h}^{-1}$, at a 4° angle and at a rotation speed of 4 rpm as determined in Chapter 9.

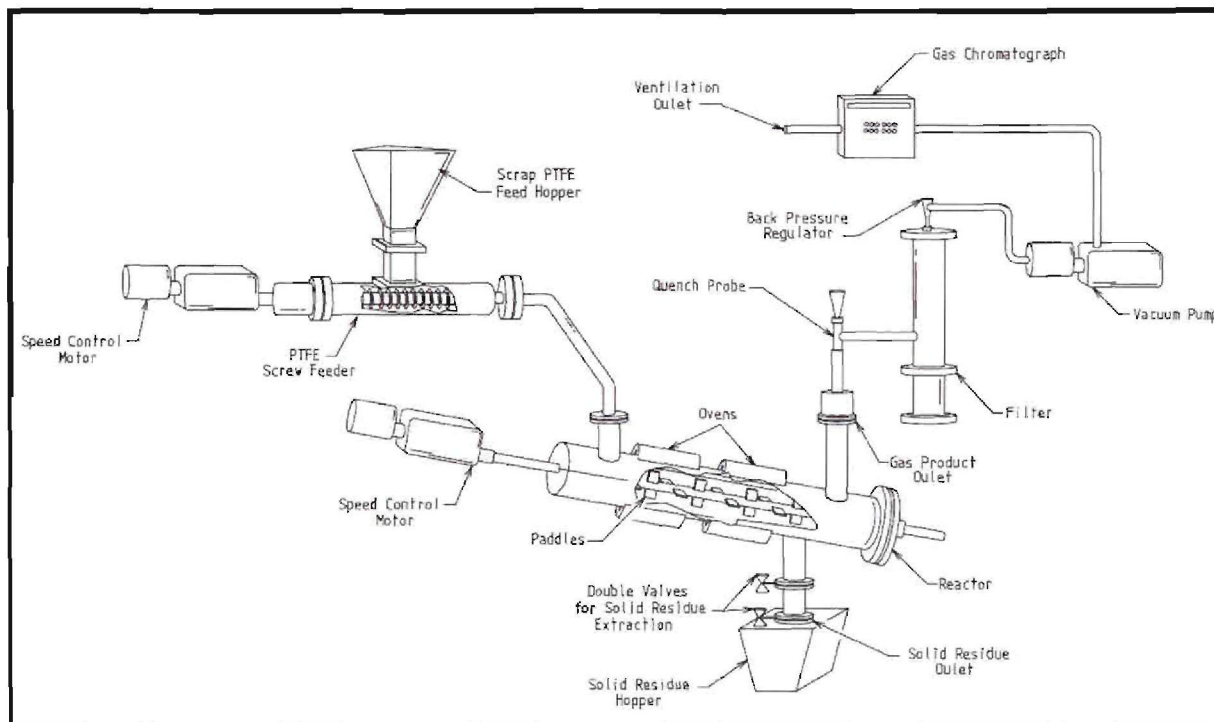


Figure 10.1: A schematic presentation of the depolymerisation Paddle Reactor and the feed and discharge system

During experimentation the following aspects regarding the system were investigated:

1. Determination of the ability of the reactor to depolymerise filled PTFE on a continuous basis;
2. The depolymerisation efficiency;
3. Analysis of the depolymerisation products.

10.3 RESULTS AND DISCUSSION

10.3.1 Depolymerisation efficiency of the Paddle Reactor

Table 10.1 is a summary of the amount of filler residue (by mass) that was generated when 5 kg of different filled and unfilled PTFE samples were depolymerised in the Paddle Reactor.

Table 10.1: Solid residue originating from filled and unfilled PTFE, collected after depolymerisation

Material	Mass PTFE fed (z) (kg)	Filler in PTFE (x) (kg)	Residue Collected (y) (kg)	Depolymerisation Efficiency (%)
PTFE (unfilled)	5.0	0	< 0.05	>99
PTFE (bronze-filled)	5.0	1.97	2.35	87
PTFE (graphite-filled)	5.0	1.19	1.52	91
PTFE (glass fibre-filled)	5.0	1.19	1.63	88

The depolymerisation efficiency was determined using the following equation:

$$\text{Depolymerisation Efficiency}(\%) = \left(\frac{z - y}{z - x} \right) \times 100\% \quad 10.1$$

As seen from Table 10.1 the depolymerisation efficiency of the Paddle Reactor at the set conditions and for this configuration was >85 %.

It was found that this type of reactor system was able to depolymerise filled as well as unfilled fluoropolymers without any blockages. No operational difficulties were experienced after 10 hours of operation. The same experimental conditions were used for all the depolymerisation experiments. Longer residence times might be needed for the filled PTFE to be depolymerised more efficiently.

10.3.2 Analyses of the depolymerisation products

After the exploratory experiments were concluded, the system was set up in such a manner as to optimise the depolymerisation of graphite-filled PTFE. The reactor was tilted at a 4 ° angle and the paddle screw was set at 4 rpm, corresponding to a solids residence time of ~4 minutes. The calculated gas residence time is ~60 seconds for a mass flow rate of 1 kg·h⁻¹ filled PTFE (calculation in Appendix 1). The reactor was operated at 600, 700 and 800 °C while the pressure was set at 10, 30, 60 and 90 kPa. Table 10.2 presents the results of the product analyses (GC) after graphite-filled PTFE was depolymerised in the Paddle Reactor.

Table 10.2: The GC analyses of the product gas after depolymerisation of graphite-filled PTFE in the Paddle Reactor (Vol %)

Pressure (kPa (abs))	Temp (°C)	TFM (%)	HFE (%)	TFE (%)	OFP (%)	HFP (%)	OFCB (%)	PFIB (%)
10	600	2.47	10.63	28.43	0.00	49.06	9.42	ND
30	600	5.64	17.04	30.79	9.42	30.22	6.89	ND
60	600	2.24	9.41	27.67	7.79	34.18	14.65	4.07
90	600	0.15	1.74	14.91	1.59	28.82	47.20	5.59
10	700	6.22	16.48	2.92	20.20	26.31	6.79	21.09
30	700	3.36	14.96	12.17	21.96	28.32	3.76	15.47
60	700	4.97	19.71	1.33	22.70	20.71	4.48	26.09
90	700	4.25	25.61	2.82	10.77	39.65	3.08	13.82
10	800	4.00	23.53	3.49	12.99	47.91	ND	8.07
30	800	7.26	32.28	1.17	11.76	40.60	ND	6.93
60	800	9.39	36.16	0.94	9.16	36.20	1.84	6.30
90	800	17.40	48.18	0.44	7.36	18.65	1.47	6.50

ND = Not Detected (Comment: All the results reported in the table above, is the average of at least three analysis with a standard deviation of less than 0.1 %)

It is clear that the product distribution is quite different from that produced in the Drop-tube Reactor (Chapter 4) with respect to the formation of high yields of HFE, OFP, HFP and TFM at most temperatures and pressures, and small concentrations of TFE. As with the Drop-tube Reactor, these products do not represent thermodynamic equilibrium conditions, but the higher yields of TFM and HFE (the thermodynamically most stable products as seen in Chapter 6) indicate that this

product distribution is closer to this equilibrium point. The formation of each product will be discussed separately below and is more clearly shown in contour plots (Figures 10.2 to 10.8).

A computer program called Axum 5.0B for Windows by Mathsoft, Inc. is used for the graphical presentation of the analytical data as a function of temperature and pressure. Axum uses the Marquardt-Levenberg nonlinear least squares algorithm to fit the curves.

The formation of TFM

TFM is formed in significant amounts (up to 17.4 %) at 800 °C and 90 kPa (Figure 10.2). At 600 and 700 °C the formation of this product with pressure increased although the yield at 700 °C was twice as high as at 600 °C. At 800 °C, the yield increased as the pressure increased. This molecule can only form if a $\text{CF}_3\cdot$ radical collides with a fluorine donor. At 600, 700 and 800 °C, the CF_4 formation competes with the HFE and OFP formation.

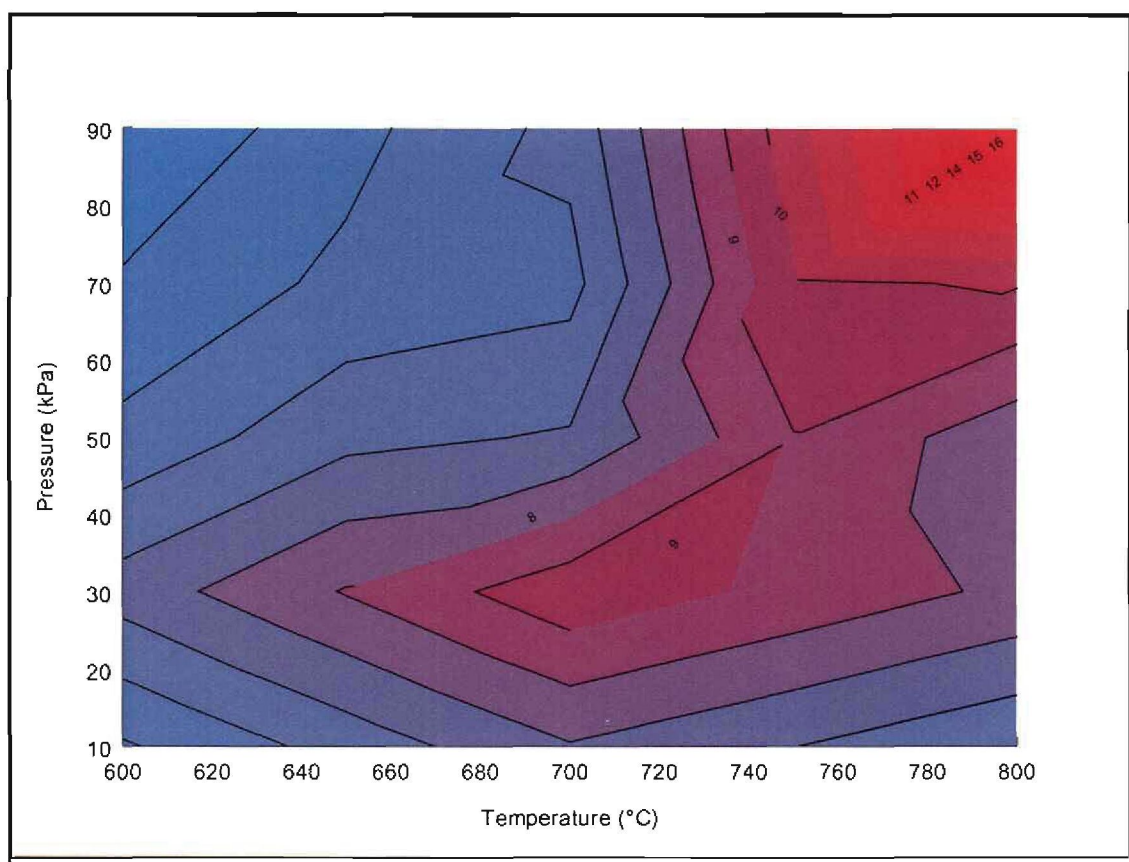


Figure 10.2: TFM concentration as produced by the Paddle Reactor

The presence of TFM is in contrast to the results found in Chapter 4 where TFM only featured at 900 °C. The reason for this might be the big difference in residence time in the reactor, between the Drop-tube system (~2 s) and the Paddle Reactor system (60 s).

The formation of HFE

Figure 10.3 gives the yield contours of HFE. The HFE formation at 600 °C decreased as the pressure increased. This might be due to an increase in the amount of PFIB that formed. At 700 to 800 °C the HFE yield increased as the pressure increased and the yield peaks at almost 50 % at 800 °C and 90 kPa.

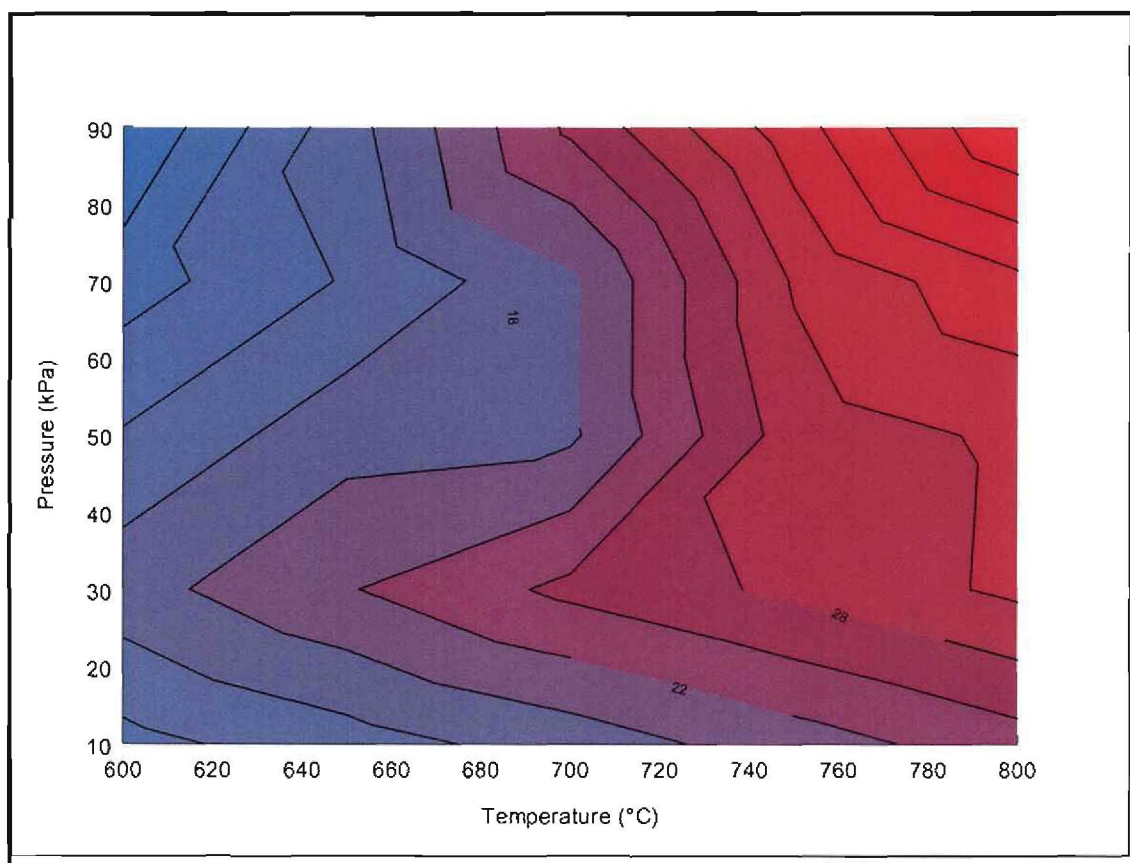


Figure 10.3: HFE concentration as produced by Paddle Reactor

These results show similar trends compared with the Drop-tube Reactor in Chapter 4, but higher yields were observed with the Paddle Reactor.

The formation of TFE

At 600 °C the TFE yield dropped as the pressure increased (Figure 10.4). The same trend was observed at 700 and 800 °C, but surprisingly much smaller amounts of TFE were found (< 5 %). The highest TFE yield (30.79 %) was found at low pressure (10 to 60 kPa) and low temperature (600 °C).

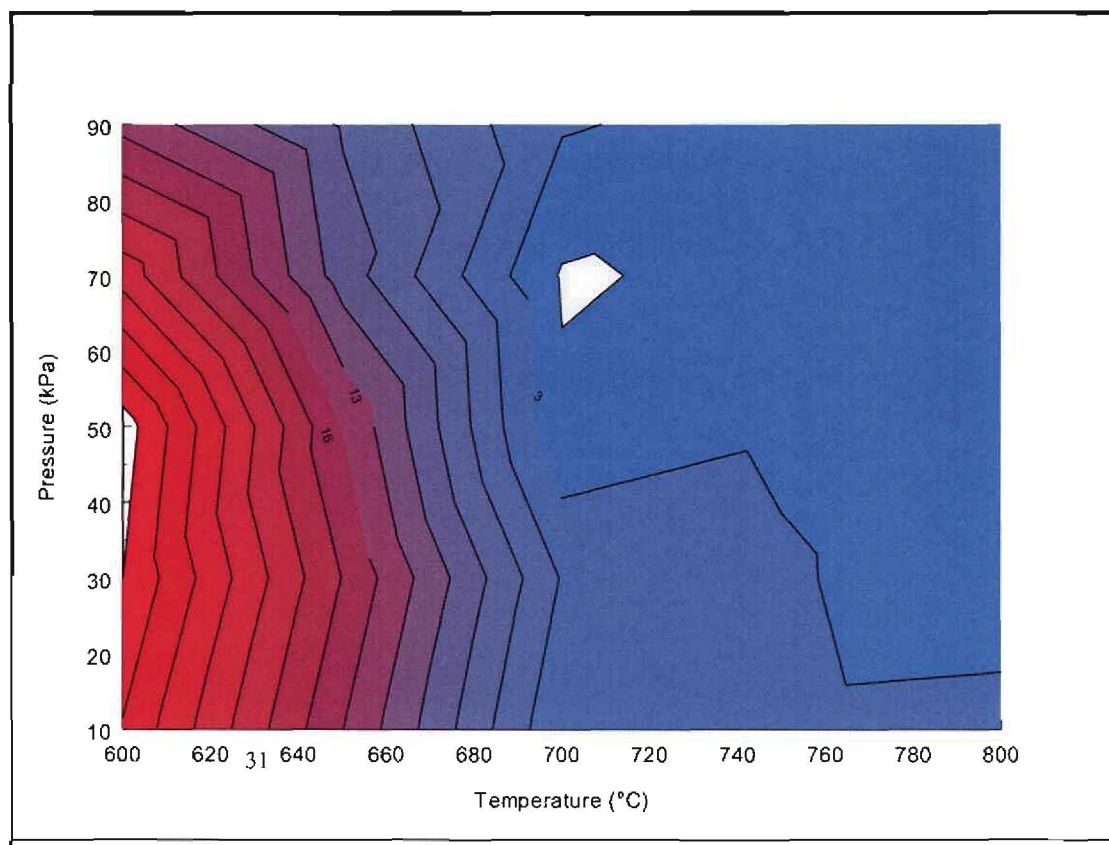


Figure 10.4: TFE concentration as produced by the Paddle Reactor

The TFE yield found with Paddle Reactor experiments is in sharp contrast with the results obtained with the Drop-tube Reactor. The TFE yield decreases as the temperature and pressure increases.

The formation of OFP

The OFP concentration contours are indicated in Figure 10.5. A maximum OFP concentration (22.7 %) was found at 700 °C and 50 kPa. At higher and lower temperatures the yield dropped.

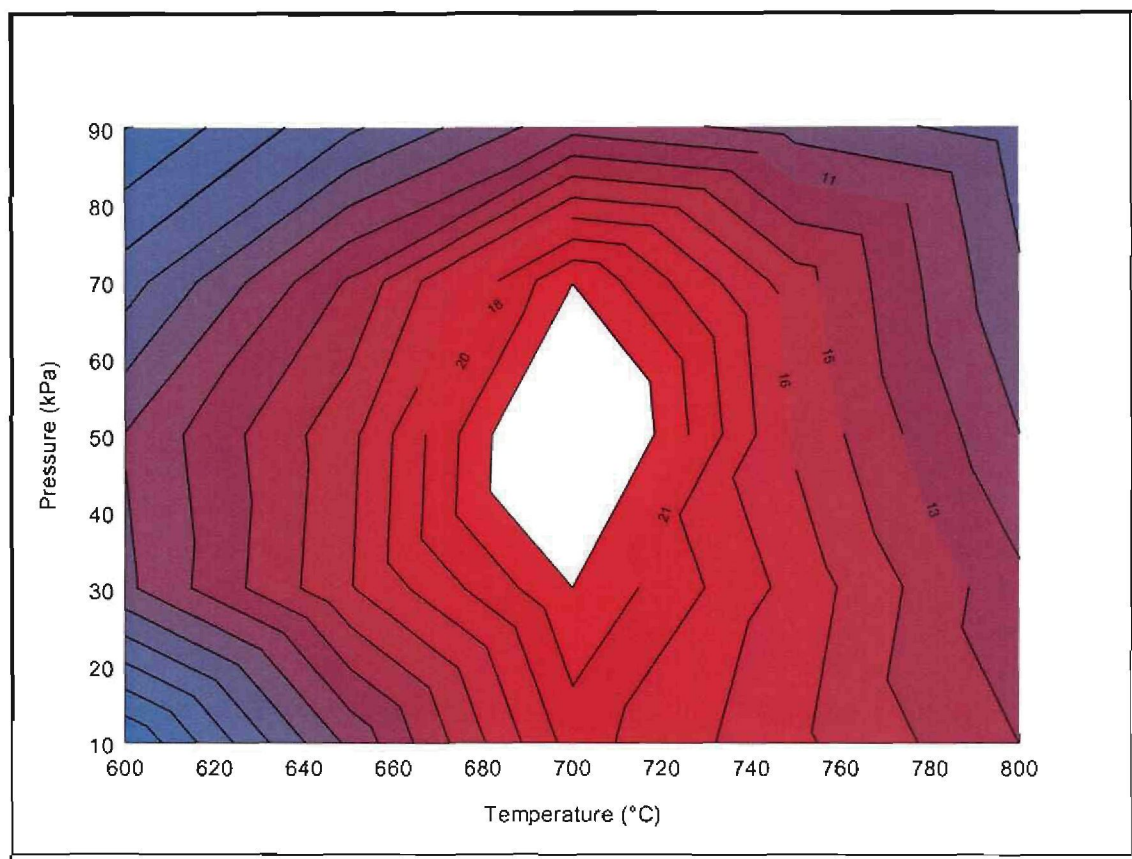


Figure 10.5: OFP concentration as produced by the Paddle Reactor

The OFP concentration produced by the Paddle Reactor is at least an order of magnitude higher than the concentration obtained by the Drop-tube Reactor under similar conditions. The trend with the Drop-tube Reactor differed as the concentration increased as the pressure increased.

The formation of HFP

The HFP yield contours are presented in Figure 10.6. Three concentration peaks were observed. The first (49 %) at 600 °C and 10 kPa, the second (~38 %) at 700 °C and 90 kPa and the third (~48 %) at 800 °C and 10 kPa. A large low-concentration dip was observed at 700 °C and 50 kPa. This is in the same region as the OFP maximum.

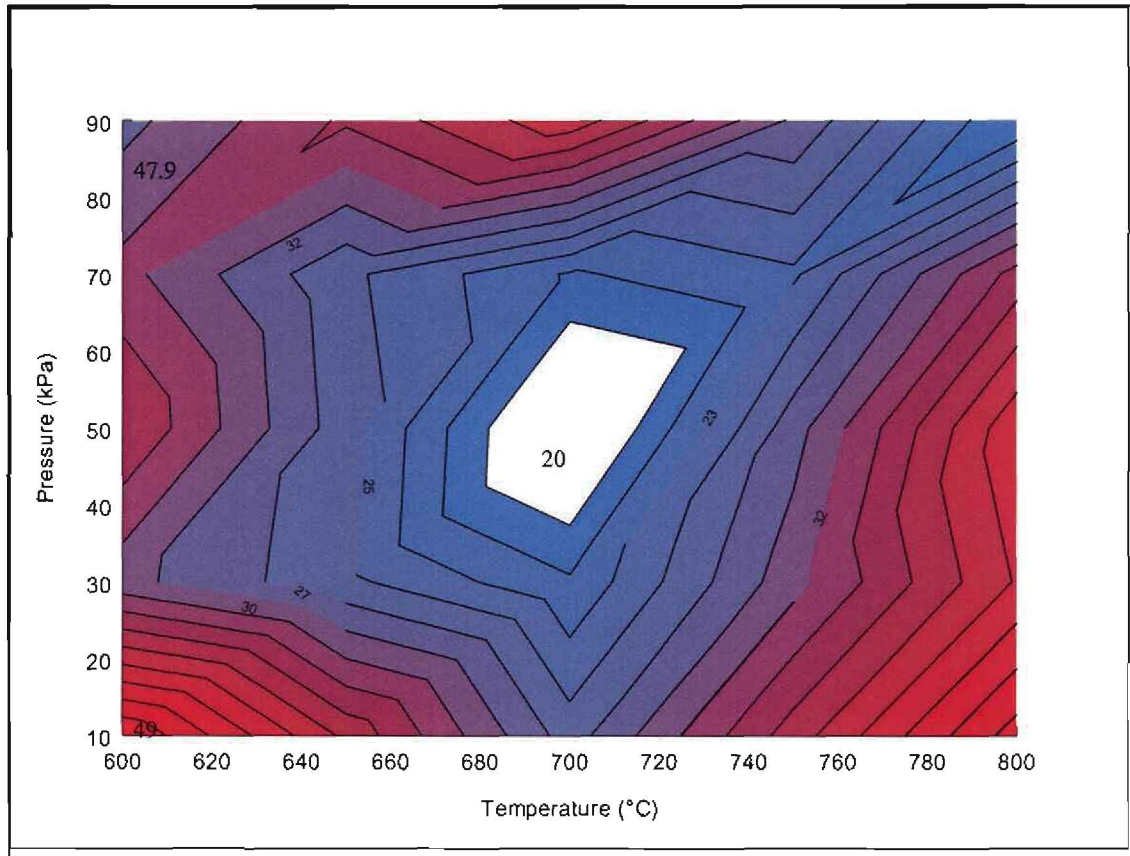


Figure 10.6: HFP concentration as produced by the Paddle Reactor

The HFP concentration in the Drop-tube Reactor (Chapter 4) generally increased as the pressure and temperature increased. The lowest yield was 4.1 % at 700 °C and 5 kPa, and the highest yield 61 % at 800 °C and 80 kPa.

The formation of OFCB

The OFCB concentration increased as the pressure was increased at 600 °C (Figure 10.7). A sharp rise in concentration was observed and a maximum yield of 47.2 % was obtained at 600 °C and 90 kPa. At 700 and 800 °C the concentration dropped significantly to below 10 %.

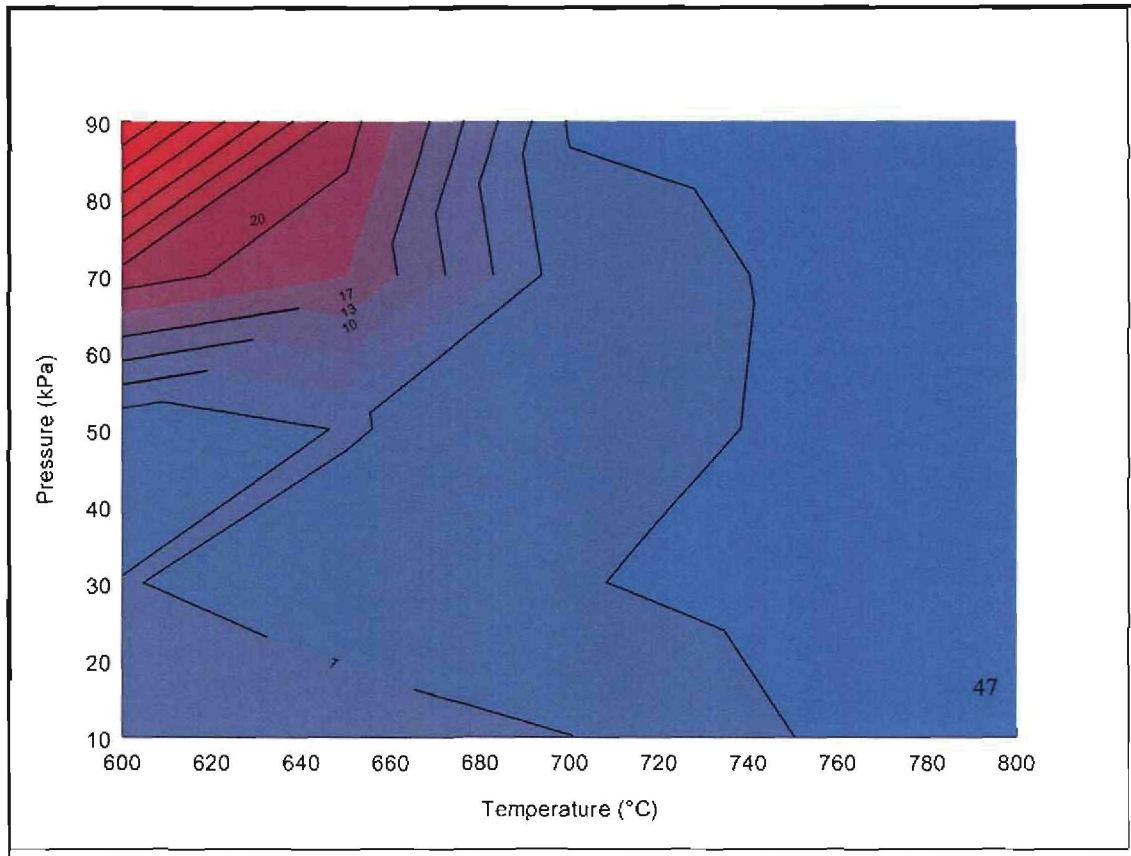


Figure 10.7: OFCB concentration as produced by the Paddle Reactor

Generally lower yields were obtained with the Drop-tube Reactor experiments. OFCB was produced in significant amounts at 600, 700 and 800 °C. The highest yield though was 25.1 % at 720 °C and 82 kPa.

The formation of PFIB

The PFIB yield produced by the Paddle Reactor was significantly higher (26.09 % max) than that was produced by the Drop-tube Reactor (1.7 %) as indicated in Figure 10.8. At 700 °C and 60 kPa the highest yield was observed. This is in the same region as the OFP maximum and the HFP minimum.

PFIB is not one of the wanted products and along with the toxicity hazard, it is one of the by-products that must be avoided as far as possible.

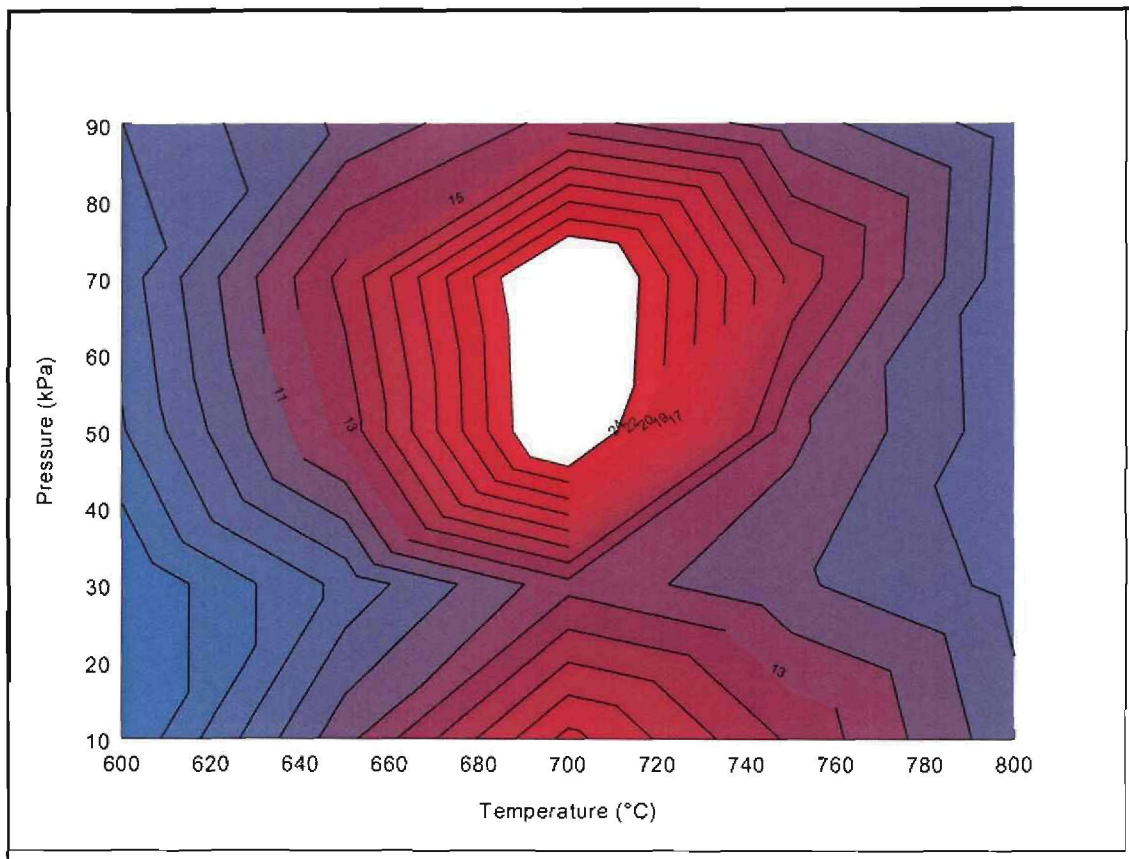


Figure 10.8: PFIB concentration as produced by the Paddle Reactor

10.4 CONCLUSIONS

A system that was able to depolymerise filled as well as unfilled PTFE at sub-atmospheric pressures, with no carrier gas (less separation necessary and less waste produced) and on a continuous basis, was successfully developed. The Paddle Reactor consisted of a screw feeder to feed the filled PTFE into a reactor that was inclined at an angle of 4 ° (as optimised in Chapter 9). This reactor was fitted with a centrally-mounted paddle screw, which enhanced the passage of the feed material through the reactor and the paddles also exerted a scraping action onto the inner wall of the reactor to prevent the residue from sticking, and to increase the heat transfer between the PTFE and the hot tube. The outlet of the reactor was designed to separate the solid residue from the depolymerised gases. When the gas exited the reactor it was quenched and analysed. The solid residue was extracted *in situ* with the double-valve system into a residue disposal hopper.

It was found that changing the temperature and pressure of the reactor can vary the product composition. Optimising the residence time of the PTFE inside the reactor can render a depolymerisation efficiency of >90 %. The product composition generated by the Paddle Reactor differed considerably from that which was generated by the Drop-tube Reactor described in Chapter 4. The reason for this is that the residence time of the gaseous product inside the Paddle Reactor was significantly longer (~60 sec) than in the Drop-tube Reactor (~2 sec).

For the Paddle Reactor the following optimum yields for the different products were obtained: An optimum TFE yield of 30 vol. % was obtained at 600 °C and 10 to 60 kPa. The abundance of other products, in comparison with the Drop-tube Reactor seems to indicate that a shorter gas residence time should be used in case is to be the major product.

The best conditions to produce HFP in the Paddle Reactor are 600 °C and 10 kPa, where 50 vol % HFP is produced. Although similar yields are observed at 800 °C and 10 kPa, the lower temperature is preferred as this will lead to lower operating and

capital cost and less carbon formation and by-products like TFM, HFE and OFP. Note that this operating condition is the same as for optimum TFE production.

The optimum conditions for OFCB production, the third commercially interesting product, are 600 °C and 90 kPa leading to a yield of 47 %.

Temperatures of 700 °C should be avoided at all cost in order to avoid the toxic PFIB from forming.

These results are in accordance with recent work from Meissner *et al*⁽³⁵⁾. He built a small system solely for the optimisation of TFE, HFP and OFCB by changing the reaction pressure, temperature and residence time. He optimised the product formation in more detail and could attain even higher yields of HFP.

Although the HFP yield was not as high as was found in the literature, this newly designed Paddle Reactor system was able to depolymerise filled and unfilled PTFE on a continuous basis without a carrier gas. This is a new and novel method and the results were accepted for publication in the Journal of Applied Polymer Science in August 2007.

Chapter 11

Continuous Conversion of Other Fluoropolymer Waste in a Vibrating Reactor

11.1. Introduction

11.2. Experimental method

11.3. Results and discussion

11.3.1. The production of fluorochemicals by the depolymerisation of unfilled and filled PTFE

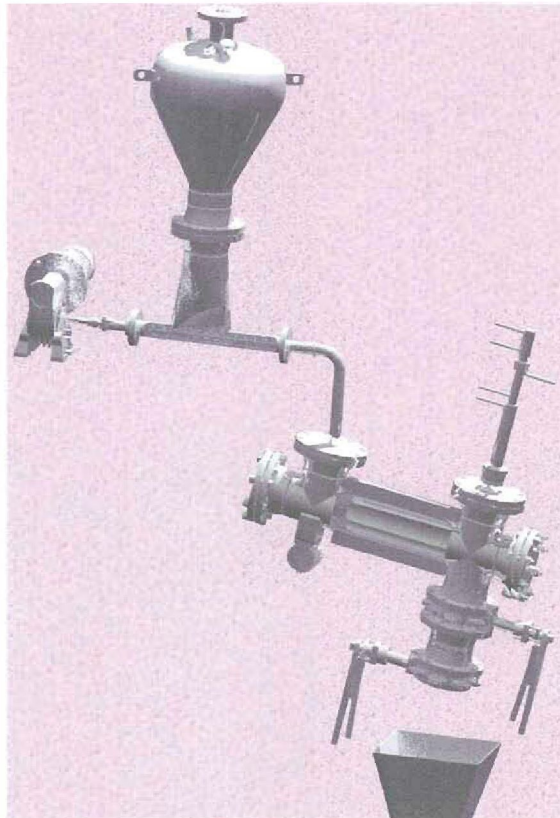
11.3.2. The production of fluorochemicals by the depolymerisation of PFA

11.3.3. The production of fluorochemicals by the depolymerisation of FEP

11.3.4. The production of fluorochemicals by the depolymerisation of THV

11.3.5. The production of fluorochemicals by the depolymerisation of ETFE and HTE

11.4. Conclusions



11.1 INTRODUCTION

Other fluoropolymers were developed during the past decades to further enhance the excellent properties of PTFE. The main disadvantage of using PTFE is the fact that it is not melt-processible.⁽⁷⁾ The addition of other monomers did solve the melt-processibility problem, but unfortunately these polymers did not have the excellent thermal qualities of PTFE.^(6, 7) The advantages, however, overshadowed the disadvantages and these polymers are used in abundance. These other fluoropolymers include Fluorinated-Ethylene-Propylene (FEP), Perfluoroalkoxy (PFA), Ethylene-Tetrafluoroethylene copolymer (ETFE), Hexafluoropropylene-Tetrafluoroethylene-Ethylene copolymer (HTE) and Tetrafluoroethylene-Hexafluoropropylene-Vinilidene fluoride (THV). These fluoropolymers can be divided into two groups, namely hydrogen-containing fluoropolymers (THV, HTE and ETFE) and non-hydrogen-containing fluoropolymers (FEP, PFA).

In this chapter the possibility of depolymerising other fluoropolymers under the same conditions as with PTFE depolymerisation will be tested, and their depolymerisation products evaluated against those for PTFE. In this case a vibrating reactor will be used because the depolymerisation properties for the other fluoropolymers are not known and a simple reactor setup is needed.

11.2 EXPERIMENTAL METHOD

As the reactor configuration plays an important role in the products formed, as was already found in Chapter 10, a series of experiments with filled and unfilled PTFE as well as with other fluoropolymers were conducted. A Vibrating Reactor was used to depolymerise the different fluoropolymers on a semi-continuous basis. The main reason was the ease of operation of the vibrating reactor with regard to the maintenance when other fluoropolymers were depolymerised. Figure 11.1 is a schematic presentation of this system. This reactor was operated at the same polymer feed rate as the Paddle Reactor, but due to its smaller volume has a typical residence time almost of 10 times shorter than the Paddle Reactor.

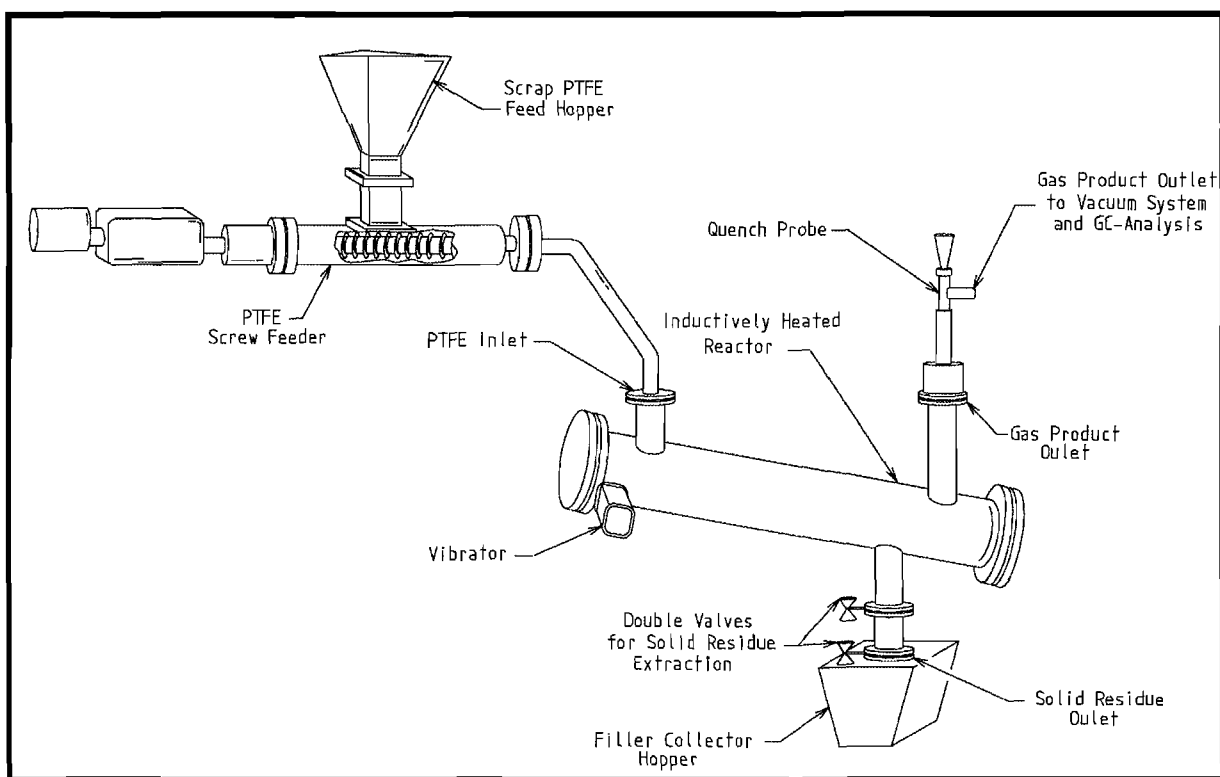


Figure 11.1: A Vibrating Reactor that was used to depolymerise different fluoropolymers

The polymer was introduced into the reactor from a feed hopper via a screw feeder at a rate of $\sim 2 \text{ kg}\cdot\text{h}^{-1}$ polymer. The reactor was fitted with a pneumatic vibrator to enhance forward movement of the polymer particles. The polymer depolymerised while moving through the reactor and was separated from the inert solids. The

back-end of the reactor was modified to accommodate the inert solids in a filler collection hopper while the gaseous product was quenched and analysed. The gas residence time for this reactor was calculated to be ~3.25 s (according to the formula presented in Appendix 1) at ambient temperature and pressure, which is close to the Drop-tube Reactor, described in Chapter 4 (~2 s). More details of the system are described in Chapter 3.

After the depolymerisation process the product gas mixture resulting from depolymerisation of the different fluoropolymers was analysed by a GC and checked by a GC/MS. The results were evaluated against that of PTFE as a reference.

The different fluoropolymers were depolymerised in the same reactor under the same experimental conditions, for comparison purposes.

11.3 RESULTS AND DISCUSSION

In this section the composition of the product gas after depolymerisation of other fluoropolymers will be analysed in order to evaluate their ability to be depolymerised to form fluorocarbon products similar to PTFE.

11.3.1 The production of fluorochemicals by the depolymerisation of unfilled and filled PTFE

The results after analysis of the depolymerisation data for unfilled and filled PTFE are presented in Table 11.1.

Table 11.1: Product composition after depolymerisation of unfilled and filled PTFE in the Vibrating Reactor

Filler	Pressure (kPa (abs))	Temp. (°C)	TFM (%)	HFE (%)	TFE (%)	OFFP (%)	HFP (%)	OFCB (%)	PFIB (%)
None	21	612	ND	ND	81.4	ND	12.4	6.0	ND
None	82	805	ND	9.0	12.8	4.5	61.0	10.7	1.7
Glass	5	600	ND	3.3	92.5	ND	4.1	ND	ND
Glass	92	818	ND	0.7	88.5	ND	9.9	0.9	ND
Graphite	5	600	ND	2.0	75.2	ND	3.4	ND	19.2
Graphite	27	864	2.2	3.9	93.9	ND	ND	ND	ND
Bronze	33	600	ND	ND	94.8	ND	5.1	ND	ND
Bronze	91	869	ND	5.2	59.0	1.2	32.6	ND	1.7

ND = Not Detected

(The results presented are the average of at least three analyses)

After analysing the data it was found that the depolymerisation products from the filled PTFE followed the same trend as for unfilled PTFE. The TFE concentration generally decreased when the pressure was increased while the HFP and OFCB concentrations increased. At ca. 80 kPa the product C₂F₆ was formed in significant amounts. The optimum conditions for high yield (> 80 %) TFE are low pressure (< 30 kPa) and low temperature (< 700 °C).

The TFE yield for the unfilled PTFE at 805 °C and 82 kPa was low and the HFP yield high in comparison with the other results. The reason for this is not clear, but a possible explanation is that the quench probe might have been partially blocked, resulting in a prolonged residence time before the gas was quenched. Bronze-filled PTFE at 91 kPa and 869 °C showed a similar trend. Another interesting result was the high PFIB yield from graphite-filled PTFE at 5 kPa and 600°C. This high yield might also be the result of an increased residence time due to a blockage.

The Vibrating Reactor, with its gas residence time between that of the Drop-tube Reactor and the Paddle Reactor produces 81 % TFE at 612 °C and 21 kPa, which falls between the TFE yield obtained with the Drop-tube Reactor and the Paddle

Reactor. A similar trend is true for HFP production at 805 °C and 82 kPa. This clearly shows that the product spectrum can be manipulated by three parameters: pressure, temperature and gas residence time. This is in line with results found in Chapter 10.

The next series of experiments were performed to determine to what extent other non-hydrogen-containing fluoropolymers like PFA, FEP and THV could be depolymerised in the new continuous depolymerisation horizontal Vibrating Reactor. A distinction was made between non-hydrogen-containing and hydrogen-containing fluoropolymers because the two reacted differently in the depolymerisation system, and the resulting hydrocarbons are contaminants in the product mixture. The oxygen concentration present in PFA is much less than the hydrogen concentration in ETFE and HTE and plays an insignificant role in product formation. This was experimentally determined in previous work that will not be discussed here.

11.3.2 The production of fluorochemicals by the depolymerisation of PFA

Depolymerisation of PFA (Table 11.2) was performed at ca. 600 °C and at pressures that ranged between 10 and 60 kPa.

Table 11.2: Results obtained during the depolymerisation of PFA

Pressure (kPa (abs))	Temp (°C)	TFM (%)	HFE (%)	TFE (%)	OFF (%)	HFP (%)	OFCB (%)	PFIB (%)
10	600	2.0	0.5	97.5	ND	ND	ND	ND
40	570	ND	ND	53	ND	24.7	22.3	ND
60	575	ND	ND	41.9	ND	24.8	12.4	20.7

ND = Not Detected (The results presented are the average of at least three analyses)

A TFE yield of 97.5% was achieved at 10 kPa, but the yield dropped to 41.9% at a pressure of 60 kPa. The HFP and OFCB yields started to increase significantly at pressures above 10 kPa. At 60 kPa PFIB was formed in significant amounts. Bad quenching or a blocked reactor (increased residence time) might have been the reason. During experimentation the reactor blocked, causing the reactor pressure to increase and the residence time to be prolonged.

Good yields of TFE, HFP and OFCB were obtained at 600 °C, but higher temperatures such as 700 and 800 °C could not be utilized because of the low melting point of PFA (301 °C). Sputtering caused blockages inside the reactor.

11.3.3 The production of fluorochemicals by the depolymerisation of FEP

FEP is elementally the same as PTFE, but as shown in Table 11.1, FEP is branched where PTFE is un-branched. The introduction of HFP in this co-polymer causes FEP to be melt-processable. The disadvantage though is that the melting temperature is lower (260 °C) compared to that of PTFE (330 °C). The results of the FEP depolymerisation experiments are presented in Table 11.3.

Table 11.3: Products from the depolymerisation of FEP

Pressure (kPa (abs))	Temp (°C)	TFM (%)	HFE (%)	TFE (%)	OPF (%)	HFP (%)	OFCB (%)	PFIB (%)
30	830	ND	ND	52.1	ND	37.8	10.1	ND
60	829	ND	ND	30.2	ND	49.9	17.4	ND
100	830	ND	ND	25.1	ND	52.4	17.9	ND
120	835	ND	ND	17.3	ND	63.7	13.8	ND
20	780	ND	ND	62.3	ND	32.2	5.4	ND
50	782	ND	ND	46.5	ND	36.6	16.7	ND
80	782	ND	ND	32.5	ND	40.8	26.6	ND
100	780	ND	ND	25.3	ND	42.3	27.9	ND
120	780	ND	ND	23.1	ND	43.9	28.0	ND
30	750	ND	ND	56.3	ND	29.9	6.8	7.0
60	750	ND	ND	33.9	ND	22.1	9.3	0.3
90	755	ND	ND	32.6	ND	39.2	26.3	1.0
120	750	ND	ND	29.3	ND	39.8	30.2	0.7

ND = Not Detected (The results presented are the average of at least three analyses)

Depolymerisation of FEP was performed successfully at 750, 780 and 800 °C and at different pressures. Because FEP is a copolymer of TFE and HFP, it was expected that the two main products from the depolymerisation process would be TFE and HFP. This was indeed the case, but OFCB was also one of the major products. The unwanted TFM, HFE, OFP and OFB were not detected.

The change in product composition with temperature and pressure is consistent with the change that takes place when PTFE is depolymerised. At low pressures the TFE yield peaks while the HFP and OFCB yields are at their lowest. Higher pressure negatively influences the TFE yield, while the HFP and OFCB yields increase as the pressure is increased.

The major difference between the products produced by the FEP in comparison with those from PTFE depolymerisation experiments, is the relatively low TFE yield and the relatively high HFP yield at low temperature (750 °C) and low pressure (20 kPa). The reason for this is the difference in the monomers used to manufacture the two polymers. In the case of PTFE only TFE was used in the polymerisation process while TFE as well as HFP was used in the FEP polymerisation process. One would expect HFP and TFE to form during the depolymerisation step.

Figures 11.2 to 11.4 are graphical presentations of the trends of TFE, HFP and OFCB emanating from the depolymerisation of FEP.

A computer program called Axum 5.0B for Windows by Mathsoft, Inc. is used for the graphical presentation of the analytical data as a function of temperature and pressure. Axum uses the Marquardt-Levenberg nonlinear least squares algorithm to fit the curves.

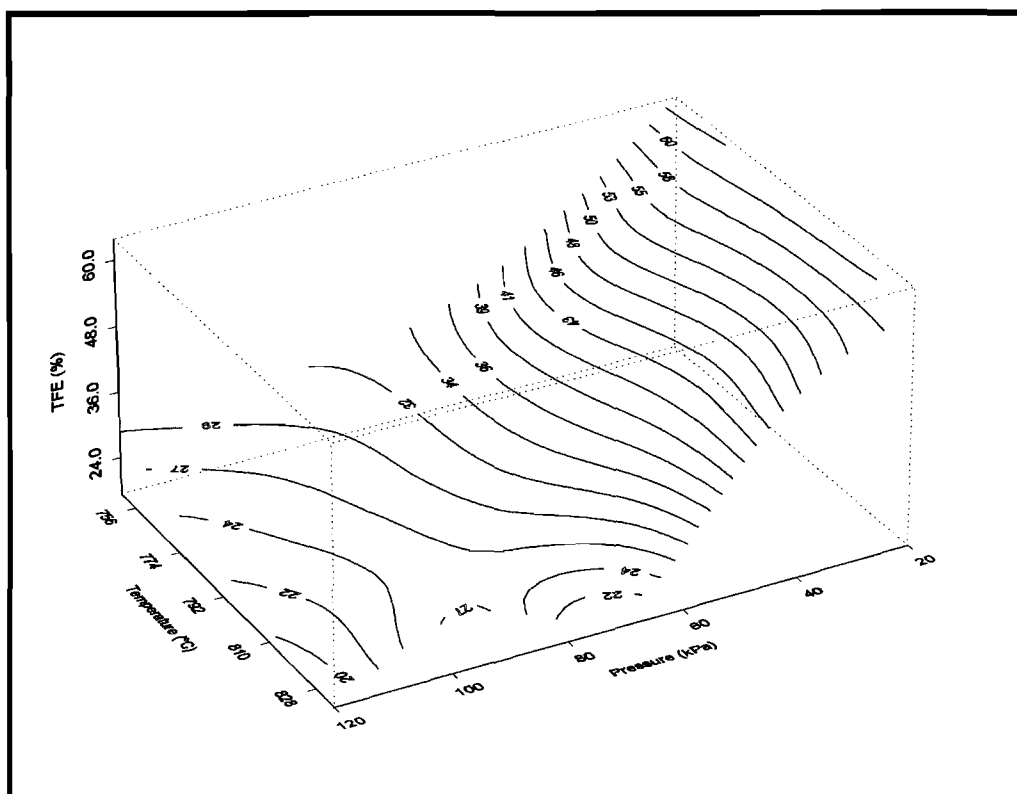


Figure 11.2: The TFE yield from FEP depolymerisation

Similar to the trend described in Chapter 4, the formation of TFE is highly dependant on the pressure and to a lesser extent on the temperature. The maximum TFE yield was found to be 62.3 % at 780 °C and 20 kPa.

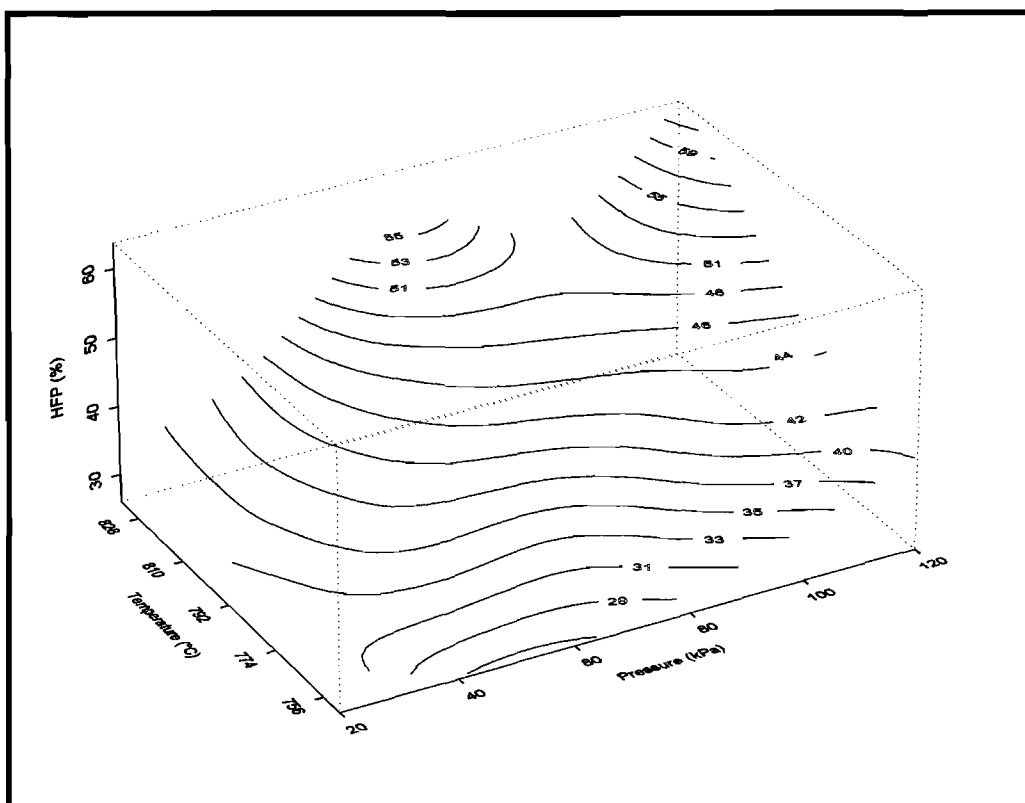


Figure 11.3: The HFP yield from FEP depolymerisation

The HFP yield showed two possible maxima. The one is at a maximum at high pressure (120 kPa) and high temperature (835 °C). The other peak value was also found at high temperature (835 °C), but at a medium pressure (60 to 70 kPa). The general trend for high HFP yield is high temperature and high pressure.

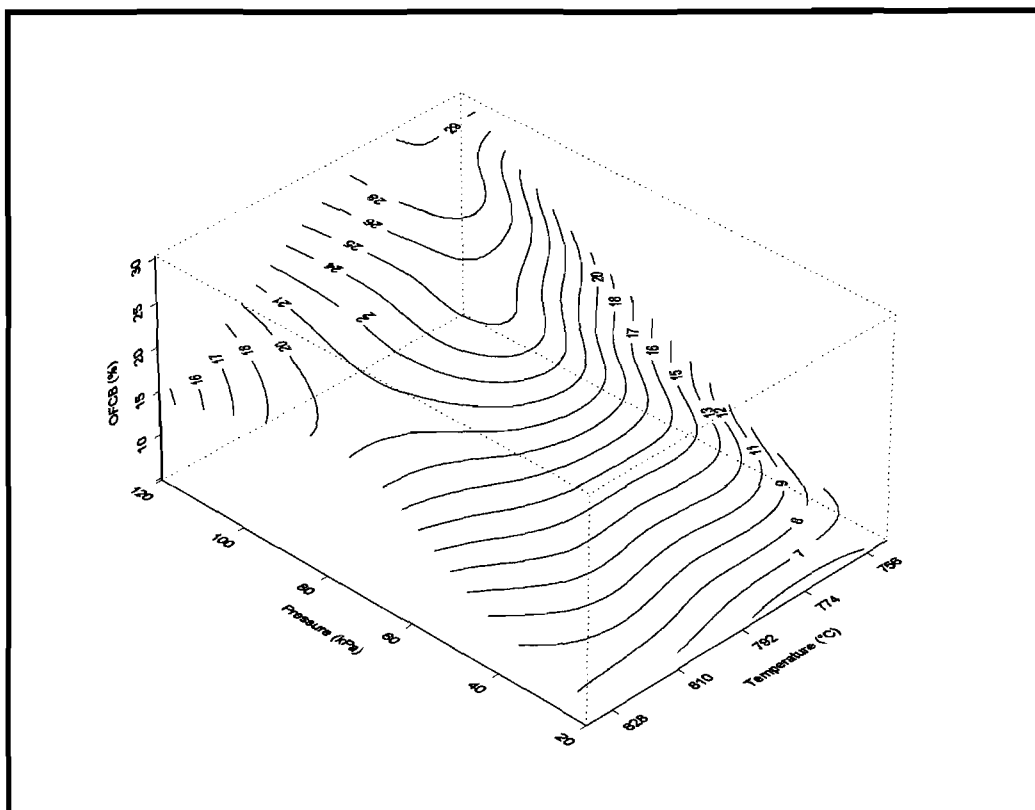


Figure 11.4: The OFCB yield from FEP depolymerisation

The OFCB yield also showed a general increasing trend towards higher pressures. The temperature dependence seems more definite as the concentration increases from 13.8 % at high temperature (835 °C) to 30.2 % at low temperature (750 °C), both at 120 kPa reactor pressure.

11.3.4 The production of fluorochemicals by the depolymerisation of THV

The last sample that was evaluated during this study was THV. Similar results as in the case of PTFE depolymerisation were obtained and similar trends were observed. Small amounts of unidentified products also appeared that might account for the oxygen. Results for the THV depolymerisation experiments are presented in Table 11.4.

Table 11.4: Results obtained during the depolymerisation of THV

Pressure (kPa (abs))	Temp (°C)	TFM (%)	HFE (%)	TFE (%)	OPF (%)	HFP (%)	OFCB (%)	PFIB (%)
10	700	ND	0.3	92.1	ND	6.4	0.3	0.9
50	700	ND	0.3	81.7	ND	11.1	5.7	1.1
80	700	ND	0.2	79.7	ND	11.5	7.8	0.6
10	800	ND	0.3	87.5	0.2	9.2	1.3	1.5
50	800	ND	0.3	74.6	0.2	16.1	6.4	2.2
80	800	ND	2.3	48.3	3.5	32.8	10.6	1.0

ND = Not Detected (The results presented are the average of at least three analyses)

No TFM was detected during the depolymerisation of THV. HFE, OPF and PFIB were detected in low concentrations of 0.2 to 3.5 %. The TFE yield decreased as both the temperature and pressure increased. The highest yield of TFE was 92.1 %. Both the HFP and OFCB yield increased as the temperature and pressure increased. These results closely resembled those for the PTFE depolymerisation.

11.3.5 The production of fluorochemicals by the depolymerisation of ETFE and HTE

Attempts to depolymerise ETFE and HTE were unsuccessful as severe blockages in the reactor occurred. Similar depolymerisation conditions as with the other fluoropolymers were used, but no results were obtained because of blockages that were experienced. Further experimentation was not done. As described in Section 11.1, the two fluoropolymers ETFE and HTE contain hydrogen in their chemical structure and it is speculated that the presence of hydrogen containing compounds caused the blockages.

11.4 CONCLUSIONS

From the results presented in this chapter, the following summarising conclusions can be made:

PTFE

Unfilled as well as filled PTFE, which included graphite-, glass fibre- and bronze-filled PTFE were successfully depolymerised in a Vibrating Reactor system. It was found that the TFE yield decreased as the temperature and pressure were increased while the HFP and OFCB yields increased as the temperature and pressure increased. This is in line with similar results obtained in Chapter 4. Relatively low yields of the other products (such as TFM, HFE, OFP and PFIB) were obtained.

PFA, FEP and THV

PFA was also depolymerised successfully. The TFE and HFP yields followed the same trends as with PTFE. A possible peak in the OFCB yield (22.3 %) was observed at 40 kPa and 570 °C. An unexpectedly high PFIB yield occurred at 60 kPa and 525 °C, but a possible blocked reactor might have been the cause.

The products from the FEP depolymerisation showed similar trends as in the case of PTFE. This was expected because this fluoropolymer is the only polymer other than PTFE that only contains perfluorinated fluorocarbons. The TFE yield decreased as the pressure and temperature increased, and the HFP and OFCB yield increased. Lower yields of TFE and generally higher yields of HFP and OFCB were observed.

The product generation from the polymer THV was similar to that of PTFE. The only difference was the detection of small amount of unidentified products. No attempt was made to analyse these products. It is speculated that these products formed due to the hydrogen contained in the compounds.

Other fluoropolymers

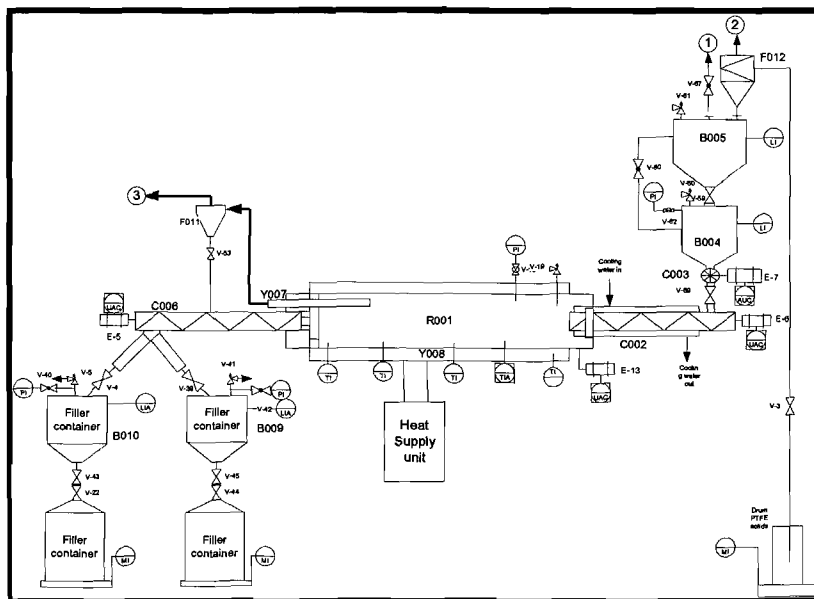
The fluoropolymers ETFE and HTE blocked the reactor when the depolymerisation conditions of PTFE were used. A different reactor design or other experimental

conditions are therefore needed for depolymerisation of these polymers. It was not part of the scope of this thesis. No conclusive results for the depolymerisation of ETFE and HTE could be generated.

Chapter 12

Design of a Depolymerisation Plant for Filled PTFE to Produce HFP

- 12.1. Introduction
- 12.2. Process description
 - 12.2.1. The feed preparation section
 - 12.2.2. The kiln reactor section
 - 12.2.3. The separation section
 - 12.2.4. The gas waste destruction section
- 12.3. Conceptual design of the HFP plant
 - 12.3.1. The feed material
 - 12.3.2. The products
 - 12.3.3. Determination of the production capacity
 - 12.3.4. Mass balance
 - 12.3.5. Reactor design
- 12.4. The techno-economy of the process
- 12.5. Conclusions



12.1 INTRODUCTION

The purpose of this chapter is to do a conceptual design of a plant that produces HFP as main product from the depolymerisation of PTFE and to do a preliminary assessment of the economic viability of such a plant.

The products produced in the depolymerisation process are speciality gases and therefore the market does not demand large volumes, but is prepared to pay much more than for other commodity products. A typical size of such a plant is in the order of 1 000 to 5 000 tpa. In this study the assumption is made that the size of the plant will be dictated by the amount of scrap filled and unfilled PTFE generated per year in the world.

This conceptual design will be based on design parameters that were obtained during experimentation that was presented in Chapter 4 (Figure 4.6, page 60), Chapter 9 (Section 9.4, page 148) and Chapter 10 (Table 10.2, page 161). The optimum conditions for production of HFP are presented in Table 12.1.

Table 12.1: Design parameters on which the conceptual design is based

Criteria	Conditions
Product	HFP (61 %)
Residence time (s)	~2
Feedstock	Filled PTFE
Operating angle (°)	4
Rotation speed (rpm)	4
Operating pres. (kPa)	82
Operating temp. (°C)	800
Other products	TFE (13 %), OFCB (11 %), By-products (15 %)
System	Drop-tube Reactor

The conditions reflect the maximum HFP yield with a residence time of 2 seconds.

12.2 PROCESS DESCRIPTION

The plant will consist of the following sections:

- The feed preparation section;
- The reactor section;
- The separation section;
- The waste destruction section.

The different sections will now be discussed.

12.2.1 The feed preparation section

The purpose of the feed preparation section, is to get rid of all cutting oil and grime that might be present on the scrap PTFE. Although this phenomenon was not investigated in this study, the assumption was made that real industrial PTFE waste, which will be used as a feed stock for this plant, will be contaminated with oil and grime. In order to prevent product gas contamination during depolymerisation, this pre-treatment step will be a necessity on industrial scale. This pre-treatment section will consist of a wash bay where the oil and grime will be dissolved with a suitable organic solvent. It is envisaged to recover the spent solvent. It is also assumed that the size and morphology of the scrap will be in the required shape and that it will present no problems when feeding it to the reactor.

12.2.2 The kiln reactor section

The envisaged kiln depolymerisation system is presented in Figure 12.1 and the operation thereof can be described as follows:

or disposal. The product gas exits the kiln via a dry quenching system Y007 and is then separated from fine solids carried over by means of a cyclone or a filter F011.

12.2.3 The separation section

The results presented in this study, showed that a mixture of product gasses will always be formed in spite of the fact that the depolymerisation conditions can be chosen to maximise the concentration of the wanted product, namely HFP in this case. The function of the separation section is to separate the HFP from the product mixture and to recycle the resultant gaseous product mixture back into the kiln reactor. The assumption is therefore made that these other products (mainly TFE and OFCB) can also be converted to HFP under the similar conditions. This assumption was not tested in this study but at parallel research done at Necsa, this was proven to be the case. Therefore, for the purpose of separation of the HFP and the other products, a two-column cryogenic distillation system is envisaged. Such a cryogenic separation system also did not form part of this study, but it is also applied at Necsa. The first column will separate TFE (BP = -75 °C) from the heavier fraction (HFP (BP = -29 °C), OFP (BP = -36 °C), OFCB (BP = -6 °C) and other C4 and C5 compounds). The second column will separate HFP from the heavier fraction, yielding > 99.5 % HFP. The HFP will then be compressed into cylinders at a pressure of 6.5 bar.

Figure 12.2 is a schematic presentation of a typical separation facility for the purification of HFP. After separation of HFP, all other products will be sent back to the reactor for conversion to HFP.

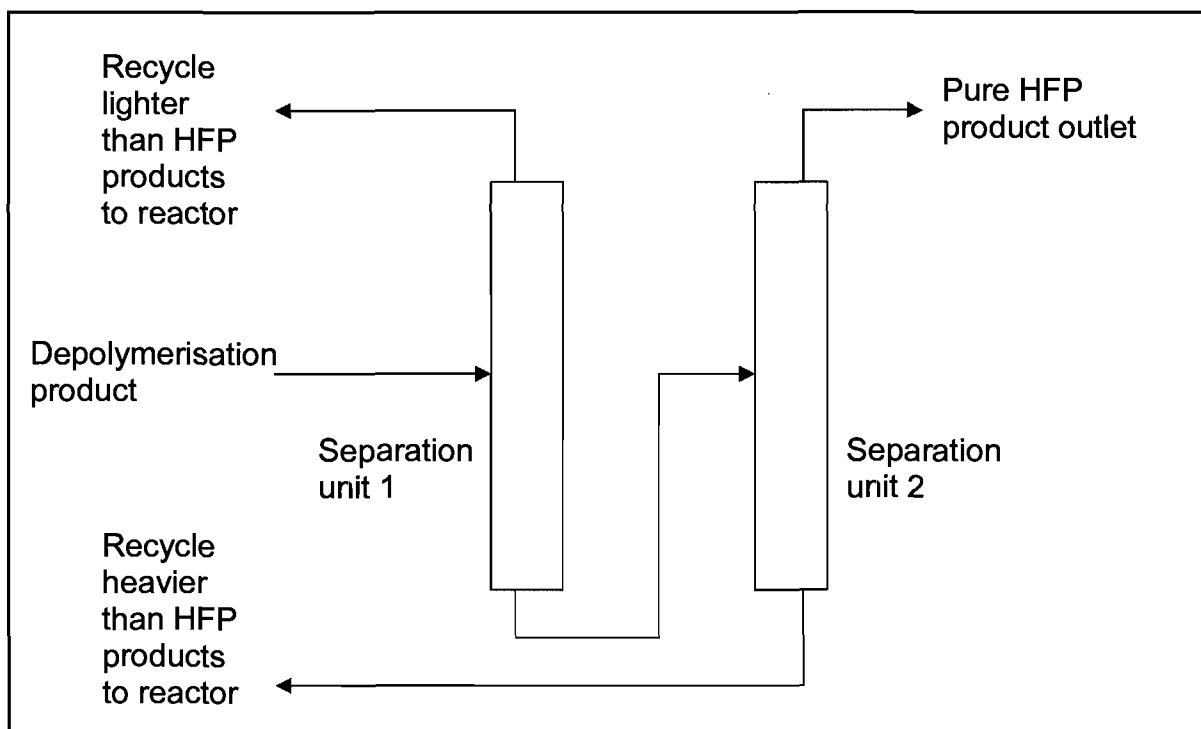


Figure 12.2: Depolymerisation product separation facility to purify HFP

12.2.4 The gas waste destruction section

The assumption is also made that during depolymerisation other products will be formed which are not recyclable. Although the formation of these products was not detected during this study, the assumption is made that such products might be present on an industrial scale plant and especially during the start-up and the shut down of the plant. Therefore, the design of the envisaged HFP plant must make provision for such an eventuality. It is assumed that this gas waste stream from this process will include HF, CO, CO₂ and NO_x compounds. Provision is therefore made for an assumed 2 % waste stream to be destroyed by burning it with propane and air at high temperature, producing mainly CO, CO₂ and possibly small amounts of NO_x type of gasses. Two scrubbers, a KOH- and NO_x scrubber, will be implemented to scrub the outlet gas before CO and CO₂ are released into the atmosphere. The spent scrubber solutions will be neutralised and disposed as a liquid waste.

12.3 CONCEPTUAL DESIGN OF THE HFP PLANT

In the conceptual design for the HFP plant the following aspects will be considered:

- The feed material;
- The products;
- The production capacity;
- Mass balance;
- Reactor design.

12.3.1 The feed material

The plant will be designed to process filled PTFE, containing 15 wt % filler. In a commercial process it is envisaged that after depolymerisation the filler material might possibly be recycled back to the manufacturer of filled PTFE, but for the purpose of this discussion it is considered to be a waste stream.

12.3.2 The products

In Table 12.2 an overview of the relevant properties is given for the compounds produced in the depolymerisation plant. The results obtained by the Drop-tube Reactor were used for this evaluation.

Table 12.2: Properties of fluorocarbon products

CF- compound	P_{sat} (kPa) at 25 °C	F/C	Max yield (Vol%) at (T/°C, P/kPa) and $\tau \approx 2$ s		Market (tpa)	Other
HFE	3344	3	77	(900, 55)	No	Inert
TFE	3271	2	93	(600, 5)	No	Explosive
OFP	883	8/3	6	(800, 56)	No	Inert
HFP	652	2	61	(800, 82)	3000	Asphyxiating
OFCB	256	2	27	(700, 82)	5	Asphyxiating
PFIB	313	2	2	(700, 82)	No	Highly toxic

Since there is no market for HFE, TFE, OFP and PFIB, these products will not be considered for this plant. Other factors that also contribute to TFE and PFIB not being considered, is the explosive nature of TFE and the highly toxic nature of PFIB. The production of both these products must be minimised.

Since the market for OFCB is very small (5 tpa), this product will also not be the end-product, although the selling price is high, \$70 to \$85 per kg in 2006 (Chapter 1).

This leads to the conclusion that HFP is the fluorocarbon product that will be produced in a PTFE depolymerisation plant, with a depolymerisation reactor operating at 800 °C, 82 kPa and a gas residence time of 2 seconds. The product distribution from the reactor at these conditions is given in Table 12.3 (Chapter 4).

Table 12.3: The product distribution at 800 °C, 82 kPa and with a gas residence time of 2 seconds

Compound	Mol fraction	Weight fraction
TFE	0.13	0.09
HFE	0.09	0.08
HFP	0.61	0.61
OFP	0.04	0.05
OFCB	0.11	0.15
PFIB	0.02	0.03
Total	1.00	1.00

The purity of HFP according to market specifications must be >99.5 %.

12.3.3 Determination of the production capacity

The capacity of this HFP plant was decided upon by the availability of scrap PTFE. The world production rate of PTFE was 16 000 tpa in 2002. Assuming that 50% of the produced PTFE is considered to be scrap PTFE in the form of shavings, cuttings, etc., and that the HFP plant will be able to collect 50% of this amount, the annual feed will be 4 000 tpa, or 500 kg·h⁻¹ for 8000 operating hours per year.

12.3.4 Mass balance

In order to calculate the mass balance the following assumptions were made:

1. The feed rate will be 500 kg·h⁻¹ of 15 % filled PTFE;

2. The depolymerisation efficiency is 100 %, implying that the filler is polymer-free and the depolymerisation products are filler-free;
3. The separation efficiency to generate the recycle streams is 100 %;
4. Although not tested, this reactor will be designed to depolymerise the filled PTFE as well as to convert the recycled gas into HFP;
5. In the reactor, six fluorocarbon products will be produced at the concentrations indicated in Table 12.3;
6. Because HFP is the required product, the operating conditions of the kiln were chosen for maximum output of HFP. According to the results presented in Chapter 4, these conditions are $T = 800\text{ }^{\circ}\text{C}$ and $P = 82\text{ kPa}$;
7. The gas products are converted to the six fluorocarbon products as indicated in Table 12.3;
8. The separation efficiency to produce the HFP product is 100 %;
9. Provision is made for two weight percent of all products formed in the reactor to be diverted to the waste destruction section. This will accommodate for start-up and shut-down product destruction;
10. The organic impurities that are removed in the feed preparation section can be ignored in the mass balance as they do not contribute to the products.

The flow sheet with recycled streams and the mass balance is schematically presented in Figure 12.3 and summarised in Table 12.4.

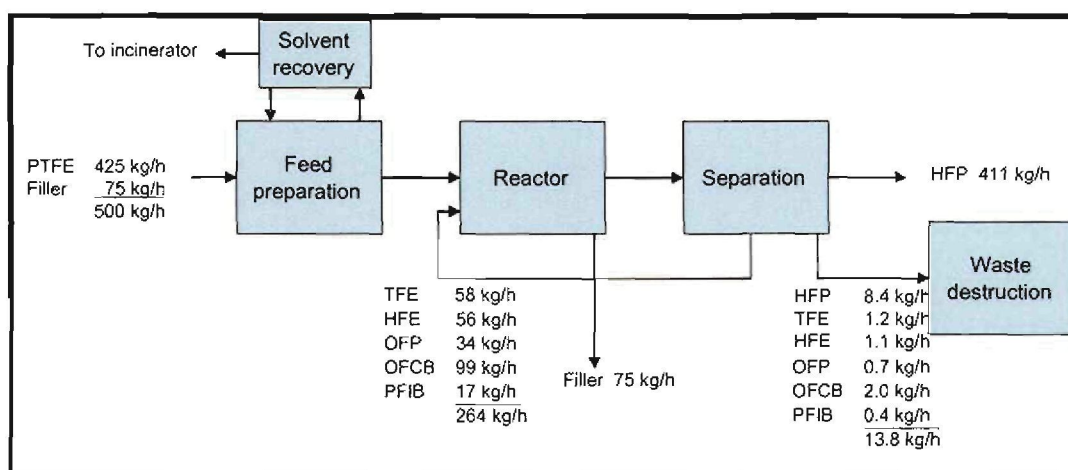


Figure 12.3: The flow-sheet with recycled streams of a HFP plant

If an amount of 500 kg of 15 % filled PTFE has to be depolymerised, this means that 425 kg·h⁻¹ PTFE will be depolymerised in the kiln. If provision has to be made for a total of 2 % (13.8 kg·h⁻¹) of the depolymerisation product to be destroyed, and the depolymerisation product mix is as mentioned in Table 12.3, the resulting HFP production rate will be 411.2 kg·h⁻¹. The HFP will be separated from the resultant product stream and the rest (264 kg·h⁻¹), recycled back to the reactor for conversion to HFP. A total of 411 kg·h⁻¹ of HFP per 500 kg·h⁻¹ filled PTFE will be produced.

Table 12.4: The mass balance of the recycle flow sheet

Compound	PTFE feed (kg·h⁻¹)	Reactor feed (kg·h⁻¹)	Reactor product (kg·h⁻¹)	To waste destruction (kg·h⁻¹)	HFP product (kg·h⁻¹)	Filler Waste (kg·h⁻¹)
PTFE	425.00	425.00	0.00	0.00	0.00	0.00
Filler	75.00	75.00	75.00	0.00	0.00	75.00
TFE	0.00	58.42	59.61	1.19	0.00	0.00
HFE	0.00	55.82	56.95	1.14	0.00	0.00
HFP	0.00	0.00	419.59	8.39	411.20	0.00
OFPP	0.00	33.79	34.48	0.69	0.00	0.00
OFCB	0.00	98.87	100.89	2.02	0.00	0.00
PFIB	0.00	17.98	18.34	0.37	0.00	0.00
Total	500.00	764.88	764.88	13.80	411.20	75.00

From Table 12.4 it can be determined that the HFP yield is 96.75% of the PTFE feed and that 3.25% of the PTFE feed ends up in the waste destruction section. For the design of the reactor volume it is important to note that the total fluorocarbon feed equals 690 kg·h⁻¹, consisting of 425 kg·h⁻¹ PTFE and 265 kg·h⁻¹ recycled CF gases.

12.3.5 Reactor design

The design of the depolymerisation kiln is based on two criteria:

1. The diameter of the kiln is determined by the filler entrainment limit of the gas velocity;

2. The volume of the reactor is determined by the gas residence time of 2 seconds.

For both criteria the density of the gas mixture at 800 °C and 82 kPa has to be estimated. The density of each compound is calculated using the ideal gas law. This calculation method is shown in Appendix 1 and the results are presented in Table 12.5, giving a density of the gas mixture of 1.74 kg·m⁻³.

Table 12.5: Density calculation of the depolymerisation gas mixture at 800 °C

Compound	Flow (kg·h ⁻¹)	Fraction (kg·kg ⁻¹)	MW (kg·mol ⁻¹)	ρ_{gas} (kg·m ⁻³)
TFE	59.61	0.086	0.100	1.121
HFE	56.95	0.083	0.138	1.547
HFP	419.59	0.608	0.150	1.681
OFFP	34.48	0.050	0.188	2.107
OFCB	100.89	0.146	0.200	2.242
PFIB	18.34	0.027	0.200	2.242
Total	689.88	1.000		1.740

The diameter of a kiln for feed of X kg·h⁻¹ and a limiting gas velocity $v_{\text{gas,lim}}$, in m·s⁻¹ is obtained from:

$$D = \sqrt{\frac{X/3600}{\frac{1}{4}\pi v_{\text{gas,lim}} \rho_{\text{gas,mix}}}} \quad 12.1$$

The limiting gas velocity, in order to avoid entrainment of filler particles, is typically equal to 1 m·s⁻¹, resulting in a kiln diameter, D, of 0.49 m in order to accommodate the feed given in Table 12.5. The length, L in m, of a kiln, the mean gas residence time τ , in s, and a gas limiting velocity for particle entrainment are related as follows:

$$L = \frac{\tau}{v_{\text{gas,lim}}} \quad 12.2$$

For a residence time of 2 seconds and a limiting gas velocity of $1 \text{ m}\cdot\text{s}^{-1}$, this gives a kiln length of 2 m.

12.4 THE TECHNO-ECONOMY OF THE PROCESS

The design of the HFP pilot plant in the section above was based on a feed rate of 500 tonnes per annum. In this techno-economic study, a full scale plant of 4000 tpa filled PTFE facility was considered. If 15 % filler material was contained inside the filled PTFE, 3400 tpa PTFE was left to be depolymerised. If it is accepted that the depolymerisation efficiency is 100 % and all the PTFE is converted into HFP with a 96.75 % yield and therefore 3290 tpa HFP would be produced. This high yield is a result of the recycle stream, where it is also assumed that the recycle stream is converted for 100 % in the product spectrum given in Table 12.3.

The costing method is based on Necsa in-house methods developed for fluorochemicals. Details on this costing can be seen in Appendix 5. The capital cost for the plant is estimated to be R107.5 million. The major contributors (~75 %) to the total capital cost are the depolymerisation reactor and the separation system. In the reactor section the kiln, instrumentation and valves contributed R9.5 million to the total depolymerisation system cost of R21 million. In the separation system the cryogenics plant contributed R22 million plus R3 million for the two distillation columns. It is envisaged that the distillation columns will contain highly flammable and explosive TFE mixtures. Therefore the columns must be specified to be spark-proof and flame-proof, adding significantly to the cost. Valves and instrumentation costs are R16.7 million.

The costing of this HFP plant is summarised in Table 12.6. In the costing exercise was included an industrial scale kiln depolymerisation system, a fluorocarbon destruction system, a PTFE feed preparation, a separation system consisting of a cryogenics plant and two distillation columns, a HFP product loading facility, safety equipment and an off-gas destruction system.

Table 12.6: Economic indicators associated with the 411 kg·h⁻¹ HFP production plant

Cost category	Units	Value
Capital cost	R Million	107.5
Payback capital + interest	R·kg ⁻¹	8.54
Fixed cost	R·kg ⁻¹	6.84
Variable cost	R·kg ⁻¹	37.59
Overheads	R·kg ⁻¹	0.16
Total production cost	R·kg ⁻¹	44.59
Sales price	R·kg ⁻¹	55.00
Profit	R·kg ⁻¹	10.41
Waste reduction of 85 %	R·kg ⁻¹	12.75

Necsa developed a budgeting model for speciality fluorochemicals such as HFP. According to this model a variable cost of R37.59 per kg was calculated. Business overheads (R0.16 per kg) and fixed costs of R6.84 per kg, add up to the total production cost per kilogram of HFP of R44.59. A profit of R10.41 per kg HFP is expected based on a selling price of HFP of R55 per kg. A capital payback amount of R8.54 per kg is also calculated. An amount of R12.75 per kg presents the cost saved by not spending \$2 = R15 (exchange rate = R7.50 / 1\$) per kg PTFE for landfilling.

Necsa marketing intelligence supported this selling price by estimating that the product could be priced between R70 to R100 per kg on the open market.

A summary of the techno-economic indicators are presented in Table 12.7.

Table 12.7: Techno-economic indicators for the HFP production plant

Indicators	Units	Value
Net Present Value [NPV] (5 years)	R Million	873
Internal Rate of Return [IRR]	%	45
Payback Period	Years	3.6
Gross Profit	%	20
Earnings Before Interest & Tax	R Million/a	56

A very healthy NPV of R873 million over 5 years can be achieved with an attractive IRR of 45 %. The fact that HFP is a speciality gas and the plant size is fairly small would prompt investors to look for an IRR above 20 %. The payback period for this plant is 3.6 years, which is quite normal for such a small speciality gas plant. A sensitivity analysis on the sales price is presented in Table 12.8:

Table 12.8: Sensitivity analysis on the sales price of HFP

Sales price (R kg ⁻¹)	IRR (%)	NPV (R million, 5 years)
50	37	713
55	45	873
60	53	1 031

A sensitivity analysis on the sales price indicated that the IRR and NPV are sensitive to a change of even 5 %. If the sales price is varied to 5 % above and below the anticipated sales price, this could cause a positive or negative change of 8 % to the IRR, and almost R160 million on the NPV, respectively, over 5 years. This is also indicated in the following sensitivity analysis graphs for IRR (Figure 12.4) and NPV (Figure 12.5). The sales price seems to be the most sensitive of the indicators.

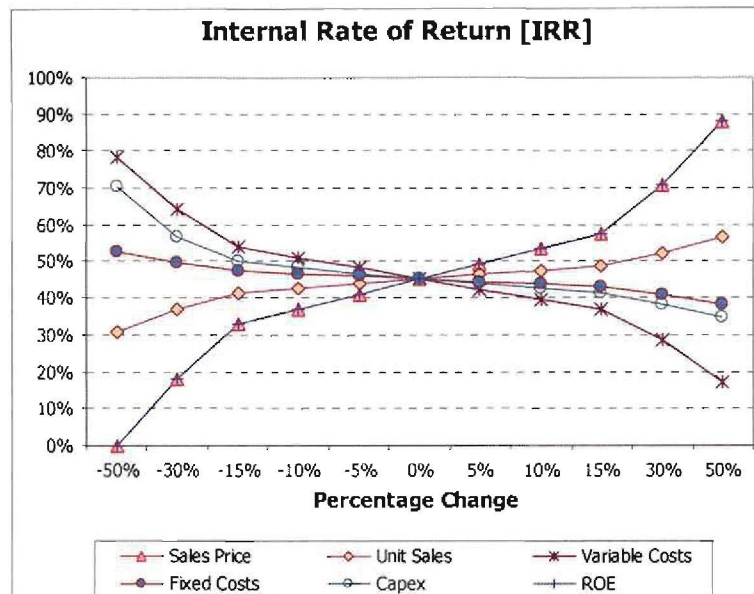


Figure 12.4: Sensitivity analysis for the IRR

The sales price and variable cost seems to be the most sensitive of the indicators for the change in IRR.

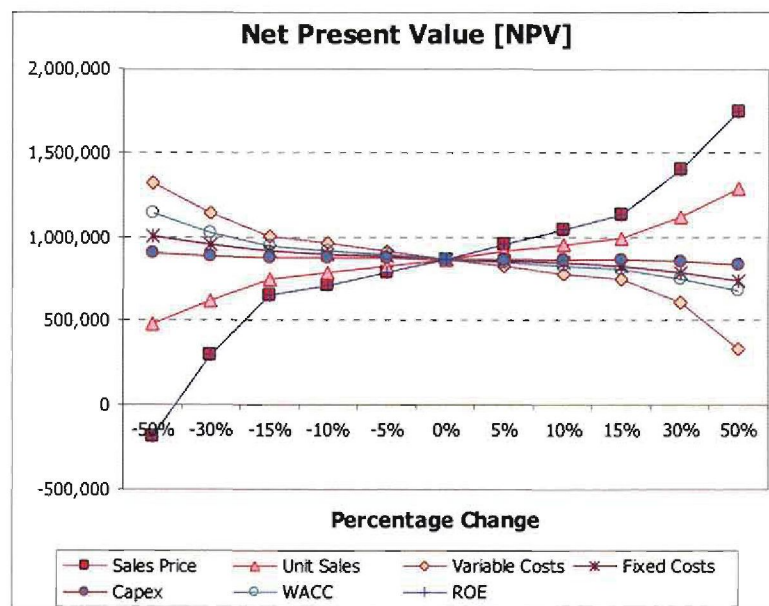


Figure 12.5: Sensitivity analysis for the NPV over a 5 year period

The sales price and return on equity (ROE) are the most sensitive for a change in NPV.

12.7 CONCLUSIONS

Based on the data obtained from a laboratory-scale pilot plant, a rotary kiln PTFE depolymerisation plant was designed, which is able to depolymerise $500 \text{ kg}\cdot\text{h}^{-1}$ of 15 % filled PTFE waste material that will produce $411 \text{ kg}\cdot\text{h}^{-1}$ HFP on a continuous basis.

For the design of this system the main product is HFP (96.75 % at $800 \text{ }^\circ\text{C}$ and 82 kPa with recycling), which is a valuable and sought-after gas. A total of 4000 tpa PTFE will be depolymerised with a potential calculated HFP selling price of R55 per kg with the variable cost the main cost driver. It was estimated that the capital cost of such a system will be R107 million. The reactor and separation sections contribute to more than 75 % of the capital cost.

This techno-economic study yielded positive results. The following techno economic indicators for the commercial plant are based on a conservative selling price of R55 per kg and sales volume of 3290 tpa HFP, and shows an IRR = 45% and a NPV of R872 million, with a payback period of 3.6 years.

Chapter 13

Conclusions



Since PTFE is synthesized via the polymerisation of TFE, it was logical to attempt to destroy waste PTFE via the reverse reaction, namely depolymerisation. The main objective of this study was to propose a method to treat and beneficiate filled and unfilled PTFE waste by producing a high value, sought-after product namely HFP. In order to optimise the HFP concentration and to understand the chemistry, a mechanism for the formation of depolymerisation products, based on PTFE depolymerisation experiments, was proposed. This mechanism was scrutinised and refined by means of scientific reasoning using thermodynamic and kinetically based arguments.

Finally an industrial scale system was proposed and designed based on a cost analysis and a preliminary techno economic study.

With this in mind a detailed study was carried out on laboratory scale. To enable this study, several laboratory systems were designed and built and appropriate experiments carried out. These systems included the following:

- Laboratory scale Rotating-kiln Reactor
- Drop-tube Reactor for depolymerisation of unfilled PTFE on a continuous basis;
- Paddle Reactor for the depolymerisation of filled and unfilled PTFE on a continuous basis;
- Vibrating Reactor for the evaluation of different fluoropolymers.

The depolymerisation of PTFE was thoroughly evaluated with these systems. In order to validate a proposed depolymerisation and product formation mechanism based on experimental data, appropriate analytical techniques had to be employed. These included the following:

- GC and GC/MS for analysis and verification of the depolymerisation product;
- SEM for analysis of the morphology of the filler material;
- EDX for the chemical analysis of the filler material;

- TGA for the analysis of the kinetic parameters (depolymerisation reaction constant, k , and the order, n , of the depolymerisation reaction) of the depolymerisation process.

Data obtained by the above techniques was then systematically analysed to test the viability of the proposed mechanism. These techniques included:

- A thermodynamic study using a computer program called HSC5.1;
- A kinetic study using the Arrhenius equation;
- A molecular modelling study using a computer program called Spartan '04 V1.0.3.

The most important findings from the study can be summarised as follows:

- From the literature study (Chapter 1) it was concluded that there is a need for the development of a continuous depolymerisation system for filled and unfilled PTFE, in order to solve the costly disposal problem manufacturers experience currently. The literature study and market research also identified several opportunities and areas in which further research and development is needed. These are:
 - The current depolymerisation processes are sub-optimal and more research is required to determine the optimal window of parameters by which PTFE can be depolymerised;
 - The output in terms of the production of valuable downstream fluoro-chemical products and the consequent recovery of expensive fluorine values, has to be maximised;
 - The conversion of the by-products TFE and OFCB into HFP needs to be optimised in order to retain the fluorine values.

It was found that unfilled PTFE could be depolymerised on a continuous basis in a Drop-tube Reactor (Chapter 4), producing high yields of TFE, HFP and OFCB and low yields of perfluorinated, unwanted compounds. For HFP the optimal window of

operation was determined to be 61 % at 800 °C and 82 kPa. and for TFE it was 94 % at 600 °C and 5 kPa. The following conclusions were also made:

- The complete mechanism, comprising two mechanistic routes, one dominating at lower- (< 700 °C) and the second one at higher (> 700 °C) temperatures was proposed (Chapter 5), based on the depolymerisation data obtained with the Drop-tube Reactor;
- After a thermodynamic study (Chapter 6) it was concluded that the depolymerisation process in the Drop-tube Reactor was not thermodynamically driven, but rather dominated by kinetic effects. The reason for this is because the product spectrum obtained experimentally was not in accordance with the equilibrium product spectrum predicted by the HSC5.1 program;
- Along with the thermodynamic results, molecular modelling was used to evaluate the depolymerisation species and a series of reaction equations for the formation of the depolymerisation products, TFE, HFE, OFP, HFP and OFCB (Chapter 7). With formation energies calculated for the intermediate radicals, the transition state species and the final products, energy diagrams could be drawn for a series of reactions involving the different final products, HFE, TFE, OFP, HFP and OFCB. Evaluation of these energy diagrams aided in proposing a two part mechanism for the product formation after depolymerisation of PTFE;
- A thermogravimetric study (Chapter 8) was performed in order to calculate the following kinetic parameters: rate (k), order (n) and activation energy (E_{act}) of the depolymerisation reaction of PTFE. The activation energy for the depolymerisation process was determined ($260 \text{ kJ}\cdot\text{mol}^{-1}$) along with the rate ($k = 4.03 \times 10^{-3} \text{ s}^{-1}$ at 600 °C and $k_0 = 1.78 \times 10^{13} \text{ s}^{-1}$) and the order ($n = 0.54$) of the depolymerisation reaction;
- After characterisation of the PTFE feed material (Chapter 9), before and during depolymerisation, it was concluded that the TGA analytical method can be used to distinguish between PTFE and different fluoropolymers;

- It was also determined using a SEM that the morphology of the different filler materials differs. It was found that this however has no significant effect on the flowability of the filled PTFE through the reactor (Chapter 9);
- The residence time for the different filled PTFE samples (glass fibre-, graphite- and bronze-filled PTFE) did not differ significantly from one another for a specific reactor angle and paddle rotation speed. The residence time of the solid PTFE inside the Paddle Reactor became sensitive for change at reactor angles $> 4^\circ$ and paddle rotation speed of ~ 4 rpm (Chapter 9);
- Visual observation of the depolymerisation process inside a laboratory Rotating-kiln Reactor and under a SEM proved that PTFE does go through a viscose liquid phase before depolymerisation starts to take place, but does not stick to the sides of a kiln metal reactor during this process (Chapter 9);
- It was demonstrated that both unfilled and filled PTFE could be depolymerised on a continuous basis at efficiencies of up to 90 % inside a Paddle Reactor system (Chapter 10). The residence time for this reactor was longer than for the Drop-tube Reactor, producing a different product ratio, with regard to TFM, HFE, TFE, OFP, HFP, OFCB and PFIB;
- The filler material (e.g. glass fibre, bronze and graphite) could be quantitatively separated from the depolymerisation product gas;
- Valuable fluorocarbon gases (TFE, HFP and OFCB) could be quantitatively recovered during the depolymerisation process;
- The laboratory reactor design that proved to be the most successful was that of a Paddle Reactor system. This system did not block during continuous operation with unfilled PTFE. The reactor also successfully separated the filler material from the depolymerised product on a continuous basis;
- A Vibrating Reactor system was designed and built for the evaluation of the product gas composition of other fluoropolymers, for example: FEP, PFA, THV, ETFE and HTE (Chapter 11). Good results were obtained for FEP, PFA and THV, but ETFE and HTE blocked the reactor before any analyses could be done;
- The product spectra obtained from three different reactors confirmed that the depolymerisation process is kinetically controlled and can be manipulated by the temperature, the pressure and the gas residence time;

- A commercial scale reactor ($\sim 500 \text{ kg}\cdot\text{h}^{-1}$ (4 000 tpa) for either unfilled or filled PTFE) was designed, based on the successful laboratory Paddle Reactor concept (Chapter 12);
- A preliminary techno-economic study based on a commercial-scale rotary kiln concept was conducted, and very promising results were obtained (Chapter 12):
 - An IRR of 45 % was calculated;
 - The NPV was calculated at MR873;
 - A payback period of only 3.6 years was predicted.

These techno-economic figures, coupled to the fact that rotary kiln systems of similar capacity have been in use globally for decades, lead to the conclusion that an industrial scale depolymerisation rotary kiln system would be very successful for the safe and economic solution of a decades-long PTFE waste disposal problem. The recovery of the valuable fluorocarbon products contributed largely to the success of this project.

Fields for further study:

Following from the results in this thesis, several opportunities are identified for further study. These are briefly discussed below:

1. Optimisation of the yields for different products like HFE, OFP, HFP and OFCB at higher pressures by means of the depolymerisation of PTFE;
2. Production of fluorocarbons from the depolymerisation of all other fluoropolymers;
3. A complete kinetic study of the formation of all the depolymerisation products;
4. Optimisation of the current Paddle Reactor and a reactor design with shorter residence times;
5. Depolymerisation inside a rotary kiln according to the design specifications in Chapter 12;
6. Evaluation of other separation techniques;
7. The influence of residence time on the depolymerisation products.

References

1. Plunkett R. J., U.S. Patent. 2,230,654, Du Pont Co., Feb. 4, 1941.
2. Drobny, J. G., Technology of Fluoropolymers, CRC Press, New York, 2001.
3. Encyclopedia of Polymer Science and Engineering, Vol. 16, John Wiley & Sons, New York, 1989, pp. 577 – 599.
4. Encyclopedia of Chemical Technology, 2nd ed., Vol. 11, John Wiley & Sons, 1966, U.S.A., pp. 1 – 50.
5. Ullman's Encyclopedia of Industrial Chemistry, 5th, Vol. A11, VCH, New York, 1989, pp. 394 – 404.
6. Ebnesajjad S., Fluoroplastics, Vol. 2, Plastics Design Library, New York, 2003.
7. Ebnesajjad S., Fluoroplastics, Vol. 1: Non-Melt Processible Fluoroplastics The Definitive User's Guide and Databook, Plastics Design Library, New York, 2000.
8. Simon C. M., Kaminski W., Chemical recycling of polytetrafluoroethylene by pyrolysis, Polymer Degradation and Stability, Vol. 62, 1998, pp.1 – 7.
9. Conesa J. A., Font R., Polytetrafluoroethylene decomposition in air and nitrogen, Polymer Engineering and Science, Vol. 41, No. 12, 2001, pp. 2137 – 2147.
10. Arkles B. C., Bonett R. N., Method for depolymerisation of polytetrafluoroethylene, US Patent 3832411, 1974.
11. Nelson G. L., Regulatory aspects of fire toxicology, Toxicology, Vol. 47, 1987, pp. 181 – 199.
12. Zook B. C., Malek D. E., Kenney R. A., Pathologic findings in rats following inhalation of combustion products of PTFE, Toxicology, Vol. 26, 1983, pp. 25 – 36.
13. Williams S. J., Baker B. B., Lee K. P., Formation of acute pulmonary toxins following thermal degradation of perfluorinated polymers, Fd. Chem. Toxic., Vol. 25, No. 2, 1987, pp. 177 – 185.

14. Townsend P. W., Vernice G. G., Williams R. L., Polymer fume fever without polymer, *Journal of Fluorine Chemistry*, Vol. 42, 1989, pp. 441 – 443.
15. Carter V. L., Bafus D. A., Warrington H. P., Harris E. S., The acute inhalation toxicology in rats from the pyrolysis products of four fluoropolymers, *Toxicology and Applied Pharmacology*, Vol. 30, 1974, pp. 369 – 376.
16. Johnston C. J., Finkelstein J. N., Mercer P., Corson N., Gelein R., Oberdorster G., Pulmonary effects induced by ultra fine PTFE particles, *Toxicology and Applied Pharmacology*, Vol. 168, 2000, pp. 208 – 215.
17. Fluorochemical products manufactured by Necsa, 2007, [Online], Available at:
<http://www.necsa.co.za/necsa/FluorineChemistry/tabid/938/default.aspx>.
18. Hintzer K., Dyneon, personal communication, 2005.
19. Naidoo V, Necsa, personal communication, 2006.
20. Barker W., Mossman A. L., Matheson Gas Data Book, Sixth ed., Matheson, USA, 1980, pp. 667.
21. Löhr G, Dyneon, personal communication, 2003.
22. Van der Walt, I. J., Investigation into depolymerisation of PTFE waste into TFE as a main product, University of Witwatersrand, M.Sc., 2002.
23. Van der Walt I. J., Bruinsma O. S. L., Depolymerization of clean unfilled PTFE waste in a continuous process, *Journal of Applied Polymer Science*, Vol. 102, 3, 2752 – 2759 (2006).
24. Van der Walt I. J., PCT Patent, PCT/IB01/0015.
25. Cotton F. A., Wilkinson G., Gaus P. L., *Basic Inorganic Chemistry*, Third ed., John Wiley & Sons, New York, 1995, pp. 465 – 467.
26. Liptrot G. F., *Modern Inorganic Chemistry*, Fourth ed., Collins Educational, London, 1992, pp. 327 – 330.
27. Lee J. D., *Concise Inorganic Chemistry*, Fourth ed., Chapman & Hall, London, 1991, pp. 582.

28. Brady J. E., Holum J. R., Fundamentals of Chemistry, John Wiley & Sons, New York, 1988, pp. 765.
29. Moore A. M. C., Die Sintese van Tetrafluoroetileen – 'n Omgewingsvriendelike Alternatief, M.Sc. Thesis, North West University, 1997, pp. 2.
30. Encyclopedia of Chemical Technology, Second ed., Vol. 9, Interscience Publishers, New York, 1966, pp. 808.
31. Grunenberg A. T., The Safety Aspects of TFE Plant Design, Internal Necsa report, Nr. PTV-TFE-GDE-02001 Rev. 2, 2002.
32. Retief W. L., A Literature Review on the Toxicology of PFIB and Particulates Origination from Fluorocarbon Polymers and Plastics, Internal Necsa Report, MX-ALG-0012, 2002.
33. Freedonia report number 1268, dated July 2002.
34. Mizuno K. et al, Method and apparatus for decomposing halogenated organic compound, US Patent 5026464, 1991.
35. Meissner E., Wroblevska A., Milchert E., Technological parameters of pyrolysis of waste polytetrafluoroethylene, Polymer Degradation and Stability, Vol. 83, 2004, pp. 163 – 172.
36. Hartwimmer, Robert., Process for preparation of fluorocarbon waxes, US Patent 4076760, Feb 28, 1978.
37. Hartwimmer, Robert., Process for preparation of perfluorinated compounds, US Patent 3816552, June 11, 1974.
38. Schottle T., Hintzer K., Staudt H. J., Weber H., Process for preparation of fluorinated monomers, US Patent 5432259, 1995.
39. Homoto Y., Ichida T., Preparation of fluoromonomers uses rotary kiln to heat decomposing fluoropolymer, Patent Application WO200374456, 2003.
40. Lungu, C.P., Lungu, A.M., Sakai, Y., Sugawara, H., Tabata, M., Akazawa, M., Miyamoto, M. C_xF_y polymer film deposition in DC and RF fluorinert vapor plasmas, Vacuum, Vol. 59, 2000, pp. 210 – 219.
41. Hikosaka, Y., Sugai, H. Radical kinetics in a fluorocarbon etching plasma, Japan Journal of Applied Physics, Vol. 32, 1993, pp. 3040 – 3044.

42. Klun, U., Kržan, A. Rapid microwave induced depolymerisation of polyamide-6, *Polymer Communication*, Vol. 41, 2000, pp. 4361 – 4365.
43. Lewis E. E., Naylor M. A., Pyrolysis of polytetrafluoroethylene, *Journal of American Chemical Society*, Arlington New York, Vol. 69, 1947, pp. 1968 – 1970.
44. Morisaki S., Simultaneous thermogravimetry-mass spectroscopy and and pyrolysis-gas chromatography of fluorocarbon polymers, *Thermochemica acta*, Vol. 25, 1978, pp. 171 – 183.
45. Holzknacht B., An analytical model for the transient ablation of polytetrafluoroethylene layers, *Journal of Heat and Mass Transfer*, Vol. 20, 1976, pp. 661 – 668.
46. Siegle J. C., Muus L. T., Lin T. P., Larsen H. A., The molecular structure of perfluorocarbon polymers II Pyrolysis of polytetrafluoroethylene, *Journal of Polymer Science*, Vol. 2, 1964, pp. 391 – 404.
47. Cox J. M., Wright B. A., Wright W. W., Thermal degradation of fluorine containing polymers. Part I. Degradation in Vacuum, *Journal of Applied Polymer Science*, Vol. 8, 1964, pp. 2935 – 2950.
48. Carrol B., Manche E. P., Kinetic parameters from temperature programmed reactions: The pyrolysis of polytetrafluoroethylene, *Journal of Applied Polymer Science*, Vol. 9, 1965, pp. 1895 – 1903.
49. Doyle C. D., Kinetic analysis of thermogravimetric data, *Journal of Applied Polymer Science*, Vol. 5, no. 15, 1961, pp. 285 – 292.
50. Atkinson B., Atkinson V. A., The thermal decomposition of tetrafluoroethylene, *Journal of Chemical Society*, 1957, pp. 2086 – 2094.
51. Atkinson B., Trenwith A. B., The thermal decomposition of tetrafluoroethylene, *Journal of Chemical Society*, 1953, pp. 2082 – 2087.
52. Moore, A. M. C., Die sintese van tetrafluoroetileen - 'n omgewingsvriendelike alternatief, M. Sc., PU vir CHO, 1997, Potchefstroom.

53. Skoog D. A., West D. M., Holler F. J., *Fundamentals of Analytical Chemistry*, Sixth ed, Saunders College Publishing, 1992, pp. 666.
54. Zenkevich I. G., Ivanova T. L., Zigel A. N., *Gas Chromatographic Identification of the Products of the Thermal Degradation of TFE and Perfluoro(Propyl Vinyl Ether) Copolymer*, *Journal of Analytical Chemistry*, Vol. 58, No. 3, 2003, pp. 251 – 256.
55. Morisaki S. *Simultaneous Thermogravimetry-Mass Spectrometry and Pyrolysis-Gas Chromatography of Fluorocarbon Polymers*, *Thermochimica Acta*, Vol. 25, 1978, pp. 171 – 183.
56. Tiedt L Dr., *Microscopy*, North West University, Potchefstroom, South Africa, 2004.
57. Verbal communication with Broly, C., Chemplast PTFE Division.
58. Roine A., HSC Chemistry 5.11, Outokumpo research Oy, Pori, Finland.
59. Fogler H. S., *Elements of Chemical Reaction Engineering*, Fourth Ed., Pearson Education International, USA, 2006, pp. 1021 – 1024.
60. Laidler K. J., Meiser J. H., *Physical Chemistry*, The Benjamin/Cummings Publishing Company, 1916, pp. 119 – 135.
61. Weast, R. C., *CRC Handbook of Chemistry and Physics*, 62nd ed. Florida: CRC Press, 1981 – 1982.
62. Daubert T. E., Danner R. P., *Physical and thermodynamic properties of pure chemicals. Data compilation*, Design Institute for Physical Property Data. American Institute of Chemical Engineers, Hemisphere Publishing Corporation, New York, (1989).
63. White W. B., Johnson S. M. and Dantzig G.B., *Chemical Equilibrium in Complex Mixtures*, *Journal of Chemical Physics*, Vol. 28, 1958, pp. 751-755.
64. Spartan '04 v1.0.3, Copyright © 1991 – 2005 by Wavefunction Inc.
65. Solomons T. W. G., *Organic Chemistry*, Fifth ed, John Wiley & Sons, 1992, pp. 216 – 225, 276 – 279.
66. Ebnesajjad S., *Fluoroplastics*, Vol. 1: Non-Melt Processible Fluoroplastics The Definitive User's Guide and Databook, *Plastics Design Library*, New York, 2000, pp. 10.

67. Laidler K. J., Meiser J. H., Physical Chemistry, The Benjamin/Cummings Publishing Company, 1916, pp. 403 – 434.
68. O. Levinspiel, Chemical Reaction Engineering, John Wiley & Sons, New York, 2006.
69. Wall L. A., Fluoropolymers, Vol. xxv High Polymers, Wiley & Sons, New York, 1972, pp. 381.
70. Van der Walt I. J., Nel J. T., Grunenberg A. T., South African provisional patent, 2005/09703.
71. Hudlicky M., Chemistry of Fluorine Compounds, First ed, The McMillan Company, New York, 1962.

Appendix 1

General Calculations

1. Residence time calculations
 - 1.1. Gas residence time for the Drop-tube Reactor
 - 1.2. Gas residence time for the Paddle Reactor
 2. Kinetic calculations
 3. Density calculations
-

1. Residence time calculations

$$P := 90 \cdot \text{kPa}$$

$$T := 873 \cdot \text{K}$$

$$R := 8.314 \cdot \frac{\text{J}}{\text{kg} \cdot \text{K}}$$

Molar mass:

$$\text{TFE}_{\text{Mr}} := 100$$

$$\text{C3F6}_{\text{Mr}} := 150$$

$$\text{c_C4F8}_{\text{Mr}} := 200$$

Average Molar mass for equal amount mixture:

$$\text{Mr}_{\text{ave}} := 0.33 \cdot \text{TFE}_{\text{Mr}} + 0.33 \cdot \text{C3F6}_{\text{Mr}} + 0.33 \cdot \text{c_C4F8}_{\text{Mr}}$$

$$\text{Mr}_{\text{ave}} = 148.5$$

Gas density

$$\rho := \frac{P \cdot \text{Mr}_{\text{ave}}}{R \cdot T}$$

$$\rho = 1.841 \frac{\text{kg}}{\text{m}^3}$$

1.1 Gas residence time for the DROP TUBE reactor

Input

$$d_{\text{reactor}} := 65 \text{ mm}$$

$$L_{\text{reactor}} := 200 \text{ mm}$$

$$\rho := 1.841 \frac{\text{kg}}{\text{m}^3}$$

$$Q_{\text{flow}} := 2 \frac{\text{kg}}{\text{hr}}$$

$$\text{Vol} := \pi \cdot \frac{D^2 \cdot L}{4}$$

At 100% volume the residence time is:

$$\text{Vol}_{100\%} = 6.637 \times 10^{-4} \text{ m}^3$$

$$\tau := \frac{\text{Vol}_{100\%}}{\left(\frac{Q_{\text{flow}}}{\rho} \right)}$$

$$\tau = 2.199 \text{ s}$$

1.2 Gas residence time for the PADDLE reactor

Input

$$Q_{\text{flow}} := 1 \frac{\text{kg}}{\text{hr}}$$

$$L := 1 \text{ m}$$

$$D := 100 \text{ mm}$$

$$\text{Vol} := \pi \cdot \frac{D^2 \cdot L}{4}$$

$$\text{Vol} = 7.854 \times 10^{-3} \text{ m}^3$$

At 25% volume the residence time is:

$$\text{Vol}_{25\%} := \text{Vol} \cdot 0.25$$

$$\text{Vol}_{25\%} = 1.963 \times 10^{-3} \text{ m}^3$$

$$\tau := \frac{\text{Vol}_{25\%}}{\left(\frac{Q_{\text{flow}}}{\rho} \right)}$$

$$\tau = 13.016 \text{ s}$$

At 50% volume the residence time is:

$$\text{Vol}_{50\%} := \text{Vol} \cdot 0.5$$

$$\text{Vol}_{50\%} = 3.927 \times 10^{-3} \text{ m}^3$$

$$\tau := \frac{\text{Vol}_{50\%}}{\left(\frac{Q_{\text{flow}}}{\rho} \right)}$$

$$\tau = 26.032 \text{ s}$$

At 75% volume the residence time is:

$$\text{Vol}_{75\%} := \text{Vol} \cdot 0.75$$

$$\text{Vol}_{75\%} = 5.89 \times 10^{-3} \text{ m}^3$$

$$\tau := \frac{\text{Vol}_{75\%}}{\left(\frac{Q_{\text{flow}}}{\rho} \right)}$$

$$\tau = 39.048 \text{ s}$$

At 100% volume the residence time is:

$$\text{Vol}_{100\%} := \text{Vol}$$

$$\text{Vol}_{100\%} = 7.854 \times 10^{-3} \text{ m}^3$$

$$\tau := \frac{\text{Vol}_{100\%}}{\left(\frac{Q_{\text{flow}}}{\rho} \right)}$$

$$\tau = 52.064 \text{ s}$$

2. Kinetic calculations

Rate equation of a chemical reaction:

$$-\frac{dm}{dt} = k \cdot m^n \quad 1$$

Separation of variables:

$$-\frac{dm}{m^n} = k \cdot dt \quad 2$$

Logarithm of 1 for determination of k and n:

$$-\ln\left(\frac{d(x)}{dt}\right) = n \ln(x) + \ln(k) \quad 3$$

$$y = mx + c \quad 4$$

Integration for simulation of experimental data by using calculated n and k values:

$$-\int_{m_0}^m \frac{dm}{m^n} = k \cdot \int_0^t dt \quad 5$$

or:

$$\int_{m_0}^m \frac{dm}{m^n} = -k \cdot \int_0^t dt \quad \rightarrow \quad \int_{m_0}^m m^{-n} dm = -k \cdot \int_0^t dt \quad 6$$

gives:

$$\left[\frac{1}{1-n} m^{1-n} \right]_{m_0}^m = -kt \quad 7$$

Rewritten:

$$\left(\frac{1}{1-n}\right)[m^{1-n} - m_0^{1-n}] = -kt \quad 8$$

$$[m^{1-n} - m_0^{1-n}] = -(1-n)kt \quad 9$$

$$m^{1-n} = (n-1)kt + m_0^{1-n} \quad 10$$

$$m^{1-n} = (n-1)kt + m_0^{1-n} \quad 11$$

$$m = \sqrt[n-1]{(n-1)kt + m_0^{1-n}} \quad 12$$

Activation energy by means of Arrhenius equation:

$$k = k_0 e^{-E_{act}/RT} \quad 13$$

Taking logarithms on either side of the Arrhenius equation:

$$\ln(k) = -\frac{E_{act}}{R} * \frac{1}{T} + \ln(k_0) \quad 14$$

$$y = mx + c$$

3. Density calculations

The density of a gas is calculated according to the ideal gas law:

$$\rho_i = \frac{P \cdot MW_i}{RT}$$

The density of the gas mixture is calculated as a summation by weight fractions,

w_i :

$$\rho_{\text{gas,mix}} = \sum_i w_i \rho_i$$

Appendix 2

Computer Program Methodology

1. HSC 5.1
2. Spartan '04 v1.0.3

1. HSC 5.1

Start HSC 5.1 by double clicking on its icon. A window similar to Figure 1 will appear. Here one can select what thermodynamic data must be calculated. In this study the reaction equations and equilibrium composition functions were used. Many other functions are available, like the calculation of the H, S, Cp and G diagrams, the addition of species to the data base, etc.

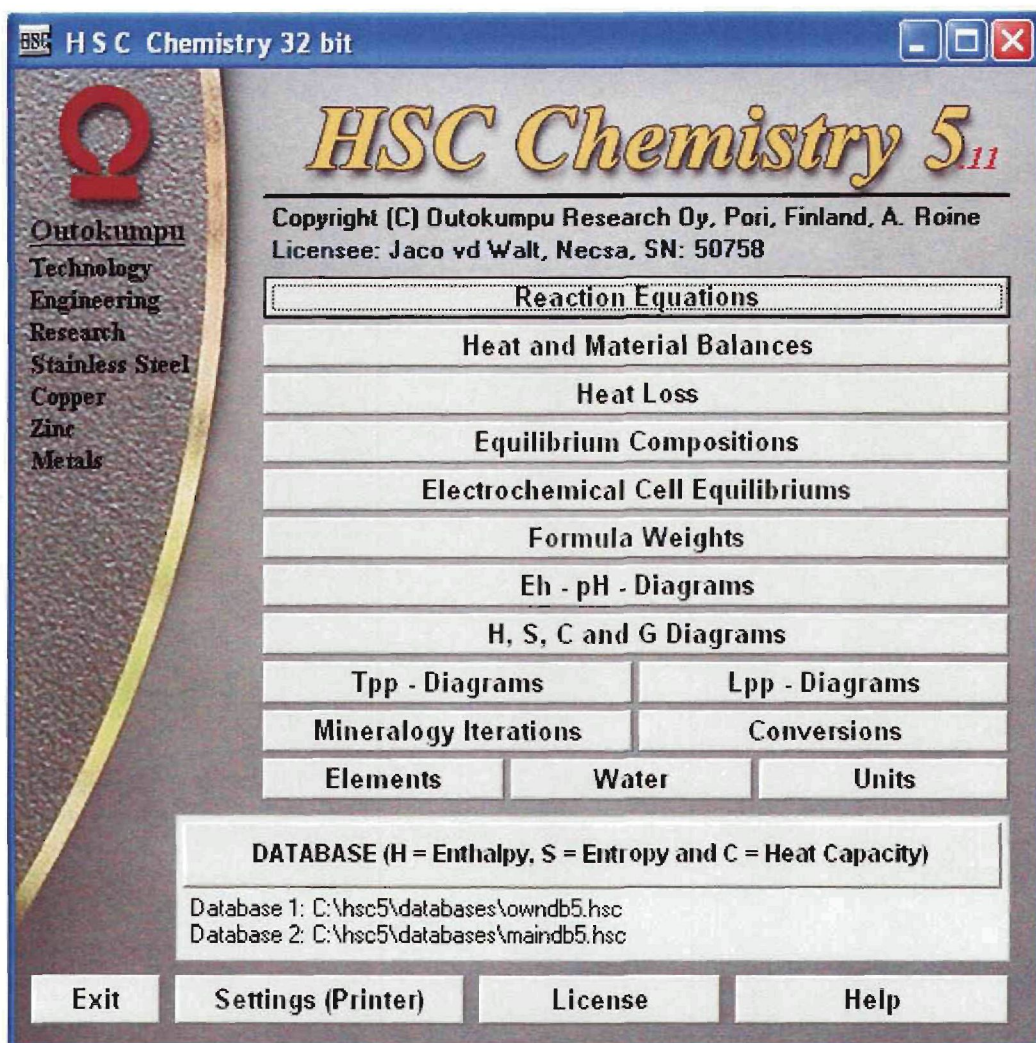


Figure 1

Reaction Equations

When the **Reaction Equations** button is pressed, the following window appears (Figure 2). Here the chemical reaction equation is typed into the blank window according to the HSC data base convention. One can search for a specie by using the **Peep Database** button. The equation must be balanced and the temperature

information amended. After choosing the correct units, the **Calculate** button can be pressed and the thermodynamic data will be presented.

Reaction Equations

Reaction Equation or Chemical Formula:

Temperature: From 0.000 To 1000.000 Step 100.000 C

Temperature Units:
 Celsius
 Kelvins

Energy Units:
 Calories
 Joules

Format of Results:
 Normal
 Delta

Collect to Sheet
 Show Transitions
 Criss-Cobble

Help File Open HSC 2 File Balance Equation Peep Database
Exit File Open ... 1 Calculate

Figure 2

Presented here is the thermodynamic data as calculated for the TFE formation reaction from two difluorocarbene radicals (Figure 3). From the data the temperature, ΔH , ΔS , ΔG and K values are presented.

	T	Cp	H	S	G	Reference
1	2CF2(g) = C2F4(g)					
2	T	deltaH	deltaS	deltaG	K	Log(K)
3	C	kcal	cal/K	kcal		
4	0.000	-70.414	-43.455	-58.544	7.007E+046	46.846
5	100.000	-70.328	-43.195	-54.210	5.661E+031	31.753
6	200.000	-70.180	-42.846	-49.908	1.134E+023	23.054
7	300.000	-69.994	-42.489	-45.641	2.541E+017	17.405
8	400.000	-69.780	-42.147	-41.409	2.789E+013	13.445
9	500.000	-69.541	-41.815	-37.211	3.308E+010	10.520
10	600.000	-69.275	-41.493	-33.046	1.871E+008	8.272
11	700.000	-68.989	-41.182	-28.912	3.117E+006	6.494
12	800.000	-68.688	-40.888	-24.809	1.129E+005	5.053
13	900.000	-68.377	-40.611	-20.734	7.294E+003	3.863
14	1000.000	-68.055	-40.348	-16.686	7.322E+002	2.865
15						
16	Formula	FM	Conc.	Amount	Amount	Volume
17		g/mol	wt. %	mol	g	l or ml
18	CF2(g)	50.008	100.000	2.000	100.016	44.827 1
19		g/mol	wt. %	mol	g	l or ml
20	C2F4(g)	100.016	100.000	1.000	100.016	22.414 1
21						

Figure 3

Equilibrium calculations

Equilibrium calculations of a mixture of species can be done by the following procedure:

Choose the **Equilibrium Calculations** button from the first window (Figure 1) and the following window will appear (Figure 4). Click on the **Create New** button.

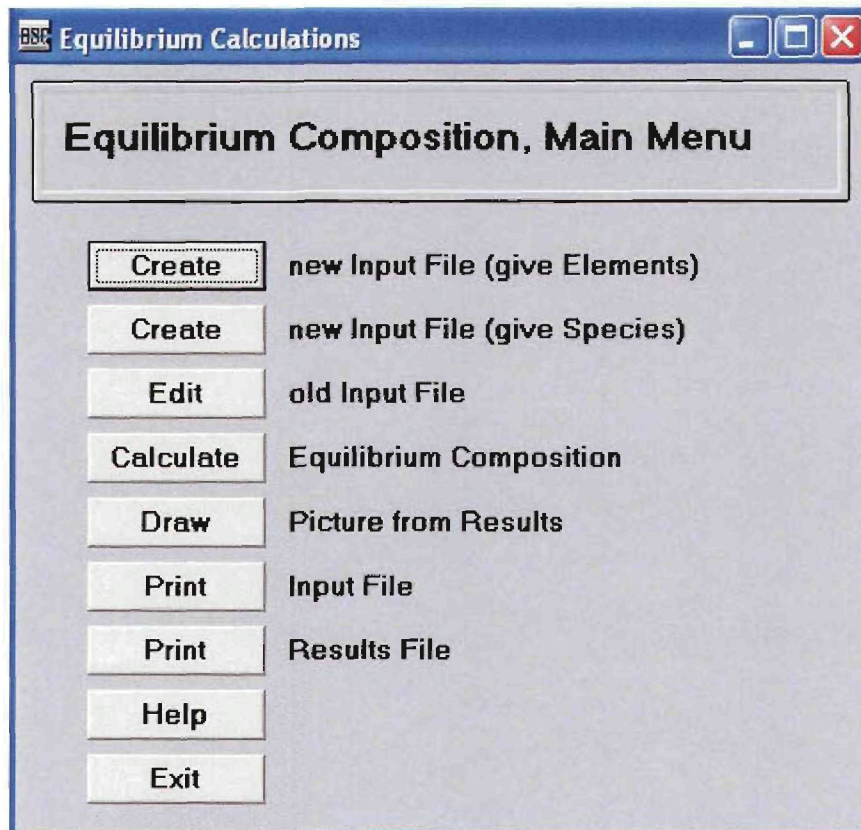


Figure 4

When the window in Figure 5 appears a selection of the elements must be made. These must include all the elements involved in the reactions. In this case C and F will be chosen.

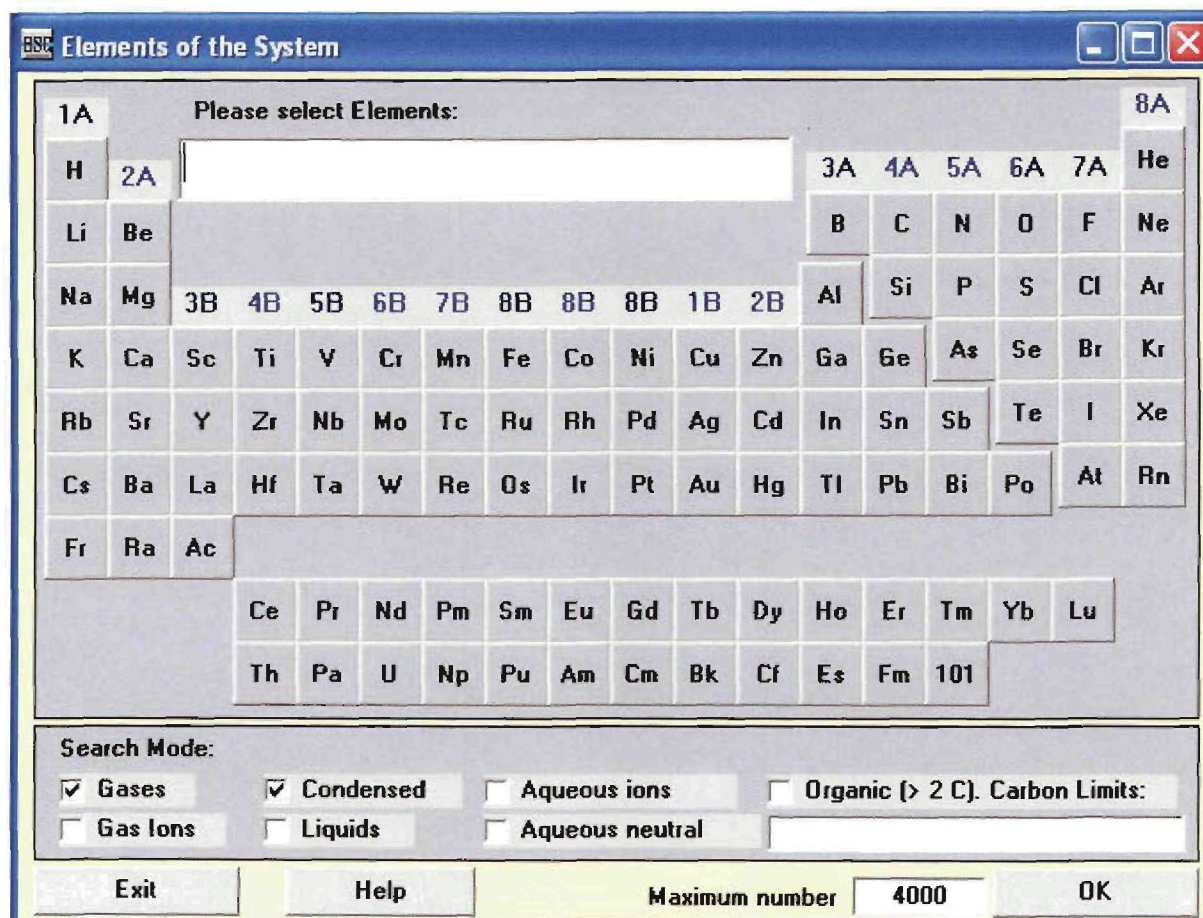


Figure 5

When the **OK** button is selected the following window appears (Figure 6). Here all the species with the particular chosen atoms were selected from the database and displayed. Now a selection can be made on the species involved in the equilibrium composition. After the unwanted species were deleted, the **Continue** button can be pressed.

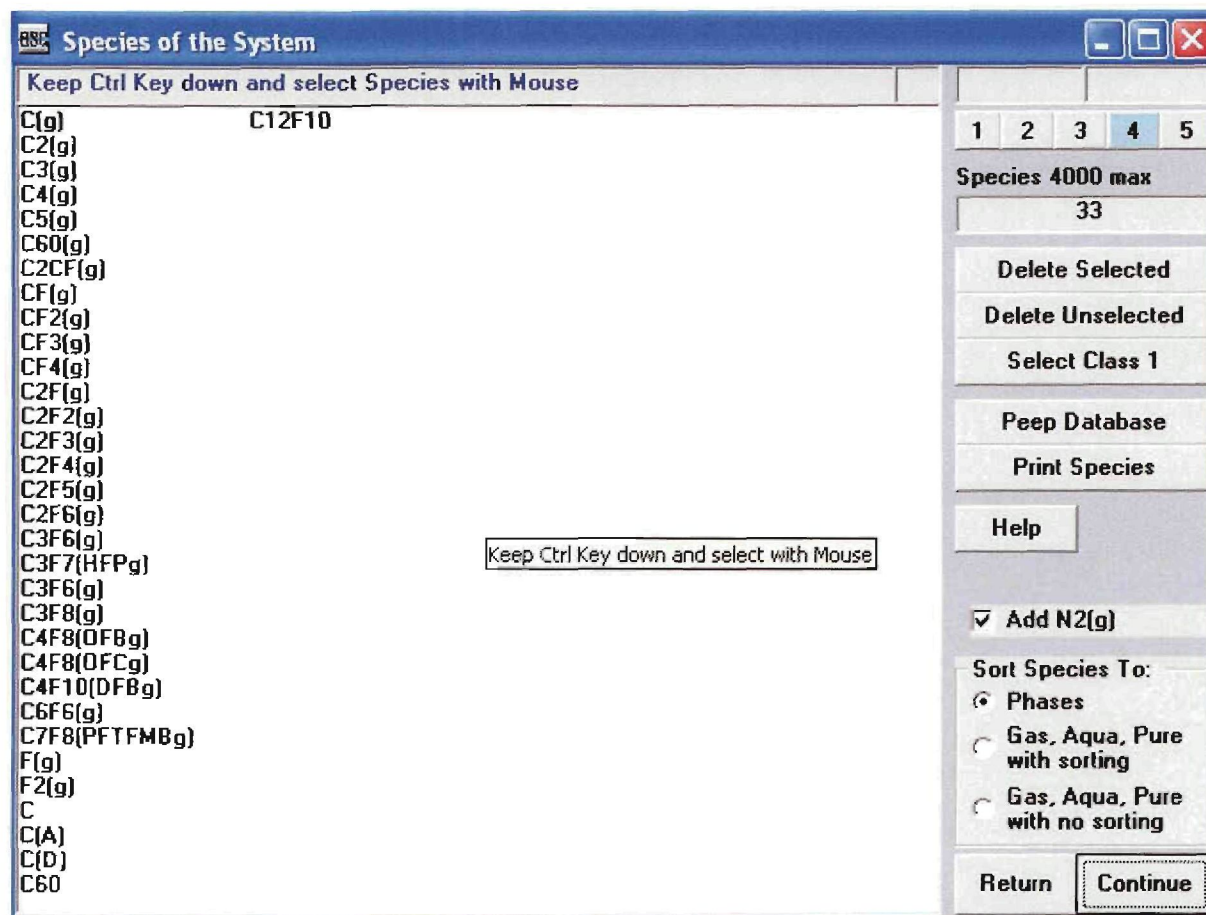


Figure 6

Now the species will be ordered into a spreadsheet according to alphabetic order and the molecules and elements separated (Figure 7). One or more species must be selected as starting species. These species must contain all the elements. Their molar ratio to one another must be filled in, into the Amount kmol column.

	SPECIES Formula	Temper. C	Amount kmol	Amount %	Step kmol	Step %	Activity Coeff.
1	GASES		1.000	100.000			
2	C(g)	25.000					1.000
3	C2(g)	25.000					1.000
4	C3(g)	25.000					1.000
5	C4(g)	25.000					1.000
6	C5(g)	25.000					1.000
7	C60(g)	25.000					1.000
8	C2CF(g)	25.000					1.000
9	CF(g)	25.000					1.000
10	CF2(g)	25.000					1.000
11	CF3(g)	25.000					1.000
12	CF4(g)	25.000					1.000
13	C2F(g)	25.000					1.000
14	C2F2(g)	25.000					1.000
15	C2F3(g)	25.000					1.000
16	C2F4(g)	25.000	1.000	100.000			1.000
17	C2F5(g)	25.000					1.000
18	C2F6(g)	25.000					1.000
19	C3F6(g)	25.000					1.000
20	C3F7(HFP)(g)	25.000					1.000
21	C3F6(g)	25.000					1.000
22	C3F8(g)	25.000					1.000
23	C4F8(OFB)(g)	25.000					1.000
24	C4F8(OFC)(g)	25.000					1.000
25	C4F10(DFB)(g)	25.000					1.000
26	C6F6(g)	25.000					1.000
27	C7F8(PFTFMB)(g)	25.000					1.000
28	F(g)	25.000					1.000
29	F2(g)	25.000					1.000
30	FLUORIDES, etc.						
31	C12F10	25.000					1.000
32	ELEMENTS						
33	C	25.000					1.000
34	C(A)	25.000					1.000
35	C(D)	25.000					1.000
36	C60	25.000					1.000

Figure 7

By selecting the **Options** tab at the bottom of the window, the following window will appear (Figure 8). Here the temperature or pressure can be varied in a predetermined amount of steps. For our purpose the temperature will be varied from 25 to 1000 °C and the pressure be kept constant at 1 bar. A tick mark must be made in the box next to **Increase Temperature**.

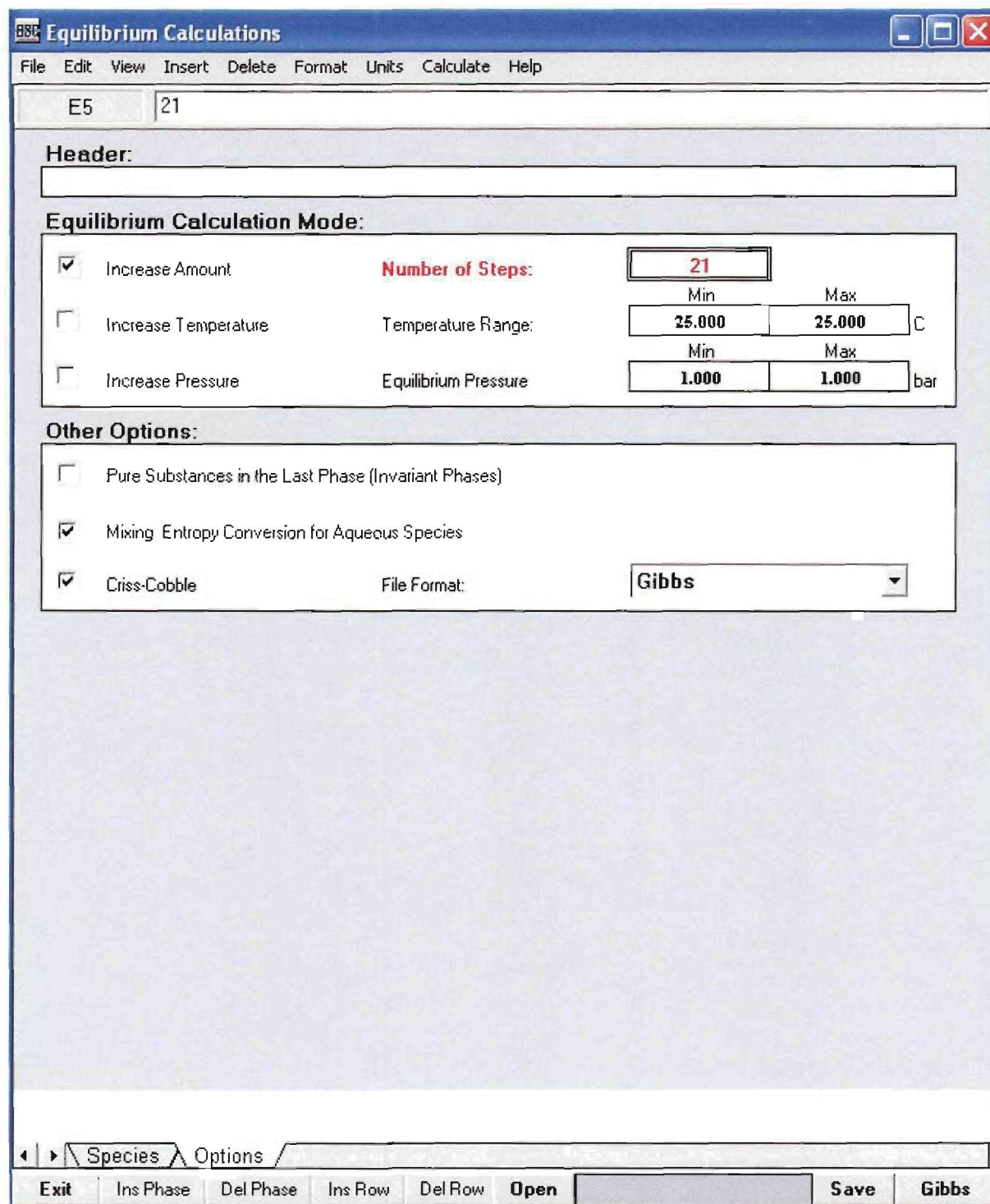


Figure 8

After **Saving** and pressing the **Gibbs** button, the following window appears (Figure 9). Press the **Calculate** button for the program to run the Gibbs energy minimisation algorithm and then the **Draw Diagram** button to display the window shown in Figure 10

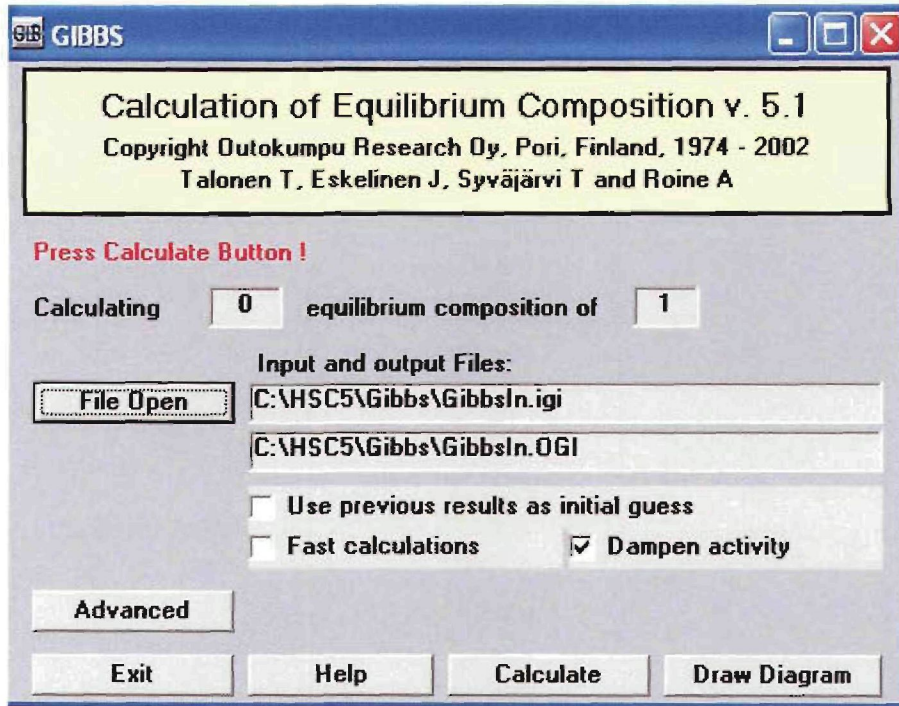


Figure 9

In order to draw the diagram one must firstly choose the X-axis. In this case it is the temperature. After pressing **OK** one usually selects the whole series of species available and press **OK** again to proceed to the next window.

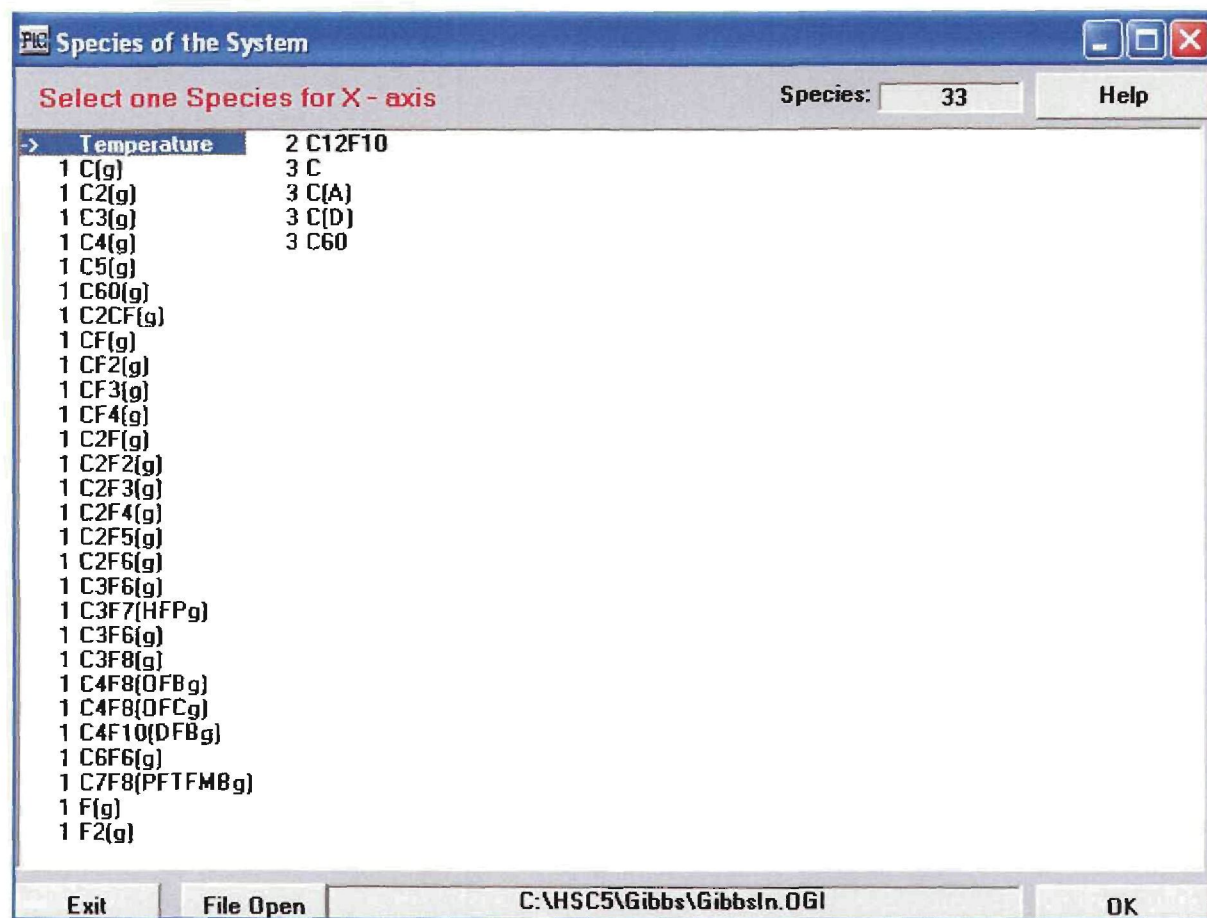


Figure 10

In the window presented in Figure 11, one can manipulate the x- and the y-axis and the units. To finally draw the diagram the **Diagram** button must be pressed.

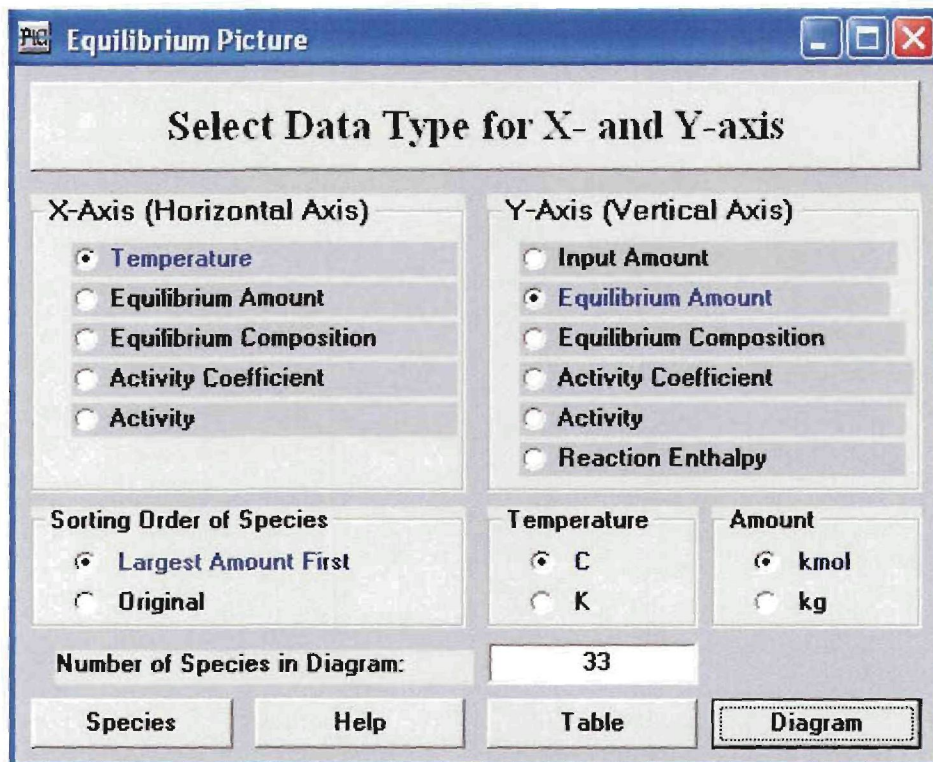


Figure 11

This diagram (Figure 12) can be Copied into a Word document or Printed. The axis of the diagram can be altered by selecting Format from the task bar and selecting the axis to be changed. In this case the Y-axis was change to view the logarithm of the concentration values.

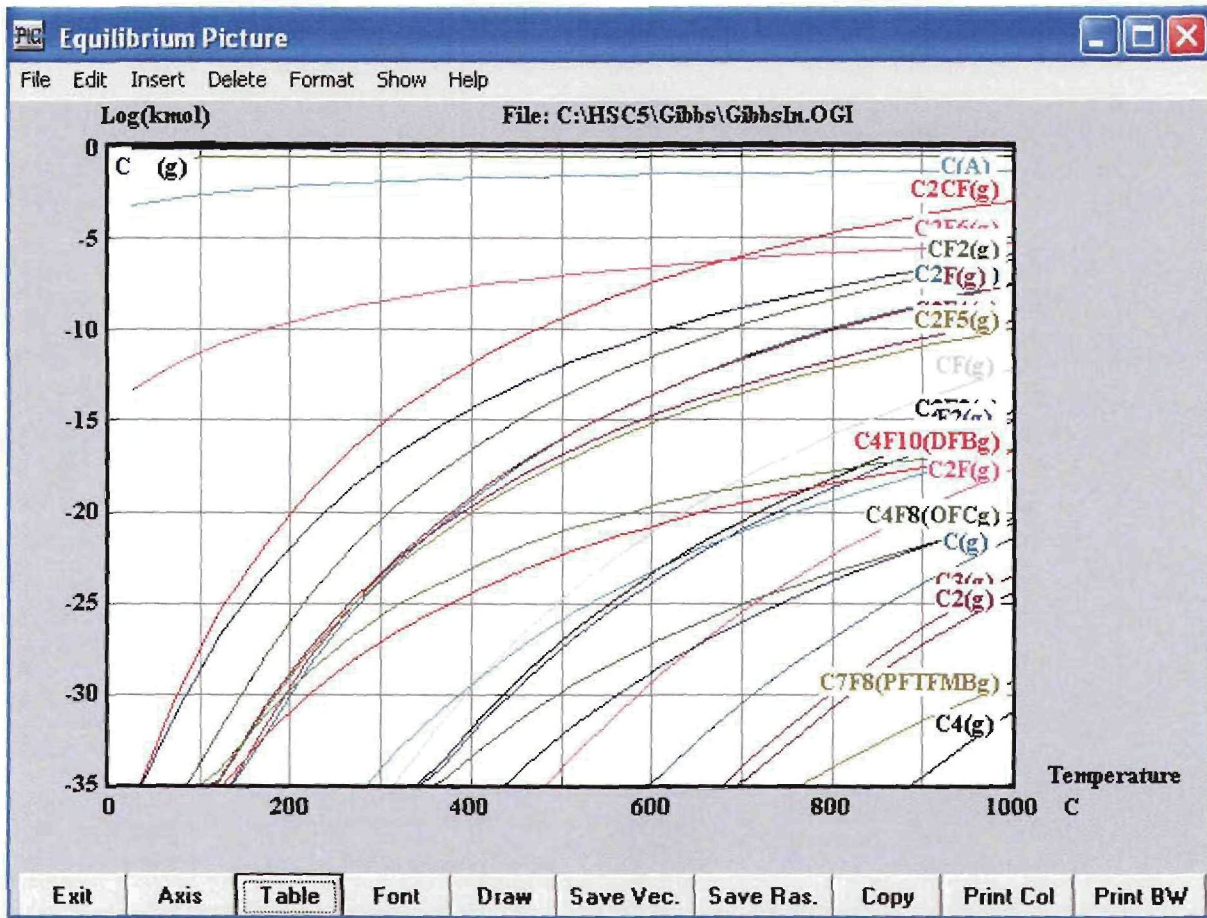


Figure 12

2. Spartan '04 v 1.0.3

When a calculation of a model is to be performed the following procedure can be followed:

After activation of the program the following window will be displayed (Figure 13).

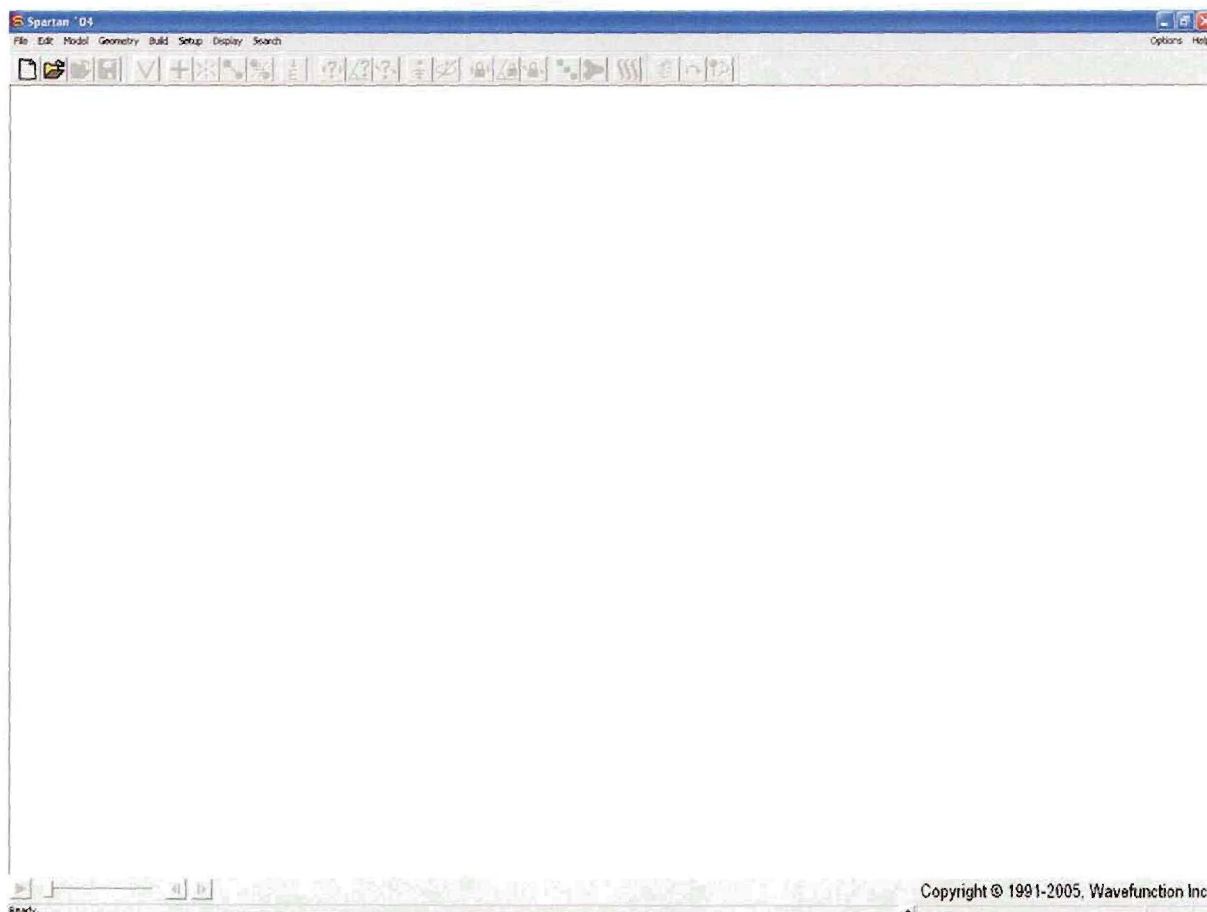


Figure 13

Now a new file can be started by clicking on the **page** icon in the top left corner.

A window, presented in Figure 14, will appear with the drawing pallet and the drawing toolbar active.

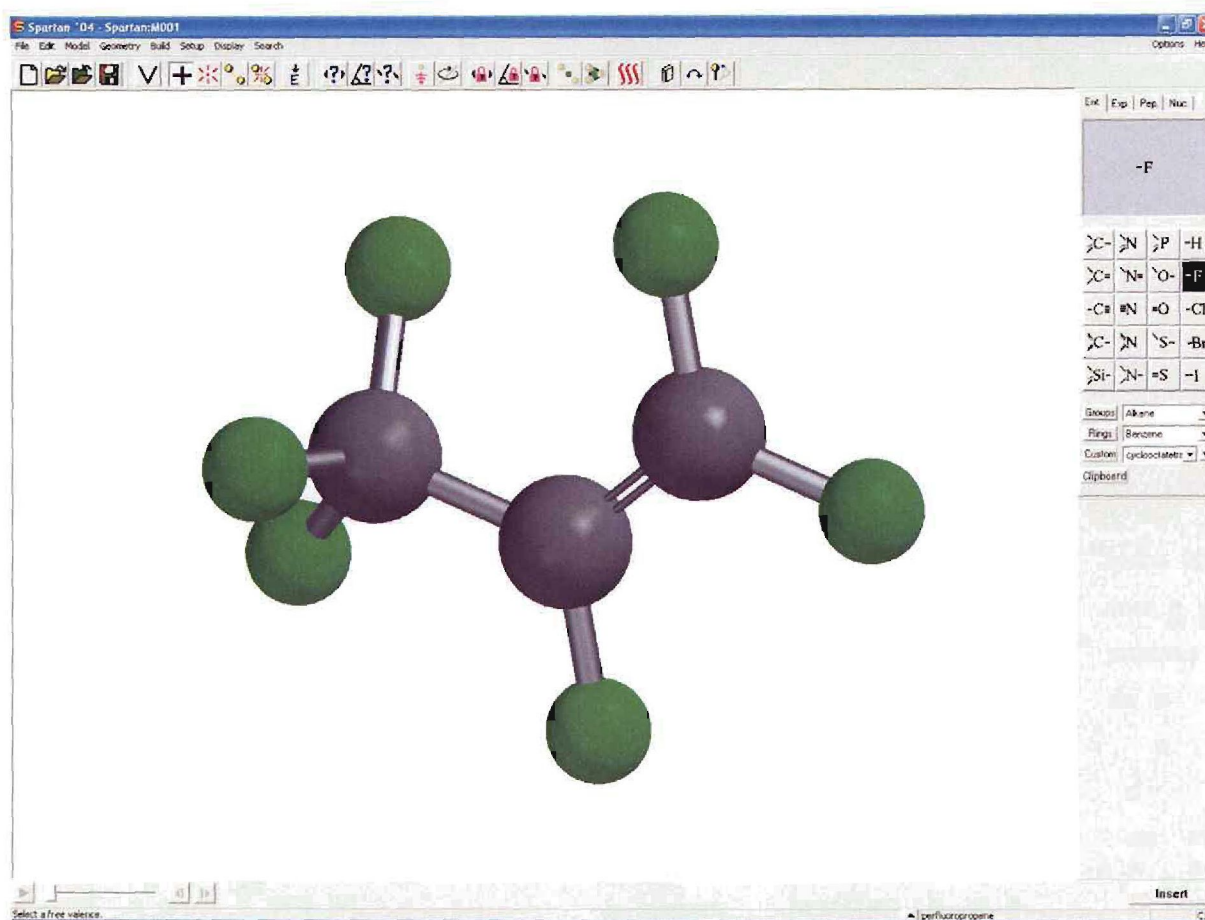


Figure 14

By using the pallet on the right hand side a molecule can be constructed. This molecule can be rotated, enlarged and modified by using a combination of the **Shift**, **Ctrl** or **Alt** keys along with the left and right mouse buttons.

After the molecule construction is finished, the calculation can be initiated by selecting the **Setup** and **Calculations** options. A calculations window will appear as indicated in Figure 15

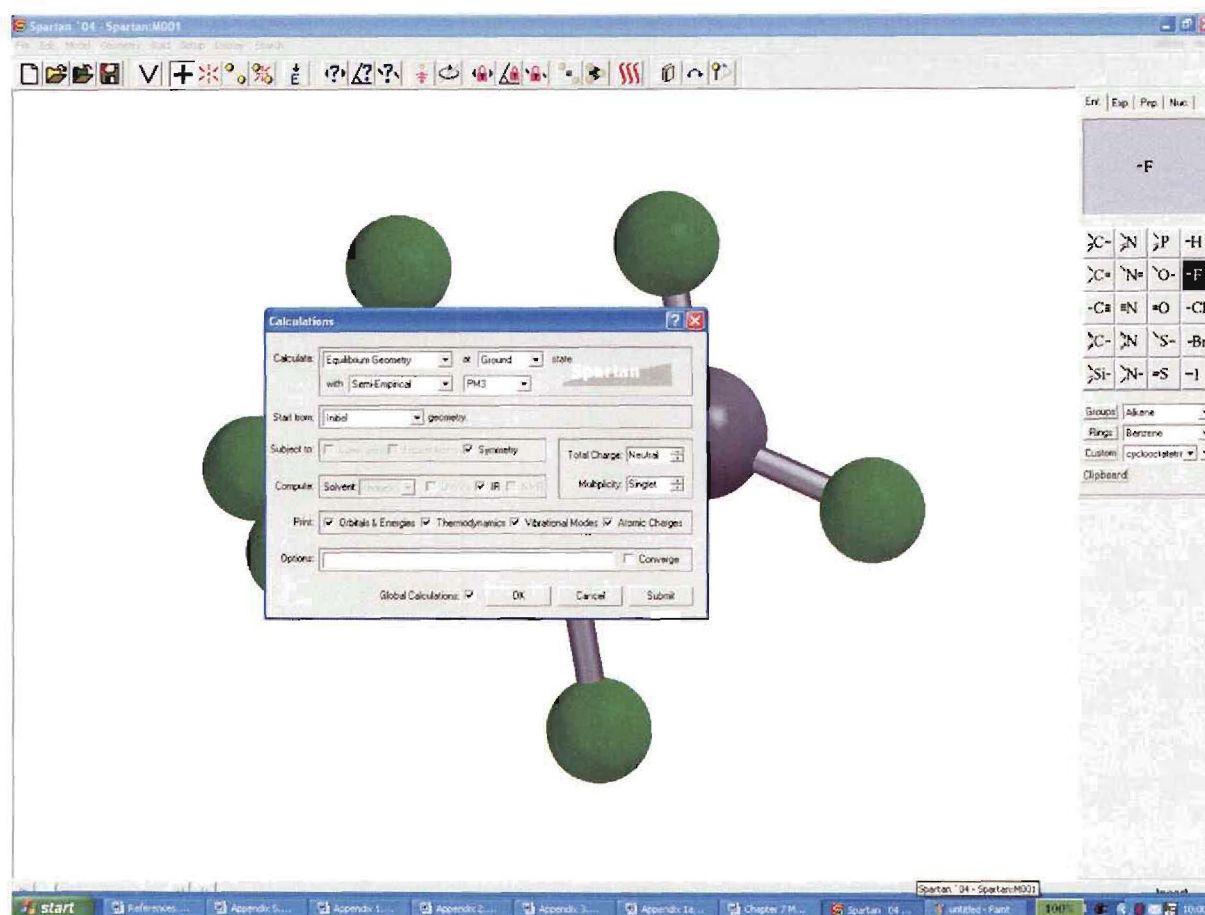


Figure 15

Different calculation methods are supported. In this study the **Equilibrium Geometry** in the **Ground** state with **Semi-empirical**, **PM3** was chosen. For this molecule the total charge is **neutral**, and the **multiplicity** is singlet. For a radical the multiplicity could be changed to doublet or triplet depending on the amount of free electrons in the radical. To calculate different thermodynamic properties, the appropriate other **check boxes** must be checked. After all the options were finalised, the **Submit** button must be pressed.

The following window (Figure 16) will appear to indicate that the calculation was started.

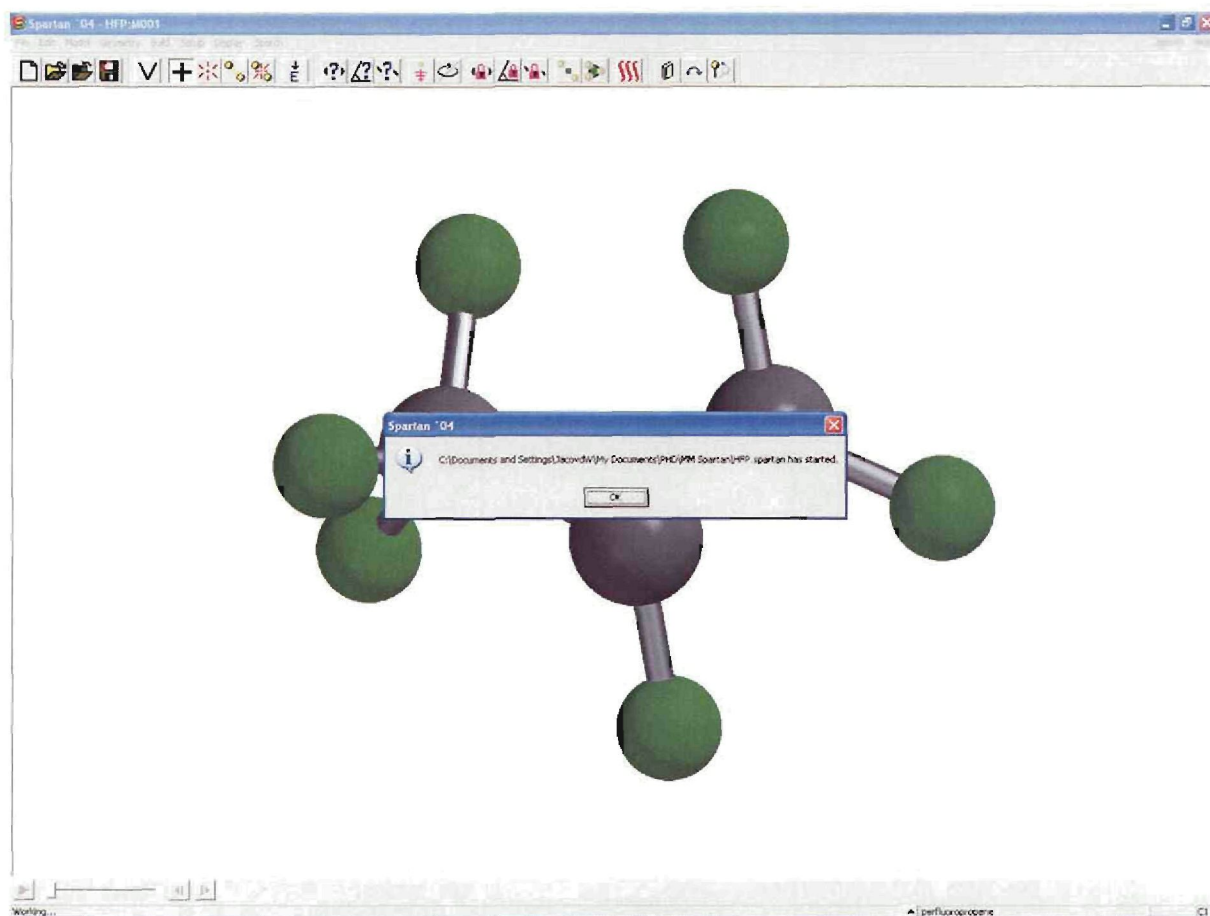


Figure 16

After clicking the **OK** button the calculation will proceed until completion.

When the calculation is finished, the following window (Figure 17) is displayed.

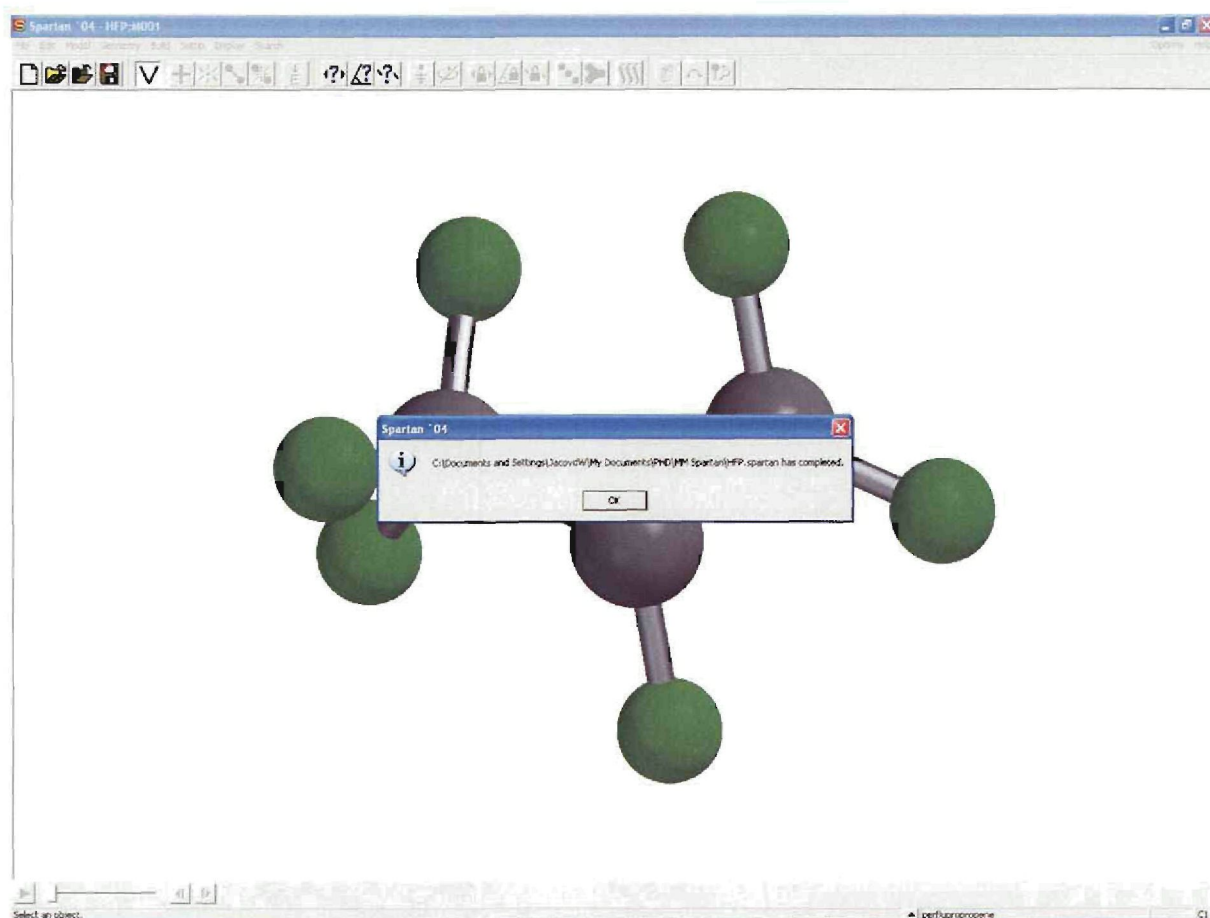


Figure 17

When this **OK** button is clicked the calculated data can be viewed.

Various windows can be activated to view the calculated data. This is presented in Figure 18.

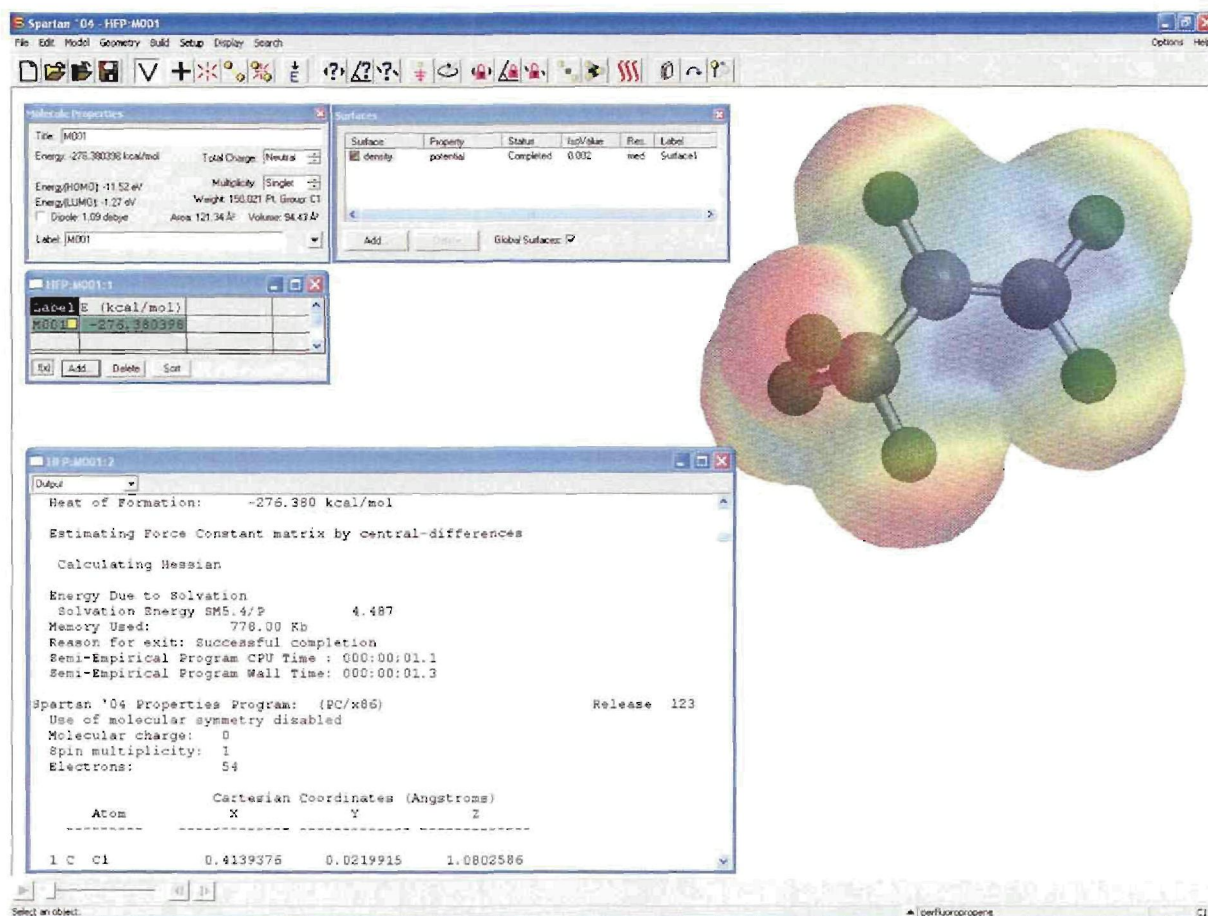


Figure 18

By selecting the **Display** option the molecule **Properties**, **Surfaces**, **Spreadsheet** and **Output** windows can be activated. Different options can be selected in order to display, for example, the charge on the surface of the molecule.

Transition states, radicals, IR spectra, animation of different frequencies, energy changes with increasing inter-atomic distances, and many more can be done. A well structured **Help** option is available in the top right corner of the screen.

Appendix 3

Evaluation of the Depolymerisation Product Formation Reactions

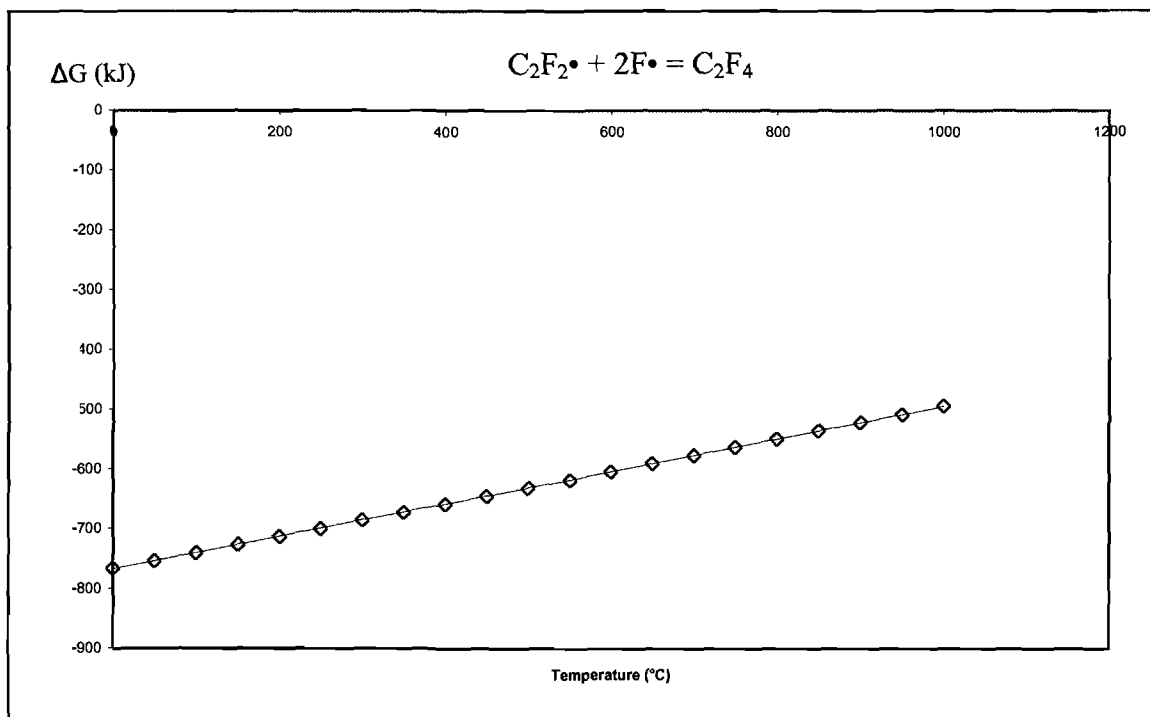


Figure 1: Change in Gibbs free energy vs Temperature for reaction 6.1

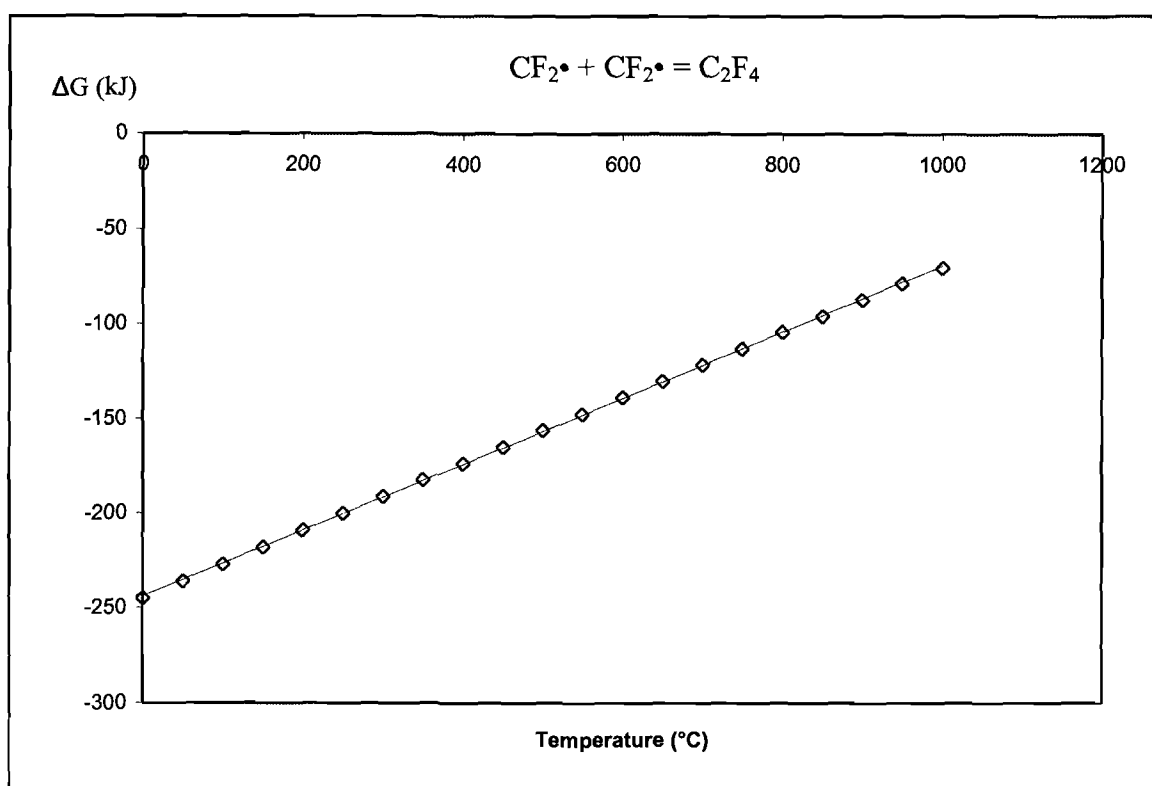


Figure 2: Change in Gibbs free energy vs Temperature for reaction 6.2

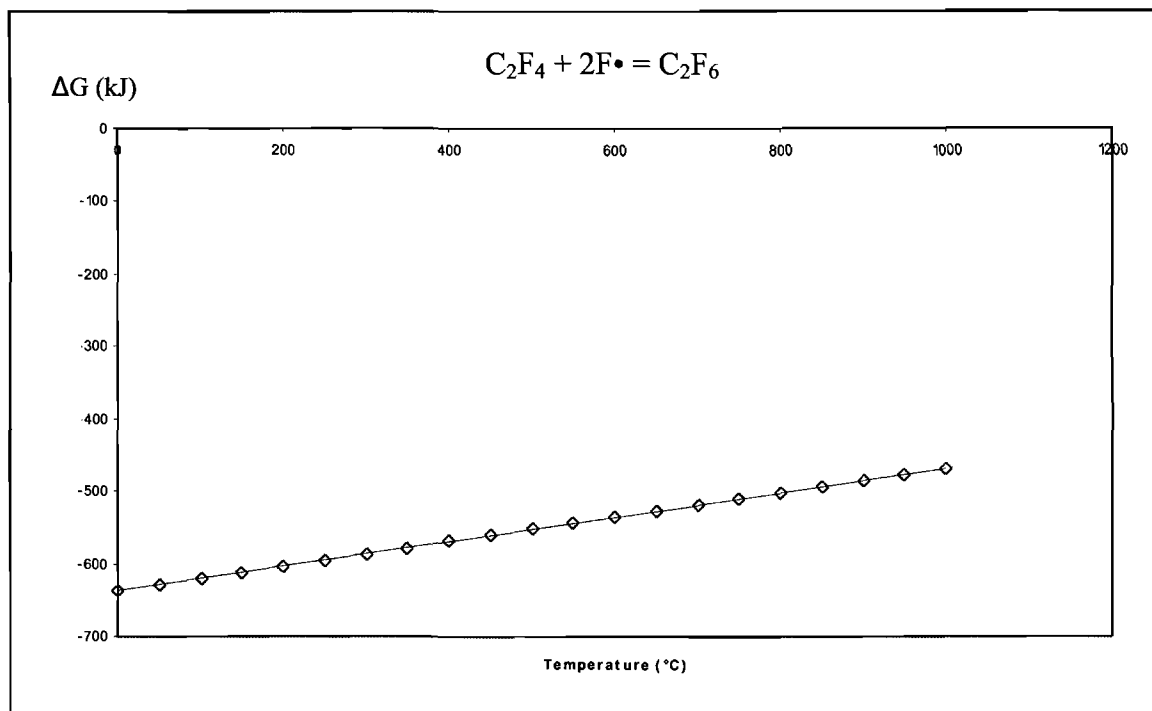


Figure 3: Change in Gibbs free energy vs Temperature for reaction 6.3

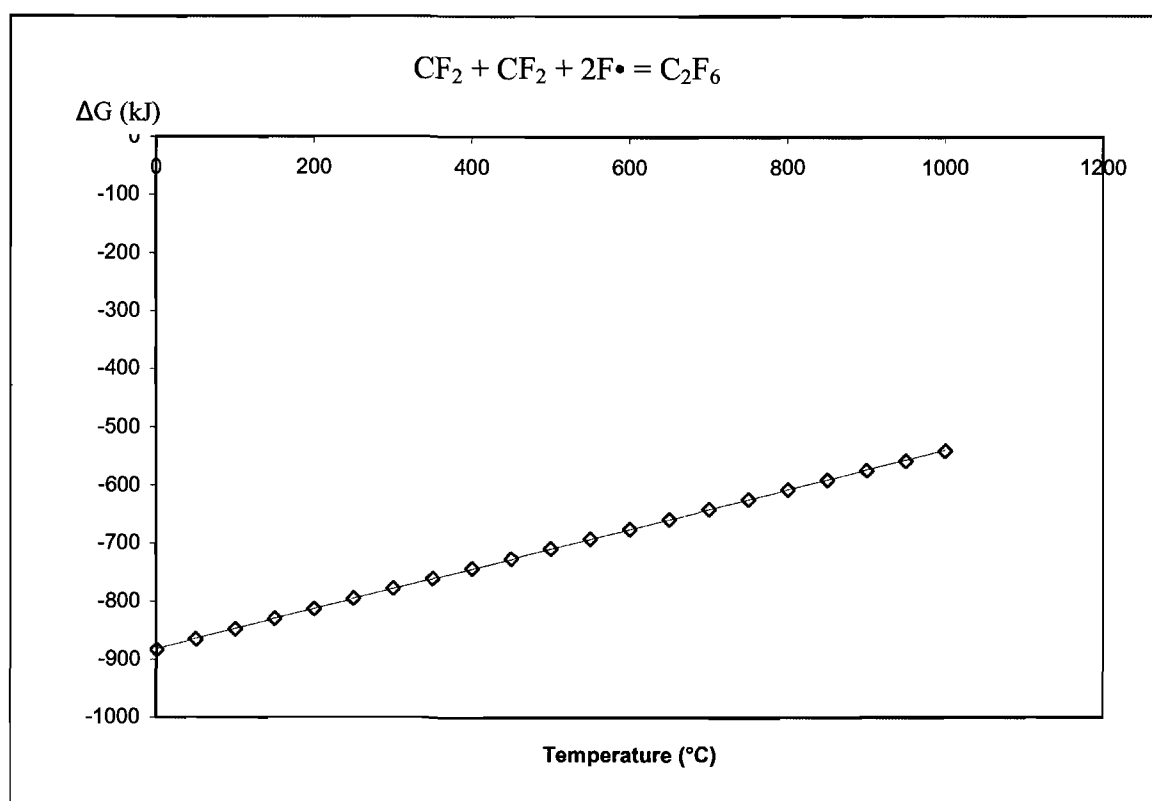


Figure 4: Change in Gibbs free energy vs Temperature for reaction 6.4

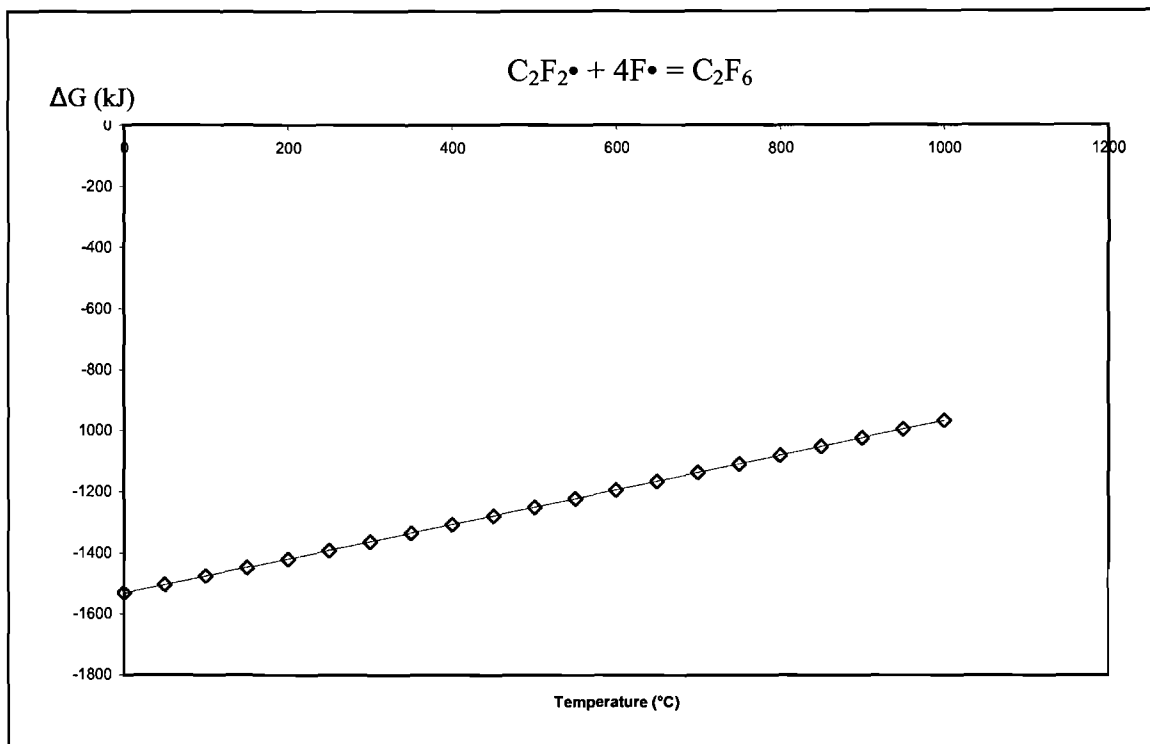


Figure 5: Change in Gibbs free energy vs Temperature for reaction 6.5

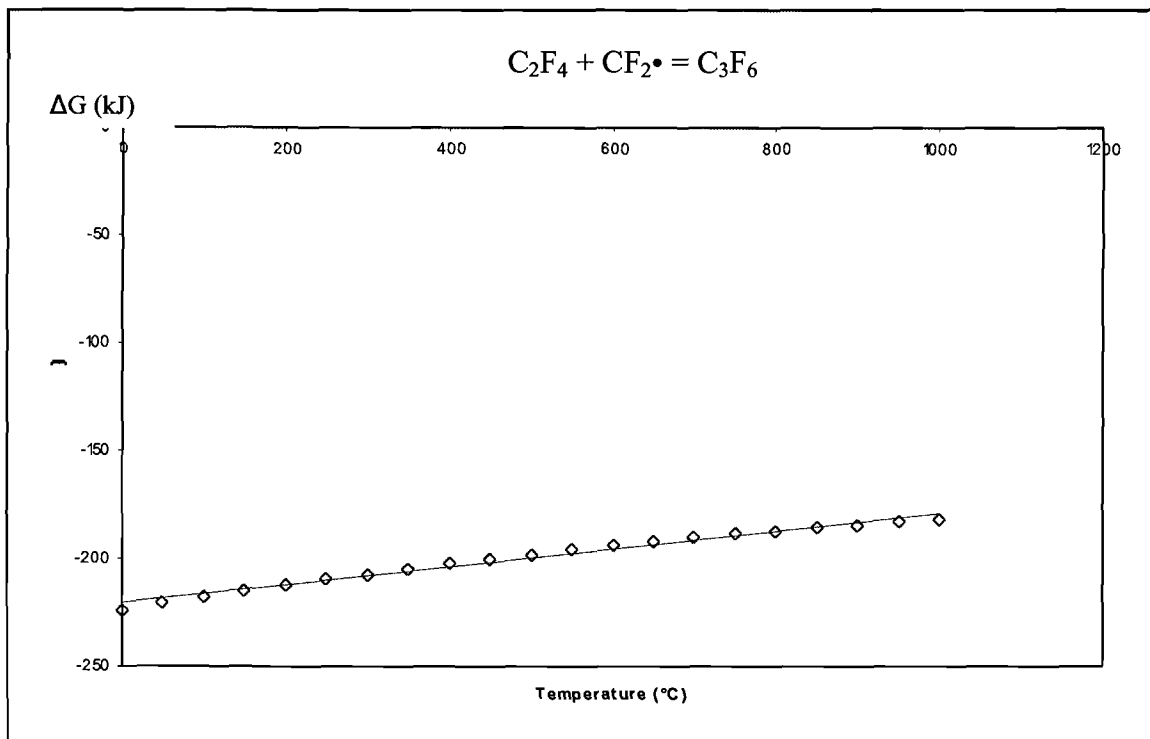


Figure 6: Change in Gibbs free energy vs Temperature for reaction 6.6

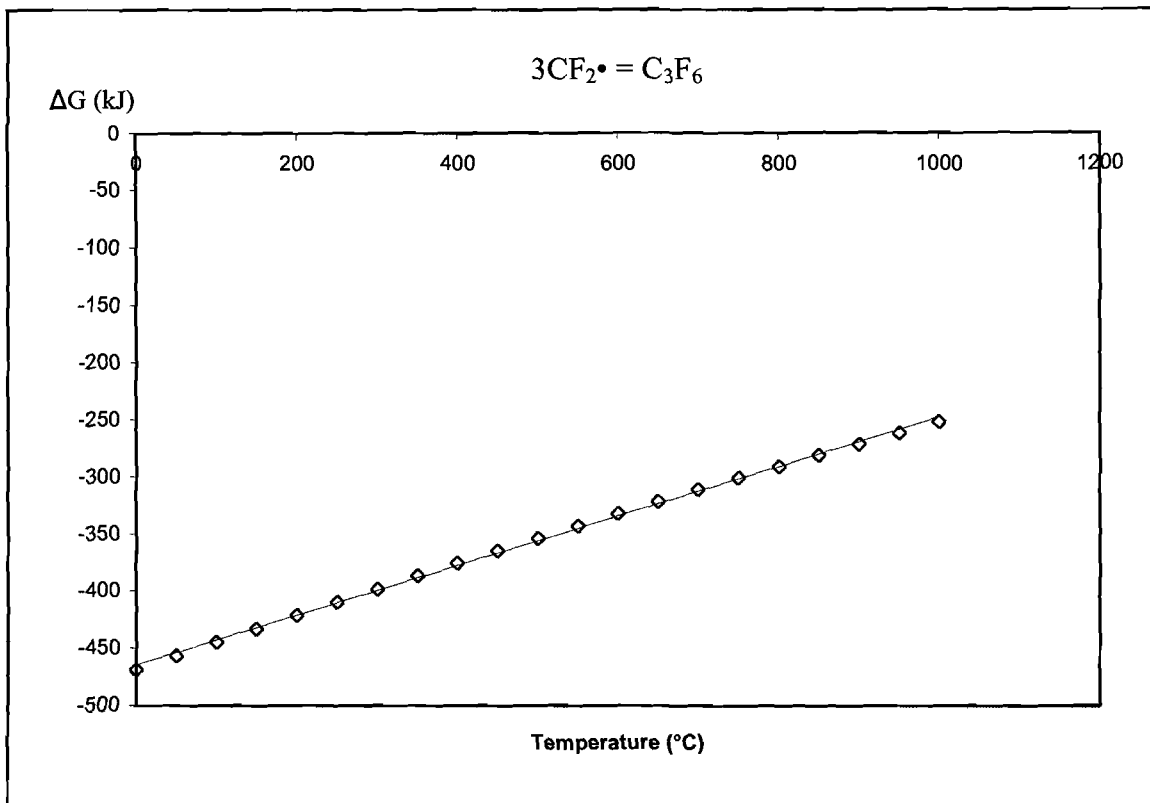


Figure 7: Change in Gibbs free energy vs Temperature for reaction 6.7

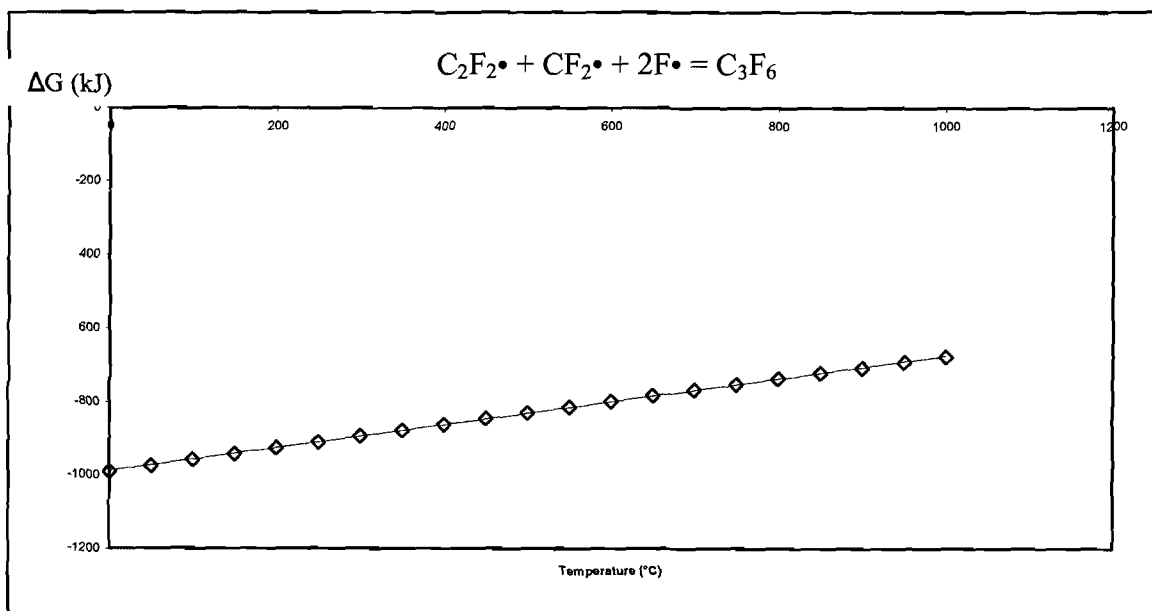


Figure 8: Change in Gibbs free energy vs Temperature for reaction 6.8

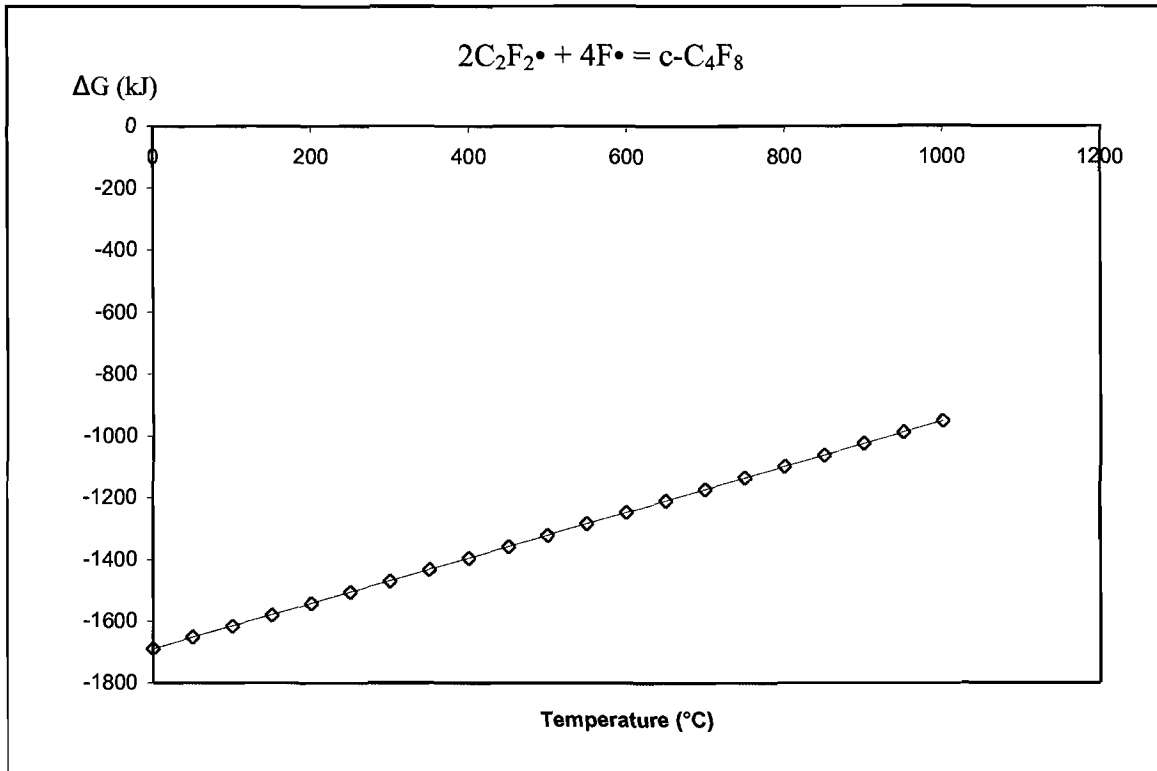


Figure 9: Change in Gibbs free energy vs Temperature for reaction 6.9

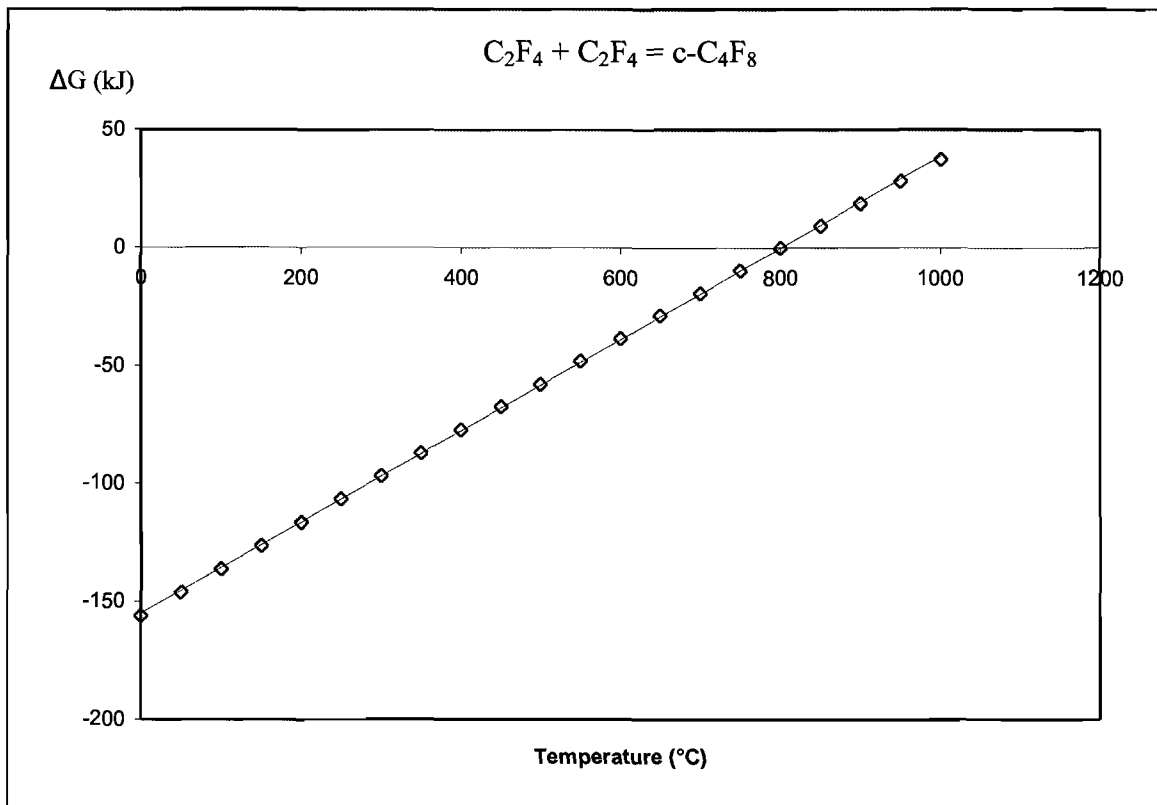


Figure 10: Change in Gibbs free energy vs Temperature for reaction 6.10

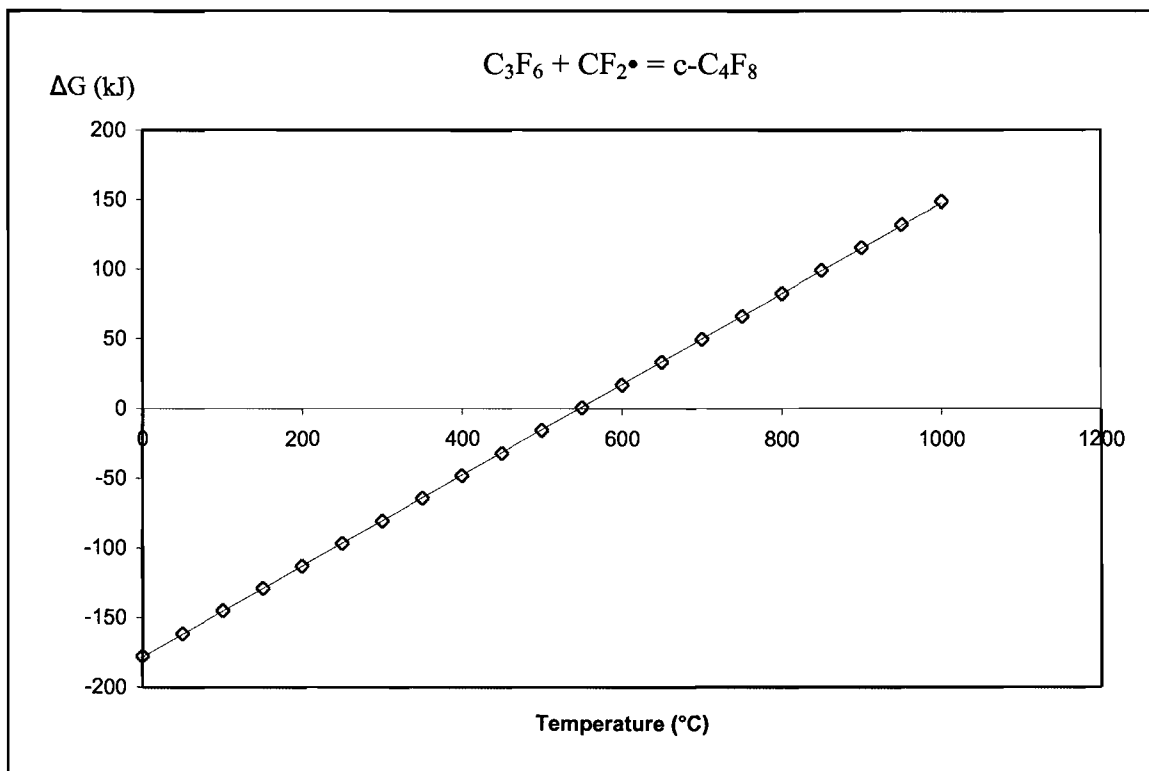


Figure 11: Change in Gibbs free energy vs Temperature for reaction 6.11

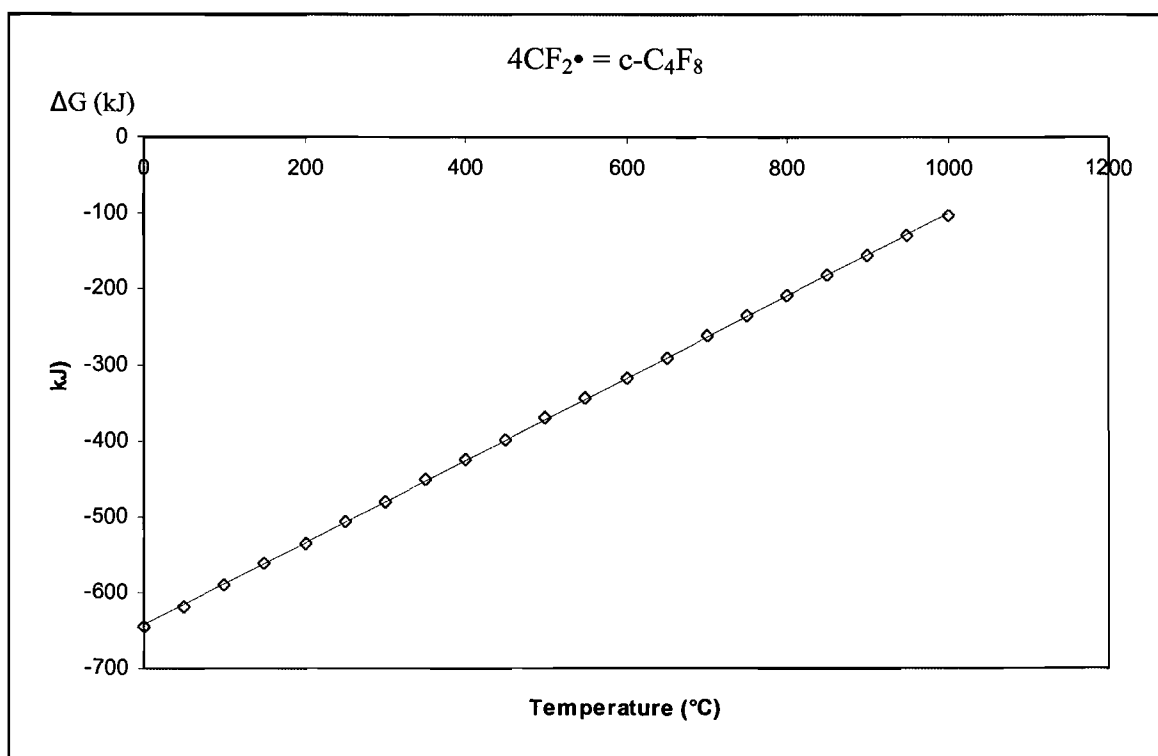


Figure 12: Change in Gibbs free energy vs Temperature for reaction 6.12

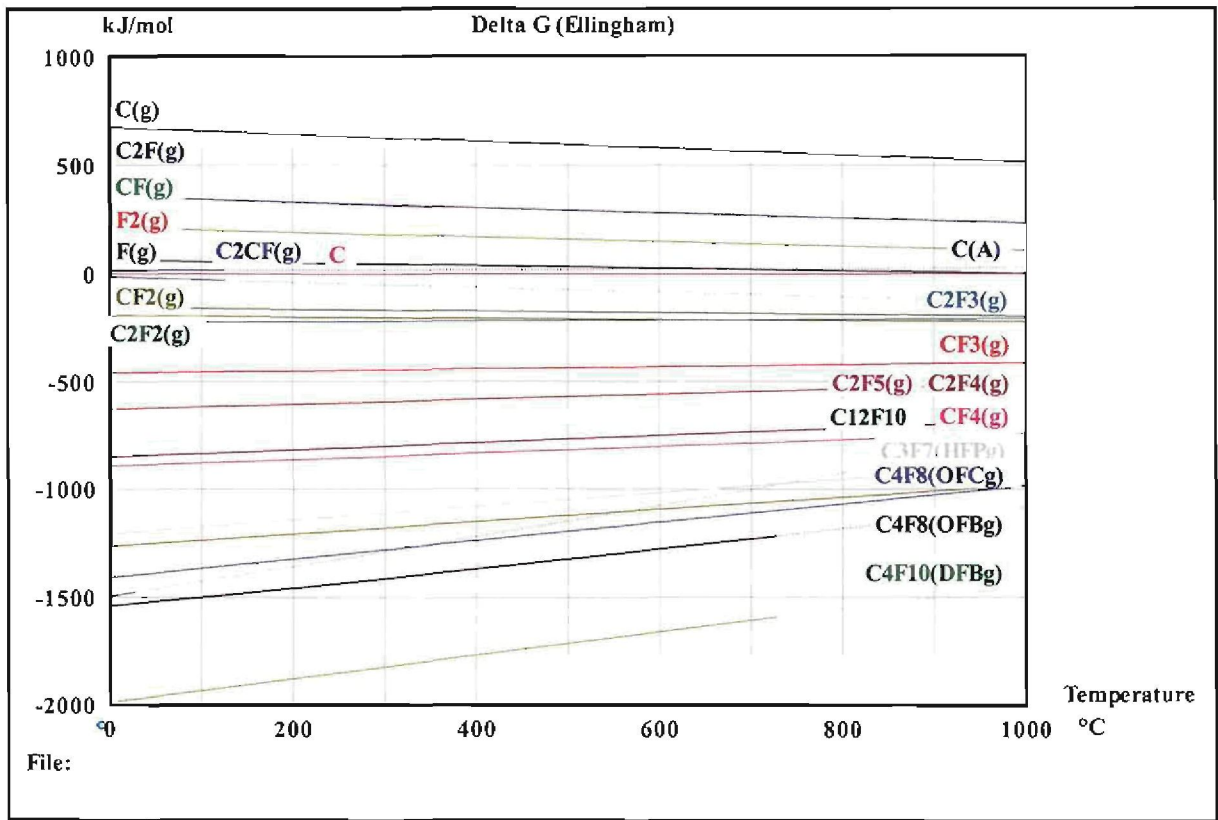


Figure 13: Ellingham plot of the depolymerisation products of PTFE

Appendix 5

Estimated Piloting Costs

HEXAFLUOROPROPENE PILOT PLANT				Total
				Cost Estimate
UNIT OPERATION 1 : High Temperature Convertor				
1.1	Wash bay			R 342,000
1.2	Filler containment			R 420,000
1.3	Fluoropolymer feeder			R 700,000
1.4	Off gas quenching system			R 600,000
1.5	Cooling water supply			R 160,000
1.6	Kiln			R 3,570,000
1.7	Other equipment			R 1,000,000
	Subtotal Main Equipment (ME)			R 6,792,000
1.16	Home Office	41%	of ME	R 2,750,760
1.16.1	Eng Design	20%	of ME	R 1,358,400
1.16.2	Risk Management	3%	of ME	R 203,760
1.16.3	Project Management	10%	of ME	R 679,200
1.16.4	Documentation	2.5%	of ME	R 169,800
1.16.5	Process Commissioning	5.0%	of ME	R 339,600
1.17	Valves	65%	of ME	R 4,414,800
1.18	Instrumentation	75%	of ME	R 5,094,000
1.19	Installation Cost	25%	of ME	R 1,698,000
				R 20,749,560
UNIT OPERATIONS 2 : MeOH Reactor				
2.1	Methanol Feed tank			R 525,000
	Subtotal Main Equipment (ME)			R 525,000
2.5	Home Office	41%		R 212,625
2.5.1	Eng Design	20%	of ME	R 105,000
2.5.2	Risk Management	3%	of ME	R 15,750
2.5.3	Project Management	10%	of ME	R 52,500
2.5.4	Documentation	2.5%	of ME	R 13,125
2.5.5	Process Commissioning	5.0%	of ME	R 26,250
2.6	Valves	65%		R 341,250
2.7	Instrumentation	300%		R 1,575,000
2.8	Installation Cost	25%		R 131,250
				R 2,785,125

UNIT OPERATIONS 3 : GAS SEPARATION SYSTEM

3.1	Cryogenics and compressor			R 22,000,000
3.2	Column 1			R 1,500,000
3.3	Column 2			R 1,500,000
	Subtotal Main Equipment (ME)			R 25,000,000
3.6	Home Office	43%		R 10,750,000
3.6.1	<i>Eng Design</i>	20%	<i>of ME</i>	R 5,000,000
3.6.2	<i>Risk Management</i>	5%	<i>of ME</i>	R 1,250,000
3.6.3	<i>Project Management</i>	10%	<i>of ME</i>	R 2,500,000
3.6.4	<i>Documentation</i>	3%	<i>of ME</i>	R 750,000
3.6.5	<i>Process Commissioning</i>	5%	<i>of ME</i>	R 1,250,000
3.7	Valves	24%		R 6,000,000
3.8	Instrumentation	43%		R 10,750,000
3.9	Installation Cost	25%		R 6,250,000
				R 58,750,000

UNIT OPERATIONS 4 : HFP PRODUCT HANDLING

4.1	HFP product loading bay and store			R 750,000
	Subtotal Main Equipment (ME)			R 750,000
4.8	Home Office	41%		R 303,750
4.8.1	<i>Eng Design</i>	20%	<i>of ME</i>	R 150,000
4.8.2	<i>Risk Management</i>	3%	<i>of ME</i>	R 22,500
4.8.3	<i>Project Management</i>	10%	<i>of ME</i>	R 75,000
4.8.4	<i>Documentation</i>	3%	<i>of ME</i>	R 18,750
4.8.5	<i>Process Commissioning</i>	5%	<i>of ME</i>	R 37,500
4.9	Valves	80%		R 600,000
4.10	Instrumentation	270%		R 2,025,000
4.11	Installation Cost	25%		R 187,500
				R 3,866,250

UNIT OPERATIONS 5 : OFF GAS DESTRUCTION				
5.1	Gas destruction system			R 2,000,000
5.2	KOH scrubber			R 450,000
5.3	Nox scrubber			R 300,000
	Subtotal Main Equipment (ME)			R 2,750,000
5.6	Home Office	41%		R 1,113,750
5.6.1	<i>Eng Design</i>	20%	<i>of ME</i>	<i>R 550,000</i>
5.6.2	<i>Risk Management</i>	3%	<i>of ME</i>	<i>R 82,500</i>
5.6.3	<i>Project Management</i>	10%	<i>of ME</i>	<i>R 275,000</i>
5.6.4	<i>Documentation</i>	3%	<i>of ME</i>	<i>R 68,750</i>
5.6.5	<i>Process Commissioning</i>	5%	<i>of ME</i>	<i>R 137,500</i>
5.7	Valves	65%		R 1,787,500
5.8	Instrumentation	90%		R 2,475,000
5.9	Installation Cost	25%		R 687,500
				R 8,813,750
OTHER COSTS				
6	Safety equipment			R 3,500,000
7	Flow meters			R 1,000,000
8	Control system			R 3,000,000
9	Ventilation - installed			R 4,000,000
10	Spares			R 1,000,000
	Subtotal others			R 12,500,000
TOTAL PILOT FACILITY COST				R 107,464,685
		% involved	Total	
OPERATORING PERSONNEL				
	Senior Process Controller	100%		R 273,420
	Junior Process Controller	100%		R 219,695
	Senior Process Engineer - Chemical	50%		R 291,699
	Process Engineer - Chemical	100%		R 654,783
	Senior Scientist	50%		R 291,699
	Senior Chemical Technologist	100%		R 674,472
	Chemical Techician X1	100%		R 510,755
	Chemical Techician X2	100%		R 461,851
	Process Engineering - Mechanical (Support)	50%		R 280,031
	Senior Artisans (Maintenance Support)	25%		R 131,033
	Electrical Artisan (Support)	15%		R 50,168
	Instrumentation Technician (Support)	25%		R 141,383
	Analytical Technician (Support)	30%		R 135,728
TOTAL OPERATING PERSONNEL				R 4,116,716
VARIABLE COST				
	Raw materials and reagents			R 170,000
	Effluents			R 270,000
	External contractors			R 250,000
	Packaging			R 1,000,000
	Utilities			R 270,000
TOTAL VARIABLE COST				R 1,960,000
TOTAL PROJECT COST				R 113,541,401